AN ENGINEERING STUDY OF THE DESIGN, INTEGRATION AND CONTROL OF ANTIBODY FRAGMENT PRODUCTION PROCESSES

A thesis submitted to the University of London
for the degree of Doctor of Philosophy

by

Leigh Caroline Bowering

June 2000

Department of Biochemical Engineering
University College London
Torrington Place
London WC1E 7JE

To Mum and Dad

ACKNOWLEDGEMENTS

I would like to thank Dr Nigel Titchener-Hooker and Professor Peter Dunnill for their supervision and support during this project. Special thanks must also go to Dr Neil Weir at Celltech Chiroscience Limited for his invaluable guidance and enthusiasm throughout the course of this research.

Much of this work would not have been possible without the technical support of Billy Doyle, Ian Buchanan and Clive Osborne; their help has been greatly appreciated.

I would like to extend my gratitude to the numerous researchers at University College London who have provided intellectual input and experimental support. In particular I would like to acknowledge Nick Murrell for his help with the large-scale fermentation and centrifugation experiments, Nik Willoughby for keeping me company during the numerous overnight fermentations and advising on expanded bed operation, and John Maybury for his input into the scale-down and modelling of the extraction and centrifugation processes.

Special thanks must go to the many friends I made during my time in London, especially Natalie and Helen for keeping me smiling, my colleagues on the first floor for the constant supply of tea, coffee and cakes, and to Layth for providing the support and encouragement I needed for the successful completion of this thesis.

Finally, I must thank my parents for their continued support throughout my career, without which none of this would have been possible.

The financial support of the BBSRC and Celltech Chiroscience Limited is gratefully acknowledged.

ABSTRACT

This project investigates process options for the production of antibody fragments from *Escherichia coli* and quantifies the effects of processing decisions on the integration of a complete bioprocess sequence.

Fab' antibody fragments were produced by *E. coli* fermentation at scales of up to 450L. Antibody expression was directed to the periplasmic space, however during initial fermentations over 50% of the Fab' leaked into the extracellular broth over the course of the induction period. Alterations to the fermentation were made to allow greater control of product location, and with the modified protocol 80-90% of the product was consistently retained within the periplasm. This fermentation strategy formed the basis for future downstream purification studies.

A novel method for the recovery of periplasmic proteins has been characterised and modelled at scales from 65mL to 100L. 85% recovery of periplasmic Fab' was achieved following resuspension of cells in a Tris-EDTA extraction buffer at 60°C. Operation at high temperature also resulted in purification of the process stream by degradation of both contaminating *E. coli* proteins and incomplete or partially degraded Fab' fragments.

Clarification of the process stream following periplasmic extraction was compared using a novel tubular bowl and an intermittent discharge disc-stack centrifuge. Operating at 95% biomass removal, 94% Fab' was recovered using the tubular bowl, compared to 73% with the disk-stack centrifuge. The improved recovery obtained with the tubular bowl was shown to be due directly to the greater level of liquid recovery. However lower throughputs were required for equivalent clarification when using this machine.

The optical biosensor has been assessed as a technique for the monitoring of Fab' in real time. The biosensor gave comparable Fab' accumulation profiles to ELISA during fermentation. During chromatographic purification, the sensor provided an

accurate indication of Fab' breakthrough during column loading and correctly identified product containing fractions during column elution.

The thesis concludes with a series of mass balance studies which compare the relative efficiencies of traditional purification processes and more novel process alternatives conducted at pilot scale. The results show that novel techniques such as whole broth extraction (performing the periplasmic extraction process on whole fermentation broth) and expanded bed adsorption offer potentially viable process alternatives, however the operational problems and reduced reliability compared to more conventional routes means further adaptation or optimisation is required before such techniques will be selected over conventional processing strategies.

TABLE OF CONTENTS

LIST OF FIGURES

LIST OF TABLES

1. INTRODUCTION

1.1 Antibody engineering

1.1.1 Project significance

Recent years have seen a rapid increase in the scientific and commercial interest in antibodies and antibody-based molecules. Currently over 30% of all biological proteins undergoing clinical trials are recombinant antibodies or antibody fragments (Hudson, 1998). Encouraging results have been obtained from phase 3 trials and several recombinant antibodies have recently received FDA (Food and Drug Administration) approval for therapeutic use.

The high affinity and specificity of antibodies for the target antigen has been exploited in a wide variety of therapeutic, diagnostic and industrial applications ranging from the treatment of inflammation and autoimmune disease to the detection and control of environmental pollution. Furthermore, the small size of engineered antibody fragments makes these molecules particularly attractive for medical applications such as imaging and cancer therapy.

The increasing commercial demand for antibody-based molecules and in particular the large dose requirements for the treatment of chronic illnesses necessitates the development of processes which allow efficient, high volume production and purification at low cost. Microbial expression systems provide a more economical means of production than the traditional mammalian cell systems based on hybridoma technology. Advances in antibody engineering techniques and elucidation of the key requirements for antibody design and efficient expression have allowed the development of low cost, high yielding production processes based on *Escherichia coli* fermentation systems.

1.1.2 Structure of antibodies and antibody fragments

1.1.2.1 Structure of whole antibodies

Whole antibody molecules consist of a Y-shaped tetramer of polypeptides composed of two heavy and two light chains (Figure 1.1.1). Both the heavy and light chains are divided into structurally discrete regions termed domains, with each light chain consisting of one variable domain (V_L) and one constant domain (C_L) and each heavy chain containing one variable domain (V_H) and three constant domains (C_H1, C_H2 and C_H3). The sequence variability within each variable domain is concentrated in three hypervariable loops. These regions form the antigen binding site of the molecule and are therefore referred to as complementary determining regions (CDRs). The remainder of the variable domain is termed the framework region. Antibody molecules are stabilised by both intra and inter chain disulphide bonds, with the number and arrangement of such bonds being determined by the immunoglobulin class and specificity of the antibody. Interchain disulphide bonds form between the two heavy chains in an area between C_H1 and C_H2 called the hinge region. Flexibility in this region permits variation in the distance between the two antigen binding sites allowing them to operate independently. Glycosylation of antibodies frequently occurs in the constant domains of the heavy chain, with glycosylation patterns also determined by the immunoglobulin class or subclass. Ordinarily glycosylation has no influence on the antigen-binding properties of the antibody, however lack of glycosylation can affect some of the antibody's effector functions (Nose and Wigzell, 1983; Leatherbarrow *et al.*, 1985).

1.1.2.2 Structure of antibody fragments

A variety of antibody fragments have been designed, the majority of which are based on either the Fv or the Fab fragment (Figure 1.1.1). The Fv fragment is a non-covalently associated heterodimer of heavy and light chain variable domains (V_H and V_L) and is the smallest antibody fragment that still contains the complete antigen

binding site. Fv fragments have been reported to have the same binding properties as the Fab fragment (Inbar *et al.*, 1972) or whole antibody (Skerra and Pluckthun, 1988). However they are quite unstable and have a tendency to dissociate into V_H and V_L upon dilution (Glockshuber *et al.*, 1990). The stability of these fragments can be increased by covalently linking the two variable domains and with this aim single chain Fv fragments and disulphide stabilised Fv fragments have been designed.

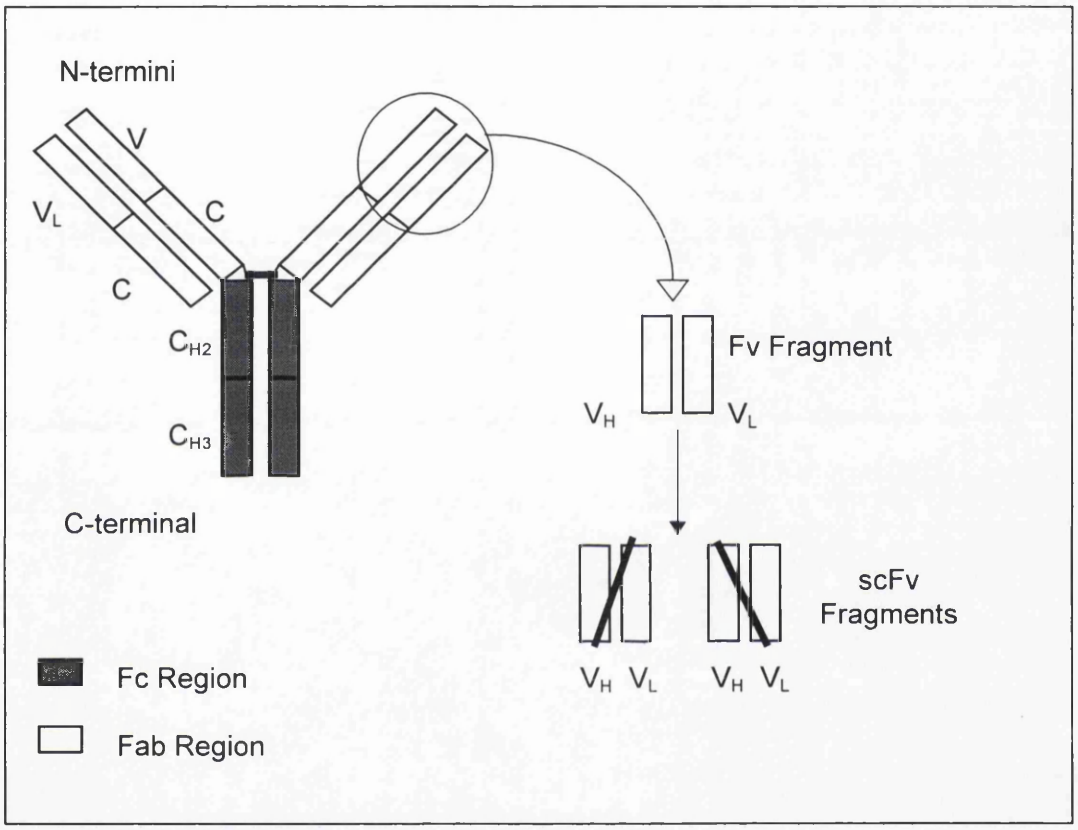

Figure 1.1.1 *Schematic representation of an antibody and derived antibody fragments. Adapted from J. Harrison (PhD Thesis, 1996).*

Single chain Fv antibody fragments (scFv) consist of the V_H domain and the V_L domain connected by a short peptide linker. Both orientations of linker (the C-terminus of V_H connected to the N-terminus of V_L and the C-terminus of V_L connected to the N-terminus of V_H) have been constructed and both arrangements give rise to fragments with antigen binding activity. Ideally the linker should be sufficiently long to span the distance between the two domains and flexible to allow V_H-V_L association. In addition the linker must not obstruct the antigen binding site or reduce antigen binding affinity. A number of linker polypeptides have been designed.

The most commonly used are 15 residues in length and consist primarily of glycine and serine residues for flexibility, with charged residues such as glutamine and lysine interspersed for flexibility (Raag and Whitlow, 1995). Although many scFvs have good binding activities, many show a reduced binding affinity when compared to the Fab fragment (Bird and Walker, 1991). This could be due to interference of the peptide linker with antigen binding or alternatively the linker may distort or not sufficiently stabilise the Fv structure. ScFvs also have a tendency to form multimers that are unstable and aggregate (Raag and Whitlow, 1995).

Disulphide-stabilised Fv fragments (dsFv) are molecules in which the V_H-V_L heterodimer is stabilised by an interchain disulphide bond. The bond can be placed in either the complementary determining regions (CDRs) or between framework residues. DsFvs are generally more stable than their scFv analogues, however both increases and decreases in dsFv binding affinities have been observed when compared to scFvs (Reiter *et al.*, 1996).

A Fab fragment contains the entire light chain (V_L + C_L) plus the variable and first constant domain of the heavy chain (V_H + C_H1, also referred to as the Fd region of the heavy chain). Interchain disulphide bonds increase the stability of the Fab compared to Fvs, and Fab fragments have been documented as having the same antigen binding activity as the whole antibody (Shibui *et al.*, 1993). Fab' fragments are Fab fragments with the heavy chain extended to include one or more hinge region cysteine residues.

A number of techniques have been developed for the conjugation of Fab or scFv molecules into dimers or higher multimers to increase their functional affinity (avidity). Di-Fabs ($F(ab')_2$) have been created by linking two Fab' arms with a disulphide bond (Carter *et al.*, 1992a) or thioether bridge (Rodrigues *et al.*, 1993), or by constrcting a linear $F(ab')_2$ molecule comprising tandem repeats of the heavy chain Fd fragment (V_H-C_H1-V_H-C_H1) (Zapata *et al.*, 1995). The $F(ab')_2$ variants all showed increased avidity compared to individual Fab or Fab' fragments. The thioether linked $F(ab')_2$ and linear $F(ab')_2$ also showed improved stability over the disulphide linked $F(ab')_2$.

A reduction in the length of the scFv linker from 15 residues to 5 residues restricts the formation of a functional Fv molecule and instead promotes combination of the V domains of two scFv molecules to form a bivalent dimer, called a diabody. Further reduction of the linker length to less than three residues prevents diabody formation, instead directing the association of three scFv molecules into a trimer (triabody) with three functional antigen binding sites. Again, increasing the number of binding sites has been shown to improve functional affinity (Kortt *et al.*, 1997).

Finally, a variety of fragments based on the Fab and scFv have been designed and engineered for clinical application. Theses include miniantibodies (scFv-CH3 fusions), dimeric miniantibodies (Pack *et al.*, 1993) and bispecific antibodies which consist of two antibodies or antibody fragments with different specificities linked together (Zhu *et al.*, 1996).

1.1.3 Commercial applications of engineered antibodies

The potential medical and diagnostic applications of engineered antibody fragments are extensive and have been reviewed by Carter and Merchant (1997) and Hudson (1998). Antibody fragments have been fused to a range of molecules including radiolabels and toxins for cancer imaging and therapy, enzymes for prodrug therapy, viruses for gene therapy and liposomes for the delivery of drugs, toxins and DNA. In addition antibody fragments are used in a wide range of *in vitro* immunoassay assays for clinical diagnosis.

Radiolabelled diabodies, dimeric minibodies and dimerised Fab have all been used for *in vivo* cancer imaging and show improved tumour targeting compared to monomeric scFv, Fab and parent Ig. The dimeric antibody fragments show improved serum residence times due to higher functional affinity (avidity) for the target antigen compared to monovalent fragments. In addition the smaller size of the antibody fragments allows more effective tumour penetration compared to whole Igs (reviewed in Hudson, 1999).

Bispecific antibodies which combine both antibody and effector function are being developed for cancer therapy (Segal *et al.*, 1999). In one example a bispecific scFv dimer was used to recruit cytotoxic T cells to kill tumour cells *in vitro* (Zhu *et al.*, 1996). A bispecific diabody was also used to cross-link colon cancer cells to serum IgG, resulting in the recruitment of effector functions to the target site (Holliger *et al.*, 1997). Bispecific antibodies also have numerous potential applications in diagnostic applications.

Immunotoxins and immunoconjugates, which direct drugs to the site of action, have been developed by recombinant or chemical fusion of whole antibodies or antibody fragments to cytotoxic drugs, proteins and peptides (reviewed in Carter and Merchant, 1997; Kreitman, 1999; Trail and Bianchi, 1999). However the toxicity and immunogenicity of such drugs has hampered their development. Human enzymes such as RNase are being investigated as potentially less immunogenic toxins (Holliger and Hoogenboom, 1998).

Antibody dependent enzyme-prodrug therapy (ADEPT) is a further technique under development designed to target toxins to the site of action. ADEPT utilises an antibody-enzyme fusion that specifically activates a prodrug into cytotoxic agent at the cell target site. ADEPT has the advantage of amplification, as the target enzyme can produce many molecules of the active drug within the tumour. However the technique again requires the development of non-immunogenic drug/ antibody-enzyme combinations (Chester and Hawkes, 1995; Bagshawe *et al.*, 1999).

Liposomes loaded with drugs or DNA can also be targeted to desired sites *in vivo* by attachment of specific antibodies or antibody fragments to the liposome surface to produce immunoliposomes. Immunoliposomes targeted against breast cancer cells and loaded with a cytotoxic drug were shown to be markedly and specifically toxic against target cells *in vitro* and were able to deliver the toxin to tumours in an *in vivo* mouse model (Park *et al.*, 1995).

The rapidly developing biotechnology industry has provided further application for antibody fragments. Fv and scFv fragments can be immobilised to porous supports allowing purification of the target antigen by affinity chromatography (Berry and

Davies, 1992). Antibodies and antibody fragments can also be immobilised on biosensors for the real-time monitoring of product during fermentation and purification processes (discussed further in section 1.4.1.3 and Chapter 7). Finally, antibody based technologies may be exploited for the detection and management of environmental pollution, reviewed by Harris (1999).

1.2 Methods for the production of antibody fragments

1.2.1 Production of whole antibodies and antibody fragments

1.2.1.1 Antibody fragments by proteolytic digestion

Antibody fragments can be produced by proteolytic digestion of whole antibodies. Fab fragments result from proteolytic cleavage of whole antibodies using papain (Porter, 1959). Cleavage by pepsin at the C-terminal side of the hinge region of a complete antibody results in the $(Fab')_2$ fragment (Petermann and Pappenheimer, 1941). Fv fragments can also be produced by digestion of Fab using pepsin (Inbar *et al.*, 1972). Production of antibody fragments by proteolytic digestion however will usually give a heterogeneous mixture due to non-specific cleavage and differences in the susceptibility of antibodies to protease action.

1.2.1.2 Production of monoclonal antibodies by mammalian cell culture

The development of hybridoma technology (Kohler and Milstein, 1975) has provided a general procedure for the production of monoclonal antibodies of defined specificity. Monoclonal antibodies have been produced from hybridomas in serum free fed-batch culture, with titres of 1-2 g L^{-1} being reported (Bibila and Robinson, 1995). Hybridoma cells have also been grown in several different types of perfusion systems including hollow fibre reactors (Altshuler *et al.*, 1986) and microencapsulated systems (Tyler, 1990). Perfusion cultures offer the advantages of higher volumetric productivity compared to fed batch culture and facilitated purification because the product is separated from the culture medium. However,

batch or fed batch cultures are simpler to operate, allow greater flexibility and generally have shorter process development and validation times.

In addition to monoclonal antibody production by hybridoma cells, recombinant gene technology has been used to develop stable cell lines expressing chimeric or humanised antibodies and antibody fragments. Expression of Fv fragments (Reichmann *et al.*, 1988), scFv fragments (Dorai *et al.*, 1994) and Fab-enzyme fusion proteins (Neuberger *et al.*, 1984) has been achieved. The major disadvantage of using mammalian cell expression systems for the synthesis of antibody fragments is the high production costs. A significantly more economical route involves the use of bacterial expression systems.

1.2.1.3 *E. coli* production of antibody fragments

The production of antibody fragments in *E. coli* offers a number of advantages over production by mammalian cell culture. *E. coli* is well characterised at the molecular level, with well-established techniques for genetic manipulation. The introduction of foreign genes can be achieved relatively easily, with proteins being expressed to high titres at specific locations within the cell. In addition the fast growth of *E. coli* to high cell density and its comparatively simple fermentation using inexpensive media and readily available fermentation equipment make the large-scale production of antibody fragments relatively straightforward. The production of antibody fragments and other recombinant proteins is well documented in *E. coli*, where expression of Fvs, Fabs, associated fragments and various antibody based molecules has been achieved successfully (reviewed by Better and Horwitz, 1989; Pluckthun and Skerra, 1989; Pluckthun, 1991).

1.2.2 Expression strategies for *E. coli*

1.2.2.1 Direct cytoplasmic expression

Initial attempts to produce antibody fragments in *E. coli* involved direct expression into the cytoplasm. Differing yields have been reported for different antibody chains, fragments and constructs, and appear to depend on the design of the translation initiation region, the proteolytic stability of the fragment and the host strain (Pluckthun, 1991). High expression levels are required to overcome degradation by *E. coli* cytoplasmic proteases and generally result in accumulation of the product as insoluble, inactive inclusion bodies.

Production of recombinant antibody fragments as cytoplasmic inclusion bodies is widely reported (Boss *et al.*, 1984; Cabilly *et al.*, 1984; Burks and Iverson, 1995), however this technique suffers the disadvantage of requiring an efficient product solubilisation and refolding process. Although successful refolding strategies have been designed, antibody recovery by this method remains inefficient (Buchner and Rudolf, 1991).

A further disadvantage of cytoplasmic expression is that polypeptide chains produced in the cytoplasm often have an initiation methionine or other additional amino acids at the N-terminus (Buchner and Rudolf, 1991) which may affect antibody function.

Cabilly (1989) reported that a soluble, functional Fab fragment could be produced in the *E. coli* cytoplasm using low temperature (20-25°C) cultures. However the levels of functional Fab obtained were very low (0.1 mg L^{-1} culture) and insoluble material was also present.

Higher expression levels have been achieved more recently by Martineau *et al.*, (1998), who reported the accumulation of a correctly folded, functional scFv fragment to titres of 3.1 g L^{-1} in the cytoplasm of *E. coli*. The scFv was produced by random mutation of the 'parent' anti-beta-galactosidase scFv, which aggregated

during cytoplasmic expression. The work illustrates that with suitable screening techniques it is possible to select antibody fragments that will fold correctly in the cytoplasm and accumulate to high yields.

1.2.2.2 Secreted fusion proteins

Antibody domains can also be fused to secreted proteins to allow accumulation in the periplasm or extracellular medium. Fusion of the Fc binding domain of *Staphylococcus aureus* protein A to the N-terminus of antibody domains results in secretion of the fusion protein to the periplasm (Gandecha *et al.*, 1992). Partial lysis of the outer membrane releases the fusion protein to the extracellular medium. Purification can then be achieved relatively easily using IgG-affinity chromatography.

Antibody V domains have also been fused to the C- or N- terminus of the periplasmic maltose binding protein (MalE) and expressed in *E. coli* (Bregegere *et al.*, 1994). The fusion proteins accumulated in the bacterial periplasm and were purified by affinity chromatography on cross-linked amylose, exploiting the binding properties of MalE.

1.2.2.3 Functional periplasmic expression

In an attempt to reproduce in *E. coli* the folding and assembly pathway of antibodies in eukaryotic cells a system was developed which allowed expression of both antibody chains in the same *E. coli* cell and secretion of both chains to the periplasmic space (Skerra and Pluckthun, 1988). This system assumes that the transport of proteins to the periplasm of *E. coli* is functionally equivalent to protein transport to the lumen of the endoplasmic reticulum in a eukaryotic cell.

Skerra and Pluckthun identified the following steps as being critical for the correct assembly of antibody chains into functional fragments.

1. Synthesis of approximately stoichiometric amounts of both chains. This is achieved by designing operons of both chains under control of the same promoter.

2. Transport of both precursor proteins to the periplasmic space. This is achieved by precise fusion of signal sequences directing protein transport to the periplasm to the N-terminus of each antibody chain.

3. Correct processing of both signal sequences, resulting in the same N-termini as in the original antibody molecule. The precise fusion of the signal sequence to the antibody molecule is necessary but not always sufficient for this to occur. Hence cleavage to produce the correct N-terminus must be confirmed experimentally.

4. In the periplasm, the two chains must fold to globular and soluble domains, intramolecular disulphide bonds must form and the two chains must assemble into the heterodimer with simultaneous oxidation of any intermolecular disulphide bonds.

This secretory system has a number of advantages over other expression systems. Firstly, the antibody fragments are produced in an assembled, functional form and hence there is no requirement for complex renaturation and refolding processes *in vitro*. Secondly, there are fewer proteases present in the periplasm compared to the cytoplasm and the folded globular domains with intrachain disulphide bonds are more resistant to protease attack. Thus the problems of proteolytic degradation found with cytoplasmic expression are greatly diminished. The correct *in vivo* assembly of the fragments also allows their purification directly by exploiting their antigen binding affinities using antigen affinity chromatography. Finally, from a process viewpoint, secretion to the periplasm is preferable over secretion to the medium because the specific release of periplasmic contents will result in lower volumes to be processed and potentially simpler purification protocols.

Potential problems associated with periplasmic expression include leakage of periplasmic proteins to the culture (Shibui and Nagahari, 1992; Harrison *et al.*, 1997; Pluckthun and Skerra, 1989) and the lysis of *E. coli* cells after long periods of antibody production (Somerville *et al.*, 1994). Such phenomena do not appear to be related to type of fragment being expressed (Fab, Fv or scFv), or the choice of signal sequence, however the host strain, plasmid and growth conditions (medium

composition, induction time and temperature) do appear to have an effect (Pluckthun and Skerra, 1989; Kipriyanov *et al.*, 1997).

Following the initial development of a periplasmic expression system by Skerra and Pluckthun, a wide variety of antibody fragments and antibody fusion proteins have been successfully produced by secretion to the periplasm of *E. coli*.

1.2.2.4 Secretion to the extracellular media

Secretion of a functional Fab to the extracellular media has also been reported by Better and co-workers (1988). Coding sequences for the heavy and light chain genes were placed in a single operon and the N-terminus of each chain was fused to the signal sequence of the bacterial *pel*B gene (pectate lyase) from *Erwinea carotova*. Pectate lyase is expressed at high levels in the periplasmic space of *E. coli*, however Fab fragments were released to the extracellular medium by an as yet unknown mechanism. 90% of the functional Fab was reported to be located in the culture medium rather than in the periplasmic space, however only very low levels of Fab were obtained (2 mg L^{-1}).

1.2.2.5 External cell surface expression

Successful expression of antibody fragments by fusion to outer membrane lipoproteins has also been reported. ScFv fragments have been expressed as a fusion to lipoprotein and ompA, resulting in 50 000-100 000 copies per cell (Francisco *et al.*, 1993). ScFvs have also been fused to the amino terminus of the peptidoglycan-associated lipoprotein (PAL) to direct cell surface expression (Fuchs *et al.*, 1991). Cleavage of the fusion proteins to release pure antibody fragments is required if such expression systems are to be used as a method of producing antibody fragments.

1.2.3 Fermentation strategies

1.2.3.1 Batch and fed-batch cultures

The large-scale production of foreign proteins in *E. coli* is influenced by a number of factors including strain selection, batch/fed-batch fermentation, temperature, composition of growth medium, the time and duration of induction and the nature of the protein being expressed. A range of antibody fragments have been produced in *E. coli* by fermentation and the use of both batch and high cell density fed-batch cultures has been investigated.

Batch fermentations generally result in low biomass concentrations and the titres of antibody fragments reported from such fermentations have varied from 40 mg L^{-1} (Berry *et al.*, 1994) up to 450 mg L^{-1} (King *et al*, 1993). Fed-batch fermentations have been used to increase cell density and hence also titres. Carter and co-workers (1992a) achieved titres of 1-2 g L^{-1} of functional cell-associated protein in a 10L fermenter using a fed batch protocol. A mineral salts media supplemented with digested casein and controlled carbon source feeding were used and gave a final cell density of 120 to 150 OD_{550}. Tight control of expression prior to induction was found to be crucial to achieving high cell densities and thus high expression titres. Conditions were optimised for high titres of functional cell associated Fab' and only low levels of Fab' (<100 mg L^{-1}) were found in the culture media.

A high cell density-fed batch fermentation of *E. coli* was also used by Horn *et al.*, (1996) to produce functional dimeric miniantibodies. Titres of 3 g L^{-1} were achieved using an optimised expression vector and high cell-density fermentation under non-limited growth conditions, with levels of biomass reaching 40 g L^{-1} by the end of the fermentation. No periplasmic leakage or cell lysis was observed during the fermentation.

For both batch and fed-batch fermentations good fermentation development is required to minimise potential problems such as substrate inhibition, limited oxygen transfer capacity and the formation of growth-inhibitory by-products.

Production of acetate is a common problem with *E. coli* cultures growing in the presence of excess glucose. A high concentration of acetate (above 5 g L^{-1} at pH 7) reduces growth rate, maximum attainable cell density and hence also product yield (Han *et al.*, 1992; Lee, 1996). Acetate formation depends on the strain, the medium and the specific growth rate and is generally greater in fed batch cultures than in batch cultures due to the extended culture period (Lee, 1996). One strategy for reducing acetate formation involves controlling the specific growth rate by limiting essential nutrients such as carbon and nitrogen (Korz *et al.*, 1995; Yoon *et al.*, 1993; Lee *et al.*, 1989). Alternatively carbon sources which do not directly produce acetate such as glycerol may be used (Holms, 1986). Lowering the temperature of the culture from 37°C to 26-30°C can also be used to reduce nutrient uptake and growth rate, hence also reducing cellular oxygen demand, the formation of toxic byproducts and generation of heat. Lowering culture temperature has the additional advantage of increasing the titres of soluble product for some recombinant proteins (Cabilly, 1989; Takagi *et al.*, 1988).

1.2.3.2 Development of growth media

The media selected for fermentations can affect both the yield of product and its location. Both complex and defined media have been used for antibody fermentations. Defined media are generally used to obtain high cell densities in fed batch culture as the nutrient concentrations are known and can be controlled during the fermentation (Pack *et al.*, 1993; Horn *et al.*, 1996). Complex media are more commonly used in batch fermentation and generally support higher specific growth rates (Shibui and Nagahari, 1992; Berry *et al.*, 1994). However nutrients in complex media can vary in composition and quality and hence fermentations are less reproducible.

The composition of the growth media during the induction period can have an effect on the expression of recombinant proteins. Overexpression of a protein often imposes a metabolic drain on the cell's energy, carbon and amino acid stores. This may result in reduced cell growth, increased plamsid instability and further physiological changes that reduce product yields. Provision of additional amino acids by supplementing the medium with casamino acids, peptone or yeast extract can significantly increase foreign protein expression and stability (Donovan *et al.*, 1996).

1.2.3.3 Induction strategies using the *lac* promoter

The *E. coli lac* promoter is one of the most commonly used promoters for regulating the expression of recombinant genes in bacteria as it is well understood and has been extensively characterised (Donovan *et al.*, 1996). A number of stronger promoters based on the *lac* system have been developed. These include the *lacUV5* promoter which contains a mutation in the *lac* consensus sequence that increases promoter strength (Reznikoff and Abelson, 1980), and the *tac* promoter, a hybrid of the tryptophan and *lac* promoters, which is reportedly 5-10 times stronger than the *lacUV5* system (Amann *et al.*, 1983).

The *lac* and associated promoters can be induced using isopropyl β-D-thiogalactoside (IPTG) or lactose. The *tac* promoter has the advantage of being lactose inducible while not being subject to catabolite repression (Donovan *et al.*, 1996). IPTG is the more commonly used inducer because it is not metabolised by the cell, hence the levels of IPTG in the growth media remain constant after induction and the effects of altering the IPTG concentration on foreign protein expression can be easily assessed. The high cost of IPTG however may limit its use in large-scale processes. In addition IPTG may be toxic to humans and consequently its presence as a contaminant in the final purified protein destined for therapeutic use is undesirable. Lactose is much cheaper than IPTG, however because it is metabolised by the cell, optimising induction conditions for maximum foreign protein expression is a much more complex procedure.

The induction process is a critical stage in the production of foreign proteins in *E. coli*. Inducer concentration, temperature, point of induction and duration of the induction phase can all influence the titres of recombinant protein obtained.

The majority of work that assesses the effect of induction conditions on yields of recombinant proteins from the *lac* and associated promoters uses IPTG as the inducer. A wide range of IPTG concentrations have been reported (0.005 to 5 $mmolL^{-1}$), however 1mmol IPTG L^{-1} is most commonly used (Donovan *et al.*, 1996). Shibui and Nagahari (1992) investigated the influence of IPTG concentration on secretion of a functional Fab in *E. coli*, and found that reducing the IPTG concentration from 1 mmol IPTG L^{-1} to 0.01-0.1 $mmolL^{-1}$ resulted in a 2-10-fold increase in the yield of secreted Fab.

Shibui and Nagahari (1992) also investigated the effect of induction temperature on Fab secretion. Yields of Fab were significantly increased by growing cultures at 30°C instead of 37°C. The formation of inclusion bodies is also less prevalent at lower temperatures. For example, Cabilly (1989) reported a 10-fold increase in yield of soluble cytoplasmic Fab fragments when cultures were grown and induced at 21°C instead of 37°C.

It is likely that reduced inducer concentration and lower temperatures enhance functional protein formation by reducing rates at which the protein is formed. Lower expression rates reduce the concentration of the unfolded intermediate in the cell, which allows the polypeptide chains to interact via the correct folding pathways rather than those leading to aggregation.

The use of lactose as an inducer has also been assessed in a small number of studies. Lactose has been shown to be as effective as IPTG for inducing recombinant calf prochymosin and tyrosine phenol lyase using the *tac* promoter (Foor *et al.*, 1993; Kapralek *et al.*, 1991). For the expression of calf prochymosin induction of a batch culture with lactose produced greater yields than induction with 1 mmol IPTG L^{-1}. High levels of product accumulated during late log and stationary phases with lactose

induction whereas recombinant protein was produced during the log phase of batch growth with IPTG.

A delayed response to induction with lactose was also observed in the production of hoof and mouth disease viral protein 1 under the control of the T7 phage promoter/polymerase system controlled by the *lac* promoter (Neubauer and Hofmann, 1994). For this system the optimal time for lactose induction was found to be just before the glucose was depleted from the medium in late log phase; the addition of lactose one hour later in the stationary phase produced poor yields of the target protein.

1.2.4 Effect of protein engineering on antibody fragment expression

The order in which the variable domains of scFv fragments are transcribed can effect expression titres (Tsumoto *et al.*, 1994). In studies examining the effect of domain order on expression levels of an anti-lysozyme scFv, V_L-linker-V_H was found to be more highly expressed than V_H-linker-V_L.

Similarly during the *E. coli* expression of Fab' antibody fragments, placing the light chain gene upstream of the heavy chain gene in a dicistronic operon enhanced both cell viability and the efficiency of antibody secretion (Weir and Bailey, 1997)

The level of secreted recombinant antibodies in *E. coli* is also influenced by the primary sequence of the antibody fragment (Knappik and Pluckthun, 1995; Forsberg *et al.*, 1997). Forsberg and co-workers studied the effect of specific framework residue substitutions on expression and location of a Fab-fusion protein in *E. coli*. A fifteen-fold increase in the level of product in the growth medium was achieved using only five light chain substitutions. In addition, the replacement of four residues on the heavy chain reduced cell lysis during the fermentation, thereby increasing retention of the product within the periplasmic space. It has been suggested that the major limiting step in the secretion of recombinant antibodies in *E. coli* is the periplasmic folding process. It is possible that the alteration of specific framework residues improves titres by improving the folding properties and solubility of the

antibody fragment and reducing the tendency for aggregation. Thus the molecular engineering of framework residues may provide a general method for increasing the expression titres of antibody fragments in *E. coli* and controlling product location.

1.2.5 Alternative host organisms for antibody fragment expression

A number of alternative host organisms are available for the expression of functional antibodies and antibody fragments. Examples include the bacteria *Bacillus subtilis*, which has been used for the expression of scFv fragments (Wong *et al.*, 1995; Wu *et al.*, 1998), and the yeast strains *Saccharomyces cerevisiae* and *Pichia pastoris*, which have been used for the expression of Fab and scFv fragments.

Better and Horwitz (1993) compared *Saccharomyces cerevisiae* with *E. coli* for the extracellular expression of Fab, Fab' and $F(ab')_2$ in 10L scale fermentations. The yeast system offered the advantages of constitutive expression and relatively few proteins in the culture supernatant other than the Fab' product, allowing more straightforward purification. However antibody yields from the yeast fermentation were found to be on average three-fold lower than yields obtained using *E. coli*. More recently *Saccharomyces cerevisiae* has been used for the expression of scFv fragments in shake flask culture, with titres of 20 mg L^{-1} active scFv achieved by a combination of expression level tuning and over-expression of folding assistants (Shusta *et al.*, 1998).

The methylotrophic yeast *Pichia pastoris* also provides a useful system for the high level expression of recombinant proteins (Fischer *et al.*, 1999). *Pichia* combines the advantages of a eukaryotic protein synthesis pathway with established techniques for genetic manipulation, an inducible expression system and a relatively straightforward fermentation utilising simple, inexpensive growth media. An additional advantage over *E. coli* as an expression host is the fact that yeast is generally recognised as a 'safe' organsim free of pyrogens and infectious viruses. A recombinant strain of *Pichia pastoris* has recently been developed, which secretes biologically active scFv into the culture supernatant at level of 1.2 g L^{-1} (Freyre *et al.*, 2000).

Insect cells offer an alternative to mammalian production systems for the expression of whole antibodies as they are capable of performing the majority of the cotranslational and post-translational processing carried out by other eukaryotic cells. Additional advantages include less complex growth medium, lower growth temperature, relatively easy scale-up and less expensive maintenance. Recent advances in the development of expression systems for the production of recombinant proteins in insect cell culture are reviewed by McCarroll and King (1997) and Pfeifer (1998).

Finally, an economical alternative for the large-scale production of antibodies and antibody fragments is the use of transgenic plants (Ma, 1995; Smith, 1996). Antibody processing in plants is also similar to the processing which takes place in mammalian cells. Antibodies and antibody fragments may be expressed in the cytoplasm or targeted for secretion by the use of a signal sequence. Secreted antibody accumulates in the apopastic fluid, which is a stable environment, allowing accumulation of the antibody product to high levels.

1.3 Recovery and purification of antibody fragments from *Escherichia coli* fermentation broths

1.3.1 Objectives of downstream processing

The objective of downstream processing is to recover and purify antibody fragments to an extent suitable for their intended use. Processing may be divided into a number of stages including primary recovery, purification, formulation and finishing. Typical methods employed in the primary recovery and purification stages are shown in Table 1.3.1.

STAGE	STEPS	TYPICAL METHODS
PRIMARY RECOVERY	EXTRACELLULAR PROTEINS: Cell removal (solid-liquid separation)	Centrifugation: tubular bowl, multichamber and disc-stack centrifugation Microfiltration: dead-end and cross-flow filtration
	CELL-ASSOCIATED PROTEINS: (a) Cell recovery (solid-liquid separation)	Centrifugation/Microfiltration
	(b) Cell disintegration	Mechanical: high pressure homogenisation and bead-milling Non-mechanical: physical methods (e.g. osmotic shock), chemical methods (e.g. chloroform addition) or enzyme lysis
	(c) Debris removal (solid-liquid separation)	Centrifugation/Microfiltration
PURIFICATION		Affinity chromatography Ion-exchange chromatography Hydrophobic interaction chromatography Gel filtration

Table 1.3.1 *Stages and methods involved in protein downstream processing. (Adapted from Lee, 1989).*

The methods and sequence of operations used in primary protein recovery depend on the final location of the antibody fragment. For extracellular fragments, the primary recovery stages involve the removal of cells from the medium. For fragments expressed in the periplasm or as intracellular inclusion bodies (cell associated antibody fragments), primary recovery generally involves (a) recovery of cells; (b) cell disruption or membrane permeabilisation to release the antibody fragments; and (c) removal of cell debris. For fragments expressed as inclusion bodies extensive solubilisation and renaturation stages are then required before the final purification stages can be employed.

Antibody purification generally involves one or more chromatography steps. Chromatographic separation techniques commonly used include affinity chromatography and ion exchange chromatography.

In the design of downstream processes it is important to consider the entire process before deciding on individual unit operations and operating conditions (Wheelwright, 1987). Methods employed in the early recovery stages can effect the efficiency of

later unit operations and the success of the primary recovery stages can have a significant effect on the success of the subsequent purification steps. A process must also be suitable for scale up and in the production of commercial proteins process efficiency is important. Recovery processes involving few steps generally have lower capital and operating costs and maintain a good yield of product. Increasing the number of steps increases product losses and therefore the aim is generally to minimise the number of steps and maximise the recovery at each stage (Ostlund, 1996).

1.3.2 Biomass Separation

1.3.2.1 Centrifugation

The removal of bulk *E. coli* biomass is a necessary operation in the recovery of antibody fragments from *E. coli* fermentation broth. For many processes separation of cells from the medium is the initial step in antibody recovery. Separation of cell debris resulting from homogenisation or cell spheroplasts following specific periplasmic release may also be required. Centrifugation is a widely used technique for solid-liquid separation and can be applied to the removal of whole cells, spheroplasts and cell debris from liquid streams (Lee, 1989). In addition centrifugation can be used in the separation of inclusion bodies from cell debris following homogenisation (Buchner and Rudolf, 1991).

Centrifugation takes advantage of the density difference between the solid and liquid phases. The density gradient is amplified through the application of centrifugal force by rotating the solid-liquid mixture at high speed. Pilot scale centrifuges are less effective than laboratory centrifuges for the separation of cells and cell debris from surrounding liquid because lower *g* forces and residence times are used.

In pilot and industrial scale biotechnology processes three different centrifuge designs are principally used; tubular bowl, multichamber and disc stack centrifuges. Multichamber centrifuges and the traditional tubular bowl machines require manual removal of solids and are operated batchwise, whereas disc stack centrifuges

discharge solids through a slots or nozzles in the bowl periphery and can be operated continuously. Dewatering however is less effective in a disc stack machine compared to tubular bowl and multichamber centrifuges.

Disadvantages associated with the use of centrifuges for the processing of recombinant proteins include aerosol production, high shear environment (which may result in damage to the product), incomplete biomass removal and high energy costs. Centrifuge theory and the use of disk stack and tubular bowl centrifugation for process stream clarification is discussed in more detail later in this work (Chapter 5).

1.3.2.2 Microfiltration

Microfiltration separates components according to their size and can be used to achieve essentially 100% removal of biomass from fermentation broths or homogenate. Microfiltration processes can be divided into two categories: dead-end filtration (feed stream flows perpendicular to the filter surface) and cross-flow filtration (feed stream flows parallel to the filter surface). Processes involving biomass removal are generally operated under cross-flow conditions as this reduces fouling of the membrane with suspended solids. Liquid retentate is recirculated around the apparatus and its concentration increases over time, however the moisture content of the final cell suspension is higher than can be achieved using dead-end filtration or centrifugation (Lee, 1989).

Both pore size and membrane composition are important in achieving good separation. Membrane pore sizes of 0.1-0.2 μm are typically used for the separation of cells or cell debris from fermentation broths and homogenates. Membrane composition is important as components of the solution can interact with the membrane surface causing fouling and reducing process efficiency. The commercial membrane modules, their properties and applications have been described (Brown and Kavanagh, 1987). The major filter designs include flat sheet (plate and frame or spiral configuration), hollow fibre, tubular and rotating filter units. Development of an effective and efficient microfiltration process will often require screening of a

number of filtration units as well as optimisation of solution conditions (pH and ionic strength) and operating conditions (cross-flow velocity and transmembrane pressure).

1.3.3 Release of cell associated antibody fragments

1.3.3.1 Mechanical cell disruption

The most commonly used methods for the disruption of microbial cells to release intracellular proteins at an industrial scale are high-pressure homogenisation (Hetherington *et al.*, 1971) and high-speed bead milling (Schutte *et al.*, 1983).

The most widely used cell disruption device in industry is the Manton-Gaulin APV homogeniser. During operation the cell suspension is forced at high pressure through an adjustable restricted orifice discharge valve. Disruption is thought to result from a number of mechanisms including shear, cavitation and impingement. Hetherington and co-workers (1971) analysed the disruption of Baker's yeast and found it to be proportional to the number of passes through the device and the operating pressure difference, raised to a characteristic power. Cell breakage may also be affected by temperature, valve unit design, organism, growth phase of cells and culture medium (Keshavarz Moore *et al.*, 1990; Sauer *et al.*, 1989). Operation at high pressures is generally desirable to increase the breakage efficiency for each pass. However, operation at high pressures and increased number of passes can produce very fine particles of cell debris which may reduce the efficiency of subsequent centrifugal clarification steps.

The advantages of homogenisation include continuous operation and low product hold up. In addition there is no requirement for outside chemicals which may affect product quality. Disadvantages include the release of large quantities of heat into the liquid stream and the possibility of mechanical failure and aerosol release.

High-speed bead milling is an alternative technique used for cell disruption (Schutte *et al.*, 1983). Bead mills consist of a vertical or horizontal cylindrical chamber containing a central motor driven agitator. The chamber is filled with the desired

amount of steel or ballotini glass beads, which provide the grinding action. Rate of cell breakage is affected by the size and concentration of beads, the type, concentration and age of cells, temperature, agitator speed, flow rate through the chamber and the arrangement of the agitator discs.

Bead milling is an efficient method of cell disruption and bead mills are well contained and resistant to blockage. Potential problems however include heat production due to impacts and friction between the grinding elements and contamination of the process stream with beads or ground glass ballotini.

1.3.3.2 Specific periplasmic release

The periplasmic expression of recombinant proteins in bacteria has a number of advantages over cytoplasmic expression for protein recovery and purification. The oxidative environment of the periplasm facilitates correct disulphide bonding and protein folding. Periplasmic product is less susceptible to protease attack as only 7 out of the 25 known *E. coli* proteases are located in the periplasm (Swamy and Goldberg, 1982). In addition the periplasm contains only 4-8% of total cell protein (Nossal and Heppel, 1966). Hence, the specific release of periplasmic contents without any contaminating cytoplasmic proteins or other intracellular material will result in lower volumes to be processed and will potentially simplify purification protocols. Complete cell disruption by homogenisation or high-speed bead milling nullifies these advantages of periplasmic expression. Complete cell disruption also exposes periplasmic proteins to cytoplasmic proteases, thus increasing the risk of proteolytic degradation. In addition such techniques may produce fine particles of cell debris which reduce the efficiency of subsequent centrifugal clarification.

Numerous laboratory scale techniques for the specific release of periplasmic material have been developed. These include physical methods such as osmotic shock (Nossal and Heppel, 1966; Zimmermann *et al.*, 1991), freeze/thaw (Johnson and Hecht, 1994), and heat treatment (Tsuchido *et al.*, 1985; Katsui *et al.*, 1982); chemical methods such as addition of Triton X-100 and guanidine (Naglak and Wang, 1990), chloroform (Ames *et al.*, 1984), EDTA (Ryan and Parulekar, 1991), tetradecyl

betainate (Ahlstrom and Edobo, 1994) and glycine treatment (Ariga *et al.*, 1989); and biological methods involving the use of lytic agents such as lysozyme (Neu and Heppel, 1964; Birdsell and Cota-Robles, 1967).

The most commonly used methods of periplasmic fractionation involve combinations of lysozyme/EDTA treatment and osmotic shock (French *et al.*, 1996; Pierce *et al.*, 1997). Lysozyme penetrates the outer membrane of *E. coli* when the cells are exposed to mild osmotic shock in the presence of EDTA. The EDTA chelates divalent cations in the outer membrane, increasing membrane permeability and allowing the lysozyme to penetrate and break down the peptidoglycan of the cell wall. This results in the release of the contents of the periplasm and the formation of spheroplasts. Various methodologies exist and for optimum lysis the balance of sucrose, Tris buffer, lysozyme and EDTA is important. In addition the phase of cell growth has been shown to have an effect on the success of periplasmic fractionation, with cells in exponential growth phase being more susceptible to osmotic shock and lysozyme treatment than stationary phase cells (Nossal and Heppel, 1966; Neu and Heppel, 1964).

Although a variety of methods based on osmotic shock and lysozyme/EDTA treatment have been developed for laboratory scale fractionation, these methods generally involve too many steps for an efficient large-scale recovery process. A simple two step fractionation method, involving enzymatic release and osmotic shock, has been developed by French *et al.*, (1996) for use at large scale.

A potential problem with the use of sucrose and lysozyme in large-scale periplasmic fractionation procedures is the effect on subsequent downstream processes. The presence of sucrose increases the viscosity of the processing stream, which may reduce the efficiency of centrifugation or microfiltration steps. Lysozyme will be expensive to use on a large scale and contamination of the process stream with lysozyme will increase the demands made on later purification stages. The effects of reducing the concentration of sucrose and lysozyme on periplasmic release have been analysed by Pierce *et al.*, (1997).

1.3.4 Purification

1.3.4.1 Affinity purification

Affinity chromatography is based on highly specific interactions between an immobilised ligand and the protein of interest and is commonly used in the purification of monoclonal antibodies and antibody fragments.

The affinity purification of antibody fragments can exploit a number of specific interactions including antibody-antigen interactions or the affinity of Staphylococcal protein A for immunoglobulins. If suitable quantities of the specific antigen are available, it can be immobilised and used to purify the antibody fragment in a single step (Skerra and Pluckthun, 1988). However the antibody-antigen interactions are often very strong and harsh elution conditions may be required to recover the antibody. Such conditions could effect antibody activity or result in elution of the entire antibody-antigen complex. A further disadvantage of this method is that scale-up is often limited by the quantity of specific antigen available.

An alternative method for antibody purification involves use of immobilised specific anti-immunoglobulin antibodies. For example Chester *et al.*, (1994) purified a chimeric Fab expressed in *E. coli* using an immobilised anti-human light chain antibody. Such techniques are more generic and do not interfere with the antigen binding activity of the antibody. However harsh elution conditions may still be required.

Affinity chromatography using immobilised Staphylococcal protein A is a well-documented method for the purification of whole monoclonal antibodies (Thommes *et al.*, 1996; Jagersten *et al.*, 1996). Protein A has two distinct binding sites on human immunoglobulins; it will bind to the Fc region of most IgG antibodies and has an additional binding site within the Fab region of certain immunoglobulins independent of their heavy chain isotype (Ibrahim *et al.*, 1993). The Fab site that binds protein A has been localised to the variable region of the Ig heavy chain (Randen *et al.*, 1993). This Fab mediated 'alternative binding' allows use of protein

A for the affinity purification of antibody fragments as well as whole antibodies. Elution conditions for recovery of antibodies or antibody fragments from protein A columns are mild and high levels of purity (close to 100%) are attainable. However leaching of protein A under such conditions has been observed (Lee *et al.*, 1986). Protein A affinity purification is discussed further in Chapter 6.

1.3.4.2 Facilitated affinity purification

The purification of antibody fragments may be facilitated by fusion to proteins or polypeptide chains possessing specific binding activities which can be utilised in affinity chromatography. For example Gandecha *et al.*, (1992) fused the Fc binding domains of Staphylococcal protein A to an scFv and utilised both binding activities of the fusion protein to purify it from *E. coli* fermentation broth.

The variable domains of antibody fragments have also been fused to the *E. coli* maltose binding protein MalE , and the binding properties of MalE used to facilitate purification of the antibody fragment by affinity chromatography on cross-linked amylose (Bregegere *et al.*, 1994).

Engineering histidine tails onto antibody fragments allows purification in a single step by immobilised metal affinity chromatography (IMAC; Skerra *et al.*, 1991; Pohlner *et al.*, 1993; Bentley *et al.*, 1998). Metal-affinity chromatography exploits the affinity for metal ions shown by functional groups on the surface of proteins. For example, the side chains of histidine residues will bind to Ni^{2+}, Zn^{2+}, Fe^{3+} and Cu^{2+} ions chelated by iminodiacetate (IDA) (Arnold, 1991). Advantages of IMAC include high protein capacities and relatively easy product elution and ligand regeneration. In addition the metal chelates used for IMAC are stable and can be recycled many times (Arnold, 1991). Pohlner *et al.*, (1993), engineered an Igase cleavage site between a His_6 peptide tail and the antibody fragment to allow enzymatic cleavage of the tail from the antibody fragment following purification by IMAC. The His_6 tail could then be removed from the protein solution by a second IMAC purification.

ScFv fragments have also been fused to the acidic protein calmodulin. Calmodulin binds specifically to certain peptides and organic ligands with high affinity in a calcium dependent manner. Thus there are three options for purifying an scFv calmodulin fusion; antigen affinity chromatography, anion exchange chromatography or calmodulin binding (Neri *et al.*, 1995).

1.3.4.3 Ion exchange chromatography

Ion-exchange chromatography has been used for the purification of antibody fragments renatured from inclusion bodies in *E. coli* (Buchner and Rudolph, 1991) and for the purification of Fab fragments secreted from *E. coli* cells (Mhatre *et al.*, 1995; Gavit *et al.*, 1992). Gavit and co-workers purified the Fab from *E. coli* fermentation broth, removing protein, endotoxin and DNA contaminants using a series of ion-exchange chromatography steps interspersed with membrane diafiltration or ultrafiltration stages.

Ion-exchange materials are relatively inexpensive and hence ion-exchange chromatography has good potential for scale-up. However the level of purification achieved is lower than for affinity chromatography. In addition the presence of high concentrations of salts in fermentation broth can significantly reduce the capacity of ion-exchange media for the desired product.

1.4 Bioprocess monitoring

The real time monitoring of product titres and location throughout a bioprocess sequence is essential for both rapid bioprocess development and effective process control. 'Real-time' or 'at-line' monitoring implies the acquisition of data regarding the state of a process within the time frame and vicinity of the bioprocess under analysis.

Currently many processes are operated 'blindly' with respect to the product of interest. Due to a lack of suitable assay procedures, the product is not directly quantified as the process is running. Process control is based on historic data or from

analysis of indirect variables such as broth optical density, pH or dissolved oxygen during fermentation and UV absorbance during chromatographic purification.

The variable nature of biological systems means such measurements do not always give a true reflection of the state of the process. If important process decisions are made incorrectly, large quantities of a high value pharmaceutical product could potentially be lost. For example, if a fermentation is harvested too early (before product titres have peaked) or too late (following product degradation or leakage of a periplasmic product into the medium) yields will be less than optimal. In cases of chromatographic purification where impurities are not always well-resolved from the product, the reliance on UV absorbance alone to determine which fractions to collect may result in the co-purification of unwanted product variants (such as aggregates) or contaminating non-product material, resulting in the requirement for additional purification steps.

The ability to monitor the specific product of interest during both production and purification can improve process efficiency by allowing process decisions to be made on a more informed basis. In addition, process monitoring allows more rapid process development, and can be used to ensure a process is functioning within established boundaries, as required by regulatory authorities for validation purposes.

Monitoring of product during fermentation is more difficult to achieve than during downstream purification because the complex components within fermentation broths often interfere with assay accuracy. Additional problems which need to be addressed before on-line fermentation monitoring can be employed include aseptic sampling, the occasional need to lyse cells prior to sample analysis and the removal of particulates.

1.4.1 Techniques available for bioprocess monitoring

Techniques developed for the real-time monitoring of specific protein products during fermentation and purification processes include chromatographic assays, biosensor analysis and flow-injection immunoassays.

1.4.1.1 Chromatographic assays

High performance liquid chromatography (HPLC) has been developed for the monitoring of monoclonal antibody production in a hybridoma cell culture (Paliwal *et al.*, 1993). The assay, which used protein A affinity chromatography to separate IgG from broth components followed by ultraviolet absorbance at 220 nm for antibody quantification, required only ~3 minutes to produce quantitative results.

HPLC has also been used for real-time monitoring and control of antibody loading during protein A affinity chromatography (Fahrner and Blank, 1999 (a and b)), and in the monitoring of product collection during preparative reversed-phase chromatography of recombinant human insulin-like growth factor-1 (IGF) (Fahrner *et al.*, 1998).

A particular advantage of HPLC is the ability to differentiate between the required product and variants such as misfolded or aggregated molecules (Fahrner *et al.*, 1998; Jacobsen *et al.*, 1997). However, fouling of the adsorbents and interference from other sample components, particularly during the analysis of fermentation samples or crude protein extracts, can limit assay rhobustness and accuracy.

1.4.1.2 Biosensors

A biosensor is an analytical device consisting of a biological 'receptor' (an enzyme, microorganism or antibody) coupled to an electronic transducer. The transducer converts a biological event (a physicochemical or biochemical change in the receptor) into an electrical signal by measuring voltage (potentiometric sensor), current (amperometric sensor), light (optical sensor), temperature (calorimetric sensor) or mass (piezo-electric sensor) (Schugerl *et al.*, 1996). Biosensor technology has been reviewed by Byfield and Abuknesha (1994). The review summarises the major types of biological molecules and systems on which biosensors can be based, provides a critical assessment of the relative strengths and weaknesses of the

respective technologies and analyses practical considerations such as sample interference, signal-to-noise ratio and biomolecule stability.

Optical biosensors have traditionally been used in the study of biomolecular interactions, for example in the determination of kinetic constants for the interaction between an antibody and its antigen (Karlsson *et al.*, 1991; Gill *et al.*, 1996). More recently biosensors have found application in the monitoring of bioprocesses, including the real time analysis of product accumulation during mammalian cell culture (Baker *et al.*, 1997) and microbial cell fermentation (Gill *et al.*, 1996; Gill *et al.*, 1998), and in the monitoring of chromatographic recovery of antibody fragments (Bracewell *et al.*, 1998).

The time required for a single biosensor assay is typically in the order 5-6 minutes (Baker *et al.*, 1997; Gill *et al.*, 1996). However, biosensor assays are also subject to interference from unknown components within complex bioprocess samples. In addition, discrepancies in the concentration of antibodies determined by ELISA and biosensor techniques have been observed (Baker *et al.*, 1997).

1.4.1.3 Flow-injection analysis

Flow-injection analysis (FIA) is a technique developed for the delivery of sample and buffers to a suitable analytical assay. FIA systems employ automated pumps and valves to control dilution and mixing of reagents before they are delivered to the 'analytical cell'.

A flow-infection immunoanalysis method for the on line monitoring of monoclonal antibodies has been described by Stocklein and Schmid (1990). The system combined a flow-injection module with immunoassays based on the principle of ELISA. The sample, assay reagents and wash buffers were pumped consecutively through a purpose-designed immunoreactor containing the immobilised capture species. The assay time varied between 15 and 25 minutes depending on the assay employed. The detection ranges for the various assays described were between 1 and 100 $\mu g\ mL^{-1}$ for mouse IgG, which is the range of interest for hybridoma cell culture.

An FIA module has also been used in conjunction with an optical biosensor for the real-time monitoring of breakthrough and elution during the chromatographic purification of antibody fragments (Bracewell *et al.*, 1998; Bracewell *et al.*, In preparation). Using the FIA regime the total biosensor assay turnaround time was reduced to ~30 seconds, and concentration data was provided within 10 seconds of sample addition to the sensing surface.

1.5 Project background

1.5.1 Industrial significance of anti p-185^{HER2} antibodies and antibody fragments

1.5.1.1 Development of anti p-185^{HER2} antibodies for cancer therapy

The HER2 protooncogene and p185^{HER2}, the growth factor receptor-tyrosine kinase it encodes, have been implicated in the pathogenesis of many human cancers including breast, lung and ovarian carcinomas. Amplification and/or overexpression of HER2 occurs in 25-30% of human primary breast and ovarian cancers and appears to contribute to cell transformation and tumour progression (Slamon *et al.*, 1989).

The p185^{HER2} receptor represents an attractive target for antibody based cancer therapies since its overexpression is unique to the malignant phenotype. Antibodies raised against p185^{HER2} may interfere with functioning of the receptor and so inhibit tumour growth, in addition to mediating antibody dependent cellular cytotoxicity and complement dependent cytotoxicity. A variety of p185^{HER2}-specific monoclonal antibodies have been developed and used for the delivery of drugs and plasmid DNA to HER2 overexpressing tumour cells in culture and in animal models (Rodrigues *et al.*, 1993).

A murine monoclonal antibody, mumAb4D5, directed against the extracellular domain of p185^{HER2} was initially developed and shown to specifically inhibit growth of p185^{HER2} overexpressing breast cancer cells in culture (Hudziak *et al.*, 1989). A

major limitation in the use of mumAb4D5 for cancer therapy is a human anti-mouse antibody response during treatment. Hence a recombinant, fully humanized version of 4D5 (humAb4D5) consisting of the mumAb4D5 antigen binding loops fused to the human variable domain framework residues and human IgG1 constant domains was developed (Carter *et al.*, 1992b). humAb4D5 was found to bind the extracellular domain of $p185^{HER2}$ 3-fold more tightly than the murine parent antibody and was almost as potent in specifically inhibiting the growth of human tumour cell lines overexpressing $p185^{HER2}$. humAb4D5, marketed under the name 'Herceptin', has recently received approval by the FDA for the treatment of breast cancer.

A variety of antibody fragments based on humAb4D5 have been designed and expressed in *E. coli*. These include Fab' fragments (Carter *et al.*, 1992a), thioether linked $F(ab')_2$ (Rodrigues *et al.*, 1993) and linear $F(ab')_2$ comprising tandem repeats of the heavy chain Fd fragment (V_H-C_H1-V_H-C_H1) and associated light chains (Zapata *et al.*, 1995). The thioether linked $F(ab')_2$ and linear $F(ab')_2$ are more stable and have longer serum permanence time compared to single disulphide linked $F(ab')_2$. Linear $F(ab')_2$ is also simpler to prepare than disulphide or thioether linked $F(ab')_2$ fragments and may be suitable for clinical applications as potentially immunogenic or mutagenic linkers are not required for attachment of the two F(ab') arms. Bispecific anti-p185/anti-CD3 $F(ab')_2$ fragments (Shalaby *et al.*, 1992) and anti-p185/anti-CD3 diabodies (bispecific $(scFv)_2$ fragments) (Zhu *et al.*, 1996) have also been developed. These target cytotoxic human T lymphocytes to tumour cells overexpressing $p185^{HER2}$.

1.5.1.2 *E. coli* expression and production of a humanised 4D5 Fab' antibody fragment

An expression system for the production of large quantities of soluble and functional humAb4D5 Fab' fragments from *E. coli* was developed by Carter and co-workers (1992a). The Fab' version of humAb4D5 consists of the Fab fragment with the hinge residues (CysAlaAla) added to the carboxy terminus of the heavy chain C_H1 domain. The cysteine provides a thiol group for conjugation to other antibody fragments, liposomes or drugs. A hinge sequence with a single cysteine was used to avoid intra-hinge disulphide bonding which may occur with hinges containing multiple

cysteines. The plasmid pAK19 was designed to express the light and heavy chain Fd' fragment of humAb4D5 from a synthetic dicystronic operon under transcriptional control of the *E. coli* alkaline phosphatase (*pho A*) promoter. Each antibody chain was preceded by the *E. coli* heat stable enterotoxin II (stII) signal sequence which directs secretion to the periplasmic space.

Using this expression system, Carter *et al.*, (1992a) have routinely obtained titres of 1-2 g L^{-1} cell associated soluble and functional Fab' using a fed-batch protocol in a 10 litre fermenter. A mineral salts medium and controlled carbon source feeding were used to obtain cell densities of 120 to 150 OD_{550}, and induction was achieved by phosphate starvation at a cell density of 80-100 OD_{550}. Tight control of Fab' expression prior to induction and precise control of the fermentation environment were found to be crucial to achieving high cell densities and hence high product titres. Under conditions which were optimised for high titres of functional cell-associated Fab', only low quantities of Fab' (<100 mg L^{-1}) were found in the culture media.

The humAb4D5 Fab' was extracted from cell pastes by lysozyme digestion of the periplasm wall and purified by Streptococcal protein G affinity chromatography. Simple osmotic shock was found to be inefficient in releasing Fab' fragments from the cell paste. humAb4D5 Fab' was also found to bind tightly to Staphylococcal protein A, allowing its use for affinity purification in place of protein G.

1.5.1.3 Development of anti-p185^{HER2} immunoliposomes for cancer therapy

Anti-p185^{HER2} immunoliposomes have been developed as a tumour-targeting vehicle in which the anti-p185^{HER2} specificity and inhibitory activity of humAb4D5 are combined with the pharmacokinetic and drug delivery advantages of liposomes (Park *et al.*, 1995). Fab' fragments of humAb4D5 were conjugated to maleimide terminated lipids within the lipososmes via the free thiol group in the Fab' hinge region. Fab' fragments were used firstly because of the high expression levels of humAb4D5 Fab' obtained in *E. coli* (Carter *et al.*, 1992a) and secondly because the free hinge thiol

group provides a singular site for covalent attachment to liposomes away from the antigen binding site and ensures correct orientation of the conjugated Fab'.

Empty immunoliposomes were shown to bind specifically to and inhibit the growth of $p185^{HER2}$-overexpressing breast cancer cells *in vitro*. The binding affinity of the immunoliposomes was comparable to that of free humAb4D5 Fab' and the intact antibody. The antiproliferative effect of liposome-associated Fab' was markedly greater than that of free humAb4D5 Fab', indicating that liposomal anchoring of these anti-$p185^{HER2}$ fragments enhances their biological activity, probably by increasing their avidity. Anti-$p185^{HER2}$ immunoliposomes loaded with the cytotoxic drug doxorubicin were also shown to be markedly and specifically toxic against $p185^{HER2}$ overexpressing cells *in vitro* and were able to deliver doxorubicin to tumours *in vivo*.

1.5.2 4D5 Fab' expression in *E. coli*: A model experimental system

In the following study expression of the 4D5 Fab' antibody fragment in *Escherichia coli* will be used as an experimental system for the study of antibody fragment production and purification processes. The expression vector, constructed by researchers at Celltech Chiroscience Limited (Slough, UK), utilises a *tac* promoter for the inducible expression of 4D5 Fab', and an *ompA* signal sequence to direct secretion of each chain to the periplasmic space. The standard route for the purification of 4D5 Fab' involves specific periplasmic release, process stream clarification by centrifugation and filtration, and Fab' purification by packed bed protein A affinity chromatography.

1.6 Project objectives

Due to the increasing commercial demand for antibody fragments and antibody-based molecules there is a requirement for the development of efficient, low cost production processes. Effective process design requires both rapid process development to minimise the time to market and successful process integration to ensure efficient process operation. This project uses a model *Escherichia coli*

expression system to study novel process options for the production of antibody fragments and to assess recently developed techniques designed to facilitate process design, integration and control.

Through the development and characterisation of a whole bioprocess sequence from fermentation to purification, this project aims to:

- Investigate the ability to control product location during fermentation to allow improved process integration.
- Assess the utility of modelling and scale-down techniques for the prediction of process scale operation.
- Apply an optical biosensor system to the real-time monitoring of a bioprocess and compare with more traditional off line monitoring techniques.
- Characterise novel processing strategies and use a mass balance approach to compare such strategies with more traditional process routes.

1.6.1 Thesis layout

The following chapters describe the experimental work performed during this study and present the results obtained and conclusions drawn. Chapter 2 details the materials and methods for the whole project. The experimental results are presented in chapters 3-7. Each results chapter has an introduction which describes the objectives of the work and gives the necessary background information or theory, a results and discussion section and a summary highlighting the major points arising from the work. Within the results and discussion sections, the relevant experimental protocols described in the Materials and Methods chapter are referred to. To facilitate flow and understanding, the relevant experimental methods have also been summarised within the results where considered appropriate.

Chapter 3 describes an *Escherichia coli* fermentation process designed for the periplasmic expression of the 4D5 Fab' antibody fragment. Modifications made to the fermentation protocol to improve control of product location are detailed and the suitability of such a protocol for large-scale operation is assessed.

In Chapter 4, the development and characterisation of a novel periplasmic extraction process designed for the specific release of periplasmic material is described. The effect of operating conditions and the use of different feed material on process yields and quality of the material produced are investigated. The extraction process is also modelled using simple first order kinetics and the effect of scale up on kinetic parameters is determined.

Chapter 5 compares a tubular bowl and a disk stack centrifuge for the clarification of *E. coli* spheroplast suspensions. The ability of current scale-down techniques to predict the clarification performance of an industrial centrifuge is also investigated.

In Chapter 6 an expanded bed adsorption process for the recovery of antibody fragments from unclarified *E. coli* periplasmic extracts is compared to the more traditional method of packed bed purification from clarified feed streams. A method is also described which enables prediction of the 'ideal' operating conditions for the maximisation of both process yield and matrix utilisation.

Chapter 7 describes the development and characterisation of ELISA and biosensor assays used for the quantitative analysis of antibody fragments during this project. The suitability of the biosensor as a technique for rapid bioprocess monitoring to allow both improved process control and faster process development is assessed. The work described was performed throughout the three years and draws on results from a number of areas of the project. For this reason this section of work has been placed at the end of the results chapters, however the ELISA assay forms an integral part of all work previously described.

Chapter 8 essentially summarises results of the studies of individual unit operations by comparing process alternatives for the purification of antibody fragments from *E. coli* fermentation broth. The processing factors which require consideration when designing a purification scheme are discussed, and a selection of process alternatives for Fab' purification are compared on the basis yield, purification and operating time.

Finally, the main findings of the work are summarised in Chapter 9 and suggestions for future work are given in Chapter 10.

2. MATERIALS AND METHODS

All reagents were purchased from BDH Chemicals (Merck Ltd., Lutterworth, Leicestershire, UK) except where otherwise stated and were of the highest grade available.

2.1 Fermentation

2.1.1 Bacterial strain and plasmid

W3110 (wild type *E. coli,* ATCC 27325) transformed with the plasmid pAGP-4 was used for all fermentations. The strain and plasmid were kindly provided by N. Weir (Celltech Chiroscience Ltd., Slough, UK). The plasmid pAGP-4 encoded the chloramphenicol resistance gene (Cm) and the 4D5 Fab' antibody fragment directed against the extracellular domain of $p185^{HER2}$ and derived from humAb4D5 (Carter *et al.*, 1992b; Kelley *et al.*, 1992). Coding sequences for the Fab' light chain and heavy chain Fd' fragment were arranged in a dicistronic operon under transcriptional control of the *E. coli tac* promoter inducible by addition of isopropyl-β-D-thiogalactopyranoside (IPTG) or lactose. Each antibody chain was preceded by the *E. coli omp A* signal sequence to direct secretion to the periplasmic space. The 4D5 Fab' expression plasmid is illustrated in Appendix 1.

2.1.2 Stock maintenance

Glycerol stocks were prepared from colonies grown on defined medium agar plates (see section 2.1.3.4). Plates were inoculated from previous -70°C stocks using a sterile loop, and were then incubated at 30°C until a suitable level of growth was obtained. The cells were aseptically transferred from the plate by pipetting 3 mL of sterile 50% (v/v) glycerol onto the plate, scraping the cells from the surface and then re-pipetting the cell suspension into a sterile bijou. The glycerol stocks were stored at -70°C and were used only once before being discarded. This approach avoided the repeated sub-culturing of cells on nutrient agar, which can lead to the cells' inability to grow on defined medium.

2.1.3 Culture media

2.1.3.1 Complex medium

The complex medium used for agar plates and shake flask cultures was 2xYT medium (Sambrook *et al.*, 1989). The composition of this medium is (g L^{-1}): tryptone, 16; yeast extract, 10; NaCl, 5. (Tryptone and yeast extract were obtained from Oxoid, Unipath Ltd., Baisingstoke, UK). The pH of the medium was adjusted to 7.0 with 4M NaOH prior to autoclaving. Chloramphenicol was filter sterilised into the sterile media using a 0.2 μm syringe filter, giving a final antibiotic concentration of 30 μg mL^{-1}.

2.1.3.2 Defined medium for low cell density fermentations

The defined medium used in low cell density fermentations had the following composition (g L^{-1}): $(NH_4)_2SO_4$, 5; NaH_2PO_4, 6.25; KCl, 3.87; $MgSO_4.7H_2O$, 0.717; citric acid, 4; trace elements, 1 mL L^{-1}; polypropylene glycol (PPG, 25% v/v), 1 mL L^{-1}; glucose, 2.5% (w/v); chloramphenicol, 30 μg mL^{-1}.

The trace element solution was composed of (g L^{-1}): Citric acid, 10; $CaCl_2.6H_2O$, 0.5; $ZnSO_4.7H_2O$, 0.246; $MnSO_4.4H_2O$, 0.2; $CuSO_4.5H_2O$, 0.05; $CoSO_4.7H_2O$, 0.0427; $FeCl_3.6H_2O$, 0.967; H_3BO_3, 0.003; NaMoO4 0.0024.

The glucose (50% w/v solution) and $MgSO_4.7H_2O$ were autoclaved separately, and the chloramphenicol was filter sterilised (0.2 μm syringe filter) into the combined glucose and $MgSO_4$ mixture immediately prior to addition to the shake flask or fermenter. The rest of the salts were sterilised in the fermenter at 121°C for 20 minutes.

2.1.3.3 Defined medium for high cell density fermentations

The defined medium used in high cell density fermentations had the following composition (g L^{-1}): $(NH_4)_2SO_4$, 5; NaH_2PO_4, 2.88; KCl 3.87; $MgSO_4.7H_2O$, 0.717; citric acid, 4; trace elements, 1 mL L^{-1}; PPG (25% v/v), 1 mL L^{-1}; glycerol, 3% (w/v); chloramphenicol, 30 μg mL^{-1}.

The trace element solution had the same composition as for low cell density fermentations (section 2.1.3.2).

$MgSO_4.7H_2O$ was autoclaved separately, and the chloramphenicol was filter sterilised (0.2 μm syringe filter) prior to addition to the shake flask or fermenter. The glycerol was sterilised in the fermenter with the rest of the salts (121°C for 20 minutes).

2.1.3.4 Agar plates

Agar plates were prepared using complex or defined media solidified with bactoagar (Oxoid) added to a concentration of 1% (w/v).

2.1.4 General Fermentation Protocols

2.1.4.1 Fermenters and associated equipment

Fermentations were carried out using four scales of fermenter; 7L, 20L, 150L and 450L. The 450L vessel was manufactured by Chemap (Alpha Laval Engineering Ltd., Middlesex, UK). All other fermenters were supplied by LH Fermentation (Inceltech UK Ltd., Berkshire, UK). Dissolved oxygen tension (DOT) and pH were measured using Ingold electrodes (Ingold, Leicester, UK). The pH probe was calibrated using standard buffer solutions and the DOT probe was calibrated against a nitrogen zero. Fermenter exit gases were monitored by mass spectrometry (MM8-80 Instrument,

VG Gas Analysis Ltd., Middlewich, UK). Exhaust gas compositions and data from the probes were logged using the software packages Real Time Data Acquisition Systems (RTDAS) or Propac (450L fermentation only). Both software packages were supplied by Acquisition Systems Ltd., Sandhurst, UK.

2.1.4.2 Inoculum preparation

The initial working volumes and volumes of inoculum cultures used at each scale of fermentation are given in Table 2.1.1. Seed cultures for the 150L and 450L inoculums were prepared as shown in Table 2.1.2.

Fermenter	Initial working volume (L)	Inoculum volume (L) (% v/v)	Inoculum vessel
LH 7L	4	0.1 (2.5)	Shake flasks (1L)
LH 20L	8	0.2 (2.5)	Shake flasks (1L)
	10	1 (10)	Shake flasks (2L)
LH 150L	87	5 (6)	LH 7L
Chemap 450L	260	15 (6)	LH 20L

Table 2.1.1 *Initial working volume and inoculum volume used with each fermenter.*

Fermenter	Inoculum vessel	Inoculum volume (L)	Volume of seed for inoculum (L) (% v/v)	Seed vessel
LH 150L	LH 7L	5	0.4 (8)	Shake flasks (2L)
Chemap 450L	LH 20L	15	1.6 (10)	Shake flasks (2L)

Table 2.1.2 *Volume of seed cultures used in preparation of inoculum for 150L and 450L fermentations.*

Shake flask cultures used in inoculum preparation were themselves inoculated with colonies from agar plates. Complex medium agar plates containing 30 μg mL^{-1} chloramphenicol were streaked from a single glycerol stock and incubated for 24 hours at 30°C in a standard microbial incubator (New Brunswick Scientific Ltd., North Mymms, UK). Cells from the 24 hour plates were resuspended in sterile water and used to inoculate shake flasks containing either complex or defined medium (with antibiotic) at a working volume of 10%. Flasks were incubated in orbital shakers (G25 Incubator Shaker, New Brunswick Scientific) at 30°C and 250 rpm for

24 hours before being used to inoculate the appropriate fermenter. Inoculum cultures for the 150L and 450L fermentations were grown to an OD_{600} of ~6 prior to inoculation of the production fermenter.

2.1.4.3 General fermentation parameters

pH was maintained at 6.95 using 15% ammonia solution (1:1 dilution of 30% ammonia with RO water) and a 1 in 20 dilution of concentrated sulphuric acid. Foaming was controlled by the addition of sterile antifoam (25% v/v PPG). Stirrer speed and air flow rates were increased manually as required to maintain levels of dissolved oxygen where possible above 20%.

2.1.4.4 Low cell density fermentations

Low cell density fermentations utilised the medium described in section 2.1.3.2. All fermentations were carried out at 30°C using an inoculum volume of 2.5% (v/v). The growth of cultures was followed by monitoring the OD at 600nm. At an OD_{600} of 20 glucose and lactose were added to give concentrations in the fermenter of 1% (w/v) glucose and 6% (w/v) lactose (concentrations are based on the *initial* fermenter working volume). Glucose was added as a 50% (w/v) solution in RO water following sterilisation by autoclaving. Lactose was also added as a 50% (w/v) solution in RO water. The solution was not autoclaved prior to addition but had to be boiled to allow the lactose to fully dissolve. At an OD_{600} of ~30 glucose was exhausted and cells switched to lactose metabolism, thereby inducing expression of 4D5 Fab'.

2.1.4.5 High cell density fermentations

For high cell density fermentations the medium described in section 2.1.3.3 was used. The inoculum volume was varied between 6% (v/v) and 10% (v/v), depending on the vessel used (Table 2.1.1). Culture growth was followed by monitoring the OD at 600nm. The growth temperature was initially maintained at 30°C and was reduced to

27°C at an OD_{600} of 40. The following additions were also made at the specified OD_{600}:

15 OD	30 g L^{-1} glycerol
35 OD	20 g L^{-1} glycerol
40 OD	$MgSO_4.7H_2O$, 14.4 mM final concentration
	$CaCl_2.6H_2O$, 1.7 mM final concentration
50 OD	10 g L^{-1} glycerol
	45 g L^{-1} lactose

Further lactose was added in 45 g L^{-1} batches as required (lactose depletion was detected by a sharp increase in DOT and concomitant decrease in oxygen uptake rate (OUR) and carbon dioxide evolution rate (CER)).

In all HCD fermentations, additions were made accounting for the increase in total liquid volume. Glycerol was added as an 80% (w/w) solution in RO water. $MgSO_4$ and $CaCl_2$ were each dissolved in a minimal volume of RO water and added separately to avoid precipitation. The salts and glycerol were autoclaved prior to addition. Lactose was added as a 50% (w/w) solution in water; the solution was boiled prior to addition to allow the lactose to fully dissolve. Due to problems dissolving and maintaining large quantities of lactose in solution at scale, lactose for the 450L fermentation was dissolved at a concentration of 75% (w/v). Also, due to foaming problems at 450L, additional lactose shots were added in batches of 22.5 g L^{-1}.

2.1.5 Fermentation harvest

The CARR P6 Powerfuge (CARR Separations Inc, Franklin, MA) and the Sharples model AS26 (Alfa-Laval Engineering Ltd, Camberly, UK) were used for the harvest of cells from fermentation broth.

Details of the centrifuge and operating conditions for each cell harvest are given in Table 2.1.3.

Fermentation	Centrifuge used for cell harvest	Operating speed	Operating flow rate
HCD 4 (10L)	CARR P6 Powerfuge	15 300 rpm (20 000g)	30 Lhr^{-1}
HCD 5 (10L)	CARR P6 Powerfuge	15 300 rpm (20 000g)	10 Lhr^{-1}
150L 2	Alfa-Laval AS26	17 000 rpm (19 000g)	60 Lhr^{-1}
450L	Alfa-Laval AS26	17 000 rpm (19 000g)	60 Lhr^{-1}

Table 2.1.3 *Centrifuges and associated operating conditions employed for the harvest of cells from fermentation broth.*

Feed was pumped through the centrifuges using a Watson Marlow 605 Di Peristaltic pump (Watson Marlow Ltd., Falmouth, UK).

2.2 General analytical techniques

2.2.1 Fractionation procedure for fermentation samples

The following procedure was used to produce extracellular and periplasmic fractions for determination of antibody fragment concentration in fermentation samples.

1 mL samples from fermenter cultures were chilled on ice for 5 minutes. Cells were harvested by centrifugation in a microfuge (13 000 rpm/~14 000g for 5 minutes) and the supernatant collected as the extracellular fraction. The pellet was resuspended in 1 mL periplasmic extraction buffer (100mM Tris HCl pH 7.4, 10 mM EDTA) and samples were incubated overnight with shaking at 30°C. Following overnight incubation spheroplasts were pelleted in a microfuge (13 000 rpm, 5 minutes) and the supernatant collected as the periplasmic fraction. Periplasmic and extracellular fractions were stored at -20°C until ELISA analysis could be performed.

2.2.2 Biomass measurements

2.2.2.1 Optical density

The biomass of fermentation samples was estimated by spectrophotometry (DU-® Spectrophotometer, Beckman Instruments (UK) Ltd., High Wycombe, UK). The

absorbance of a suitable dilution of the sample was measured at 600nm using RO water as a blank (samples were diluted so that the measured OD was <0.8).

2.2.2.2 Dry cell weight determination

For dry cell weight determination, 1 mL samples were spun for 5 minutes at 13 000 rpm in a pre-weighed Eppendorf tube and the supernatant was discarded. Samples were resuspended in RO water and re-spun to rinse off extracellular protein. Cell pellets were then dried to constant weight at 105°C.

2.2.3 Analysis of total protein

2.2.3.1 Bradford assay

Protein concentration was determined by the Bradford (1976) assay technique, using Coomassie Plus assay reagent (Pierce and Warriner (UK) Ltd., Chester, UK) and Bovine Serum Albumin (BSA) protein (Pierce and Warriner) as the standard. Dilutions of BSA in the range 0.1-1.0 mg mL^{-1} were prepared. Samples were also diluted to a concentration of 0.1-1.0 mg mL^{-1}. 150 μL of the assay reagent was added to 5 μL of sample or standard on a microtitre plate. Colour was left to develop for 5 minutes and the A_{595} measured using a Dynatech MR 7000 microplate reader (Dynex Technologies, Billingshurst, UK). Protein concentrations of the samples were determined from a calibration curve of A_{595} vs BSA concentration prepared on each microtitre plate. The Bradford protein assay allows determination of protein concentration to within ± 5%.

2.2.3.2 SDS-PAGE

SDS-PAGE was performed using a dual mini-lab system (Atto System AE 6400, Genetic Research Instruments Ltd, Dunmow, UK) according to the method of Laemmli, (1970). 12% acrylamide gels were used for the resolution of protein bands and were prepared as shown in Table 2.2.1.

STOCK SOLUTION	RESOLVING GEL COMPOSITION (mL)	STACKING GEL COMPOSITION (mL)
Acrylamide - bisacrylamide (30:0.8 % w/v)	6.25	1.25
Resolving gel buffer	1.88	-
Stacking gel buffer	-	2.5
Water	7.1	6.1
10% SDS	0.150	0.100
10% ammonium persulphate	0.225	0.150
TEMED	0.015	0.015

Table 2.2.1 *Composition of 12% acrylamide gels used for SDS-PAGE analysis of protein solutions.*

All stock solutions were prepared and stored as described by Hames and Rickwood (1990). Resolving gel buffer comprised 3.0 M Tris HCl (pH 8.8) and stacking gel buffer comprised 0.5 M Tris HCl pH 6.8. The volumes shown are sufficient for the preparation of two 12% acrylamide gels.

Samples for electrophoresis were prepared by dilution in a 1:1 ratio with sample buffer (60mM Tris-HCl pH6.8, 10% glycerol, 2% SDS, and 0.001% Bromophenol blue) and boiling for 5 minutes. A suitable volume of sample (up to 20µl) was loaded into the sample wells. Gels were run in reservoir buffer (0.025M Tris, 0.192M glycine, 0.1% SDS pH 8.3) at a voltage of 8 V/cm gel (stacking gel) and 15 V/cm gel (resolving gel).

Low molecular weight markers (Amersham Pharmacia Biotech, St. Albans, UK) were used for estimation of molecular weight of protein bands and were prepared according to manufacturer's instructions. The sizes of the low molecular weight markers used are given in Table 2.2.2.

COMPONENT	M.W. (Da)
Phosphorylase b	97 400
Serum albumin	66 200
Ovalbumin	45 000
Carbonic anhydrase	31 000
Trypsin inhibitor	21 500
Lysozyme	14 400

Table 2.2.2 *Low molecular weight marker proteins for SDS-PAGE.*

Gels were stained with 0.1% (w/v) Coomassie Brilliant Blue R-250 (Bio-Rad Laboratories, Hemel Hempstead, UK) in a solution of 50% water, 40% methanol and 10% acetic acid. Gels were stained for 1 hour and then transferred to destain solution (50% water, 40% methanol, 10% acetic acid) until protein bands became visible.

2.2.4 Glucose-6-phosphate dehydrogenase (G-6-PDH) assay

G-6-PDH is a cytoplasmic enzyme in *E. coli* and as such was used as a marker for cell breakage. G-6-PDH catalyses the following reaction:

Glucose-6-phosphate + $NADP^+$ $\Leftrightarrow$ 6-phosphogluconolactone + NADPH + H^+

NADPH, but not $NADP^+$, absorbs at 340nm. Hence G-6-PDH activity can be determined by following the production of NADPH spectrophotometrically.

An assay mixture was prepared, composed of 3 mM glucose-6-phosphate (Sigma Chemical Company, Poole, UK), 0.4 mM $NADP^+$ (Sigma), 7mM $MgCl_2$ and 50 mM Tris HCl pH7.5. 50µL sample (diluted appropriately) was added to 1 mL assay mix at 25°C and the rate of absorbance change at 340nm recorded. Enzyme activity was then determined from the equation:

$$\text{Activity (in enzyme units)} = \frac{\Delta OD_{340}}{\Delta t}\left[\frac{1}{E}\right]\left[\frac{V}{v}\right]D \qquad \textbf{(2.1)}$$

Where:

Enzyme units	= µmol (substrate converted) $min^{-1}mL^{-1}$
$\frac{\Delta OD_{340}}{\Delta t}$	= rate of change in absorbance at 340nm (OD units/ time)
E	= extinction coefficient (NADPH = 6220 OD units for a Molar solution)
V	= Total volume in cuvette (mL)
v	= volume of sample in cuvette (mL)
D	= dilution factor

2.2.5 Measurement of viscosity

Liquid viscosity was measured using a Rheomat 115 viscometer (Contraves Industrial Products Ltd, Middlesex, UK) fitted with a double gap, cup and bob measuring system. The measuring bob was rotated at 15 pre-set speeds from 5 to 780 rpm, producing shear rates over the range 24.3 s^{-1} to 3680 s^{-1}. The corresponding shear stress for each speed was recorded. Sample viscosity was determined from the gradient of the linear regression of shear stress against shear rate. The measuring system was maintained at a constant temperature using a Haake re-circulating glycol/water bath (Haake, Germany).

2.3 Analysis for quantification of antibody fragments

2.3.1 ELISA

NUNC 96 well maxisorp immunoplates (Life Technologies Ltd., Paisley, UK) were coated overnight at 4°C with HP6045 (a mouse antihuman monoclonal antibody supplied by Celltech Chiroscience Ltd) at 2 μg mL^{-1} in phosphate buffered saline (PBS, 10mM phosphate, 145 mM NaCl). After washing 4x with PBS containing 0.05% (v/v) Tween-20, serial 1 in 2 dilutions of samples and standards were performed on the plate in 100 μL of sample/conjugate buffer (100 mM Tris HCl pH 7, 100 mM NaCl, casein 0.2% (w/v), Tween-20 0.0002% (v/v)), and the plate was placed on a rocker (Luckman 4RT rocking table, Denley Instruments Ltd, Billinghurst, UK) at room temperature for 1 hour. The wash step was repeated, 100 μL of the revealing antibody GD12 peroxidase (The Binding Site Ltd., Birmingham, UK) was added, diluted 1 in 2000 in sample/conjugate buffer, and the plate again incubated on a rocker at room temperature for 1 hour. After further washing, 100 μL of substrate solution was added, consisting of 0.1 M sodium acetate/citrate pH 6, 100 μg mL^{-1} TMB, H_2O_2 0.02% (v/v)). The A_{630nm} was recorded with a Dynatech MR 7000 microplate reader (Dynex Technologies, Billingshurst, UK) after 4-6 minutes. The concentration of Fab' was determined from a standard curve prepared each time the ELISA was performed.

2.3.2 Biosensor analysis

2.3.2.1 The sensor

The IAsys optical biosensor (Affinity Sensors, Cambridge, UK), which employs a resonant mirror (Cush *et al.*, 1993), was operated according to the 'user documentation' supplied with the instrument. The resonant mirror is assembled within a disposable cuvette which has a working volume of 200 µL. During operation the instrument temperature was controlled at 25°C and the contents of the cuvette mixed with a micro stirrer. The instrument was controlled using a Microsoft Windows™ based package supplied by the manufacturers. Binding interaction profiles were analysed by linear regression to determine the initial rate of binding using the Fastfit software programme also supplied by Affinity Sensors.

2.3.2.2 Ligand Immobilisation

The biosensor capture species (protein A (Sigma) or HP6045) was immobilised onto the sensing surface of cuvettes derivatised with a coating of carboxymethyl dextran (CMD). Covalent coupling of the ligand to CMD was achieved through the formation of amide linkages between carboxyl groups on the dextran and amino groups on the protein.

After placing the cuvette in the instrument, 200 µL PBS/T (10mM phosphate, 2.7 mM KCl, 138 mM NaCl, 0.05%(v/v) Tween-20, made by dissolving one PBS/T sachet (Sigma) in 1 L RO water) was added and the response followed for 5 minutes to establish an initial baseline. Buffer was removed from the cuvette by aspiration. The carboxymethyl groups on the dextran coating of the cuvette were activated over a period of 8 minutes by addition of a solution of 400 mM 1-ethyl-3-(-3 dimethylamino propyl) carbodiimide (EDC, Sigma) and 100 mM N-hydroxysuccinimide (NHS, Sigma). Following activation the cuvette contents were replaced with PBS/T and the instrument response followed for a further 3 minutes to establish a pre-immobilisation baseline. Immobilisation was then initiated by

addition of ligand at the appropriate concentration (protein A, 30 μg mL^{-1}, HP6045 250 μg mL^{-1}), in 10 mM acetate buffer (pH 5.0). After 5 minutes the solution was replaced with 1 M ethanolamine (Affinity Sensors) to quench residual NHS ester activated carboxymethyl groups. Following 2 minutes incubation the ethanolamine was replaced with PBS/T to establish a post-immobilisation baseline. The difference between the pre- and post-immobilisation baselines was used to indicate the amount of ligand that had been immobilised. Non-covalently attached protein was removed prior to interaction studies by washing with 10 mM HCl for 2 minutes.

2.3.2.3 Monitoring of ligand interaction with 4D5 Fab'

Prior to the recording of each interaction profile 180 μL PBS/T/S (PBS/T buffer containing 0.5M NaCl) was added to the cuvette for 30 seconds to establish a baseline. Interaction was initiated by the addition of 20 μL of sample. Thus each sample was diluted 1 in10 during interaction with the surface immobilised ligand. The dilution step minimises the effects of changes in temperature and refractive index on sample addition, both of which can affect instrument response. Interaction was allowed to continue for 30 seconds before the surface was regenerated by the addition of 10 mM HCl (HP6045 assay) or 50 mM HCl (protein A assay). The surface was then washed three times with PBS/T/S, following which 180 μL PBS/T/S was added to the cuvette to establish a new baseline prior to the next sample application. The interaction profiles obtained were analysed using linear regression as described in Holwill *et al.*, 1996. Concentration data was obtained from a standard curve prepared for each biosensor cuvette using purified Fab' diluted in PBS/T/S.

2.3.3 Production of Fab' standards

4D5 Fab' standards for the calibration of ELISA and biosensor assays were purified from periplasmic extracts of cells harvested from HCD fermentations (section 2.1.4.5). Cells were resuspended in periplasmic extraction buffer (100mM Tris HCl pH 7.4, 10 mM EDTA) at a concentration of 0.14 g mL^{-1} and incubated with shaking overnight at 60°C, 250 rpm. Following extraction, spheroplasts were removed by centrifugation at 10 000 rpm for 40 minutes using a Beckman J2-M1 centrifuge

(Beckman Instruments (UK) Ltd, High Wycombe, UK) with a JA 10 rotor. 4D5 Fab' was purified from clarified periplasmic extracts by packed bed affinity protein A chromatography as described in section 2.4.3.1.

Purified Fab' was buffer exchanged into 100 mM acetate pH5.5 containing 125 mM sodium chloride and 0.02% sodium azide for long term storage. Buffer exchange was carried out by dialysis (14 mm diameter dialysis tubing, Fisons Scientific, Loughborough, UK) overnight at 4°C. The concentration of the resulting solution was determined from the absorbance at 280 nm, using the equation:

$$A = \varepsilon c l \qquad \textbf{(2.2)}$$

where: A = absorbance at 280 nm

ε = extinction coefficient

c = concentration (mg mL^{-1})

l = path length (1 cm)

For 4D5 Fab' the extinction coefficient, ε, is equal to 1.43 for a 1 mg mL^{-1} solution (personal communication, D. King, Celltech Chiroscience Ltd). Purity and quality of the Fab' standard was assessed by SDS-PAGE (section 2.2.3.2) and Western blotting (section 2.3.4).

2.3.4 Western blotting

To enable specific detection of bands of antibody fragments, SDS-PAGE gels (section 2.2.3.2) were blotted onto Immobilon-P PVDF transfer membranes (Millipore (UK) Ltd, Watford, UK) using a Trans-Blot semi-dry transfer cell (Bio-Rad Laboratories), operating at 15V for 30 minutes using tris-glycine buffer (0.039M glycine, 0.048M tris base, 0.037% SDS, 20% methanol, 80% water) at pH 8.4. So that the success of transfer to the blotting membrane could be readily assessed, pre-stained low molecular weight markers (Bio-Rad Laboratories) were run on the gel (Table 2.3.1). These markers also aided the identification of protein bands on the

blot. Following transfer the membrane was blocked for 1 hour by incubation with shaking in PBST (PBS + 0.1% tween 20) containing 2% milk powder.

COMPONENT	M.W. (Da)
Phosphorylase B	111 000
Bovine serum albumin	77 000
Ovalbumin	48 200
Carbonic anhydrase	33 800
Soybean trypsin inhibitor	28 600
Lysozyme	20 500

Table 2.3.1 *Pre-stained low molecular weight marker proteins for Western blotting.*

2.3.4.1 Fab' light chain detection

For Fab' light chain detection the membrane was incubated overnight with an anti-human kappa light chain antibody-HRP conjugate (Dako Ltd., High Wycombe, UK) diluted 1/1000 in PBST containing 2% milk powder. The membrane was washed on a shaker in three changes of PBST, 5 minutes per wash. Colour was developed by incubating the membrane in a substrate solution containing 34ml PBS, 6ml methanol, 20mg 1-chloro-4-naphthol and 20 µl of 30% H_2O_2 for 15 minutes.

2.3.4.2 Fab' heavy chain detection

For Fab' heavy chain detection the membrane was incubated for 1 hour with a sheep anti-human IgG (Fd) polyclonal antibody (The Binding Site, Birmingham, UK) diluted 1/10 000 in PBST containing 2% milk powder. Following three 5 minute washes in PBST, the membrane was incubated for another hour in an Fc fragment specific peroxidase conjugated affinipure $F(ab')_2$ fragment rabbit anti-sheep IgG (Jackson, Luton, UK) diluted 1/10 000 in PBST containing 2% milk powder. The wash step was repeated and colour was developed by incubating the membrane in substrate solution (34ml PBS, 6ml methanol, 20mg 1-chloro-4-naphthol and 20 µl of 30% H_2O_2) for 15 minutes.

2.4 Downstream processing

2.4.1 Periplasmic extraction

2.4.1.1 General extraction protocols

The procedure used to produce periplasmic fractions for the determination of periplasmic antibody concentration in fermentation samples is given in section 2.2.1.

The standard periplasmic extraction protocol, used to release antibody fragments from cells, involved incubation of cells overnight (~16 hours) in periplasmic extraction buffer (100 mM Tris HCl, 10 mM EDTA) at an OD_{600} of ~80. The concentration of cell paste required to give an OD_{600} of ~80 was determined to be 0.14 mg mL^{-1}. Standard incubation conditions were 60°C and 250 rpm unless otherwise stated.

2.4.1.2 Equipment used for the characterisation and scale up of periplasmic extraction

Periplasmic extraction experiments for the characterisation of antibody release and protein degradation were performed at three scales of operation; 0.065L, 2L and 100L. The small scale extractions were carried out in 0.1L stirred tanks whereas 2L and 100L extractions were performed in a 3L and a 150L bioreactor respectively (both bioreactors supplied by LH Fermentation, Inceltech UK Ltd., Berkshire, UK). Temperature within the stirred tanks was maintained by heating coils containing water pumped from a hot water bath maintained at 85°C. Temperature within the bioreactors was maintained using the bioreactors' in-built temperature control systems.

Dimensions of the vessels and associated impellers used for the extraction experiments are given in Table 2.4.1.

Extraction vessel	0.1L Stirred tank	3L Bioreactor	150L Bioreactor
Extraction volume (L)	0.065	2	100
Vessel height (m)	0.058	0.2	1.205
Vessel diameter (m)	0.046	0.14	0.4
Impeller type	6-bladed disk turbine	6-bladed disk turbine	6-bladed disk turbine
Impeller diameter (m)	0.024	0.056	0.125
Number of impellers	1	2	3
Impeller Power number (-)	5	10	15

Table 2.4.1 *Dimensions of vessels used for the characterisation and scale up of periplasmic extraction.*

Impeller speeds used in the extraction experiments were calculated to give a constant power per unit volume of 45 Wm^{-2}. Calculations are given in Appendix 4. The impeller speeds used were 250 rpm (0.1L stirred tank), 150 rpm (3L bioreactor) and 130 rpm (150L bioreactor).

For the small scale extractions (0.1L stirred tank), cells were resuspended in extraction buffer in a 100 mL Duran bottle (approximate dimensions 6 cm height × 4.6 cm diameter). Resuspension was achieved using a six-bladed disk turbine impeller (diameter 2.4 cm) rotated at a speed of ~1800 rpm for 15 minutes. Cell suspensions were transferred to the stirred tanks following complete resuspension.

For the large scale extractions (performed in the 3L and 150L bioreactors) cell paste was added directly to the bioreactor containing extraction buffer at the required temperature. Resuspension was performed at the impeller speed employed for the extraction process and took up to 45 minutes.

2.4.1.3 Production of spheroplast suspensions for centrifugation trials

Spheroplast suspensions used in the large-scale centrifugation trials were produced using the standard periplasmic extraction procedure described in section 2.4.1.1. Extraction was performed in the 150L bioreactor at a temperature of 60°C and an impeller speed of 130 rpm.

2.4.2 Centrifugation

2.4.2.1 Measurement of shear sensitivity

The rotating disc shear device was used to shear purified Fab' and spheroplasts. The device, illustrated in Figure 2.4.1, consisted of a single flat aluminium disk, 3 cm in diameter and 0.1 cm in thickness, mounted within a cylindrical Perspex chamber. The chamber had a diameter of 4 cm and a height of 1.5 cm. The disk was rotated within the chamber by a small battery driven high speed motor (Groupher Speed 500 BB RACE, UK). For the experiments carried out in this study, the disk was rotated at 27 000 rpm for 15 seconds, corresponding to a shear rate of approximately $1.1\times10^{6}\ s^{-1}$.

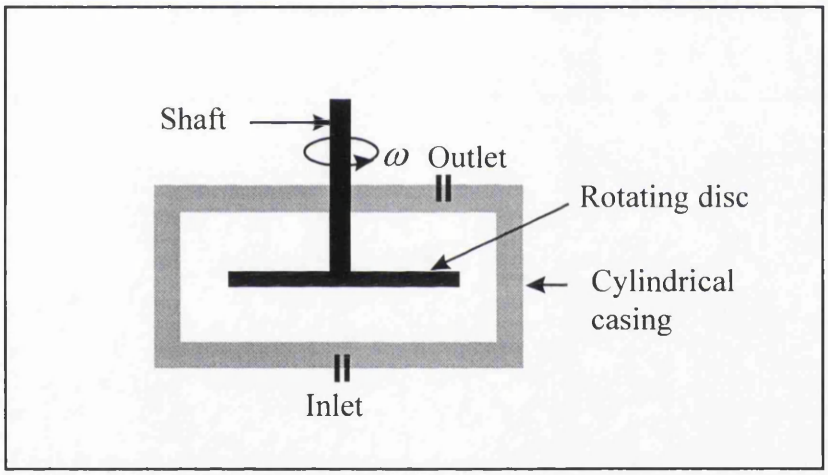

Figure 2.4.1 *Schematic diagram of the rotating disk shear device.*

2.4.2.2 Laboratory spin test

Laboratory spin tests were performed on spheroplast suspensions using the Beckman J2-M1 centrifuge (Beckman Instruments (UK) Ltd, High Wycombe, UK) with a JS 13.1 swing-out rotor. The centrifuge tubes used were 10 mL open, lipless tubes filled to capacity. During centrifugation, the tubes were rotated such that the axis of each tube was at right angles to the axis of rotation. Spheroplast suspensions were spun at 6720 rpm (3720g) for 3.5, 6, 10, 15, 20, 29 and 47 minutes. The equivalent Q/Σ corresponding to each run time is given in Appendix 8. Following centrifugation the supernatant in each tube was carefully decanted. The optical density of all

supernatants was measured at 600nm using a spectrophotometer (Uvikon 922, Kontron Instruments Ltd., Watford, UK). The OD_{600} of the initial spheroplast suspension ('feed') and a 'well spun' sample of the feed (obtained by centrifuging at 10 000 rpm/ 8200g for 90 minutes) was also measured. The clarification efficiency obtained at each equivalent Q/Σ was calculated using the equation in section 2.4.2.3.

2.4.2.3 Clarification efficiency

Clarification efficiencies were calculated using the following equation:

$$\text{Clarification efficiency (\%)} = 100 * \left(1 - \left(\frac{OD_{600}(\text{supernatant}) - OD_{600}(\text{well spun})}{OD_{600}(\text{feed}) - OD_{600}(\text{well spun})}\right)\right) \quad \textbf{(2.3)}$$

The well spun sample represents a feed sample centrifuged in the laboratory centrifuge (Beckman J2-M1 centrifuge) at 10 000 rpm (8200g) for 90 minutes. Optical densities were measured using a spectrophotometer (Uvikon 922).

Clarification efficiencies were also determined on the basis of solids volume fraction by replacing the OD_{600} terms in Equation 2.2 with solids volume fractions. Solids volume fractions were estimated as described in section 2.4.2.5.

2.4.2.4 Clarification of spheroplast suspensions

Two centrifuges were used for the clarification of spheroplast suspensions, the CARR P6 Powerfuge (CARR Separations Inc, Franklin, MA) and the Westfalia CSA-1 variable speed, steam sterilisable disk stack with semi-hermetic bowl (Westfalia Separator, Milton Keynes, UK). Feed suspension was pumped through the CARR Powerfuge using a Cole-Parmer Instrument Company model 7523-27 pump (Barnant Co., Barrington, IL). The pump used with the CSA-1 was a Watson Marlow 605 Di Peristaltic pump (Watson Marlow Ltd., UK). Technical specifications of the centrifuges are given in Appendix 6 (CARR) and Appendix 7 (CSA-1).

2.4.2.4-a Centrifuge recovery

Recovery curves were produced to determine the relationship between flow rate and clarification for each centrifuge. Centrifuges were operated at the following flow rates: CARR, 15, 20, 30, 50, and 90 Lhr^{-1}; CSA-1, 10, 20, 30, 50 and 100 Lhr^{-1}. The clarification efficiency at each flow rate was calculated and plotted against Q/Σ. The Q/Σ values corresponding to the flow rates used for each centrifuge are given in Appendix 9.

2.4.2.4-b Centrifuge mass balances

Mass balances were performed by processing one 'centrifuge bowl' volume of spheroplast suspension (i.e. the volume required to fill the centrifuge bowl with solids) at the estimated operating flow rate for 95% clarification (determined from centrifuge recovery curves). The suspension volume required to fill the bowl was initially determined by pumping the suspension through the centrifuge at the required flow rate until solids breakthrough occurred. Following the processing of one bowl volume, collected solids were discharged and the volume of the supernatant and solids recorded.

Solids volume fraction of the feed, supernatant and solids (CSA-1 only) streams were estimated using the method described in section 2.4.2.5. The supernatant obtained following centrifugation of each stream for solids fraction determination was assayed for Fab' and protein. This allowed a full mass balance of each centrifuge run to be conducted using the equations given below. The nomenclature used to represent stream properties in the mass balance equations is given in Table 2.4.2.

Process stream	Feed	Supernatant	Solids
Protein concentration	C_{PF}	C_{PS}	C_{PD}
Fab' concentration	C_{AF}	C_{AS}	C_{AD}
Volume	V_{FEED}	V_{SUP}	V_{DIS}
Solids fraction	v_{FF}	v_{FSUP}	v_{FDIS}

Table 2.4.2 *Nomenclature used to represent stream properties in mass balance equations.*

Protein balance: $C_{PF}(1- v_{FF})\, V_{FEED} = C_{PS}(1- v_{FSUP})\, V_{SUP} + C_{PD}(1- v_{FDIS})\, V_{DIS}$

Fab' balance: $C_{AF}(1- v_{FF})\, V_{FEED} = C_{AS}(1- v_{FSUP})\, V_{SUP} + C_{AD}(1- v_{FDIS})\, V_{DIS}$

Protein yield (%)	Supernatant stream	$\frac{C_{PS}(1- v_{FSUP})\, V_{SUP}}{C_{PF}(1- v_{FF})\, V_{FEED}} * 100$
	Solids stream	$\frac{C_{PD}(1- v_{FDIS})\, V_{DIS}}{C_{PF}(1- v_{FF})\, V_{FEED}} * 100$
Fab' yield (%)	Supernatant stream	$\frac{C_{AS}(1- v_{FSUP})\, V_{SUP}}{C_{AF}(1- v_{FF})\, V_{FEED}} * 100$
	Solids stream	$\frac{C_{ADIS}(1- v_{FDIS})\, V_{DIS}}{C_{AF}(1- v_{FF})\, V_{FEED}} * 100$
Liquid (%)	Supernatant stream	$\frac{(1- v_{FSUP})\, V_{SUP}}{(1- v_{FF})\, V_{FEED}} * 100$
	Solids stream	$\frac{(1- v_{FDIS})\, V_{DIS}}{(1- v_{FF})\, V_{FEED}} * 100$

2.4.2.5 Estimation of solids volume fraction

The fractional volume of solids in any given process stream was determined by centrifuging known volumes of material in graduated, transparent Perspex process tubes. The process tubes were graduated in increments of 50μL to allow direct measurement of the volume of solids. Samples were centrifuged in the Beckman J2-M1 centrifuge using the JS 13.1 rotor, at 10 000 rpm (8200g) for 30 minutes.

2.4.2.6 Scale-down operation of the CSA-1 disk stack centrifuge

Scale-down of the CSA-1 centrifuge was achieved using stainless steel conical inserts made by Westfalia Separator. Four interlocking conical top inserts were used to reduce the bowl volume, solids holding space volume and the number of active disks. In addition, a conical bottom insert was used to reduce the bowl volume and

lift the disk stack off the bottom of the centrifuge. Specifications for the full stack and scale-down configurations are given in Table 2.4.3.

No. reducing inserts	Active disks		Bowl volume		Solids holding volume	
	No.	%full-scale	Vol (L)	% full-scale	Vol (L)	% full-scale
0 (full stack)	45	100	0.44	100	0.25	100
4 (scale-down)	12	27	0.13	30	0.089	36

Table 2.4.3 *Specifications for the CSA-1 full-scale and scale-down configurations.*

Operational flow rates used in the preparation of recovery curves (section 2.4.2.4-a) for the CSA-1 were as follows: Full stack configuration, 100, 50, 30, 20 and 10 L hr^{-1}; Scale-down configuration, 27, 13, 8, 5.3 and 2.7 L hr^{-1}. The corresponding Q/Σ values have been calculated in Appendix 10.

2.4.3 Chromatography

2.4.3.1 Packed bed affinity protein A chromatography

Purification of 4D5 Fab' from periplasmic extracts was routinely performed by packed bed affinity protein A chromatography using a BioCAD™ 700E workstation (Perceptive Biosystems, Warrington, UK). Three types of protein A media were used for Fab' purification; details of the media, associated columns and operating flow rates are given in Table 2.4.4.

Chromatography Matrix	Column			Flow rate (mL min^{-1})
	Type	Dimensions	Matrix volume (mL)	
Streamline rProtein A (Amersham Pharmacia Biotech, Uppsala, Sweden)	Pharmacia HR 10/10	10 mmD × 100 mmL	7	3
POROS® 50A protein A (Perseptive Biosystems)	POROS®	4.6 mmD × 100 mmL	1.66	2
rProtein A Sepharose® Fast Flow (Pharmacia)	Pharmacia HiTrap	7 mmD × 25 mmL	1	1

Table 2.4.4 *Protein A chromatography media and associated columns and flow rates used for the packed bed affinity purification of 4D5 Fab'.*

2.4.3.1-a Sample preparation

Periplasmic extracts were clarified by centrifugation at 10 000 rpm for 40 minutes using the Beckman J2-M1 centrifuge (Beckman Instruments (UK) Ltd, High Wycombe, UK) with a JA 10 rotor. Glycine was then added to the extracts to a concentration of 1M and the pH of the extract adjusted to 7.5 using 50% (w/v) sodium glycinate. Prior to application to the column, extracts were filtered through a Sartobran 300 0.2 μM filter (Sartorius, Goettingen, Germany).

2.4.3.1-b Process operation

Sample was applied to a protein A column equilibrated in 1M glycine/ glycinate (pH 8.0) at the operating flow rate given in Table 2.4.4. The column was washed with 15 column volumes of equilibration buffer. The Fab' was then eluted with a 10 column volume linear gradient from 1M glycine pH 8.0 to 0.1M citrate pH 3.0. Column flow through was collected in 10 mL fractions during the load and wash cycles; 2mL fractions were collected during elution. Fab' containing fractions were adjusted to pH 6.0 with 2M tris-HCl pH 8.5.

2.4.3.2 Expanded bed affinity protein A chromatography

Fab' was purified by expanded bed affinity chromatography using a Streamline 25 expanded bed column packed with 25 mL Streamline rProtein A matrix. The system was controlled using a modified Pharmacia FPLC system comprising an LCC-500 controller and two P-500 pumps. UV monitoring at 280nm was carried out using a UV-1 monitor; conductivity and pH of the eluant stream were also monitored. Column flow through was collected in fractions using a FRAC-100 fraction collector. The Streamline column and matrix, all components of the FPLC system and the fraction collector were supplied by Amersham Pharmacia Biotech, Uppsala, Sweden. UV and conductivity/ pH were logged using a PE Nelson 900 interface and Turbochrom v. 4 software (both Perkin Elmer, California). The layout of the expanded bed system is illustrated in Figure 2.4.2.

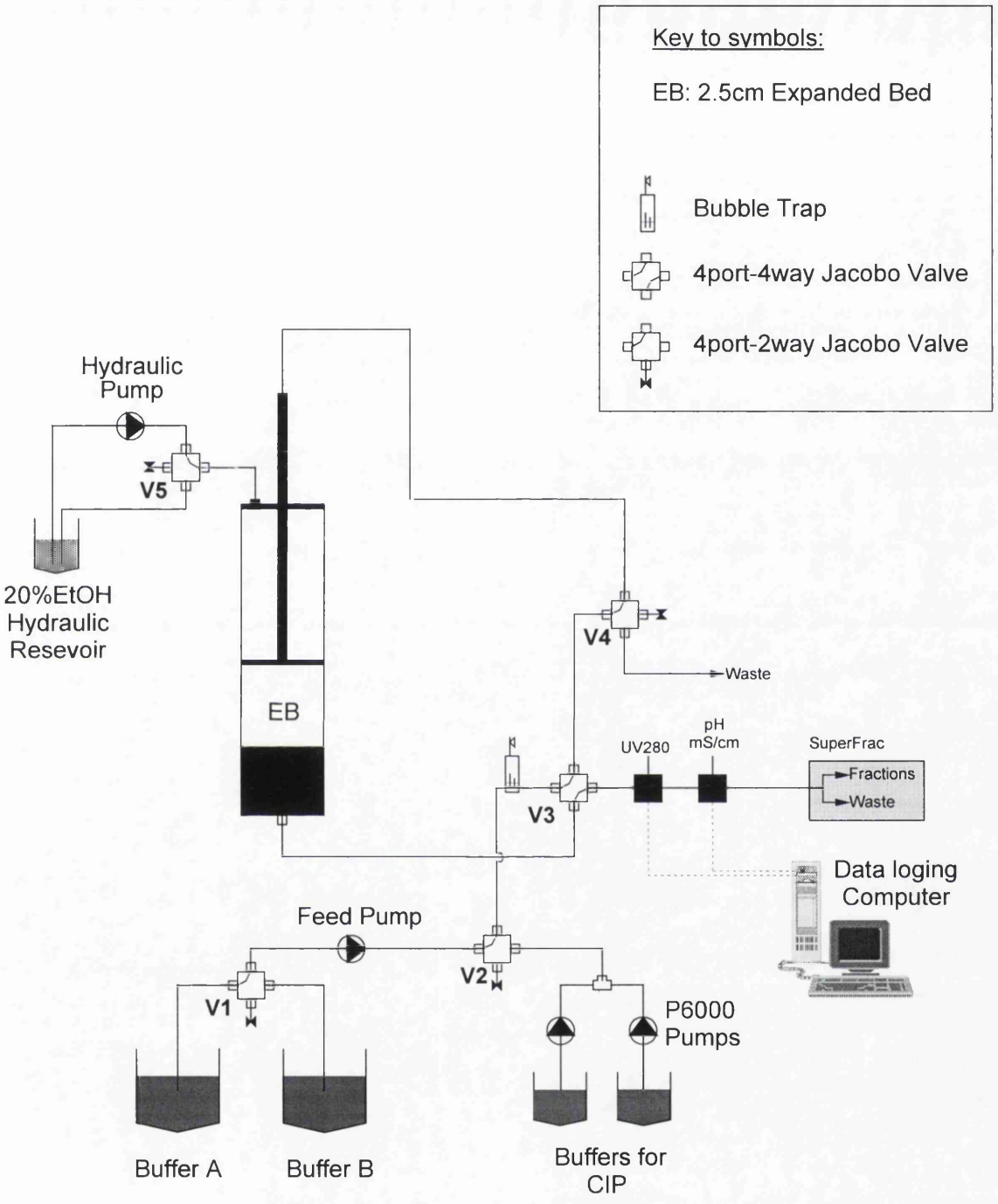

Figure 2.4.2 *Schematic diagram of the Streamline 25 expanded system used for the purification of 4D5 Fab'.*

2.4.3.2-a Sample preparation

Glycine was added to unclarified periplasmic or whole broth extract to a concentration of 1M and the pH of the extract was adjusted to 7.5 using 50% (w/v) sodium glycinate. The extract was then adjusted to 2 mM $MgCl_2$ and 20 μL L^{-1} benzonase and incubated for 3 hours at 34°C to allow degradation of extracellular nucleic acids.

2.4.3.2-b Process operation

- **Expansion and equilibration.** The settled bed was expanded by pumping water through in an upward direction, gradually increasing the linear fluid velocity from 0 to 185 cm hr^{-1}. The system was then switched to run through buffer A (1M glycine/ glycinate, pH 8.0) for 20 minutes to equilibrate the bed.
- **Sample loading.** The prepared feed was loaded onto the column in an upward direction at a linear velocity of 185 cm hr^{-1}.
- **Washing.** The column was washed in an upwards direction using buffer A at 185 cm hr^{-1} for 50 minutes to remove unbound protein and particulate matter.
- **Elution.** Following washing, flow to the column was stopped and the bed was allowed to settle. The upper adapter was then lowered until it reached the surface of the settled bed. The direction of liquid flow was reversed and the liquid linear velocity lowered to 90 cm hr^{-1}. Fab' was eluted by switching from buffer A to buffer B (0.1M Tri-sodium citrate, pH 3.0), giving a step change in pH.

During loading and washing, column flow through was collected in 15 mL fractions. During elution, column eluate was collected in 7.5 mL fractions. Fab' containing fractions were adjusted to pH 6.0 with 2M tris-HCl pH 8.5.

2.4.4 General procedures

2.4.4.1 Homogenisation

Complete cell disruption was achieved using a Gaulin Micron Lab 40 homogeniser (APV Gaulin GmbH, Lubeck, Germany). 40 mL samples were passed once through the homogenising valve at an operating pressure of 1200 bar. Glycol cooling was supplied to the equipment to reduce the disruption temperature to 4°C.

2.4.4.2 Ultrafiltration

Ultrafiltration was performed using a Millipore Labscale™ TFF system operated with three 50 cm^2 Pellicon XL regenerated cellulose membranes (Millipore (UK) Ltd., Watford, UK). Process fluid was circulated through the system at a pump speed of 2.5 and an operating pressure of ~200 psi until an eight-fold concentration was achieved.

3. PRODUCTION OF A Fab' ANTIBODY FRAGMENT BY *Escherichia coli* FERMENTATION

3.1 Introduction

This chapter describes the design and characterisation of a fermentation process for the periplasmic expression of Fab' antibody fragments. Section 3.2.1 details characteristics of the 'low cell density' fermentation initially used for Fab' production. Although this fermentation produced high antibody titres, notable leakage of the antibody into the extracellular broth was observed over the course of the induction period. The fermentation was therefore modified to allow greater control of product location. Alterations made to the fermentation protocol are discussed in section 3.2.2, with the characteristics of the resulting 'high cell density' fermentation described in section 3.2.2.1-3.2.2.3. Finally, in order to provide sufficient material for downstream processing studies, the high cell density fermentation was scaled up to 450L as described in section 3.2.3.

The production of antibody fragments by *E. coli* fermentation has been reviewed in Chapter 1. A number of factors contribute towards product titres achieved, including the primary sequence of the antibody (Knappik and Pluckthun, 1995) and the rate of antibody expression. It has been suggested that the major limiting step during the production of antibody fragments in *E. coli* is the periplasmic folding process (Skerra and Pluckthun, 1991). If the antibody expression rate is too high, folding pathways are saturated and the antibody accumulates as insoluble aggregates. Therefore, to ensure the high level accumulation of soluble, correctly folded antibody fragments, it is important to limit production rates whilst maintaining sufficient levels of expression to allow high titres to accumulate. Factors affecting the rate of recombinant protein expression include promoter strength (Kipriyanov, *et al.*, 1997), strength and concentration of the inducer (Shibui and Nagahari, 1992, Takagi *et al.*, 1988), design of the translation initiation region (Simmons and Yansura, 1996) and the induction temperature (Cabilly, 1989, Shibui and Nagahari, 1992, Takagi *et al.*, 1988). The order in which the individual chains are transcribed can also have an effect on expression titres and cell viability (Tsumoto *et al.*, 1994, Weir and Bailey,

1997). All such factors must be taken into consideration during design of the expression plasmid and fermentation system to achieve optimal rates of antibody fragment expression.

For a process study such as this to be considered both useful and relevant, the fermentation system employed should be comparable to current industrial practice. Additionally, it is desirable for the fermentation to show consistency in terms of both biomass levels and product titres. The initial development of recombinant antibody expression systems in *E. coli* usually involves growth and expression trials using complex media, antibiotic selection and chemical inducers such as IPTG. However, the use of such materials during the production of recombinant proteins destined for therapeutic use is inadvisable because evidence of clearance of these materials from the final product must be provided before regulatory approval can be obtained. Demonstrating clearance can be both difficult to achieve and extremely expensive. Therefore, current industrial systems tend to employ fully defined media with the avoidance of antibiotic selection or use of potentially harmful chemical inducers in the production fermenter.

The expression plasmid and fermentation system chosen for use in this study have been designed to allow controlled, high level expression of antibody fragments. As with current industrial practise, a fully defined growth medium is employed, and lactose rather than IPTG is used for the induction of recombinant protein expression from a *tac* promoter. The use of lactose as an inducer has the additional advantage of providing a slower, more controlled induction. The rate of product accumulation is also limited by the use of a sub optimal growth temperature during the induction phase. A diagram of the expression plasmid utilised for Fab' production is illustrated in Appendix 1. The two antibody chains are expressed from a dicistronic operon to ensure the transcription of equal quantities of both chains. Furthermore, the light chain is situated upstream of the heavy chain so that it is transcribed first, to enhance both cell viability and the efficiency of antibody secretion.

3.2 Results and discussion

3.2.1 Low cell density fermentations

Initial fermentations of *E. coli* strain W3110 pAGP-4 were carried out to assess fermentation characteristics and 4D5 Fab' expression patterns. Three runs were performed using the low cell density (LCD) protocol described in section 2.1.4.4. In all runs fermenters were inoculated with 24 hour shake flask cultures using an inoculum volume of 2.5 % (v/v). Growth conditions were controlled at 30°C and pH 6.95, and the DOT was maintained above 20% by manual increases in stirrer speed and airflow rate. 4D5 Fab' expression was induced with lactose at an OD_{600} of 30. Fermentations were run for 15-20 hours after the carbon source switch from glucose to lactose.

3.2.1.1 General fermentation characteristics

Details of the three fermentations are summarised in Table 3.2.1. To allow for comparisons, Fab' titres shown are those measured at 15 hours after the switch in carbon source from glucose to lactose metabolism.

Run	Scale (Initial wv, L)	Inoculum medium	DCW (gL^{-1})	Fab' (mgL^{-1})			
				Ex	Pp	Total	% Pp
LCD 1	4	Complex	14.5	45	25	70	36
LCD 2	8	Complex	16.3	89	86	175	49
LCD 3	8	Defined	14.1	46	43	89	48

Table 3.2.1 *Summary of low cell density fermentations. Ex, extracellular Fab'; Pp, periplasmic Fab'; %Pp, percentage of total Fab' located in the periplasm. Fab' titres recorded 15 hours after the switch from glucose to lactose metabolism.*

The initial fermentation was carried out to gain a general indication of the time scale and growth characteristics. The culture was grown in a 7L vessel using a 4L initial working volume. During LCD fermentation runs 2 and 3 fermentation characteristics were monitored more closely. Due to fermenter availability, these runs were carried out in a 20L fermenter using an initial working volume of 8L.

The aeration and respiration profiles for LCD run 2 are shown in Figures 3.2.1 and 3.2.2. The respiration profile shows typical diauxic growth kinetics. A very long initial lag phase (~18 hours) was observed, followed by a shorter lag of 3 hours after ~35 hours, indicating glucose depletion and the onset of lactose metabolism. The OUR increased exponentially during growth on glucose and peaked at 90 $mmolL^{-1}h^{-1}$ just prior to glucose depletion. The specific growth rate during exponential growth was calculated as 0.22 h^{-1}, based on dry cell weight (DCW) (data illustrated in Figure 3.2.4). Biomass levels of 16 g(DCW) L^{-1} were attained by end of the fermentation.

The sudden drop in oxygen uptake rate (OUR) and carbon dioxide evolution rate (CER) and rise in DOT at ~35 hours, indicative of the switch from glucose to lactose metabolism, was accompanied by a tautological rise in extracellular pH, as shown in Figure 3.2.3. During growth on glucose, the pH of the medium dropped due to the synthesis of acidic by-products and alkali was added by the pH controller to maintain the culture pH at 6.95. The pH rise following glucose depletion was thought to be caused by the proton symport associated with lactose uptake (Straight *et al.*, 1989). After growth began to increase as cells adapted to lactose metabolism, medium pH again dropped and alkali was consumed.

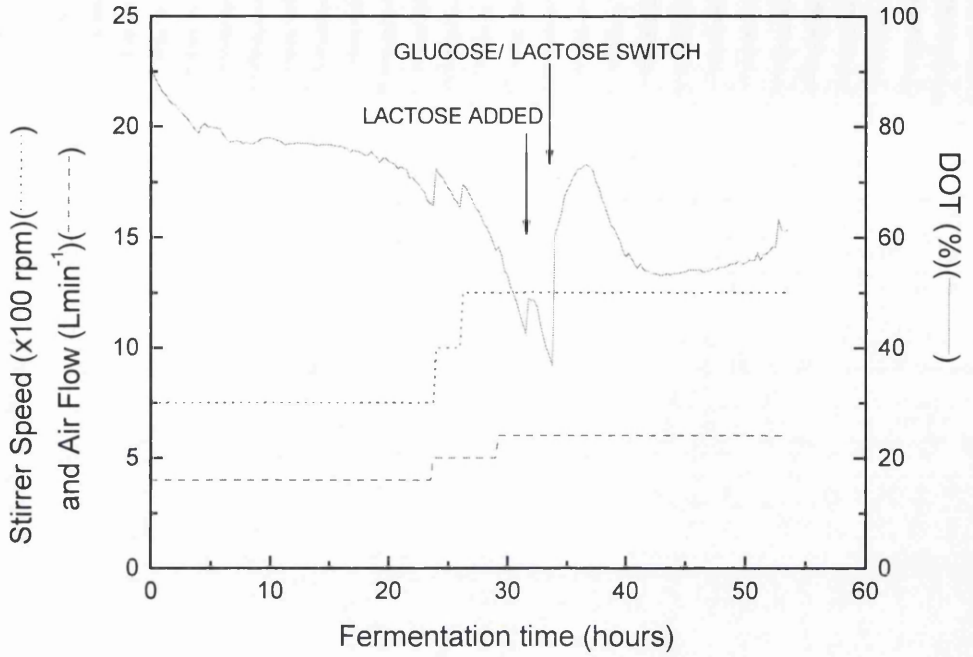

Figure 3.2.1 *Aeration profile for fermentation LCD 2 showing changes in dissolved oxygen tension (DOT) during fermentation and effects of changing stirrer speed and airflow to maintain dissolved oxygen above 20%.*

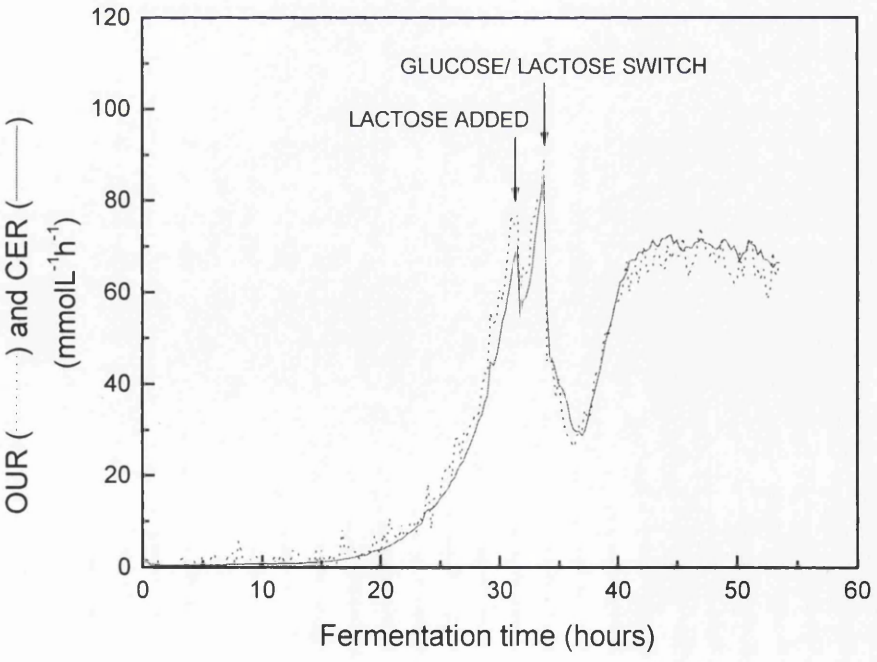

Figure 3.2.2 *Respiration profile showing oxygen uptake rate (OUR) and carbon dioxide evolution rate (CER) for fermentation LCD 2.*

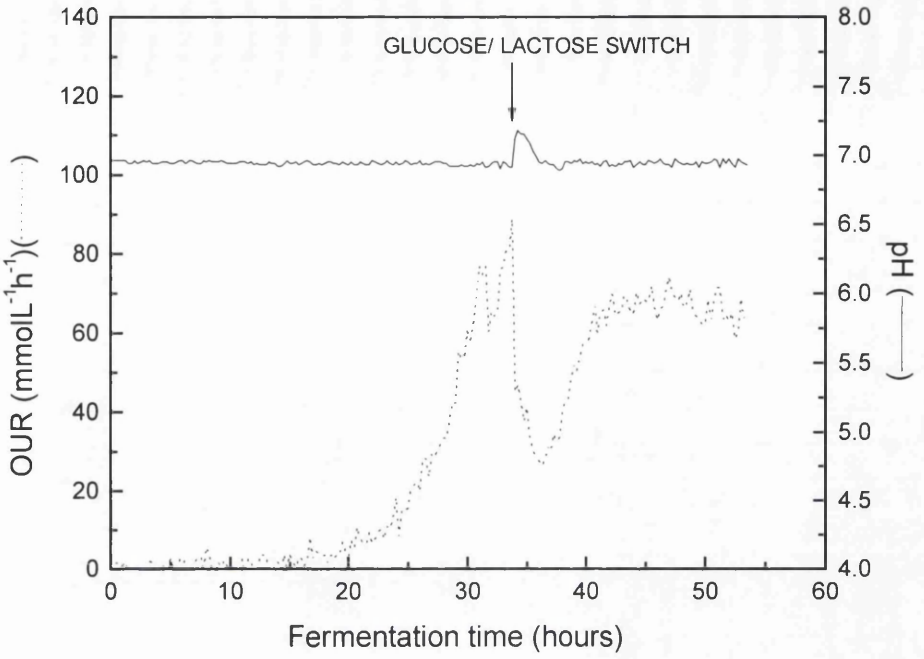

Figure 3.2.3 *Oxygen uptake rate (OUR) and pH profiles indicating point of switch from glucose to lactose metabolism for fermentation LCD 2.*

3.2.1.2 Fab' production

Fab' accumulation was monitored from the time of lactose addition to 20 hours after the glucose/ lactose switch. Fab' concentrations of both periplasmic and extracellular fractions of fermentation samples were determined by ELISA. Periplasmic fractions were obtained using the extraction protocol described in section 2.2.1. All concentrations obtained from ELISA analysis were converted to mg Fab' per litre of original fermentation broth.

Total Fab' accumulation for run 2 is illustrated alongside OUR and DCW data in Figure 3.2.4. It is evident from this that Fab' production occurred mainly during late exponential and stationary growth phases, following the addition of lactose at 32 hours. Figure 3.2.5 shows how the distribution of Fab' between the periplasm and the extracellular medium varied over the course of the induction period. Periplasmic Fab' reached peak titres (70-80 mg L^{-1}) 8 hours after the glucose/ lactose switch. Titres remained fairly constant for the following 10 hours and then began to decline.

Extracellular Fab' accumulated more slowly initially but titres continued to increase throughout the induction phase with levels reaching 132 mg L^{-1} (and still increasing) at the end of the fermentation. Total Fab' titres appear to level off over the final three hours of the fermentation. Thus the increase in extracellular Fab' and decrease in periplasmic Fab' could be attributed to cell lysis or leakage of antibody from the periplasmic space into the medium. The time for optimal harvest therefore depends on whether extracellular Fab', periplasmic Fab' or both are being harvested. However, it is inadvisable to harvest from the extracellular broth after extended periods of induction as any cell lysis occurring in the latter stages of fermentation will result in the release of proteases, DNA and lipids into the medium. This will reduce process stream purity and may hinder downstream purification operations.

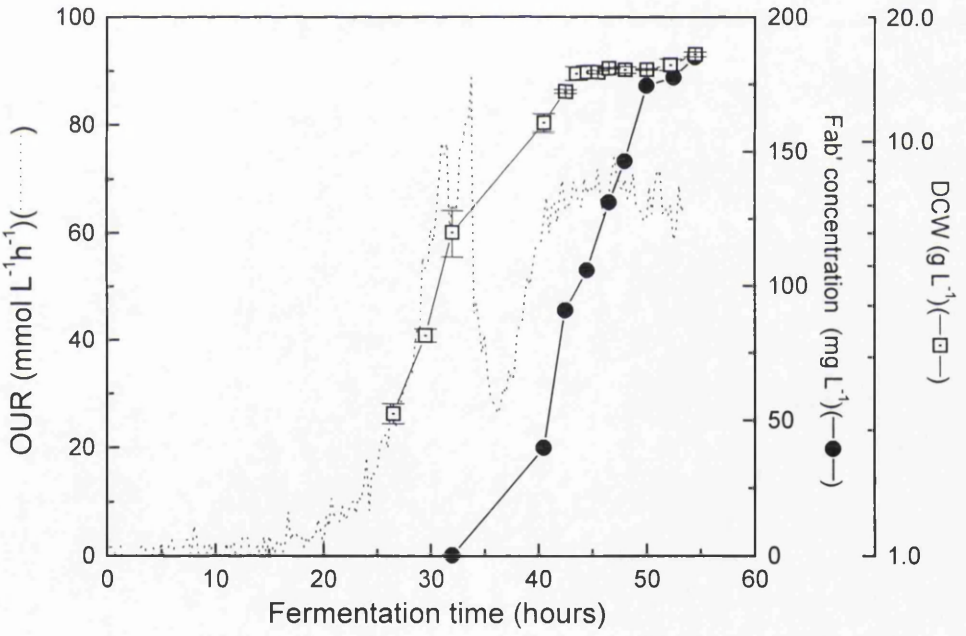

Figure 3.2.4 *Growth and Fab' accumulation profiles for fermentation LCD 2. Growth indicated by oxygen uptake rate (OUR) and dry cell weight (DCW) data. Error bars represent the standard deviation of duplicate measurements (DCW data) or the standard deviation determined from multiple dilutions of duplicate samples (ELISA data).*

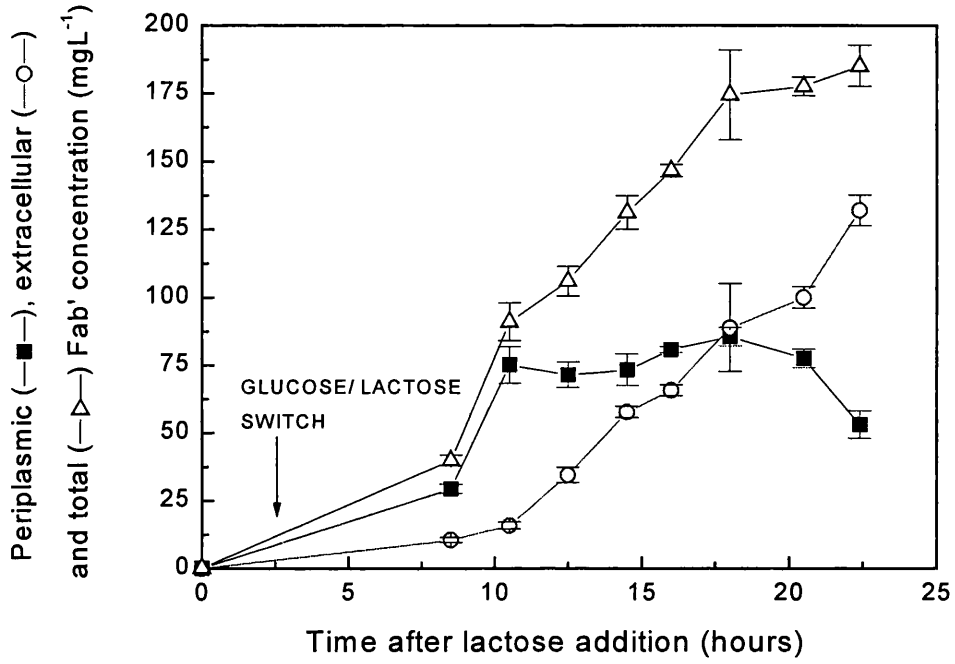

Figure 3.2.5 *Periplasmic, extracellular and total Fab' accumulation during fermentation LCD 2. Fab' concentrations determined by ELISA. Error bars represent standard deviations determined from multiple dilutions of duplicate samples.*

It can be seen from the data in Table 3.2.1 that the level of cell growth was similar in all three fermentations whereas Fab' titres varied quite widely. E. Fischer (PhD thesis, 1996) also observed notable variation in titres of periplasmically expressed α-amylase despite biomass levels being relatively consistent. This variation is difficult to explain but may result from differences in inoculum cultures, specific problems encountered during individual fermentations and slight variations in operating conditions which are generally determined by the specific requirements of each fermentation.

3.2.1.3 Reduction of initial lag

The respiration profile in Figure 3.2.2 shows a long initial lag as the cells adapt to the environment within the fermenter. The lag was estimated at ~18 hours from the OUR profile (Figure 3.2.6) and a ln-linear plot of OD against time (Figure 3.2.7). The lag was thought to be a direct result of transfer of the culture from complex medium in the shake flasks to defined medium in the fermenter. Bacterial cells find growth on defined medium more difficult as they are required to synthesise essential nutrients such as amino acids and nucleic acids which come 'ready made' in the complex medium. Following transfer to defined medium, cells must initially produce the enzymes required for synthesis of complex nutrients from the defined medium components before culture growth can resume. The time taken for the cells to adapt in this way can be considerable and is both inefficient and costly for production.

In order to try and reduce the lag phase, run 3 was carried out using an inoculum culture grown on the defined medium used in the production fermenter instead of the complex broth used in runs 1 and 2. Use of defined medium in the shake flasks is also preferable in terms of regulatory issues as discussed previously (section 3.1). Again an inoculum volume of 2.5% (v/v) was used. Analysis of the OUR profile and a ln-linear plot of the OD profile for run 3 (Figures 3.2.6 and 3.2.7) showed the lag had been reduced to ~14 hours as a result of the alteration in growth medium. However, a 14 hour lag still exceeds the ideal and therefore in an attempt to reduce it further the inoculum volume used in subsequent fermentations was increased (as discussed in section 3.2.2.1).

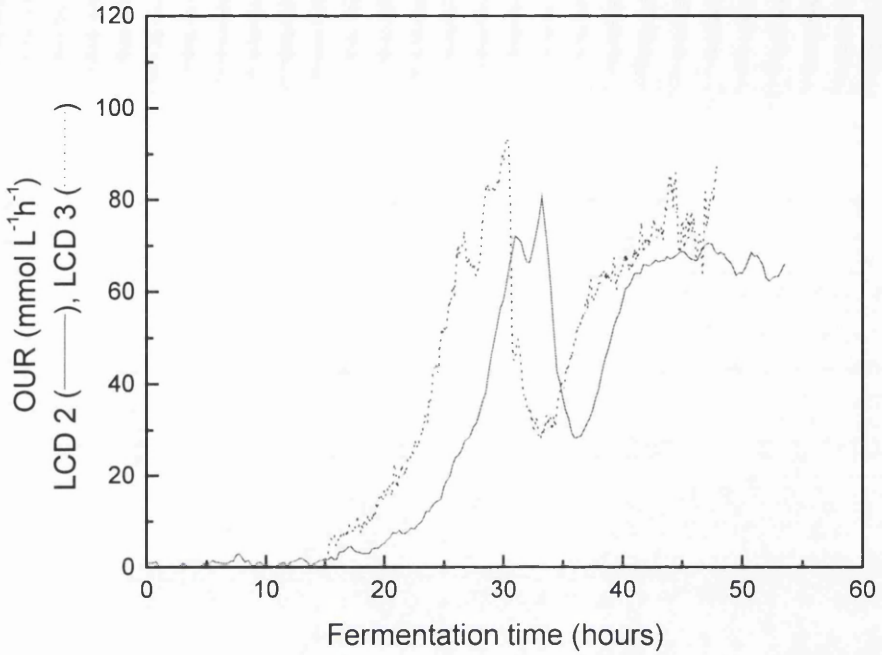

Figure 3.2.6 *Comparison of oxygen uptake rate (OUR) traces indicating different lengths of lag phase for fermentations LCD 2 and LCD 3. (OUR data was not available for LCD 3 over the period 0-15 hours).*

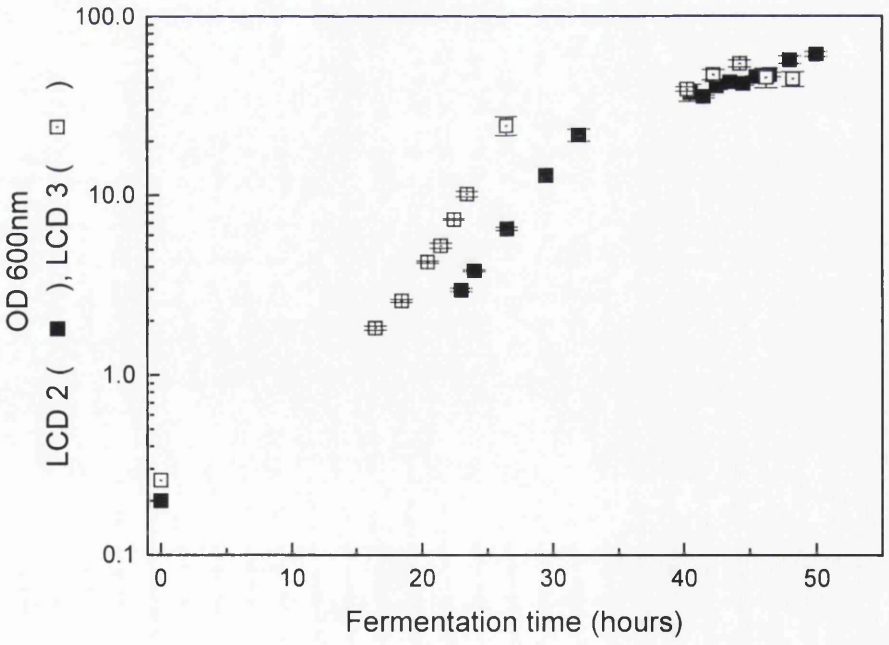

Figure 3.2.7 *Comparison of biomass accumulation shown by OD 600nm, indicating different lengths of lag phase for fermentations LCD 2 and LCD 3.*

3.2.2 High cell density fermentations

Downstream processing studies carried out later in this work focus on harvesting material from the periplasmic space. For processes where recovery from the periplasm is the chosen purification route, a fermentation is required which will minimise leakage of product into the extracellular medium. In order to try and achieve this a number of alterations were made to the original fermentation protocol described above. As well as allowing increased control over product location, these changes were designed to give higher biomass and thus increased antibody titres. The protocol changes can be summarised as follows:

1. Alteration of carbon source. The initial carbon source was changed from glucose to glycerol to reduce potential acetate production and growth inhibition, allowing growth to higher cell densities (Holms, 1986). Cells also grow more slowly on glycerol than on glucose (Korz *et al.,* 1995) which aids plasmid stability. The glycerol was added in batches to increase total biomass.

2. Addition of calcium and magnesium during fermentation. Calcium and magnesium salts were added prior to induction to increase the strength of the outer membrane and thereby reduce leakage of periplasmic material into the medium. Calcium and magnesium ions play an essential role in outer membrane integrity by electrostatically linking together the lipopolysaccharide molecules which cover the outer membrane surface (Vaara, 1992).

3. Temperature reduction. Culture temperature was reduced to 27°C prior to induction to slow culture growth and thereby increase the efficiency of antibody folding. Culturing at low temperatures reduces the rate of protein production and secretion into the periplasm, which improves folding efficiency, allowing the accumulation of higher titres of soluble and functional Fab (Cabilly, 1989; Shibui and Nagahari, 1992).

4. Use of phosphate limited medium. A reduced phosphate concentration in the growth medium was used to aid plasmid stability and enhance periplasmic retention. The stability of small, low copy number plasmids has been shown to be increased in continuous culture by phosphate limitation (Caulcott, 1984, Caulcott *et al.*, 1987). Phosphate limitation can also have an effect on the cell wall of Gram-negative bacteria, with phospholipids being replaced with glycolipids (Tempest and Wouters, 1981). It is thought that the changes in cell wall structure also aid the retention of proteins within the periplasmic space (personal communication, N Weir).

The protocol followed for high cell density (HCD) fermentations is described in section 2.1.4.5. All inoculum cultures for HCD fermentations were grown on defined medium. Culture pH was maintained at 6.95, and the DOT was as far as possible maintained above 20% by manual increases in stirrer speed and airflow rate. Glycerol was used as the initial carbon source at a concentration of 3% (w/v) in the fermentation medium. Further glycerol was added in batches at specific ODs, as described in section 2.1.4.5. The growth temperature was initially maintained at 30°C and was reduced to 27°C at an OD of 40. $MgSO_4$ and $CaCl_2$ were also added at 40 OD to final concentrations of 14.4 mM and 1.7 mM respectively. Fab' expression was induced at an OD of 60 by addition of 45 g L^{-1} lactose with the final glycerol shot. Further lactose was added in 45 g L^{-1} batches as required.

3.2.2.1 General fermentation characteristics

Initially four HCD fermentations were performed at a scale of 10L (initial working volume). Additions during the fermentation resulted in an increase in culture volume of at least 15% (depending on how many lactose shots were required). The inoculum volume for the 10L HCD fermentations was increased to 10% (v/v) (compared to 2.5% (v/v) used for the LCD fermentations) with the aim of minimising the initial lag. Fermentations were run for 13 hours after the switch in carbon source from glycerol to lactose. The characteristics of each run are summarised in Table 3.2.2.

Run	Scale (Initial wv, L)	Inoculum medium	DCW (gL^{-1})	Fab' (mgL^{-1})			
				Ex	Pp	Total	% Pp
HCD 1	10	Defined	40	250	358	608	59
HCD 2	10	Defined	38	105	573	678	85
HCD 3	10	Defined	33	34	189	227	83
HCD 4	10	Defined	37	15	202	217	93

Table 3.2.2 *Summary of high cell density fermentations. Initial wv, initial working volume; Ex, extracellular Fab'; Pp, periplasmic Fab'; %Pp, percentage of total Fab' located in the periplasm. Fab' titres recorded 13 hours after the switch from glycerol to lactose metabolism.*

Figures 3.2.8-3.2.11 show data obtained from fermentation HCD2. The respiration profile (Figure 3.2.9) again shows diauxic growth kinetics. The culture was oxygen limited for a brief period between ~13 and 18 hours. This was because the stirrer speed and airflow rate had been set too low to sustain growth overnight. Dissolved oxygen also fell below 20% for a short period immediately prior to glycerol depletion. At this stage the stirrer speed and airflow rate were both operating on maximum settings, hence a brief period of oxygen limitation could not be avoided. The OUR peaked at 175 $mmolL^{-1}h^{-1}$ just prior to glycerol depletion. This compares to 90 $mmolL^{-1}h^{-1}$ for the LCD fermentation. Oxygen demands of the HCD fermentations are considerably increased because the cultures are grown to higher biomass (achieved by batch-feeding of glycerol). A disadvantage associated with this is that cultures are at risk of becoming oxygen limited when oxygen demands are greatest, just prior to the carbon source switch.

The switch from glycerol to lactose metabolism during HCD fermentations was indicated not only by a large drop on OUR and CER and an increase in medium pH (as for LCD fermentations) but also by an increase in RQ, illustrated in Figure 3.2.10. The RQ during growth on glycerol was ~0.7, a typical value for *E. coli*. Following glycerol depletion and the onset of lactose metabolism the RQ increased to 1.0. Such a change was not observed for LCD fermentations as the RQ for growth of *E. coli* on glucose (the initial carbon source in LCD) fermentations was also 1.0.

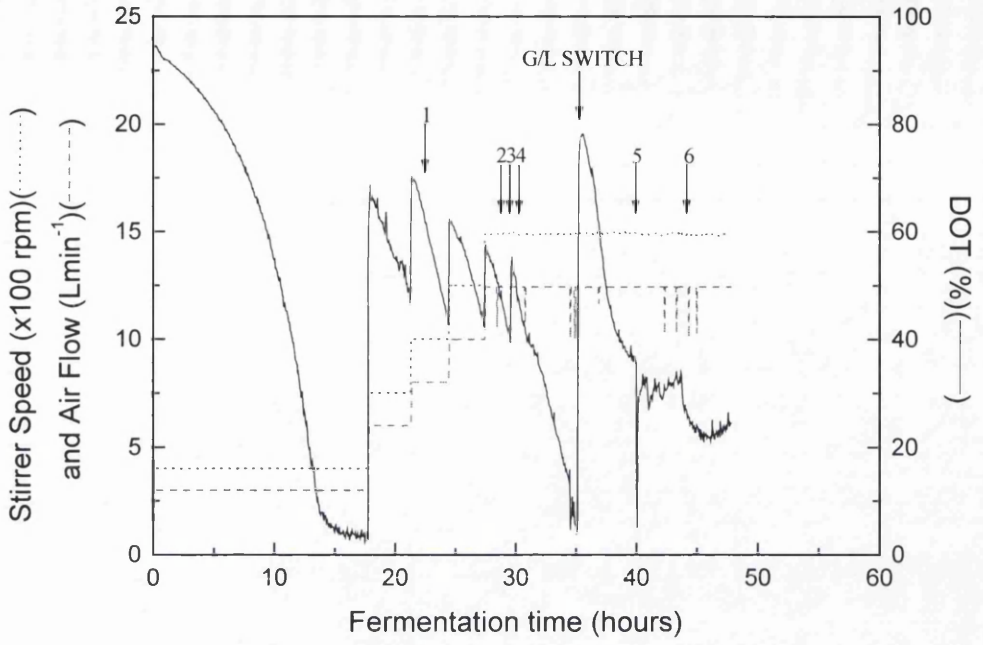

Figure 3.2.8 *Aeration profile showing changes in dissolved oxygen tension during fermentation HCD 2 and effects of changing stirrer speed and airflow to maintain dissolved oxygen where possible above 20%. Additions were as follows: 1. 30 g* L^{-1} *glycerol; 2. 20 g* L^{-1} *glycerol; 3. 14.4 mM* $MgSO_4$ *and 1.7 mM* $CaCl_2$*, temperature reduced to 27°C; 4. 10 g* L^{-1} *glycerol and 45 g* L^{-1} *lactose; 5. and 6. 45 g* L^{-1} *lactose; G/L SWITCH = glycerol/ lactose switch.*

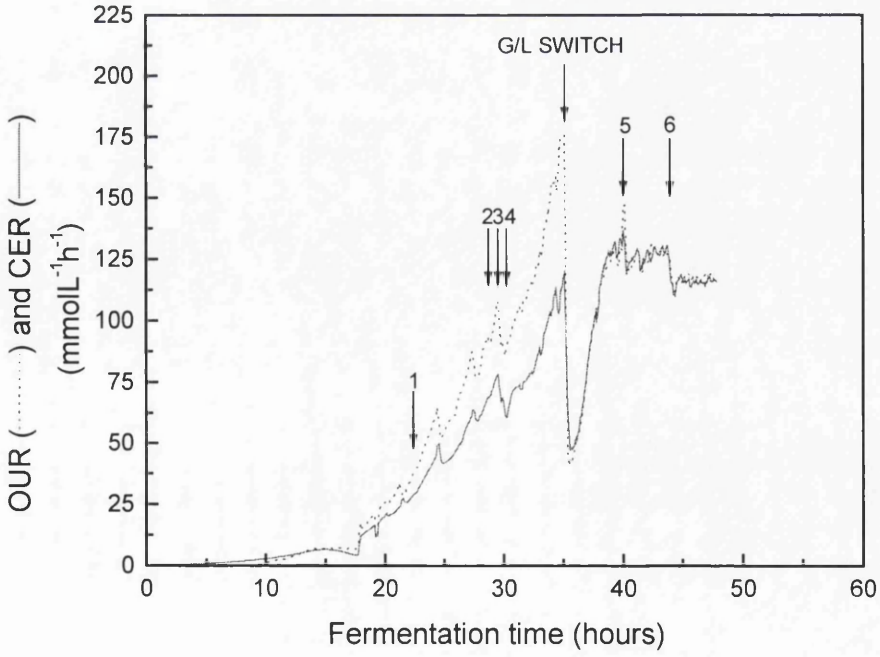

Figure 3.2.9 *Respiration profile showing carbon dioxide evolution rate and oxygen uptake rate for fermentation HCD 2. Additions as for Figure 3.2.8.*

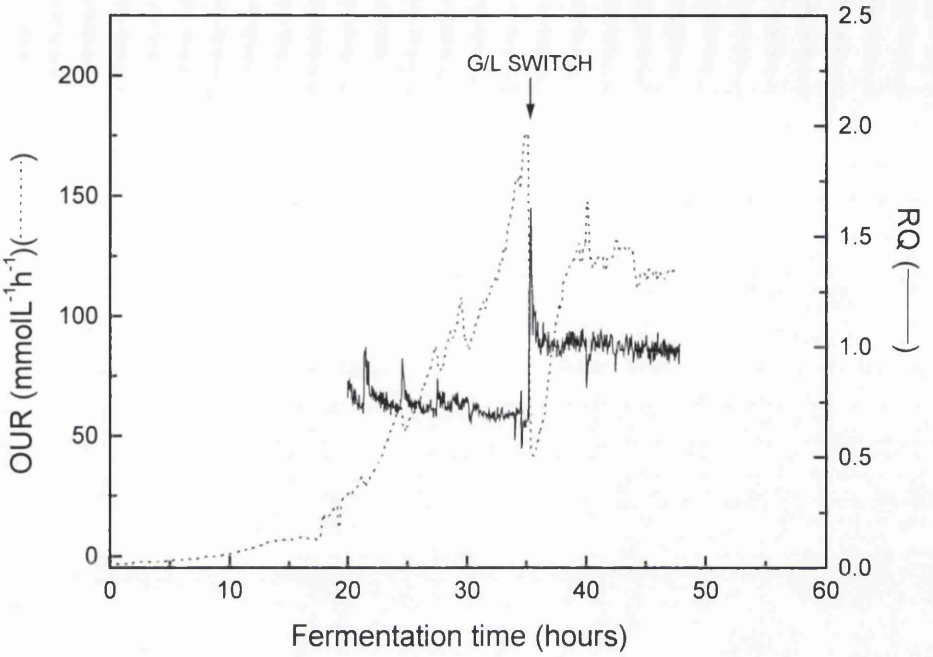

Figure 3.2.10 *Switch from glycerol to lactose metabolism during fermentation HCD 2, indicated by a drop in OUR and an increase in RQ from 0.7 (growth on glycerol) to 1.0 (growth on lactose). (Due to excessive noise resulting from inaccuracies in OUR and CER measurements, RQ over the period 0-20 hours is not shown). G/L SWITCH = glycerol/ lactose switch.*

The initial lag for HCD run 2 was estimated from OUR and DCW data to be approximately 10 hours. This is lower than the lag observed in LCD fermentations using an inoculum culture grown on defined medium and an inoculum volume of 2.5% (v/v). Thus increasing the inoculum volume to 10% (v/v) for the HCD appeared to further reduce the initial lag.

Specific growth rate for exponential growth on glycerol was calculated to be 0.14 h^{-1} based on OD and DCW data. This is lower than the equivalent figure for growth on glucose (0.22 h^{-1}) as expected from Korz *et al.,* 1995. The altered carbon source and batch feeding routine resulted in higher biomass; 33-40 g L^{-1} dry cell weight were routinely obtained (Table 3.2.2).

3.2.2.2 Fab' production

Fab' accumulation profiles were monitored following lactose addition in all HCD fermentations. The profile for run 2 is illustrated in Figure 3.2.11. This fermentation showed a considerable increase in titres compared to the LCD fermentations. Levels of periplasmic antibody reached 573 mg L^{-1} and extracellular antibody titres reached 105 mg L^{-1}. This appears to result from an increase in Fab' yield per unit biomass as well as an increase in total biomass. The maximum Fab' yield for the LCD fermentation was 13 mg Fab'$(gDCW)^{-1}$, compared to 18 mg Fab'$(gDCW)^{-1}$ for HCD run 2.

Accumulation of Fab' to high titres within the periplasmic space was also indicated by an SDS-PAGE gel showing periplasmic extracts prepared from samples taken throughout the induction period (Figure 3.2.12). Periplasmic extracts were prepared as described in section 2.2.1 with samples incubated in extraction buffer overnight at 60°C. SDS-PAGE was performed as described in section 2.2.3.2. The Fab' protein runs as a single band on the gel at a molecular weight of approximately 48kDa. A band at this molecular weight appears in lanes 6-11 of the gel (representing samples taken between 7 and 16 hours after the addition of lactose). The intensity of the band increases as induction continues indicating increasing Fab' concentration.

It is apparent from Figure 3.2.11 that induction of Fab' expression began after lactose addition but before the switch from glycerol to lactose metabolism. This is because Fab' is expressed from a *tac* promoter which is not subject to catabolite repression. It is also evident that Fab' titres were still increasing when the fermentation was stopped. HCD fermentations were terminated at 13 hours post carbon source switch despite the fact that Fab' was generally still accumulating. This is because the aim was not to produce the highest titres of antibody possible, but simply to produce biomass with suitable levels of antibody for detection in downstream processing studies.

In addition to high antibody titres, the HCD fermentations also showed considerably reduced leakage of periplasmic material into the external medium (Table 3.2.2). Three of the four fermentations showed over 80% retention of material in the periplasmic space throughout the induction period. The reduced leakage was thought to result from a combination of changes made to the initial LCD protocol, including the addition of calcium and magnesium salts prior to induction, reduced phosphate concentration and reduced growth temperature during induction.

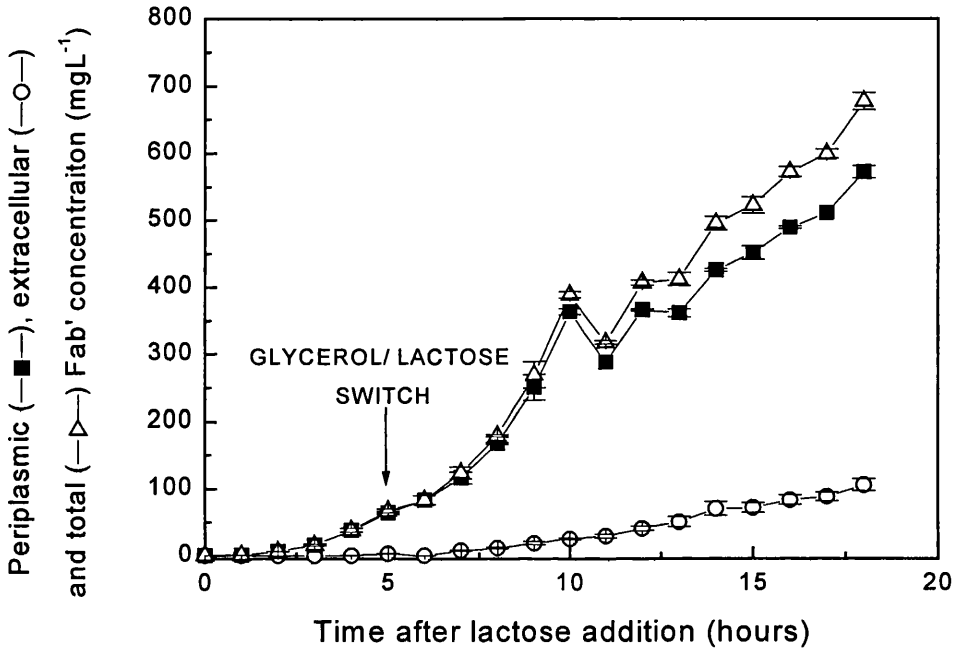

Figure 3.2.11 *Periplasmic, extracellular and total Fab' accumulation during fermentation HCD 2. Fab' concentrations determined by ELISA. Error bars represent standard deviations determined from multiple dilutions of duplicate samples.*

As with LCD fermentations, the HCD fermentations showed consistent levels of cell growth but notable variation in product titres (Table 3.2.2). Again, variations in titres are likely to result from differences in inoculum cultures and slight variations in the operating conditions of individual fermentations. In addition, the use of different Fab' standards for calibration of ELISA assays was thought to contribute towards the variation in measured titres.

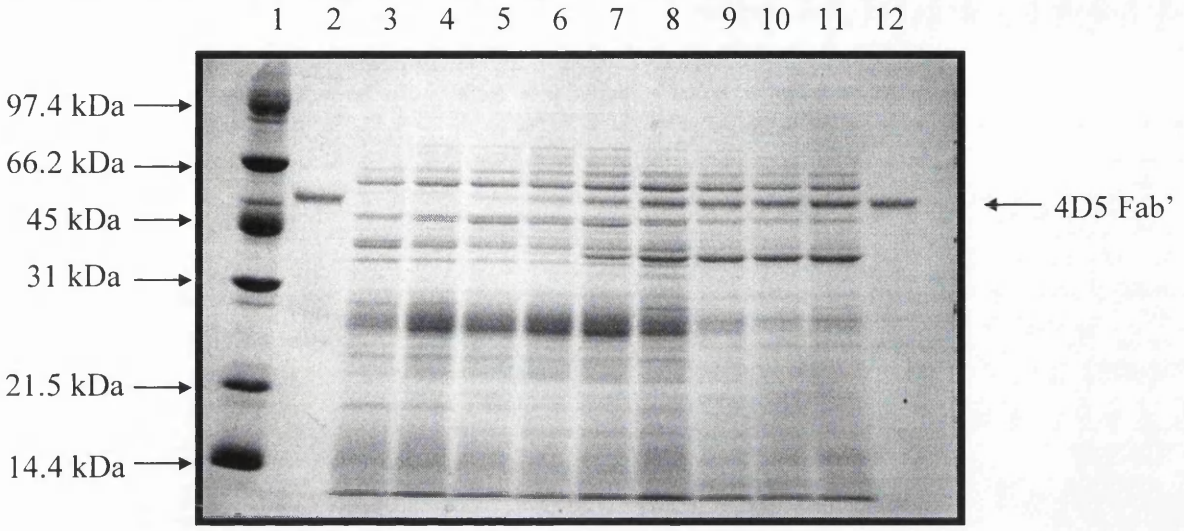

Figure 3.2.12 *SDS-PAGE gel showing Fab' accumulation within the periplasm during the induction phase of HCD fermentation. Periplasmic fractions obtained by overnight incubation in extraction buffer at 60 ℃.*

Lane 1 Low molecular weight markers
Lane 2 Purified 4D5 Fab' standard

Lanes 3-11 Periplasmic samples at the following time intervals after lactose addition:

Lane 3 0 hours
Lane 4 3 hours
Lane 5 5 hours
Lane 6 7 hours
Lane 7 9 hours
Lane 8 11 hours
Lane 9 13 hours
Lane 10 15 hours
Lane 11 16 hours

Lane 12 Purified 4D5 Fab' standard

The effects of methods employed for standard preparation on quality of the standards and on assay calibration are discussed in Chapter 7. In summary, two different Fab' standards were used for ELISA calibration during the assay of fermentation samples. The initial standard, used for quantification of Fab' titres in LCD fermentations and HCD runs 1 and 2, was later found to contain a considerable proportion of incomplete or partially degraded Fab'. The consequence of using such a standard would have been to overestimate the Fab' concentration in unknown samples. Alterations made to the production protocol allowed the preparation of an improved quality standard, used in the assay of samples from HCD runs 3 and 4. Thus, titres in the later HCD runs are considered to be more accurate, but should not be directly compared with previous fermentations. Because the same standard was used for assay calibration during the analysis of samples from LCD fermentations and HCD run 2, it is felt that comparisons of titres between these fermentations are valid.

3.2.2.3 Effect of calcium and magnesium on periplasmic retention

During the latter stages of this project a fermentation was carried out with the aim of increasing leakage into the extracellular broth to allow recovery of both extracellular and periplasmic material (section 4.2.5). In order to try and achieve this, a fermentation was carried out at 10L scale following the protocols described for the HCD fermentations, but with the omission of the calcium and magnesium addition prior to induction (fermentation HCD 5). This allowed the effect of calcium and magnesium addition on periplasmic retention to be assessed.

The fermentation showed similar characteristics to previous HCD fermentations with biomass levels reaching 38 g L^{-1} (DCW). Fab' accumulation was monitored for 18 hours following the carbon source switch (it was envisaged that during the latter stages of induction leakage would increase, as in LCD fermentations, and hence higher concentrations of extracellular Fab' would be attained). However it is evident from the Fab' accumulation profile (Figure 3.2.13) that omission of the calcium and magnesium addition did not have a major effect on Fab' distribution. Following 13 hours induction, 71% of the total Fab' was located in the periplasm, and by the end of

the fermentation (18 hours after the glycerol/ lactose switch) the proportion of periplasmic antibody had barely changed at 73%. This compares to an average of 80% retention of periplasmic material following 13 hours induction for standard HCD fermentations.

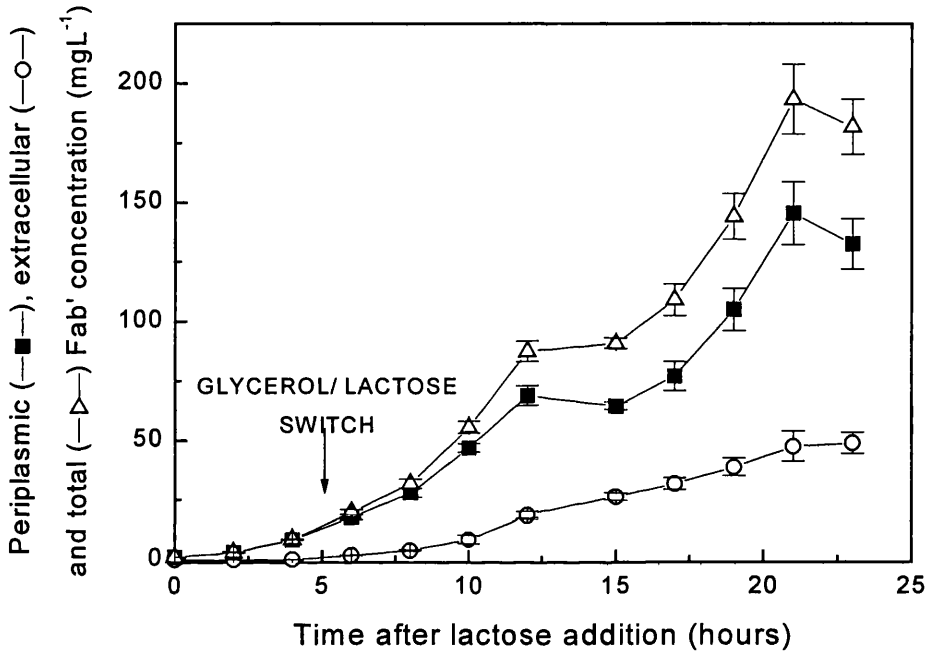

Figure 3.2.13 *Effect of omission of the calcium and magnesium addition prior to induction on distribution of Fab' between the periplasm and the extracellular broth during the induction phase of HCD fermentation. Fab' concentrations determined by ELISA. Error bars represent standard deviations determined from multiple dilutions of duplicate samples.*

Thus, despite the fact that calcium and magnesium ions form an integral part of the *E. coli* outer membrane (Vaara, 1992), it would appear that the addition of calcium and magnesium salts prior to induction was not singularly responsible for the increased retention of material within the periplasmic space observed with the HCD fermentations.

3.2.3 Fermentation scale up

In order to produce sufficient material for the large scale downstream processing experiments, it was necessary to operate the fermentation at increased scale. Rather than carrying out a detailed investigation into fermentation scale up, the aim was simply to increase the scale of the fermentation following the protocol designed at 10L as closely as possible. This allowed identification of a number of the problems associated with the large scale operation of such a protocol. The work described was carried out in collaboration with N. Murrell (Department of Biochemical Engineering, University College London).

The HCD fermentation was scaled up initially to 87L (initial working volume) in a 150L fermenter and later operated at 260L (initial working volume) in a 450L fermenter. Details of inoculum preparation for both scales of operation are given in section 2.1.4.2. Because of fermenter availability at the time, it was necessary to use a smaller inoculum volume (6% instead of 10%). To compensate for the decreased volume, inoculum cultures were grown to a higher optical density ($OD_{600} \approx 6$) compared to the 10L fermentations ($OD_{600} \approx 3$).

Growth media for the large scale fermentations was identical to that used at 10L with one alteration; the phosphate concentration was increased from 24 mmol to 30 mmol. As explained in section 3.2.2, phosphate concentration was lowered for the HCD fermentations to aid plasmid stability and help retain material within the periplasmic space. The medium was designed such that the phosphate would become depleted during the stationary phase. This improves plasmid stability by preventing growth of plasmid free cells which arise during the later stages of the fermentation. Studies performed at Celltech Chiroscience Limited (Slough, UK) illustrated that higher concentrations of phosphate were required to support the same level of growth at increased scale, although the reason for this was not known (personal communication, N. Weir). Therefore the phosphate concentration was increased to avoid any potential problems associated with phosphate limitation on scale up.

Three fermentations were operated at 150L scale and one at 450L. Similar results were obtained at both scales of operation, therefore only the data from the 450L fermentation will be discussed.

3.2.3.1 Fermentation characteristics

Aeration and respiration profiles for the 450L fermentation are shown in Figures 3.2.14 and 3.2.15. It is evident from the aeration profile that the culture was oxygen limited for short periods both prior to the carbon source switch and during lactose metabolism. This was due to higher oxygen demands and the reduced aeration capacity of the fermenter compared to the small scale fermentations. Higher oxygen demands are shown by the increase in maximum OUR, which peaked 3½ hours after the carbon source switch at ~220 $mmolL^{-1}hr^{-1}$. This compares to a maximum OUR of 175 $mmolL^{-1}hr^{-1}$ just prior to glycerol depletion for the 10L HCD fermentations. In order to try and satisfy oxygen demands, it was necessary to operate the fermentation under a head pressure of ~1 bar.

Growth and product accumulation profiles for the 450L fermentation are illustrated in Figure 3.2.16. The maximum specific growth rate was calculated at 0.22 h^{-1} from DCW data, and biomass levels of 48 g L^{-1} were attained. Both these figures are higher than the equivalent values recorded for small scale fermentations. At 10L scale, the maximum specific growth rate was ~ 0.14 h^{-1}, and biomass levels of 33-40 g L^{-1} were routinely achieved. Growth in the small scale fermentations is thought to be limited by phosphate availability. Phosphate concentration in the initial growth medium for the large scale fermentations was increased to support the same level of growth at scale. However, the results suggest the increased phosphate allowed growth to higher biomass. Evidence for this is provided by the 450L OUR data which shows both a higher maximum oxygen demand compared to the 10L fermentations, and an increase in oxygen utilisation after the carbon source switch, indicating continued culture growth. In the 10L fermentations growth was limited from the onset of lactose metabolism.

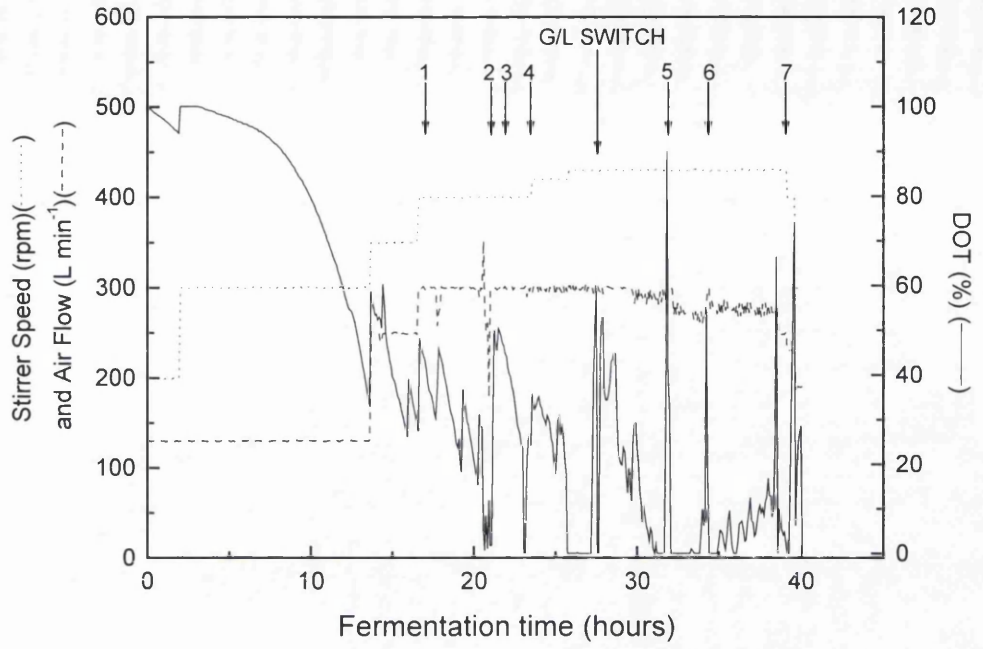

Figure 3.2.14 *Aeration profile showing changes in dissolved oxygen tension during 450L fermentation and effects of changing stirrer speed and airflow. Additions were as follows: 1. 30 g L^{-1} glycerol; 2. 20 g L^{-1} glycerol; 3. 14.4 mM $MgSO_4$ and 1.7 mM $CaCl_2$; 4. 10 g L^{-1} glycerol and 45 g L^{-1} lactose; 5, 6 and 7. 22.5 g L^{-1} lactose; G/L SWITCH = glycerol/ lactose switch.*

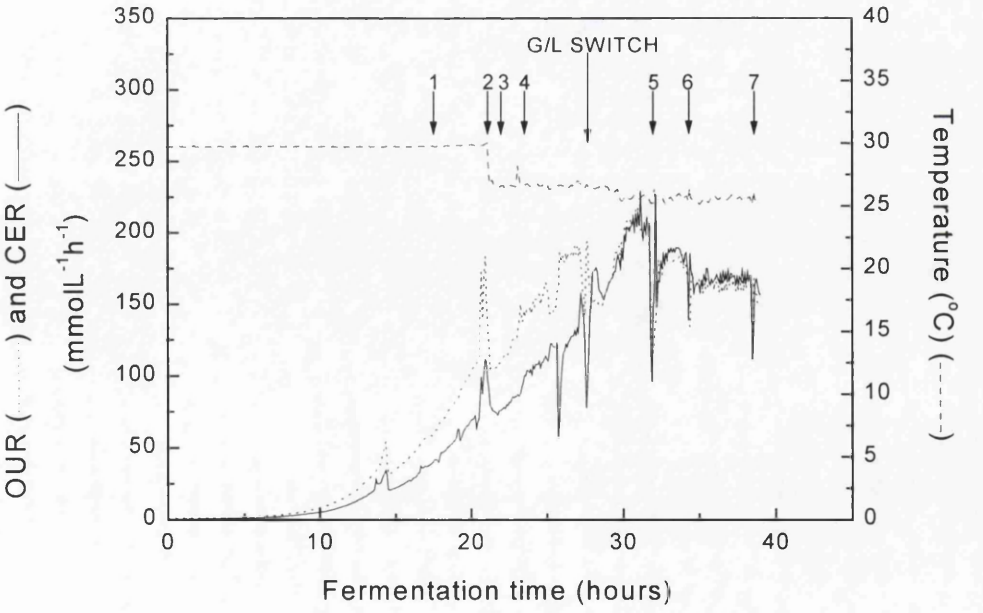

Figure 3.2.15 *Temperature and respiration profile showing oxygen uptake rate and carbon dioxide evolution rate during 450 L fermentation. Additions as for Figure 3.2.14.*

During the induction phase of the 450L fermentation Fab' levels accumulated to titres of 100 mg L^{-1}. Titres can be compared to those obtained for HCD fermentations 3 and 4 as the same Fab' standard was used for ELISA calibration. Antibody titres in the 450L fermentation were approximately half those achieved at 10L. Slower rates of antibody accumulation may result from the reduced growth temperature during induction (shown in Figure 3.2.15); problems with the controller caused the temperature to fluctuate between 25 and 26°C instead of being maintained at 27°C as for the small scale fermentations. Alternatively, reduced plasmid stability caused by the increased growth rate or use of a higher phosphate concentration may have had an effect.

Distribution of Fab' between the periplasm and the extracellular medium throughout the induction period is illustrated in Figure 3.2.17. As with the 10L fermentations, good control of product location was achieved, with 78% Fab' retained within the periplasm following 13 hours induction. Contradictory results were obtained by researchers at Celltech Chiroscience Limited, who found that increasing the phosphate concentration at large scale resulted in increased leakage of periplasmic material into the extracellular broth (personal communication, N. Weir). The effect of scale on product location was not investigated further. However, the ability to control product location at increased scale is essential for efficient process operation; if successful periplasmic retention cannot be achieved it may be necessary to employ processes for the recovery of extracellular material. Methods for the recovery of both extracellular and periplasmic product are described in Chapter 4, and are compared to the more traditional processing route for the recovery of purely periplasmic product in Chapter 8.

Additional problems associated with operating the fermentation at increased scale were identified. These include maintaining large quantities of lactose in solution, foaming following lactose addition and temperature control problems during the 150L fermentation (where the cooling capacity of the fermenter was insufficient to reduce the culture growth temperature to 27°C during the induction phase).

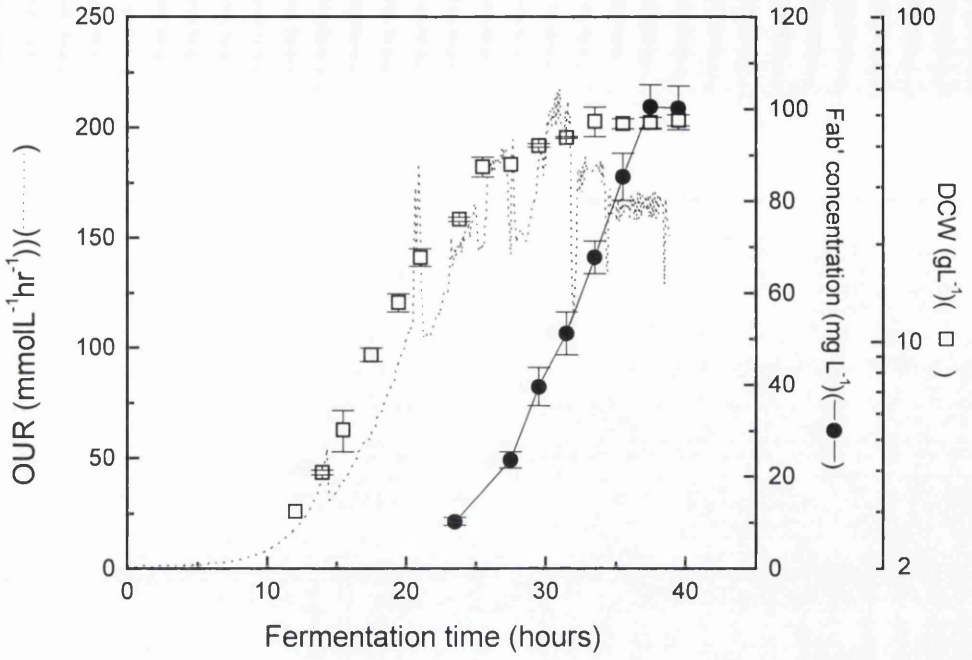

Figure 3.2.16 *Growth and Fab' accumulation profiles for 450L fermentation. Growth indicated by oxygen uptake rate (OUR) and dry cell weight (DCW) data. Error bars represent the standard deviation of duplicate measurements (DCW data) or the standard deviation determined from multiple dilutions of duplicate samples (ELISA data).*

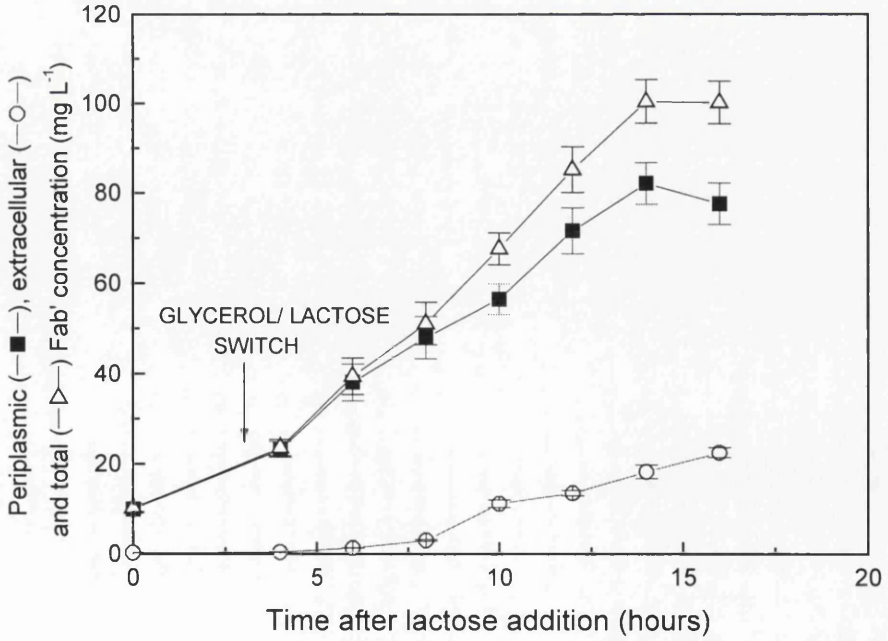

Figure 3.2.17 *Periplasmic, extracellular and total Fab' accumulation during 450L fermentation. Fab' concentrations determined by ELISA. Error bars represent standard deviations determined from multiple dilutions of duplicate samples.*

3.2.4 Harvest of fermentation material for use in downstream processing studies

Biomass produced during fermentations HCD4, HCD5, 150L2 and 450L was harvested for use in downstream processing studies. Methods for the centrifugal cell harvest are given in section 2.1.5. All cell paste was stored at -70°C until required for use in downstream processing trials. The properties of each batch of fermentation material and details of the experiments for which each batch was used are given in Appendix 2.

3.3 Summary

Two fermentation protocols for the production of 4D5 Fab' have been characterised. Using the original 'low cell density' protocol, biomass levels of 14-16 g(DCW) L^{-1} were achieved with Fab' titres reaching 175 mg L^{-1} following 15 hours induction. However, over 60% of the Fab' had leaked from the periplasmic space into the fermentation broth by the end of the fermentation.

As this project focuses on the recovery of periplasmic material, the fermentation protocol was modified with the aim of enhancing periplasmic retention. The changes made to the original protocol include alteration of the initial carbon source from glucose to glycerol and batch feeding of the glycerol, use of a phosphate limited growth medium, addition of calcium and magnesium prior to induction and reduction in the growth temperature for the induction period.

This combination of changes gave a higher cell density fermentation with biomass levels of 33-40 g(DCW) L^{-1} routinely achieved. However, increased levels of biomass resulted in greater oxygen demands with the risk of the fermentation becoming oxygen limited when demands were highest, just prior to the carbon source switch.

Fab' titres also increased to ~680 mg L^{-1} following 13 hours induction. Improved titres appeared to result from an increase in specific antibody production in addition to higher total biomass. More importantly, over 80% of product was retained within the periplasm at the end of the fermentation.

The specific factors responsible for increasing periplasmic retention were not identified, however omission of the calcium and magnesium addition prior to induction did not result in an increase in product leakage, suggesting that the salt addition alone is not singularly responsible for the increased periplasmic retention.

The high cell density fermentation was scaled up to 450L. Operation at large scale resulted in higher specific growth rate, increased oxygen demands and oxygen limitation. Fab' titres recorded at large scale were approximately half those obtained at 10L, thought to be due to either the reduced growth temperature or reduced plasmid stability. However, tight control of product location was maintained, with 70% of material retained within the periplasm following 15 hours induction.

In addition to oxygen limitation, problems associated with large scale operation of the fermentation include difficulties maintaining large quantities of lactose in solution, foaming following lactose addition and poor temperature control. Such problems will prove increasingly significant on further scale-up.

4. PERIPLASMIC EXTRACTION

4.1 Introduction

Periplasmic extraction is the process by which product is released from cells following cell harvest at the end of the fermentation. The aim of the extraction process is to release selectively periplasmic material whilst maintaining cell integrity so that the process stream does not become contaminated with intracellular material such as proteases, DNA or lipids which may degrade the product or cause problems in subsequent stages of purification.

General methods for the selective release of periplasmic material from bacterial cells have been reviewed in Chapter 1. A novel technique for the extraction of periplasmic antibody fragments has recently been developed by Weir and Bailey (1997). The technique involves suspension of cells in a Tris-EDTA extraction buffer at elevated temperature for periods of up to 24 hours. The Tris and EDTA act synergistically in permeabilising the outer membrane of *E. coli* and the elevated temperature both enhances periplasmic release and degrades contaminating *E. coli* proteins, thereby purifying the process stream. However, little data is available regarding the kinetics of antibody release and protein degradation or the effect of scale on the extraction process.

The Tris-EDTA extraction could potentially be performed on whole fermentation broth to allow recovery of both extracellular and periplasmic product. This could significantly increase product yields in processes where control of product location is difficult to achieve, and has the additional advantage of removing the requirement for a cell harvest step following fermentation.

This chapter aims to characterise the effects of temperature, time and scale of operation on the periplasmic extraction of 4D5 Fab' from *E. coli* strain W3110 using the Tris-EDTA extraction method developed by Weir and co-workers. In section 4.2.1 the thermal stability of purified 4D5 Fab' is assessed to determine the highest temperature at which the extraction process can be operated. Section 4.2.2 examines

the effect of temperature on Fab' release, purification of the process stream, quality of Fab' and process stream viscosity following 16 hour extraction at laboratory scale. The kinetics of antibody release and protein denaturation are analysed in section 4.2.3. Section 4.2.4 examines the effect of increasing scale on the rate of antibody release and protein degradation. Finally, the extraction process is performed on whole fermentation broth in section 4.2.5 and a comparative analysis of periplasmic and whole broth extraction is made.

4.2 Results and discussion

4.2.1 Thermal stability of 4D5 Fab'

The thermal stability of 4D5 Fab' was assessed to determine the highest temperature at which the extraction process could be performed. A sample of purified 4D5 Fab' (obtained from Celltech Chiroscience Ltd) was initially shown to consist of entirely complete, disulphide bonded 4D5 Fab' by SDS-PAGE analysis (data not shown). The purified Fab' was diluted to a concentration of ~100 μg mL^{-1} in periplasmic extraction buffer (100 mM Tris HCl pH 7.4, 10 mM EDTA) at a range of temperatures for up to 8 hours. 2 mL samples of the diluted antibody were incubated in Eppendorf tubes in water baths at 30°C, 45°C, 60°C, 70°C and 80°C. 200 μL samples were removed at regular intervals for assay by ELISA. Because of the nature of the ELISA assay it was not possible to assay samples immediately, therefore all samples were stored overnight at 4°C and assayed together the following day. It was assumed that denaturation of the antibody would be detected by a reduction in the concentration measured by ELISA.

No decrease in concentration recorded by ELISA was observed over the 8 hour period for samples incubated at 30°C and 45°C. Figure 4.2.1 shows the results for samples incubated at 60°C, 70°C and 80°C. The graph shows that the Fab' was stable for 8 hours at 60°C and 70°C, however at 80°C the antibody fragment was degraded. Over 70% of the antibody fragment was denatured after one hour at this temperature, with no detectable antibody remaining after 8 hours incubation.

The stability of Fab' to temperature in the presence of cells was also assessed. Purified Fab' was spiked into a suspension of control cells obtained from another *E. coli* fermentation (*E. coli* strain BMH 71-18 which does not produce 4D5 Fab', supplied by D. Bracewell, Department of Biochemical Engineering, UCL). Cells were suspended in periplasmic extraction buffer to a concentration of 0.14 g L^{-1} (the standard cell concentration used during periplasmic extraction). 2 mL samples were again incubated in Eppendorf tubes in water baths maintained at 30°C, 45°C, 60°C, 70°C and 80°C. 200 μL samples removed at intervals were spun in a microfuge at 13 000 rpm for 5 minutes to pellet the cells and the supernatant was assayed for Fab' concentration by ELISA. Again, no Fab' degradation was observed at 30°C or 45°C. The results for incubations at 60°C, 70°C and 80°C are illustrated in Figure 4.2.2.

The results show the Fab' to be stable over an 8 hour period at 60°C, however the stability in the presence of cells at 70°C and 80°C was significantly reduced compared to the purified antibody fragment. It is assumed that a certain degree of 'unfolding' of the antibody fragment occurs at these higher temperatures. In purified form the Fab' then renatures as the solution is cooled. When cells are present it is likely that hydrophobic regions of the Fab' which are exposed as the protein unfolds at higher temperatures 'stick' to the hydrophobic cell walls and are taken down into the cell pellet when the samples are centrifuged.

The proportion of detectable Fab' in the sample incubated at 70°C decreased to ~30% of the original concentration over the first three hours of incubation and then remained at 30% for the next five hours. This suggests the Fab' preparation consists of a population of fragments differing in their thermal stability. At 70°C a proportion of the fragments are sufficiently stable to remain folded in such a way that they do not bind to the cells and hence remain in the supernatant when the samples are centrifuged.

The results of the stability experiments indicate that of the temperatures tested, the highest the extraction process can be effectively operated at is 60°C.

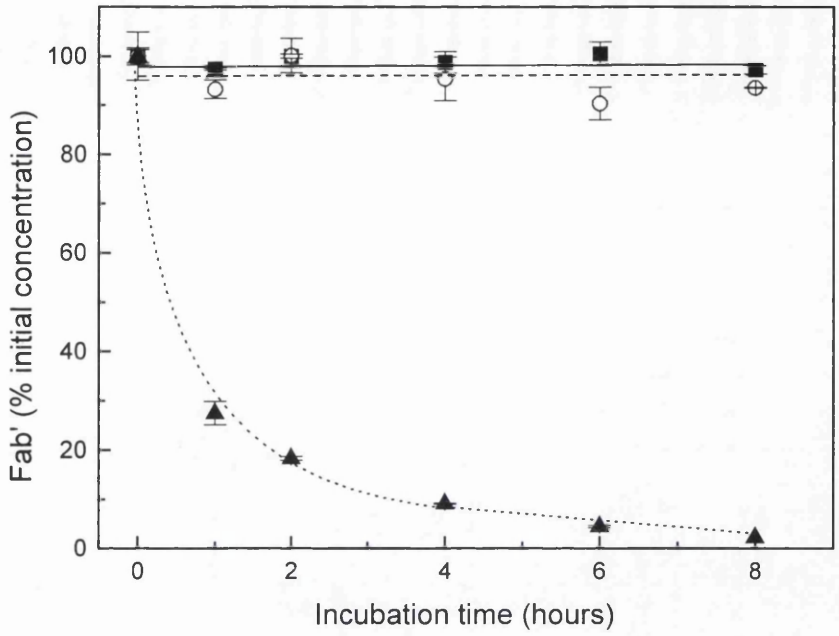

Figure 4.2.1 *Thermal stability of 4D5 Fab' diluted in periplasmic extraction buffer. Samples were incubated at 60℃ (–■–), 70℃ (--O--) and 80℃ (···▲···). Concentrations were determined by ELISA and converted to % initial concentration. Error bars represent the standard deviation of multiple sample analyses.*

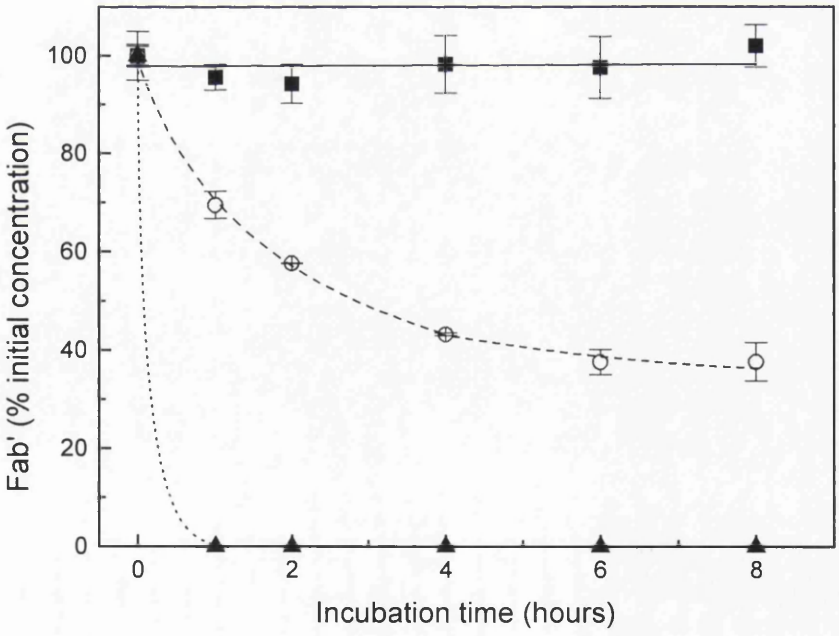

Figure 4.2.2 *Thermal stability of 4D5 Fab' spiked into E. coli cells suspended in periplasmic extraction buffer. Samples were incubated at 60℃ (–■–), 70℃ (--O--) and 80℃ (···▲···). Concentrations determined by ELISA and converted to % initial concentration. Error bars represent the standard deviation of multiple sample analyses.*

4.2.2 Characterisation of periplasmic release

The periplasmic extraction process was initially characterised in terms of the effect of temperature on Fab' release, protein degradation and process stream viscosity following overnight extraction at laboratory scale (75 mL). Cells (harvested from HCD fermentation 4, section 3.2.2, and stored at -70°C) were resuspended in 200 mL periplasmic extraction buffer at a concentration of 0.14 g mL^{-1}. Following complete resuspension, a 1 mL sample was centrifuged (5 minutes at 13 000 rpm) and the supernatant assayed to determine the initial extracellular protein and Fab' concentration. In addition, a 50 mL sample of the cell suspension was homogenised (section 2.4.4.1) and the supernatant assayed to allow determination of total cellular protein and total Fab' available for release. The remaining cell suspension was divided between two sealed 200 mL shake flasks, one of which was incubated in an orbital shaker at 30°C and 250 rpm while the other was incubated in a hot water bath maintained at 60°C, also with agitation at 250 rpm. Following incubation for 16 hours, 1 mL samples of each spheroplast suspension were centrifuged and the supernatant assayed to ascertain the extracellular Fab' and protein concentrations following extraction. The remaining suspensions were each divided into two; one half was homogenised for determination of total Fab' and protein at the end of the extraction procedure, whilst the other half was used for measurement of viscosity as described in section 2.2.5.

The results of the extraction experiment are shown in Table 4.2.1. Extremely good recovery of Fab' was observed at both temperatures, with 94% Fab' released by overnight periplasmic extraction at 30°C, compared to 85% for extraction at 60°C. The reduced Fab' recovery at 60°C was thought to be primarily due to Fab' degradation. Both recovery figures were based on total Fab' available for release measured in a homogenised sample at the beginning of the extraction procedure. Samples of cell suspension were also taken following 16 hours extraction and homogenised to determine total Fab' remaining at the end of extraction. The initial and final Fab' concentrations were within error for samples extracted at 30°C, however during this and subsequent experiments, a 10-15% decrease in total Fab'

was consistently observed following overnight extraction at 60°C. The reduction in total Fab' was thought to be due to the presence of free Fab' heavy and light chain which associate in solution and are therefore recorded by ELISA in the initial homogenised sample, but which are degraded by the high temperature extraction. Evidence for degradation of free heavy and light chain is presented below, however with the assays available it was not possible to quantify precisely and therefore distinguish between degradation of free heavy and light chain and degradation of complete Fab'. Quantification of Fab' variants within a sample could be achieved by quantitative Western blotting, HPLC or biosensor analysis. However, the appropriate assays were not developed during the course of this study.

Extraction temperature	30°C	60°C
% Fab' recovery	94	85
Specific Fab' (mg(Fab') mg(protein)$^{-1}$)	0.073	0.27
Purification factor	2.5	9.2
Viscosity (mPaS)	1.7	1.7

Table 4.2.1 *Effect of extraction temperature on Fab' recovery, purification of the process stream and process stream viscosity during periplasmic extraction. Cells were incubated in periplasmic extraction buffer at 30℃ or 60℃ and 250 rpm for 16 hours.*

The % Fab' recovery is specifically the extracellular Fab' concentration at the end of the extraction process expressed as a percentage of the total Fab' available for release, measured in a homogenised sample taken at the beginning of extraction. The specific Fab' is the extracellular Fab' concentration divided by the extracellular protein concentration at the end of extraction. The purification factor is the specific Fab' measured at the end of extraction divided by the specific Fab' recorded at the beginning of extraction.

The major difference between the two extraction temperatures relates to the degradation of contaminating protein observed at the higher temperature. This is illustrated by the difference in specific Fab' at the end of the extraction process, and the higher purification factor (PF) for the 60°C extraction (PF = 9.2) compared to extraction at 30°C (PF = 2.5). (Purification factor is defined as the specific Fab' concentration (mg Fab'/ mg protein) at the end of the extraction process divided by the specific Fab' concentration at the beginning of extraction).

The reduction in concentration of contaminating protein in the extracellular fractions is thought to result from denaturation of the proteins at high temperature. The proteins partially unfold as they denature, exposing hydrophobic regions which interact with the hydrophobic bacterial cell wall. The denatured proteins are consequently pelleted with the cells during centrifugation. The reduction in soluble protein is also evident from an SDS-PAGE gel comparing total protein in extracellular samples taken at the end of each extraction process (Figure 4.2.3). The higher protein concentration following extraction at 30°C is shown by the more intense staining and increased number of protein bands in lane 3 of the gel (30°C extract) compared to lane 4 (60°C extract).

Western blotting (section 2.3.4.1) of the gel shown in Figure 4.2.3 to reveal the Fab' light chain gave two major bands (Figure 4.2.4(a)). The band of higher molecular weight (~48 kDa) represents assembled Fab' and the second band at ~23 kDa reveals free light chain. Although not strictly quantitative, the Western blot indicates that significant free light chain was present in the 30°C extract whereas at 60°C free light chain was denatured whilst the assembled Fab' remained intact. A similar effect is shown in a blot probed for Fab' heavy chain (Figure 4.2.4(b)). Although some free heavy chain was still present in the 60°C periplasmic extract, the amount was significantly decreased compared to extraction at 30°C. As explained previously, the free heavy and light chain degraded by the high temperature extraction assemble in solution and therefore would have been detected in a pre-extraction sample. Degradation of free heavy and light chain may therefore account for some, if not all the observed Fab' degradation during extraction at 60°C.

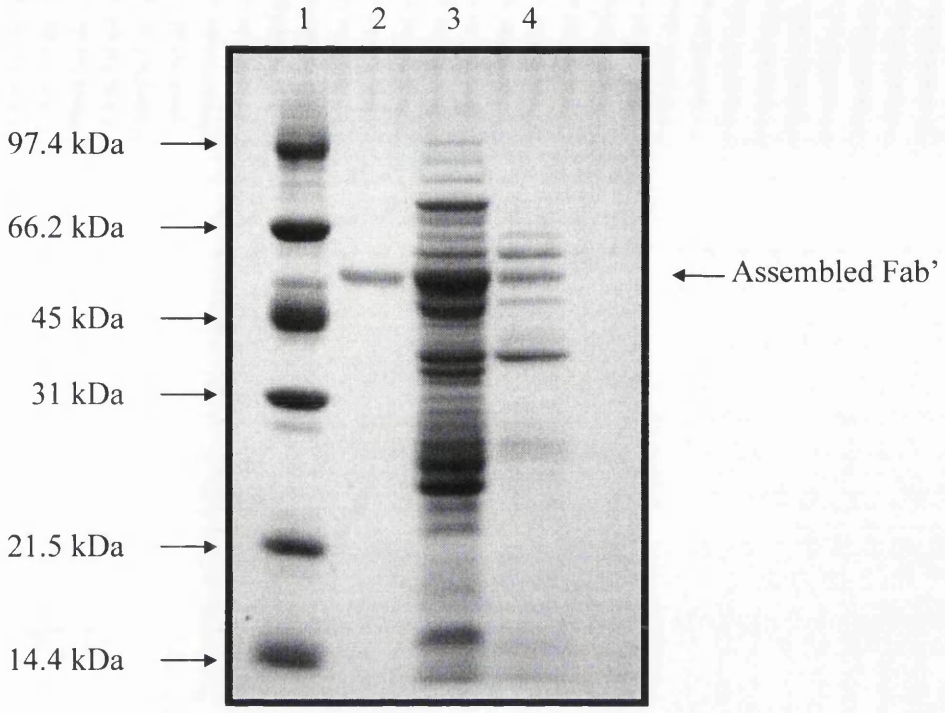

Figure 4.2.3 *SDS-PAGE gel showing the effect of periplasmic extraction temperature on purification of the process stream.*

Lane 1 Low molecular weight markers
Lane 2 Purified 4D5 Fab' standard
Lane 3 Extracellular protein following overnight extraction at 30℃
Lane 4 Extracellular protein following overnight extraction at 60℃

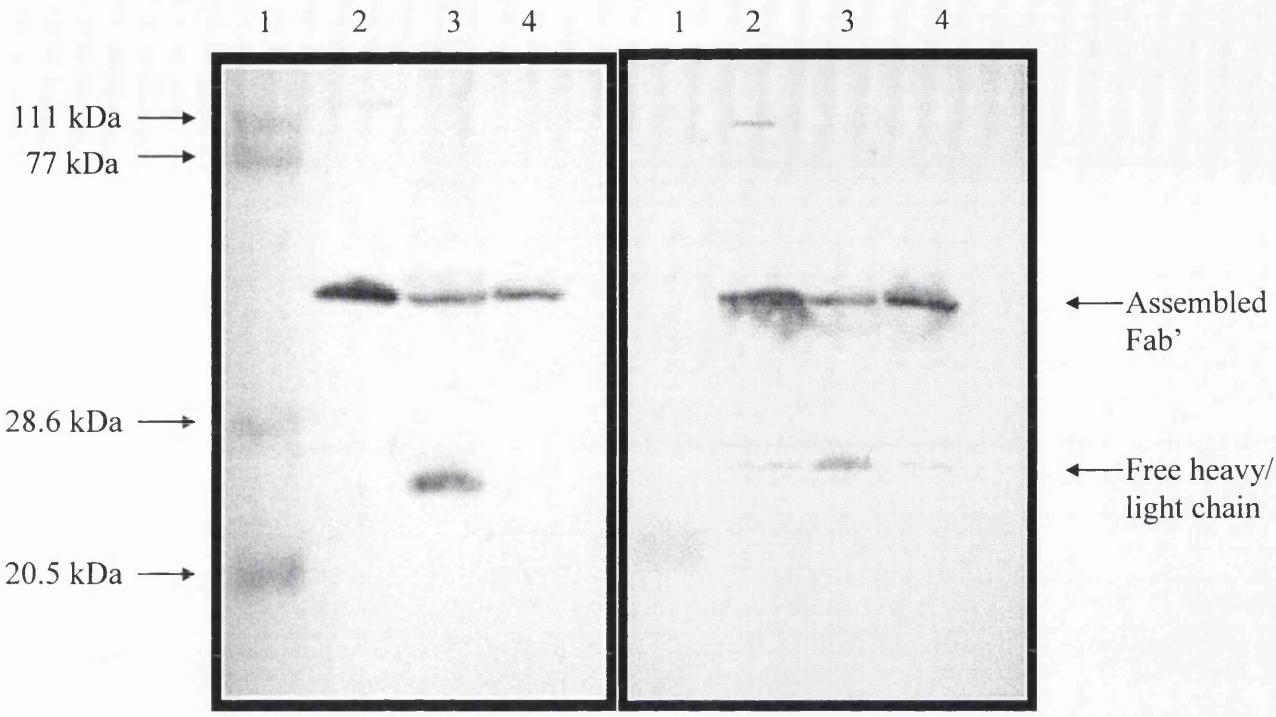

Figure 4.2.4 *Western blots showing effect of periplasmic extraction temperature on presence of free Fab' heavy and light chain in the process stream.*

(a) Western blot probed for 4D5 Fab' light chain

Lane 1 Prestained low molecular weight markers
Lane 2 Purified 4D5 Fab' standard
Lane 3 Periplasmic extract following overnight incubation at 30℃
Lane 4 Periplasmic extract following overnight incubation at 60℃

(b) Western blot probed for 4D5 Fab' heavy chain.

Lane 1 Prestained low molecular weight markers
Lane 2 Purified 4D5 Fab' standard
Lane 3 Periplasmic extract following overnight incubation at 30℃
Lane 4 Periplasmic extract following overnight incubation at 60℃

Fab' released by overnight periplasmic extraction at 30°C and 60°C was purified on a protein A column (as described in section 2.4.3.1) to assess the effect of extraction temperature on quality of the Fab' preparation following affinity purification. An SDS-PAGE gel showing column load and eluate for 30°C and 60°C extracts is shown in Figure 4.2.5. It is clear from the number of bands in lane 4 of the gel that a large proportion of incorrectly assembled, incomplete or partially degraded Fab' was present in the 30°C extract and was co-purified with the complete Fab' by protein A affinity chromatography. This material was degraded by overnight extraction at 60°C and thus affinity purification of Fab' from 60°C extracts gave a much purer Fab' preparation (shown by the presence of predominantly assembled Fab' with only a small proportion of free heavy and light chain in lane 6 of the gel). (Western blot analysis identified all bands in lanes 4 and 6 as Fab' related material, data not shown). This highlights another advantage of high temperature extraction: degradation of incomplete or incorrectly assembled Fab' which would otherwise be co-purified with the complete Fab' by protein A chromatography.

Finally, Fab' may be purified from periplasmic extracts either by packed bed affinity chromatography following spheroplast removal by centrifugation or by expanded bed affinity purification directly from the whole spheroplast suspension. Performance of the expanded bed is affected by viscosity of the process stream and therefore the viscosity of the spheroplast suspension following overnight extraction at 30°C and 60°C was measured. The results, given in Table 4.2.1, show that extraction temperature had no effect on process stream viscosity. The viscosity of both spheroplast suspensions following extraction was only slightly higher than that of water, at 1.7 mPaS.

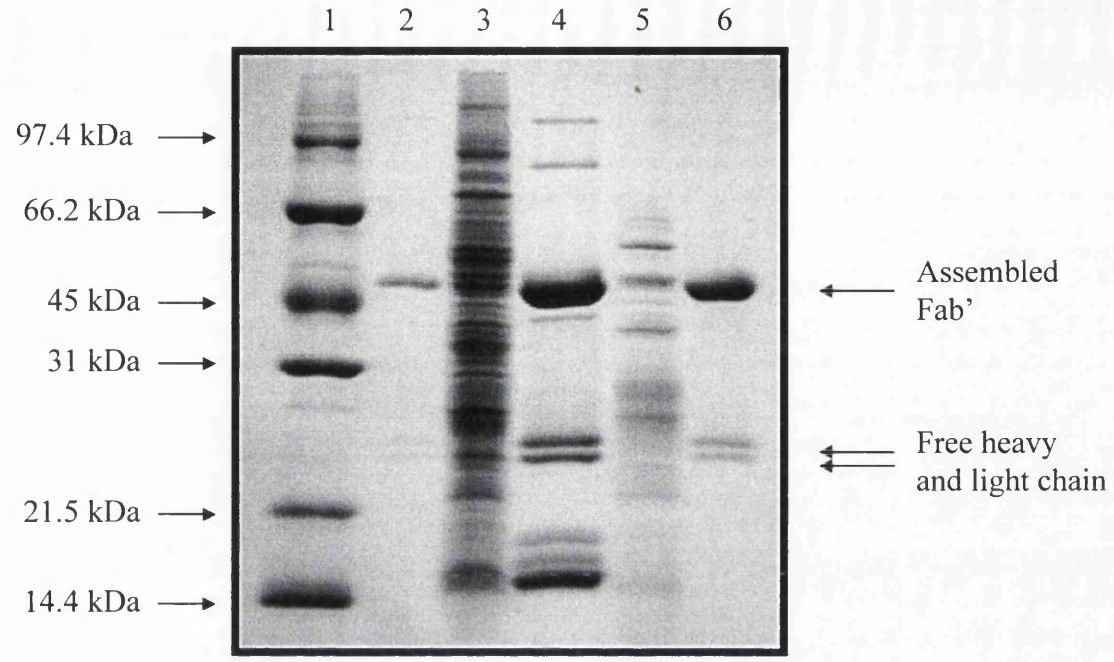

Figure 4.2.5 *SDS-PAGE gel showing effect of periplasmic extraction temperature on purity of the process stream before and after protein A affinity purification of 4D5 Fab' from periplasmic extracts.*

Lane 1 Low molecular weight markers
Lane 2 Purified 4D5 Fab' standard
Lane 3 Periplasmic extract following overnight incubation at 30℃ (Column load)
Lane 4 Fab' preparation purified from 30℃ periplasmic extracts (Column eluate)
Lane 5 Periplasmic extract following overnight incubation at 60℃ (Column load)
Lane 6 Fab' preparation purified from 60℃ periplasmic extracts (Column eluate)

4.2.3 Kinetics of Fab' release and protein degradation

Fab' release and protein degradation were monitored during periplasmic extraction to gain an indication of the time scale of these events. Cells (harvested from HCD fermentation run 4) were resuspended in 65 mL periplasmic extraction buffer or PBS (control) at a concentration of 0.14 g mL^{-1}. The buffers were heated to the required temperature prior to resuspension. Resuspension was achieved by rapid mixing in a 100 mL Duran bottle for 15 minutes. Following resuspension, cells were incubated in 100 mL stirred tanks for up to 5 hours at temperatures of 30°C, 45°C and 60°C. Dimensions of the tanks and agitators are given in section 2.4.1.2. The temperature in the tanks was maintained to within ±2°C by coils heated with water pumped from a hot water bath maintained at 85°C. Samples were taken at intervals and cells were removed by centrifugation (5 minutes at 13 000 rpm). The extracellular Fab' and protein concentration were measured by ELISA and Bradford protein assay respectively. After 5 hours incubation each suspension was homogenised and Fab' concentrations in the homogenate were used to define 100% antibody release.

The results obtained are illustrated in Figures 4.2.6-4.2.8. Figure 4.2.6 shows the effect of incubation time and temperature on Fab' release. Release appears to be temperature dependent, with higher temperatures giving higher rates of Fab' release. The effect of heat on the outer membrane of *E. coli* strain W3110 has been described by Katsui *et al.*, (1982), who showed that exposure of cells to a temperature of 55°C for 30 minutes resulted in blebbing and vesiculation of the outer membrane, leading to the release of the 52% the periplasmic enzyme alkaline phosphatase, with no associated release of the cytoplasmic enzyme glucose-6-phosphate dehydrogenase. Thus high temperature alone may account for the release of a significant proportion of the periplasmic Fab'.

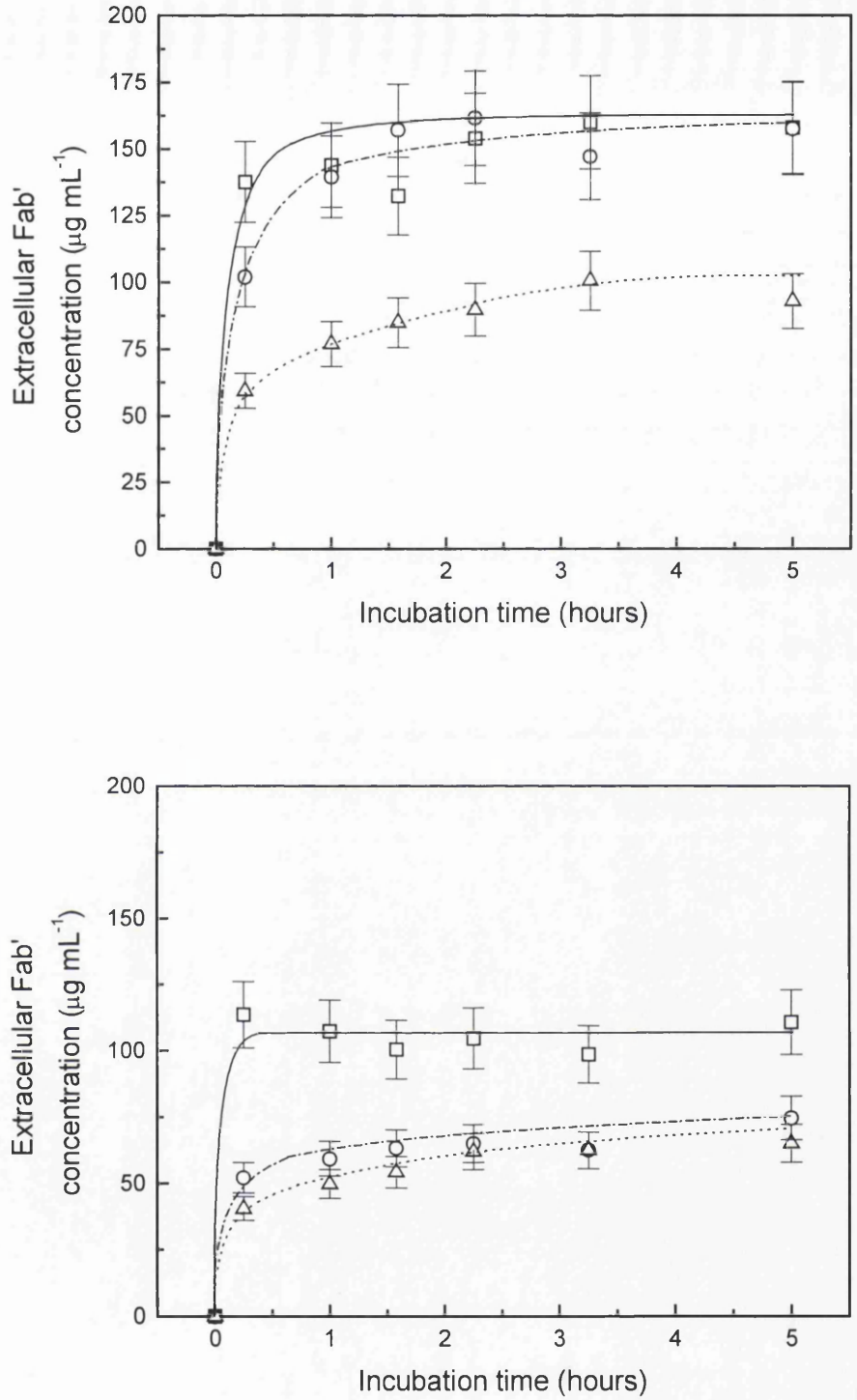

Figure 4.2.6 *Effect of incubation time and temperature on Fab' release during periplasmic extraction. Incubation temperatures were 60℃ (–□–), 45℃ (- -O- -) and 30℃ (···Δ···). Cells were resuspended in periplasmic extraction buffer (upper plot) and PBS (lower plot). The same vertical axis has been used to allow for comparisons between the two graphs. Error bars represent the error of the ELISA assay (± 11%).*

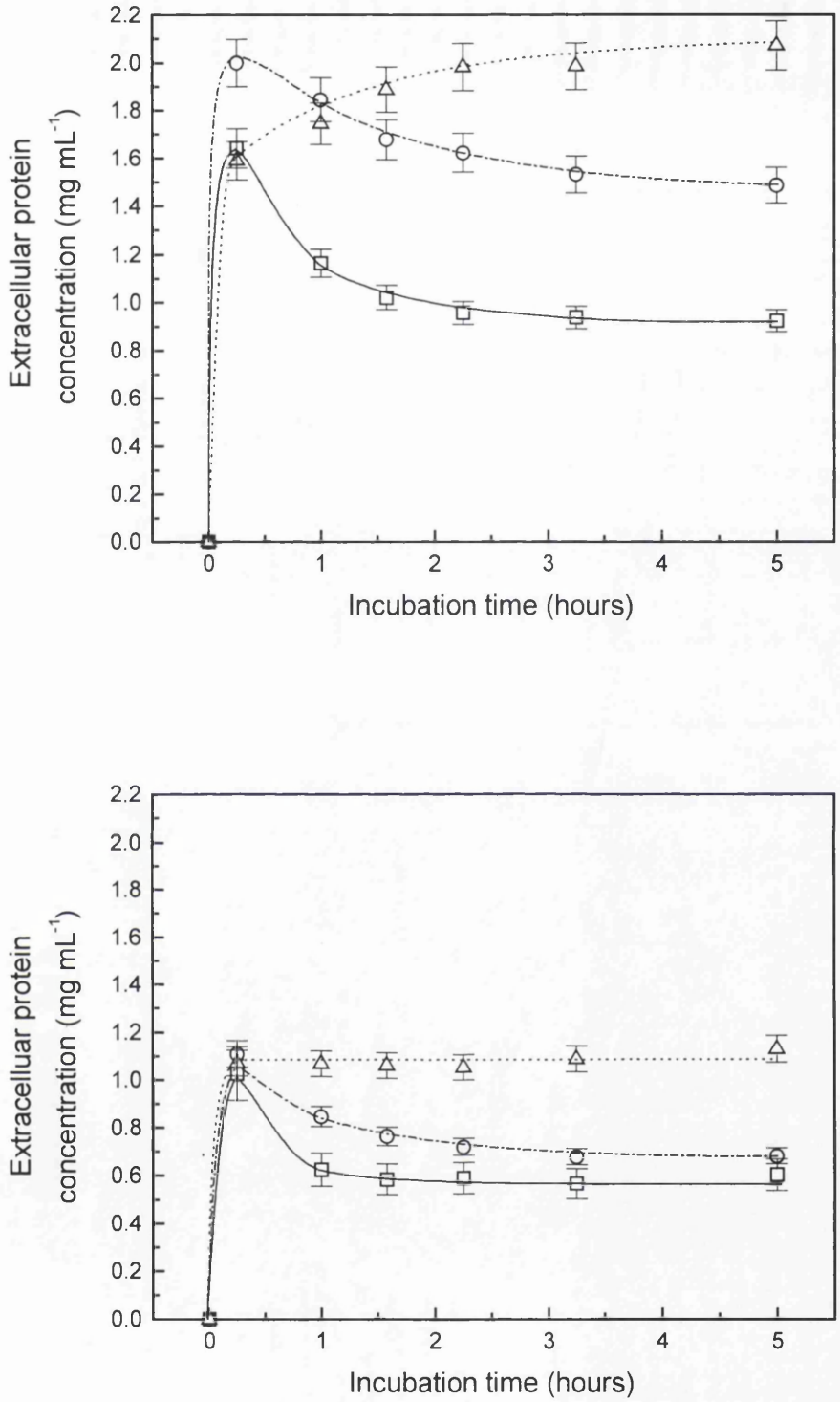

Figure 4.2.7 *Effect of incubation time and temperature on extracellular protein concentration during periplasmic extraction. Incubation temperatures were 60℃ (–□–), 45℃ (--O--) and 30℃ (···Δ···). Cells were resuspended in periplasmic extraction buffer (upper plot) and PBS (lower plot). The same vertical axis has been used to allow for comparisons between the two graphs. Error bars represent the error of the protein assay (± 5%).*

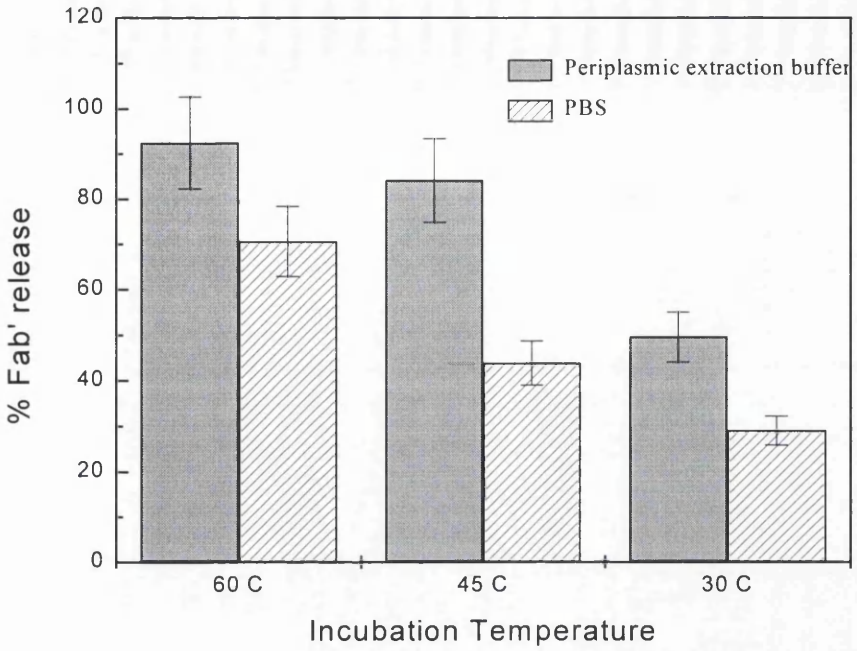

Figure 4.2.8 *Effect of incubation temperature and extraction buffer on antibody release. Cells were incubated in periplasmic extraction buffer or PBS at 60℃, 45℃ and 30℃ for 5 hours. Following incubation the extracellular antibody concentration was recorded. 100% antibody release is defined as the Fab' concentration in a homogenised sample (1 pass, 1200 bar). Error bars represent the error of the ELISA assay (± 11%).*

The Tris-EDTA extraction buffer gave higher release at each temperature than the PBS (shown in Figure 4.2.6 and Figure 4.2.8), illustrating the effect of Tris and EDTA in permeabilising the outer membrane of *E. coli*. EDTA removes by chelation the divalent cations that stabilise the lipopolysaccharides (LPS) coating the bacterial outer membrane. It has been suggested that Tris binds to the LPS, replacing the stabilising Ca^{2+} and Mg^{2+} ions, and thus reducing the interaction between LPS molecules (Varra, M., 1992).

Protein release under the different extraction conditions is illustrated in Figure 4.2.7. Again, Tris-EDTA gave higher release than PBS, as expected. Following the initial resuspension at 30°C, extracellular protein concentration either increased (cells suspended in Tris-EDTA) or remained constant (cells suspended in PBS). However, at higher temperatures protein concentration decreased as a proportion of the *E. coli* proteins were denatured. Denaturation was more rapid and occurred to a greater extent at 60°C compared to 45°C. This is to be expected as there will be a population of protein molecules which are stable at 45°C but not at 60°C. Maximum denaturation occurred within the first 2-3 hours of incubation.

4.2.3.1 Modelling of Fab' release

The ability to model Fab' release and protein degradation during periplasmic extraction at different temperatures and different scales of operation would allow prediction of the incubation time necessary to achieve the required product yield and levels process stream purification.

The release of Fab' from cells during the process of periplasmic extraction was modelled using first order release kinetics following the approach of Hetherington *et al.*, (1971). Hetherington and co-workers showed that the release of protein from suspensions of baker's yeast (*Saccharomyces cerevisiae*) by disruption in an industrial homogeniser can be described by the first-order equation:

$$\ln \frac{R_m}{(R_m - R)} = KNP^{2.9} \qquad \textbf{(4.1)}$$

where R is the protein released, R_m is the maximum protein available for release, K is the dimensional constant, which is a function of temperature, N is the number of passes through the homogeniser and P is the operating pressure.

It was proposed that the release of Fab' from the periplasm of *E. coli* also followed first order kinetics and hence could be described by the first order equation:

$$\ln\left(\frac{A_m}{A_m - A}\right) = k_1 t \qquad \textbf{(4.2)}$$

or rearranged, $A = A_m(1 - e^{-k_1 t})$ **(4.3)**

where A is the antibody released (μg mL^{-1}), A_m is the maximum antibody available for release (μg mL^{-1}), k_1 is the rate constant for release (a function of temperature, s^{-1}) and t is the incubation time (s). The derivation of this equation is given in Appendix 3.

Fab' release data shown in Figure 4.2.6 (upper plot) was initially plotted as the percentage Fab' released (where 100% release was defined as the total Fab' following homogenisation). First order release curves (described by Equation 4.3) were fitted to the data using the non-linear curve-fitting program of Microcal™ Origin™ (Microcal Software Inc., Northampton, MA). The Origin program derives best-fit curves by minimising the Chi-square value using the Levenberg-Marquardt algorithm. Equation 4.3 assumes that at t = 0, A = 0 (i.e. antibody release starts at time zero), and as $t \rightarrow \infty$, $A \rightarrow A_m$. For curve fitting, the value for A_m was set at 100%.

The best-fit release curves are shown in Figure 4.2.9. It can be seen from the results that the release data is poorly described by first order kinetics. It was thought that the method of cell resuspension may have effected release kinetics by enhancing antibody release. Cell paste was resuspended in Tris-EDTA buffer in 100 mL Duran bottles (approximate dimensions 6 cm height × 4.6 cm diameter) using a 6-bladed disc turbine impeller (impeller diameter 2.4 cm) rotated at ~1800 rpm. High agitation rates were required for cell resuspension, which took approximately 15 minutes. The extraction buffer was at the correct temperature at the beginning of the resuspension process, however temperature was not controlled during resuspension. It is suspected

that high shear rates during the resuspension process (caused by high rates of agitation) may have enhanced antibody release by damaging the bacterial outer membrane. This, together with the variations in temperature, makes it difficult to model release using a simple first order equation and draw valid conclusions from the results obtained. More accurate release data may have been obtained if cells had been resuspended in the stirred tanks at the impeller speed at which extraction was performed. However, it is likely that at low impeller speeds, the time taken for complete cell resuspension would have been significantly increased (particularly at low extraction temperatures), which would have had the opposite effect of impairing antibody release.

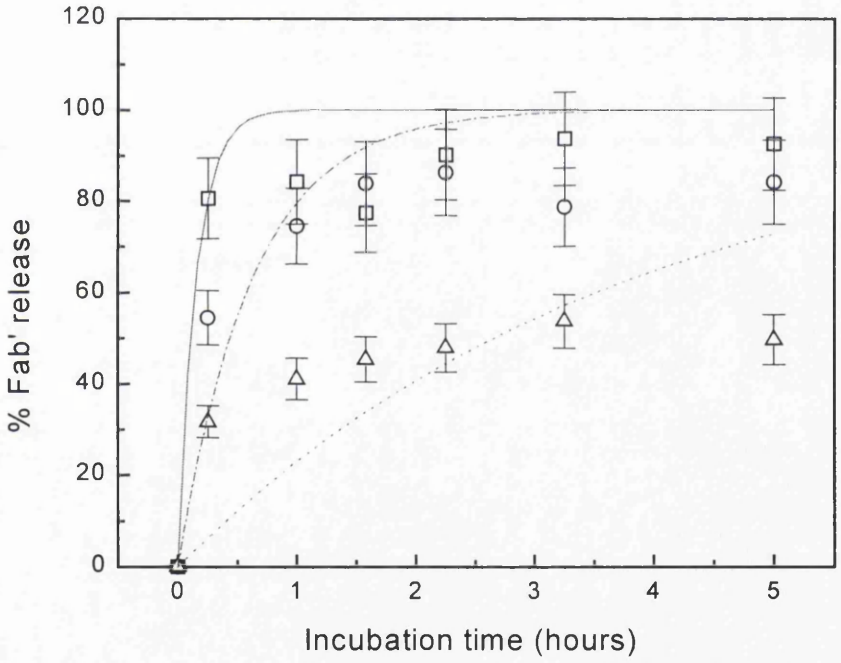

Figure 4.2.9 *Comparison of experimental data (points) and theoretical data (lines) for Fab' release during periplasmic extraction at 60°C (–□–), 45°C (- -O- -) and 30°C (···Δ···). Periplasmic release was modelled using first order kinetics; curves shown are the curves of best-fit obtained using the non-linear curve fitting program of Microcal™ Origin™. Data is modelled from the beginning of cell resuspension. Error bars represent the error of the ELISA assay (± 11%).*

To determine whether antibody release *following* complete cell resuspension was a first order process, release was modelled from the time of complete resuspension using the following modified first order equation:

$$A = A_m\left(1 - e^{-k_1 t}\right) + A_o e^{-k_1 t} \qquad \textbf{(4.4)}$$

Equation 4.4 is again based on first order release kinetics, but assumes that at t = 0, A = A_0. Curve fitting using Equation 4.4, setting A_m at 100% and A_0 as the measured antibody release at the time of complete cell resuspension (time zero) gave the results illustrated in Figure 4.2.10. Rate constants, k_1, for antibody release following complete cell resuspension were estimated at 0.10 s^{-1} at 30°C, 0.46 s^{-1} at 45°C and 0.22 s^{-1} at 60°C. The graphs illustrated in Figure 4.2.10 suggest that in the controlled environment within the stirred tank reactors, antibody release following complete cell resuspension is a first order process. However, rate constants for release in these models are determined not only by temperature, but also by the release occurring during the resuspension process. Therefore the rate constants at the different extraction temperatures cannot be directly compared.

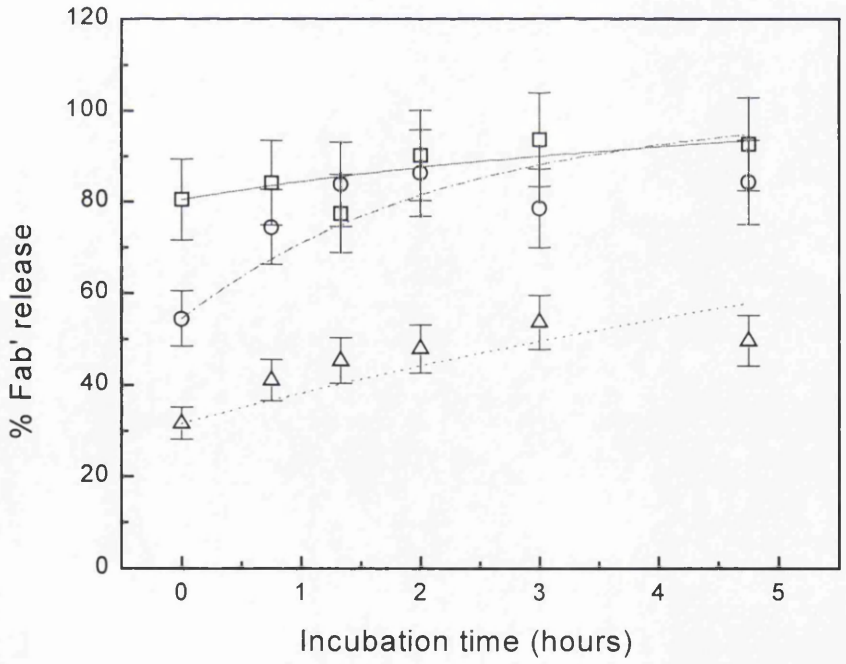

Figure 4.2.10 *Comparison of experimental data (points) and theoretical data (lines) for Fab' release during periplasmic extraction at 60°C (–□–), 45°C (- -O- -) and 30°C (···Δ···). Periplasmic release was modelled using first order kinetics; curves shown are the curves of best-fit obtained using the non-linear curve fitting program of Microcal™ Origin™. Data is modelled from the time of complete cell resuspension. Error bars represent the error of the ELISA assay (± 11%).*

4.2.3.2 Modelling of protein degradation

Protein degradation was also modelled using first order kinetics. If it is assumed that protein degradation is a first order process, then is can be described by the modified first order equation:

$$P = P_m e^{-k_2 t} + P_f(1 - e^{-k_2 t}) \qquad \textbf{(4.5)}$$

where P is the available functional (non-denatured) protein (mg mL^{-1}), P_f is the functional protein remaining at the end of the denaturation process (i.e. protein which is stable at the temperature employed) (mg mL^{-1}), k_2 is the rate constant for degradation (s^{-1}) and t is the incubation time (s).

The derivation of Equation 4.5 is given in Appendix 3, and assumes that at t = 0, P = P_m (where P_m is the total protein available for denaturation), and as $t \rightarrow \infty$, $P \rightarrow P_f$, (i.e. at each extraction temperature there is a proportion of protein which is stable and will not be denatured).

Prior to curve fitting, it was necessary to convert the data given in Figure 4.2.7 (upper plot) to curves representing the degree of protein degradation. To do this the following assumptions were made:

1. % protein released ≡ % Fab' released
2. % protein degraded = % protein released - % assayed protein
   (≡ % Fab' released -% assayed protein)
3. Remaining functional protein = Total available protein (100%)-%protein degraded

Assumption (1) was used to estimate the total protein available for release (and hence also degradation) from 30°C extraction data. The protein detected by assay (assayed protein) was then converted to percentage of total available protein. Finally, assumption (2) was used to calculate the percentage of available protein degraded during the course of the extraction. Data was plotted as the percentage of available

protein remaining functional (assumption (3)), illustrated in Figure 4.2.11. Figure 4.2.11 also shows the best-fit curves using Equation 4.5, setting P_m as 100%. It is apparent from the graph that protein degradation can be described reasonably accurately by first order equations, and that both the rate of degradation and the functional protein remaining at the end of the extraction procedure are a function of temperature. Rate constants, k_2, for protein degradation at 45°C and 60°C were estimated at 1.1 $s^{-1}$and 3.4 s^{-1} respectively.

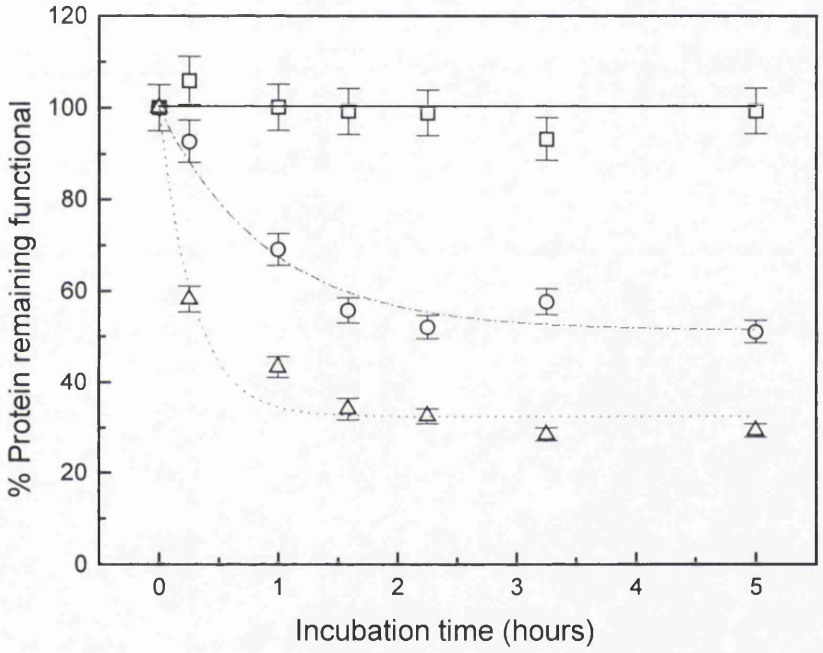

Figure 4.2.11 *Comparison of experimental data (points) and theoretical data (lines) for protein degradation during periplasmic extraction at 60°C (–□–), 45°C (- -O- -) and 30°C (···Δ···). Protein degradation was modelled using first order kinetics; curves shown are the curves of best-fit obtained using the non-linear curve fitting program of Microcal™ Origin™. Data is modelled from the beginning of cell resuspension. Error bars represent the error of the protein assay (± 5%).*

4.2.4 Effect of scale on periplasmic extraction

High temperature periplasmic extraction was performed at 2L and 100L to allow the effect of increasing scale on Fab' release and protein degradation to be assessed. The 2L and 100L extractions were carried out in a 3L and a 150L bioreactor respectively. The dimensions of the bioreactors and associated impellers are given in section 2.4.1.2. Cells (harvested from the 450L and 150L3 fermentations for extraction at 2L and 100L respectively) were resuspended in periplasmic extraction buffer (preheated to 60°C) to 0.14 g L^{-1} (the same concentration as for small-scale extractions). Resuspension was performed in the bioreactor at the impeller speed employed for the extraction process (given in section 2.4.1.2); complete resuspension took ~20 minutes at 2L and ~45 minutes at 100L. Samples were taken following complete cell resuspension, then at regular intervals for the initial 5 hours of extraction and finally following 16 hours incubation. A sample taken at the end of extraction was homogenised to allow determination of total Fab' available for release. Impeller speed during extraction was set to maintain constant power per unit volume at each scale of operation to maintain a constant degree of agitation (as described in Hoare *et al.*, 1982). The formula and calculations used to determine the required impeller speed are given in Appendix 4.

Antibody release and protein degradation curves obtained for 2L and 100L extractions are shown in Figure 4.2.12. The curves shown are best-fit first order release (Equation 4.3) and degradation (Equation 4.5) curves, fitted using Microcal™ Origin™ as described previously.

Results show similar patterns of Fab' release and protein degradation as for small scale extraction, with maximum release occurring within the first hour of extraction and maximum degradation occurring within the first five hours of incubation. At both scales of operation, release and degradation kinetics were accurately modelled by first order rate equations. It was difficult to make comparisons of Fab' release kinetics because release was so rapid that the value obtained for the rate constant was dependent on the time at which the first sample was taken.

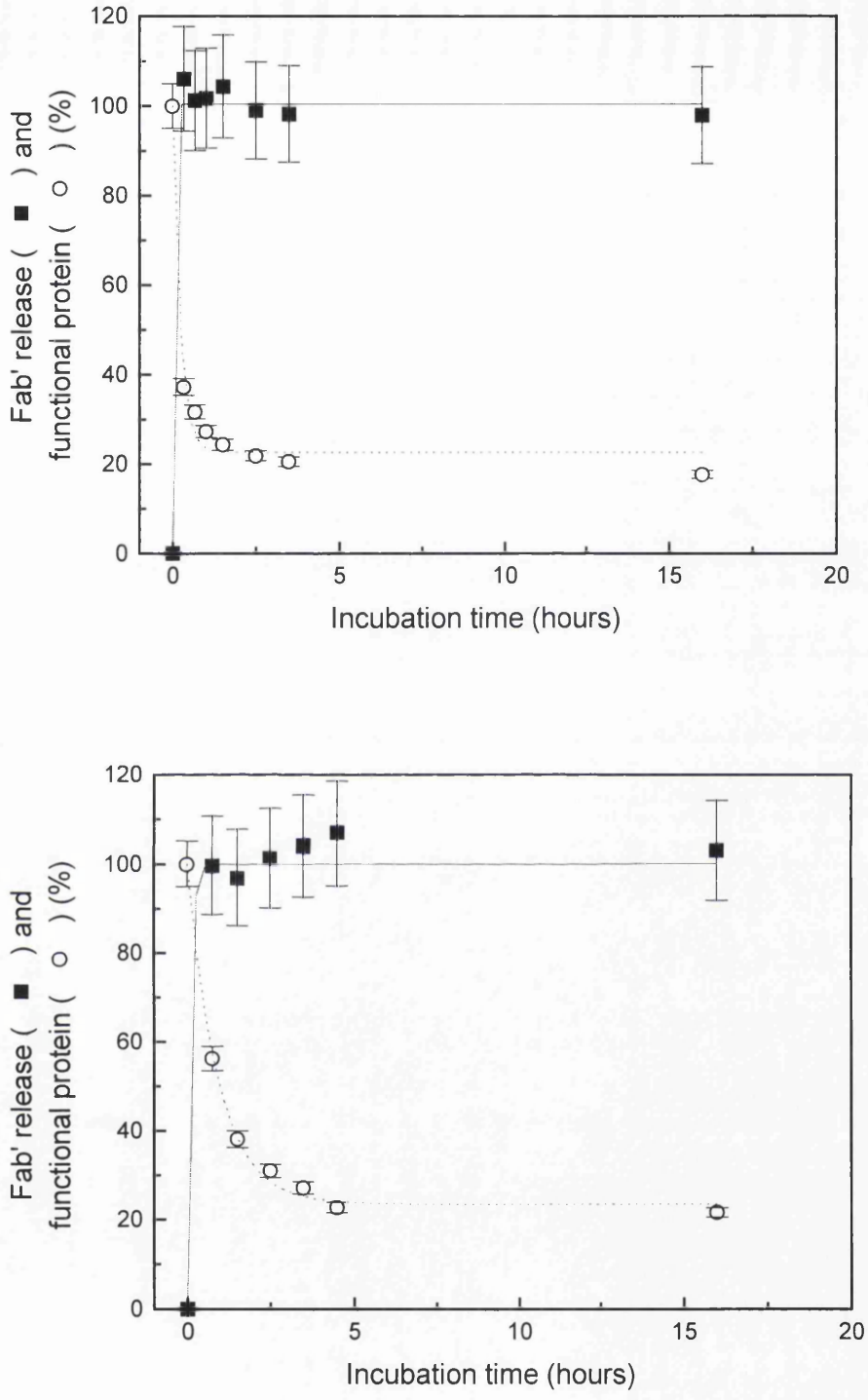

Figure 4.2.12 *Fab' release and protein degradation during 2L (upper plot) and 100L (lower plot) periplasmic extraction at 60°C. Curves represent the best fit first-order release and degradation curves obtained using the non-linear curve fitting program of Microcal™ Origin™. Data is modelled from the beginning of cell resuspension. Error bars represent the error for each assay (ELISA, ±11%; protein assay, ±5%).*

Values of the rate constant, k_2, obtained for protein degradation, and the percentage available protein remaining at the end of the extraction procedure are given in Table 4.2.2. Variation is observed in both the figures, and may be attributed to the use of different feed material, giving different populations of proteins which vary in their thermal stability. This highlights one of the problems associated with the use of modelling to predict process performance; differences in feed material in biological systems are both difficult to predict and therefore also difficult to account for when designing models.

Extraction vessel	0.1L Stirred tank	3L Bioreactor	100L Bioreactor
Extraction volume (L)	0.065	2	100
k_2 (s^{-1})	3.4	4.5	1.1
P_f (%)	32	23	23

Table 4.2.2 *Rate constant for protein degradation (k_2) and percentage of available protein remaining functional at the end of the extraction process for 60°C periplasmic extraction at different scales of operation.*

Degradation of incomplete Fab' was also monitored for 100L periplasmic extraction. Western blot analysis (Figure 4.2.13) of extracellular protein over the course of the extraction process reveals significant degradation of free light chain within the first 1.5 hours of extraction.

Thus, at scales up to 100L, maximum Fab' release occurs within the time taken for complete cell resuspension, and the time required to achieve maximum degradation of contaminating *E. coli* protein is approximately 5 hours. It is likely that the degradation of contaminating incomplete or degraded Fab' fragments will also take place within this time frame.

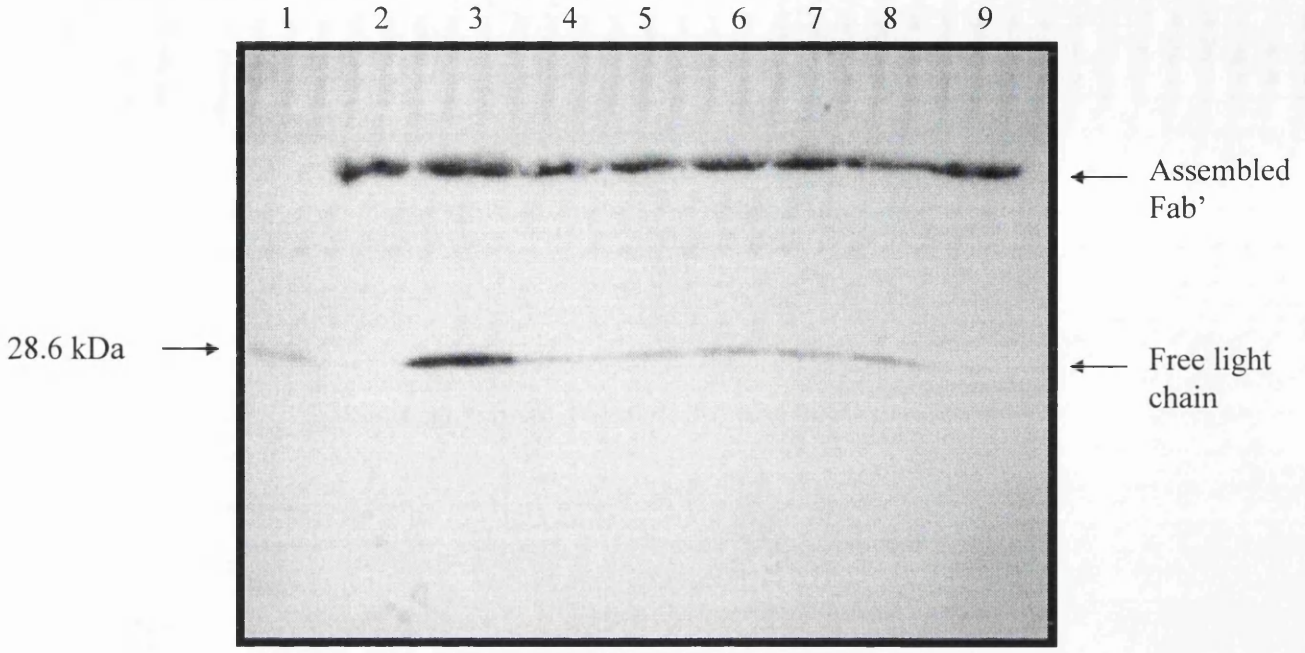

Figure 4.2.13 *Western blot probed for 4D5 Fab' light chain, showing complete Fab' and free light chain in periplasmic extracts during 100L periplasmic extraction.*

Lane 1 Prestained low molecular weight markers
Lane 2 Purified 4D5 Fab' standard

Lanes 3-9 Periplasmic extracts (extracellular protein) at the following time intervals after cell resuspension:

Lane 3 45 minutes
Lane 4 1.5 hours
Lane 5 2.5 hours
Lane 6 3.5 hours
Lane 7 4.5 hours
Lane 8 16 hours

Lane 9 Purified 4D5 Fab' standard

4.2.5 Whole broth extraction

Chapter 3 describes development of a fermentation to improve control of product location. Following modification of the original protocol, over 80% retention of Fab' product within the periplasmic space was routinely achieved. However, studies have shown that retention of material within the periplasm can be harder to achieve at large scale (personal communication, N. Weir). In cases where product location is more difficult to control and excessive leakage of product into the extracellular broth occurs, it may be more economically desirable to concentrate on harvesting material exclusively from the extracellular medium, or alternatively attempting to purify both extracellular and periplasmic product.

Initial studies were therefore carried out to assess the feasibility of recovering both extracellular and periplasmic material by performing the extraction process on whole fermentation broth (whole broth extraction). Whole broth extraction was compared to periplasmic extraction (i.e. performing the extraction on cell paste) by assessing Fab' recovery, process stream purification, process stream viscosity and quality of the Fab' purified from each process stream by expanded bed protein A affinity chromatography (section 2.4.3.2).

Before the process of whole broth extraction could be characterised, it was necessary carry out a fermentation to produce a stock of fresh fermentation supernatant. In order to simulate the increased leakage observed at scale, the addition of calcium and magnesium salts prior to induction was omitted from the fermentation protocol as this was thought to be one of predominant factors contributing towards the increased retention of periplasmic material (fermentation HCD5, section 3.2.2.3). However, the measurement of extracellular and periplasmic Fab' in samples taken at the end of the fermentation showed that leakage had increased only slightly, with 70% of product still retained within the periplasmic space. Extracellular Fab' titres however were sufficiently high (~50 $\mu g\ mL^{-1}$) to allow experiments to be performed using the material produced.

Cells harvested from fermentation HCD5 were frozen (-70°C) and the supernatant stored at 4°C until the experiments could be performed. Periplasmic and whole broth extraction were compared at laboratory scale. Cell paste was resuspended at a concentration of 0.14 g L^{-1} in either 300 mL periplasmic extraction buffer or 270 mL fermentation supernatant and 30 mL 10X periplasmic extraction buffer (so that the concentration of Tris and EDTA in each extraction process was identical). A 1 mL sample of each suspension was spun (13 000 rpm, 5 minutes) to provide a supernatant sample for assay of extracellular Fab' and protein concentration prior to extraction. In addition, 30 mLs of each suspension were homogenised to allow determination of initial total protein and total Fab' available for release. The remaining suspensions were each divided into two sealed 200 mL shake flasks, one of which was incubated in an orbital shaker at 30°C, 250 rpm, whilst the other was incubated in a hot water bath maintained at 60°C, 250 rpm. All suspensions were incubated for 16 hours, after which samples were taken for measurement of extracellular Fab' and protein, total Fab' and protein (after homogenisation) and viscosity.

The results are given in Table 4.2.3. Two values for Fab' recovery are shown, the first is based on total Fab' available for release at the beginning of extraction, whereas the second (in brackets) shows Fab' release based on total Fab' available at the end of extraction. The two figures are similar for extraction at 30°C, however significant differences are observed for 60°C extraction. The differences are due to Fab' degradation; total Fab' concentrations before and after extraction at 60°C are shown in Figure 4.2.14. Initial differences in total Fab' for periplasmic and whole broth extraction resulted from the presence of 42 μg mL^{-1} Fab' in the broth supernatant. Following periplasmic extraction at 60°C, total Fab' was reduced by ~15%; as explained in section 4.2.2, such levels of degradation were routinely observed and are thought to be due to denaturation of free heavy and light chain. Whole broth extraction at 60°C resulted in 35% degradation of Fab'. The actual quantity of Fab' denatured was approximately equal to the amount lost during periplasmic extraction plus the amount present in the extracellular broth. Hence it is postulated that the extracellular material is less heat stable than periplasmic Fab',

possibly as a result of chemical reactions that occur in the supernatant, and therefore is denatured by the high temperature.

Extraction Temperature	30°C		60°C	
	Periplasmic extraction	Whole broth extraction	Periplasmic extraction	Whole broth extraction
% Fab' recovery	66 (63)	50 (49)	57 (68)	41 (63)
Specific Fab'	0.0508	0.0393	0.174	0.135
Purification factor	1.8	2.2	4.0	6.0
Viscosity (mPaS)	1.8	1.8	1.9	2.2

Table 4.2.3 *Comparison of Fab' recovery, purification of the process stream and process stream viscosity during periplasmic and whole broth extraction.*

The % Fab' recovery gives the extracellular Fab' concentration at the end of the extraction process expressed as a percentage of the total Fab' available for release, measured in a homogenised sample taken at the beginning (first figure) and the end (second figure in brackets) of the extraction procedure. Specific Fab' and purification factor as for Table 4.2.1.

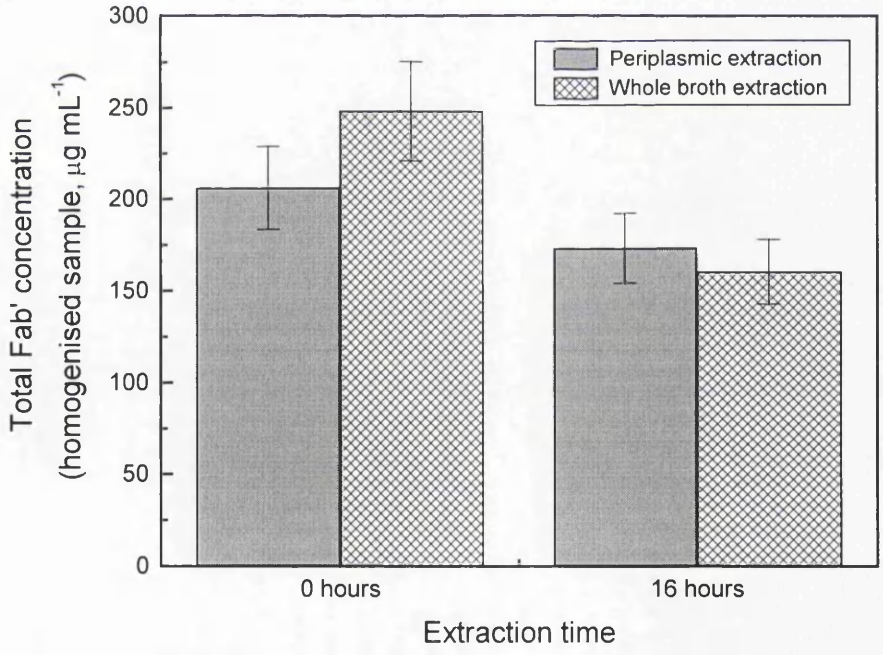

Figure 4.2.14 *Total Fab' available for release, measured in a homogenised sample at the beginning and end of periplasmic and whole broth extraction at 60°C. Error bars represent the error for the ELISA assay (±11%).*

In all cases, recovery was lower for whole broth extraction compared to periplasmic extraction, indicating that the extraction process was less efficient in the presence of fermentation supernatant. It is possible that EDTA in the extraction buffer, which functions as a membrane permeabilising agent by chelating the divalent cations which form an integral part of the bacterial outer membrane, interacts with cations within the fermentation supernatant and is thereby prevented from binding the calcium and magnesium ions in the outer membrane.

The periplasmic extraction process performed on cells from fermentation HCD5 was also observed to be significantly less efficient than previous extractions performed on cells harvested from standard high cell density fermentations. Of the Fab' recorded at the end of extraction, 68% had been released from the periplasm, compared to 100% release frequently achieved during previous extractions. The only difference in protocols for the standard high cell density fermentations and the fermentation used to produce material for the experiments described in this section was the omission of the calcium and magnesium additions prior to induction. It is possible that the reduced concentration of calcium and magnesium resulted in a change in the structure of the bacterial outer membrane such that it was more resistant to treatment with Tris and EDTA.

The high temperature extraction resulted in purification of the process stream for whole broth extraction as well as periplasmic extraction, indicated by the higher specific Fab' obtained at 60°C compared to 30°C. Purification was marginally higher for whole broth extraction, shown by the higher purification factor. Evidence for the high temperature purification is also provided by SDS-PAGE analysis of extracellular protein after cell resuspension and following extraction at 30°C and 60°C (Figure 4.2.15). Lower levels of protein contaminants are shown by the reduced number of protein bands in the 60°C extracts.

Purification by degradation of free heavy and light chain and incomplete Fab' is also observed for whole broth as well as periplasmic extraction, as illustrated by Western blots detecting Fab' light and heavy chain (Figures 4.2.16 and 4.2.17 respectively). Both blots show a considerably 'cleaner' Fab' preparation obtained by extraction at

60°C. The increased intensity of staining of the bands representing complete Fab' in the 60°C extracts suggests a higher concentration of disulphide bonded Fab' compared to 30°C extracts. However, the reduced staining intensity in 30°C extracts is thought to result from 'hindered binding' of detecting antibodies due to much higher levels of protein within the sample, rather than lower Fab' concentration.

Quality of Fab' purified from periplasmic and whole broth extracts by expanded bed adsorption (section 2.4.3.2) was assessed by SDS-PAGE analysis, illustrated in Figure 4.2.18. The gel indicates Fab' purified from whole broth extracts to be of equivalent quality in terms of purity compared to Fab' purified from periplasmic extracts.

Finally, the viscosity of each suspension was measured following extraction. The results, shown in Table 4.2.3, indicate that the viscosity following whole broth extraction was slightly higher compared to periplasmic extraction, however the increase was thought not to be significant in terms of processing.

The comparisons made between the two extraction processes indicate that no significant advantage is gained from whole broth extraction in terms of product yield or purity, however performing the extraction on whole fermentation broth does remove the requirement for a cell harvest step following fermentation (discussed further in Chapter 8). Further work is required to fully characterise the process of whole broth extraction, including an assessment of Fab' stability in the fermentation supernatant and optimisation of the extraction process in the presence of fermentation broth. In addition, more detailed analysis of the quality of Fab' purified from whole broth extracts would be required before the operation could be included as a purification stage in the preparation of material for clinical use. Quality is assessed in terms of degree of deamination, oxidative state of the thiol group used for conjugation to other elements such as PEG, toxins or liposomes, affinity of the antigen and *in vivo* stability and efficacy.

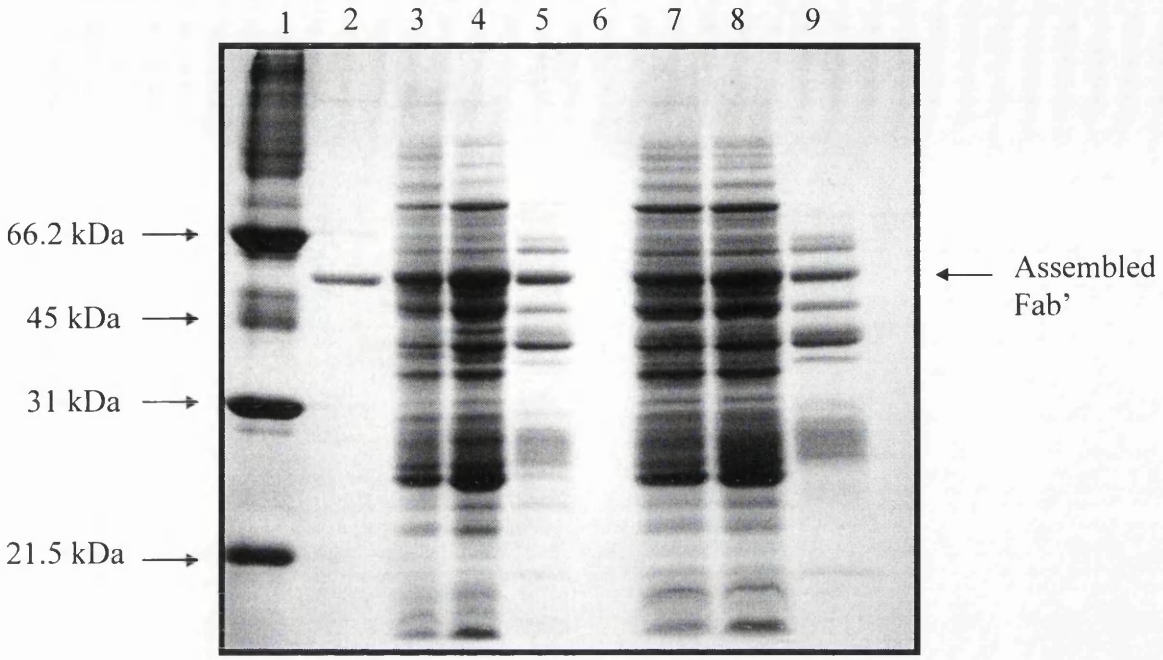

Figure 4.2.15 *SDS-PAGE gel showing process stream purity following periplasmic and whole broth extraction at 30℃ and 60℃.*

Lane 1 Low molecular weight markers
Lane 2 Purified 4D5 Fab' standard

Lanes 3, 4 and 5, Periplasmic extraction

Lane 3 Extracellular protein following cell resuspension
Lane 4 Extracellular protein following overnight extraction at 30℃
Lane 5 Extracellular protein following overnight extraction at 60℃

Lane 6 -

Lanes 7, 8 and 9, Whole broth extraction

Lane 7 Extracellular protein following cell resuspension
Lane 8 Extracellular protein following overnight extraction at 30℃
Lane 9 Extracellular protein following overnight extraction at 60℃

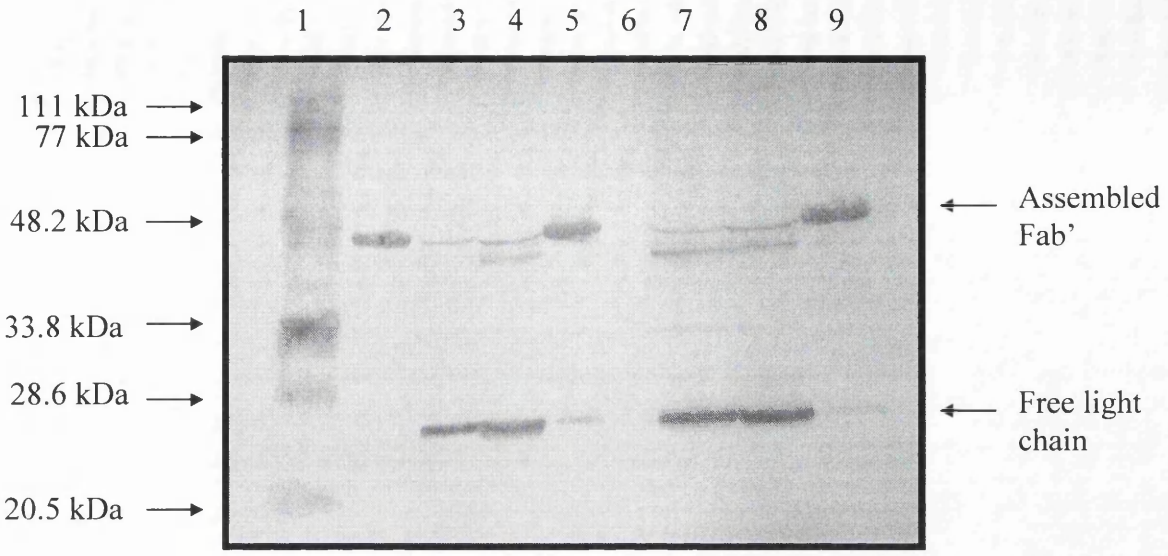

Figure 4.2.16 *Western blot probed for 4D5 Fab' light chain, showing process stream purity following periplasmic and whole broth extraction at 30℃ and 60℃.*

Lane 1 Low molecular weight markers
Lane 2 Purified 4D5 Fab' standard

Lanes 3, 4 and 5, Periplasmic extraction

Lane 3 Extracellular protein following cell resuspension
Lane 4 Extracellular protein following overnight extraction at 30℃
Lane 5 Extracellular protein following overnight extraction at 60℃

Lane 6 -

Lanes 7, 8 and 9, Whole broth extraction

Lane 7 Extracellular protein following cell resuspension
Lane 8 Extracellular protein following overnight extraction at 30℃
Lane 9 Extracellular protein following overnight extraction at 60℃

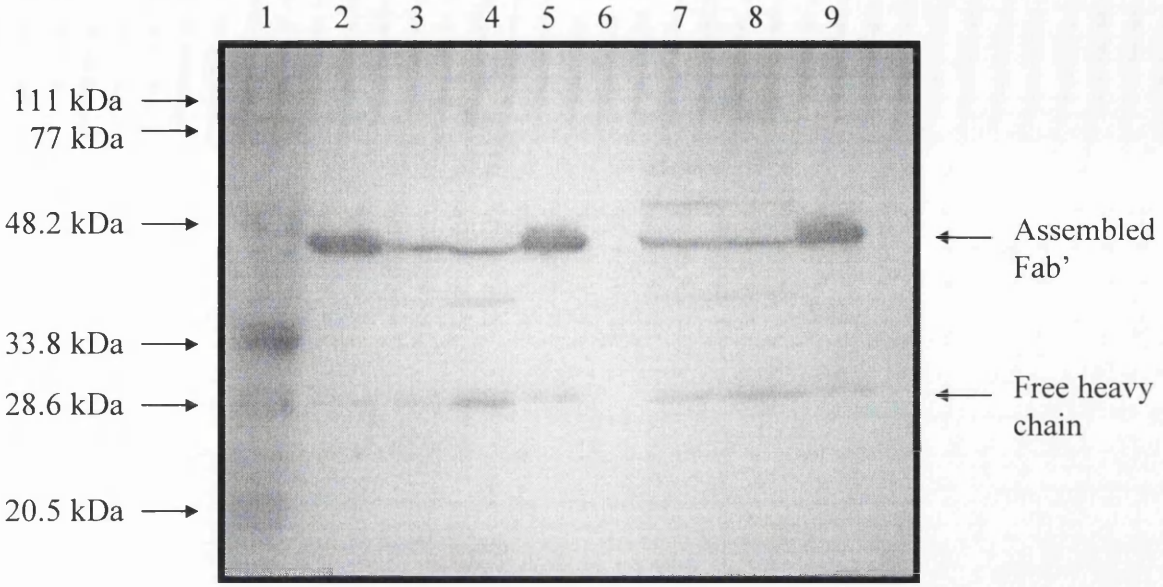

Figure 4.2.17 *Western blot probed for 4D5 Fab' heavy chain, showing process stream purity following periplasmic and whole broth extraction at 30℃ and 60℃.*

Lane 1 Low molecular weight markers
Lane 2 Purified 4D5 Fab' standard

Lanes 3, 4 and 5, Periplasmic extraction

Lane 3 Extracellular protein following cell resuspension
Lane 4 Extracellular protein following overnight extraction at 30℃
Lane 5 Extracellular protein following overnight extraction at 60℃

Lane 6 -

Lanes 7, 8 and 9, Whole broth extraction

Lane 7 Extracellular protein following cell resuspension
Lane 8 Extracellular protein following overnight extraction at 30℃
Lane 9 Extracellular protein following overnight extraction at 60℃

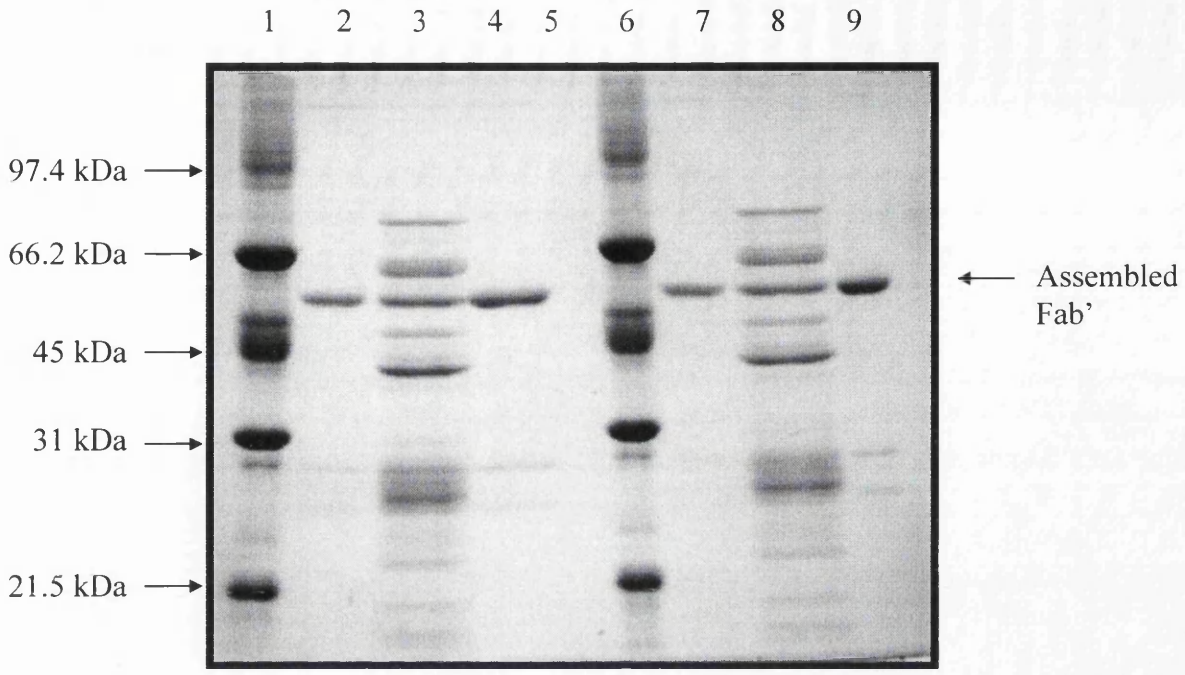

Figure 4.2.18 *SDS-PAGE gel showing quality of Fab' preparations purified from 60℃ periplasmic and whole broth extracts by expanded bed adsorption.*

Lane 1 Low molecular weight markers
Lane 2 Purified 4D5 Fab' standard
Lane 3 Periplasmic extract following overnight incubation at 60℃ (column load)
Lane 4 Fab' preparation purified from 60℃ periplasmic extract (column eluate)

Lane 5 -

Lane 6 Low molecular weight markers
Lane 7 Purified 4D5 Fab' standard
Lane 8 Periplasmic extract following overnight incubation at 60℃ (column load)
Lane 9 Fab' preparation purified from 60℃ whole broth extract (column eluate)

4.3 Summary

A novel process of periplasmic extraction, involving the incubation of cells in a Tris-EDTA extraction buffer at elevated temperature, has been characterised. An initial assessment of the thermal stability of 4D5 Fab' concluded that the highest temperature at which the extraction process could be effectively operated was 60°C. Performing the extraction at both low (30°C) and high (60°C) temperature produced high Fab' yields (>85%). However, high temperature extraction offered the additional advantage of process stream purification by the degradation of both contaminating *E. coli* proteins and incomplete or partially degraded Fab' fragments which would otherwise be purified with the complete Fab' during protein A affinity chromatography.

The monitoring of Fab' release and protein degradation during periplasmic extraction revealed that both processes are temperature dependent, with higher temperatures giving higher rates of release and degradation. At 60°C, Fab' release occurred almost instantaneously during cell resuspension, and maximum protein denaturation took place within the first five hours of incubation.

Fab' release and protein degradation were modelled at different temperatures and scales of operation using first order rate equations, however the method of cell resuspension appeared to interfere with release, making it difficult to model accurately. Release following complete cell resuspension and protein denaturation both followed first order kinetics, however the rate and extent of protein degradation varied with the use of different feed material.

Finally, the Tris-EDTA extraction process was performed on whole fermentation broth. Yields achieved with whole broth extraction were lower than for periplasmic extraction due to a combination of increased Fab' degradation and a less efficient extraction procedure. However, the degree of process stream purification during 60°C whole broth extraction was slightly higher than that achieved with periplasmic extraction. Further work is required to assess the thermal stability and quality of extracellular Fab', and to optimise extraction in the presence of fermentation supernatant before a complete characterisation of the process and valid comparisons with periplasmic extraction can be made.

5. CLARIFICATION OF SPHEROPLAST SUSPENSIONS

5.1 Introduction

This chapter examines the centrifugal removal of spheroplasts from the process stream following periplasmic extraction and assesses the ability of scale-down techniques to predict recovery performance in industrial centrifuges.

Following the release of 4D5 Fab' from *E. coli* cells by periplasmic extraction, either of two purification routes may be followed. Fab' may be recovered directly from the spheroplast suspension using expanded bed chromatography. Alternatively, spheroplasts can be removed from the process stream by centrifugation and/or microfiltration, and the Fab' purified by packed bed chromatography.

One disadvantage of the latter method relates to the observed product losses during large-scale centrifugation to clarify spheroplast suspensions. N. Weir and co-workers (Celltech Chiroscience Ltd) observed that during the large-scale disk stack centrifugation of spheroplast suspensions following periplasmic extraction, ~50% Fab' was lost with the solid phase despite only ~10% loss of liquid volume. This loss of product has also been observed by G. Zapata at Genentech (San Fransisco, CA) (Erdmann, 1998). During large-scale centrifugation to remove cell debris following lysis of *E. coli* cells expressing periplasmic antibody fragments, the antibody partitioned preferentially with the pellet resulting in reduced recovery. The problem was solved by diluting the process stream in high ionic buffer prior to centrifugation.

Another common problem associated with the centrifugation of biological material is the damage resulting from exposure to high shear rates. Shear damage to the product can reduce yields, and shear-associated cell breakage will result in contamination of the process stream with proteases, DNA and lipids, which may degrade product or cause problems in subsequent purification stages.

This chapter aims to investigate the problems of shear damage and preferential partitioning of antibody product with the solid phase during the centrifugal clarification of spheroplast suspensions. In addition, the scale-down techniques developed to allow investigation of processing problems at laboratory and pilot scale are assessed in their ability to mimic the performance of an industrial centrifuge.

The following sections (5.1.1-5.1.5) provide an introduction to the tubular bowl and the disk stack centrifuges, centrifugation theory and the techniques developed for the scale-down of centrifugal recovery. In sections 5.2.1 and 5.2.2 an assessment is made of the sensitivity of 4D5 Fab' and spheroplasts to shear. The centrifugal removal of spheroplasts using a disk stack and a tubular bowl centrifuge is characterised and compared in section 5.2.3. Finally, section 5.2.4 compares process stream clarification achieved using full-scale and scale-down equipment.

5.1.1 Tubular bowl centrifuge

The tubular bowl centrifuge is the simplest of all centrifugal separators. Feed is pumped through a nozzle into the bottom of a cylindrical tube, which rotates at high speed. As the feed enters, it is rapidly accelerated and is distributed to the inner walls of the bowl. As the liquid moves upwards through the bowl, solids sediment against the sides of the cylinder. Clarified supernatant flows out of the top of the bowl and the solids, which collect as a paste layer on the bowl inner walls, are collected separately. The design of the tubular bowl is illustrated in Figure 5.1.1.

The simple design of the tubular bowl means extremely high relative centrifugal forces can be attained (up to 20 000g on an industrial scale), therefore good separation and high solids dewatering are achieved. However, limitations on the length of the cylinder due to mechanical stresses at high rotational speed mean the particle residence time within the bowl is relatively short, which can limit both separation efficiency and centrifuge capacity. In addition, conventional machines require solids to be removed manually, which can be cumbersome and may present biosafety hazards. As a result, tubular bowl centrifuges are applied mainly for

difficult separations which require high relative centrifugal forces or where a low solids content is present in the feed suspension (1-5%).

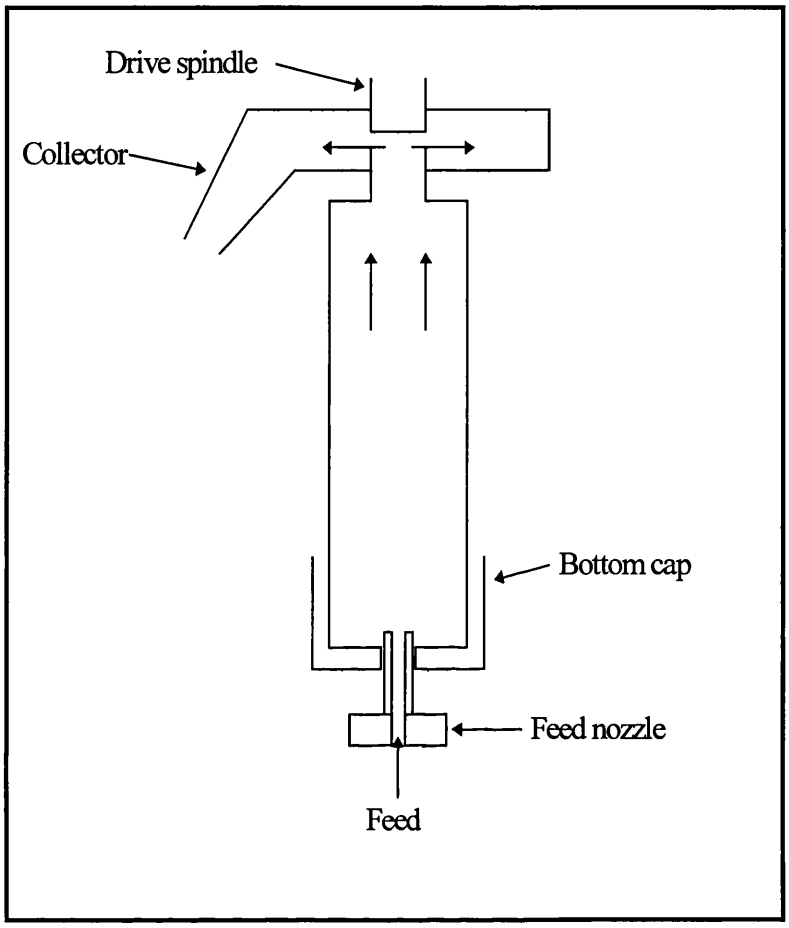

Figure 5.1.1 *Schematic diagram of a tubular bowl centrifuge.*

Recent years have seen the development of a tubular bowl centrifuge which is capable of automated solids discharge during operation. The centrifuge design is considerably more complex than traditional tubular bowls, however high relative centrifugal forces (up to 20 000g) can still be achieved. Feed is introduced at the top of the centrifuge bowl, solids are retained within the bowl and supernatant is discharged over a weir at the base of the centrifuge. Compressed solids are removed periodically during a fully automated cycle in which bowl speed is reduced and a knife within the bowl 'scrapes out' the solids. The machine also has the capacity for fully automated sterilisation in place and cleaning in place.

5.1.2 Disk stack centrifuge

The disk stack centrifuge is considerably more complex than the tubular bowl. A number of designs of disk stack machine exist, the principal difference between them being the method of removal of accumulated solids. In the simplest of designs, solids must be removed periodically by hand. The majority of disk stack centrifuges however are capable of solids discharge during operation without reducing the bowl speed. Solids may be ejected continuously through nozzles in the periphery of the bowl, or alternatively centrifuges may be fitted with valves to allow the intermittent discharge of solids when required.

The internal structure of a disk stack centrifuge is illustrated in Figure 5.1.2. The central feature of the design is a stack of conical disks that rotate with the bowl and split the liquid into thin layers. This has the effect of both reducing the sedimentation distance and increasing the settling area. Feed enters the centrifuge through the central pipe of the centripetal pump and is rapidly accelerated to the speed of the bowl. Feed then passes through the distributor to the bottom of the stack, and flows upwards between the disks where separation occurs. Disks are held apart by spacer ribs (or caulks) on the surface of each disk, giving separation distances of 0.4-2 mm. The high centrifugal force causes the heavier particles within the feed suspension to be thrown outwards towards the undersides of the disks whilst lighter fluid is displaced towards the centre of the bowl. Solids collect on the lower surface of the disks and slide downwards into the conical holding space where solids discharge occurs through nozzles or slots in the periphery of the bowl. Clarified liquid moves upwards into the centripetal pump chamber, above the disk space, where it is discharged from the machine.

The disk stack centrifuge used in the following work is an automated intermittent solids discharging machine. Discharge is achieved by injecting high-pressure water into the space between the fixed lower bowl component and the top of the sliding piston (Figure 5.1.2). This forces the piston to move downwards, exposing six evenly spaced slots in the periphery of the bowl through which collected solids are discharged by centrifugal force. Removal of the water allows the piston to close,

sealing the bowl to allow further solids accumulation. Discharged solids are ejected into the surrounding hood and fall down a chute for collection in a container.

Two types of discharge can be performed; a full and a partial discharge. During a full discharge, the feed valve is closed and the sliding piston is lowered for sufficient time (typically ~ 10 seconds) to allow complete removal of the entire contents of the bowl. When the centrifuge reaches capacity, the bowl will contain a mixture of solids (approximately half the bowl volume) and liquid (feed and partially clarified supernatant). Therefore a full discharge will produce a 'wet' solid (25-30% solids on a volume fraction basis). Considerably drier solids are achieved using a partial discharge, where the bowl is opened for the time it takes to eject the sedimented solids only (typically 1-2 seconds). The feed valve remains open during a partial discharge, however the pump can be stopped manually to prevent feed entering the bowl whilst discharging. In industrial operation, disk stack centrifuges are normally operated with four partial discharges followed by a full discharge.

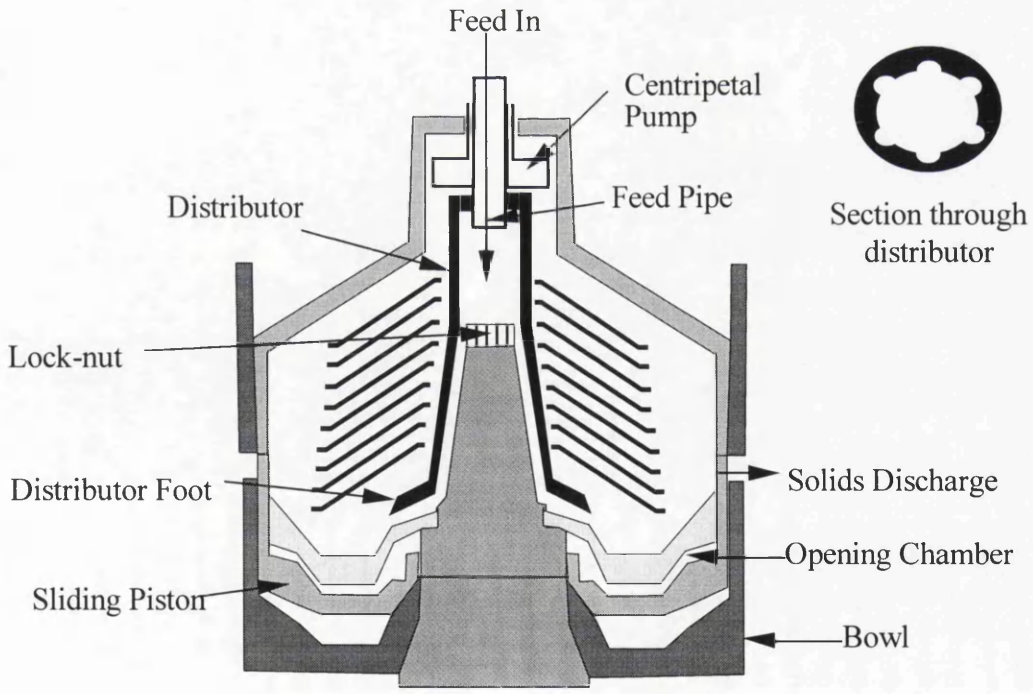

Figure 5.1.2 *Schematic diagram of a disk stack centrifuge.*

The complicated design of the disk stack machine limits rotational speeds, with industrial machines designed to operate at forces of up to 10 000g. In addition, the discharge mechanism requires that the solids must remain sufficiently wet to flow through the machine. Despite the ability to release solids during operation, the limited solids capacity of disk stack machines means only feed suspensions of up to ~10% solids content by volume can be handled efficiently (Brunner and Hemfort, 1988). However, the ability to process large batches with minimal operator intervention means that for many bioprocessing operations, disk stack centrifuges are the machine of choice. Disk stack centrifugation has been reported for the separation of both mammalian cell cultures (Kempken *et al.*, 1995) and *Escherichia coli* cultures (Datar and Rosen, 1987).

5.1.3 Centrifugation theory

5.1.3.1 Relative centrifugal force

The effectiveness of centrifugation is characterised by the ratio of particle velocity achieved in a particular centrifuge to particle settling velocity under gravity.

The settling velocity under gravity of a small, spherical particle in dilute suspension is given by Stoke's law:

$$V_g = \frac{(\rho_S - \rho_L) d_s^{\,2} g}{18\mu} \qquad \textbf{(5.1)}$$

where V_g = settling velocity under gravity (m s^{-1})

ρ_S = density of the particles (kg m^{-3})

ρ_L = density of the suspending fluid (kg m^{-3})

μ = suspension dynamic viscosity (Ns m^{-2})

d_s = diameter of particle (m)

g = acceleration due to gravity (m s^{-2})

In a centrifugal field, the acceleration the particle experiences under gravity is replaced with that due to centrifugal force. The settling velocity is therefore given by:

$$V_Z = \frac{(\rho_S - \rho_L) d_S^2 \omega^2 r}{18\mu} \qquad \textbf{(5.2)}$$

where V_Z = settling velocity in a centrifugal field (m s^{-1})

ω = angular velocity of the centrifuge (rad s^{-1})

r = radial position of particle (m)

The ratio of velocity in the centrifuge to velocity under gravity is termed the relative centrifugal force (RCF, also called the centrifuge effect or g number):

$$RCF = \frac{V_Z}{V_g} = \frac{\omega^2 r}{g} \qquad \textbf{(5.3)}$$

Hence a centrifuge can be characterised by the relative centrifugal force it generates, which determines particle settling velocity in the centrifugal field and thus influences the rate of sedimentation. Sedimentation is also affected by the time of exposure to the centrifugal force. In batch centrifuges, exposure time is increased by increasing the centrifuge spin time. In continuous centrifuges, residence time within the centrifuge is increased by decreasing the feed flow rate.

5.1.3.2 Sigma theory

The performance of different designs and scales of centrifuge is commonly compared using sigma theory which was developed by Ambler (1952). Each centrifuge has an associated 'Sigma factor' (Σ), which physically represents the cross-sectional area of a gravity settler with the same sedimentation characteristics as the centrifuge, and hence has the units m^2. The basic equation for Σ, derived in full by Ambler (1959), is given by:

$$\Sigma = \frac{V \omega^2 r_e}{g s_e} \qquad \textbf{(5.4)}$$

where V = volume of liquid in the bowl (m^3)

r_e = effective radius of the centrifuge (m)

s_e = effective settling distance (m)

Equations for evaluating Σ depend on centrifuge design; equations for the Σ factor of the laboratory batch centrifuge, the tubular bowl and the disc stack centrifuge are given in Appendix 5.

The relationship between Σ and the flow rate of material through a continuous centrifuge is given by the equation:

$$\Sigma = \frac{Q}{2V_g} \qquad \textbf{(5.5)}$$

where Q = volumetric flow rate through the centrifuge ($m^3 s^{-1}$)

It can be seen from Equations 5.1 and 5.4 that V_g depends entirely on the physical characteristics of the system whereas Σ depends entirely on centrifuge design. Therefore, it should be possible to compare centrifuges of different designs and sizes operating on the same feed stream, on the basis that V_g is constant and hence:

$$\frac{Q_1}{\Sigma_1} = 2V_g = \frac{Q_2}{\Sigma_2} = \frac{Q_3}{\Sigma_3} = \text{etc} \qquad \textbf{(5.6)}$$

Equation 5.6 implies that any centrifuges operating with the same feed stream will recover particles with identical efficiency if the ratio of flow rate to Sigma factor for all machines is the same. This is used as the basis for centrifuge scale up, however caution is required when comparing different machine types because sigma theory is based on the assumption of laminar flow and ideal operating conditions. In reality, centrifuge performance can deviate from theoretical prediction due to factors such as particle shape and size distribution, aggregation of particles, non-uniform flow

distribution in the centrifuge and interaction between particles during sedimentation. To account for non-ideal conditions in different machines, empirically derived correction factors are introduced as shown:

$$\frac{Q_1}{c_1 \Sigma_1} = \frac{Q_2}{c_2 \Sigma_2} \qquad \textbf{(5.7)}$$

where c_1 and c_2 are the appropriate correction factors for the particular centrifuge. The correction factor is defined as 1.0 for the laboratory batch centrifuge. For the tubular bowl centrifuge, flow patterns are simple and the correction factor is close unity (0.9-1.0; Ambler, 1959). A variety of correction factors for disk stack centrifuges have been quoted in the literature, ranging from 0.4 (Maybury *et al.*, 2000) to 0.73 (Murkes and Carlsson, 1978). In reality, comparisons between different machines should not be made unless the appropriate correction factor for the particular machine and feed material has been determined.

5.1.4 Centrifuge scale-down

The aim of scale-down is to simulate the conditions and performance of pilot plant equipment at reduced scale, so that the performance of unit operations can be predicted using reduced volumes of process material. This will allow meaningful process data to be collected early in process development when material is limited, thus accelerating process design.

Three approaches to scale-down exist:

- Use of a small scale, geometrically similar model of the industrial machine.
- Modification of existing pilot scale equipment so that lower volumes of process material are required whilst maintaining comparable process performance.
- Operation of traditional bench-top equipment to simulate the poorer performance of pilot-scale machines.

The initial approach, the development of small-scale replicas, is unfeasible and cost-prohibitive when applied to complex industrial machines such as the disk stack centrifuge.

The approach of modifying existing equipment has been used by Maybury *et al.*, (1998) to scale-down an industrial disk-stack centrifuge. The volume of process material required for the study of centrifugal clarification was minimised by reducing the number of active separating disks and also reducing the liquid and solid hold-up of the centrifuge bowl. Maximum scale-down gave a 76% reduction in the separation area and a bowl volume reduction of 70%. The recovery performance of the full-scale machine was closely mimicked by the scale-down variant during the processing of dilute streams of polyvinyl acetate and yeast cell debris. However, solids dewatering and compaction were not assessed. In addition, no changes were made to the feed zone of the centrifuge, hence shear rates in the feed zone of the scale-down configuration are likely to have been lower than in the full-scale version, which may affect the recovery performance during processing of shear sensitive particulates.

The final approach, involving the operation of bench-top equipment to simulate the performance in pilot-scale machines, has been termed ultra scale-down. Techniques have been developed which allow recovery performance of an industrial disk stack separator to be predicted using a standard laboratory centrifuge (Maybury *et al.*, 2000). The laboratory centrifuge was operated at the same relative centrifugal force and equivalent Q/Σ as the industrial machine. The equation defining Q/Σ for a laboratory centrifuge, developed by Ambler (1959), was initially modified to account for the centrifuge acceleration and deceleration stages (as shown in Appendix 8). The ability to mimic recovery performance in the industrial separator using the laboratory centrifuge was then assessed using a dilute suspension of polyvinyl acetate particles, yeast cell debris and protein precipitates. Recovery of polyvinyl acetate particles was found to be well predicted by the laboratory centrifuge. However, the laboratory centrifuge over predicted the recovery of shear sensitive yeast cell debris and protein precipitates. It is suspected that the high shear in the disk stack centrifuge feed zone caused breakage of debris aggregates and precipitates, resulting in poorer performance. Particulates are exposed to only low shear rates in the laboratory centrifuge, resulting in an over prediction of the recovery achieved with the industrial

machine. Improvement of laboratory prediction requires the development of a device which mimics the conditions of high shear combined (in some cases) with air-liquid interfaces in the industrial machine.

5.1.5 The rotating disc shear device

The laboratory rotating disc shear device has been developed at University College London to generate controlled levels of shear. The device, described in detail in section 2.4.2.1, consists of a single flat aluminium disc rotated in a closed Perspex cylindrical chamber at fixed rotational speeds between 5 000 and 27 000 rpm. The device generates shear rates of up to 1.1×10^6 s^{-1} and has previously been used to determine the effects of shear on plasmid DNA in solution (Levy *et al.*, 1999).

5.2 Results and discussion

5.2.1 Shear sensitivity of 4D5 Fab'

The effect of shear on 4D5 Fab' was assessed using the rotating disc shear device described in section 2.4.2.1. Purified 4D5 Fab' was diluted to a concentration of 100 μg mL^{-1} in PBS and ~12 mL of this solution was fed into the reservoir of the shear device (so that the reservoir was ~2/3 full). This left a small pocket of air at the top of the reservoir to allow air entrainment as the solution was sheared. The disc was rotated at a rate of 27 000 rpm for 15 seconds, which corresponds to an average shear rate of approximately 1.1×10^6 s^{-1}. This is the highest shear rate possible using the rotating disc device. Samples were taken before and after shearing and the concentration measured by ELISA. It was assumed that any shear damage to the antibody fragment would result in a decrease in the concentration recorded by ELISA. The experiment was performed on triplicate Fab' samples.

The results of the experiment, illustrated in Figure 5.2.1, show no appreciable decrease in the signal detected by ELISA and thus no apparent damage to the antibody as a result of exposure to high shear in the presence of air-liquid interfaces.

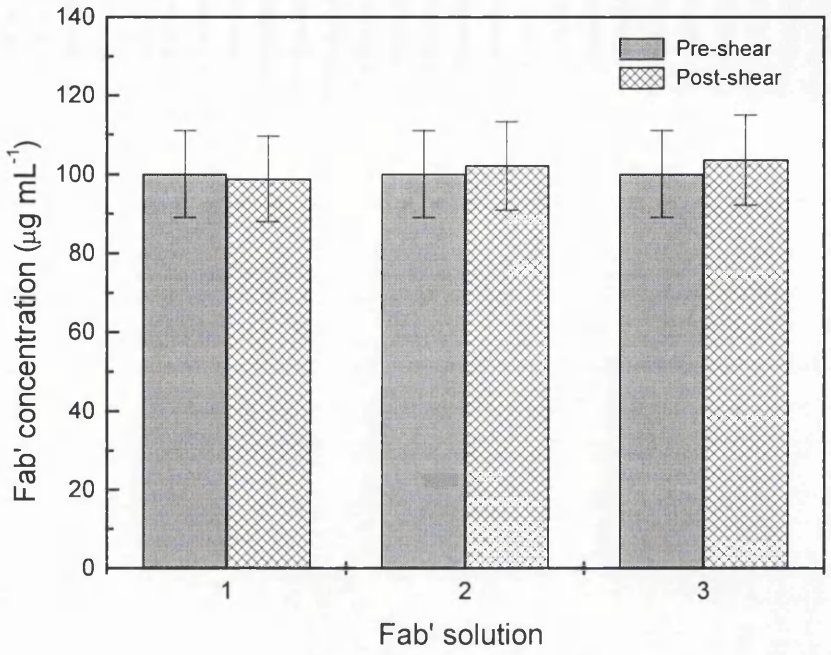

Figure 5.2.1 *Concentration of a solution of purified 4D5 Fab' measured by ELISA before and after exposure to shear in the presence of air-liquid interfaces. Purified Fab' was sheared at a rate of ~1.1×10^6 s^{-1} for 15 seconds in a rotating disc shear device. Error bars represent the error of the ELISA assay (± 11%).*

The shear studies performed indicate the Fab' to be stable at shear rates up to 1.1×10^6 s^{-1}. During processing the Fab' is exposed to highest shear in the feed zone of a centrifuge. Maximum shear rates in the feed zones of the disk stack and tubular bowl centrifuges used later in this study were calculated to be in the range 10^5-10^6 s^{-1} (S. Yim, University College London), which is comparable to the shear rates produced by the rotating disk device. Thus it is unlikely that the Fab' will be damaged by the shear it experiences in the centrifuge feed zone.

5.2.2 Shear sensitivity of spheroplasts

The shear sensitivity of spheroplasts was investigated by assessing the degree of cell breakage caused by exposure to shear and the effect of shearing on centrifugal clarification efficiency.

Spheroplast breakage following exposure to shear was estimated from the release of total cellular protein and the intracellular enzyme glucose-6-phosphate

dehydrogenase, G-6-PDH. Cells (harvested from HCD run 4) were resuspended to a concentration of 0.14 g mL^{-1} in periplasmic extraction buffer and incubated overnight at 30°C and 60°C. 1mL samples of each suspension were centrifuged in a microfuge (13 000 rpm/~14 000g for 5 minutes) and the supernatant collected for the measurement of pre-shear extracellular protein and G-6-PDH concentration. (This method assumes that centrifugation in the microfuge causes minimal damage to the cells. The assumption has previously been experimentally confirmed by N. Murrell, PhD Thesis, 1998).

Samples of the 30°C and 60°C spheroplast suspensions were then sheared (in triplicate) using the rotating disc shear device. The reservoir of the disc device was filled with ~12 mL suspension (so that it was ~2/3 full) and the disc was rotated at 27000 rpm for 15 seconds to produce a shear rate of 1.1×10^{6} s^{-1} with air entrainment. Following shearing, 1 mL samples were centrifuged as before and the supernatant collected to determine the post-shear extracellular protein and G-6-PDH concentration. Total protein and G-6-PDH available for release was measured in homogenised samples of pre-shear suspensions (section 2.4.4.1). Protein and G-6-PDH assays are described in sections 2.2.3.1 and 2.2.4 respectively.

The concentrations measured were used to determine the level of release due to spheroplast damage that had occurred during shearing. The percentage release was calculated as follows:

$$\% \text{ Release} = \frac{P_S - P_0}{P_{100} - P_0} * 100\% \qquad \textbf{(5.8)}$$

Where P_S = Extracellular protein/ enzyme concentration in sheared sample

P_0 = Background protein/ enzyme concentration (i.e. extracellular concentration in pre-shear sample)

P_{100} = Total enzyme/ protein available for release, measured in a homogenised sample.

The results are given in Tables 5.2.1-5.2.3. G-6-PDH release was only measured in 30°C spheroplast suspensions as incubation at 60°C destroyed all enzyme activity.

Sample	Pre-shear extracellular protein (mg mL^{-1})	Post-shear extracellular protein (mg mL^{-1})	Total protein available for release (mg mL^{-1})	% release
1	2.67	2.96	9.35	4.3
2	2.67	2.89	9.35	3.3
3	2.67	2.70	9.35	0.04

Table 5.2.1 *Protein release resulting from shearing of a spheroplast suspension produced by overnight extraction at 30℃. Spheroplasts were sheared at a rate of ~1.1×10^6 s^{-1} for 15 seconds in a rotating disc shear device.*

Sample	Pre-shear extracellular G-6-PDH (IUmL^{-1})	Post-shear extracellular G-6-PDH (IUmL^{-1})	Total G-6-PDH available for release (IUmL^{-1})	% release
1	0.11	0.14	1.21	2.5
2	0.11	0.13	1.21	2.3
3	0.11	0.14	1.21	2.4

Table 5.2.2 *G-6-PDH release resulting from shearing of a spheroplast suspension produced by overnight extraction at 30℃. Spheroplasts were sheared at a rate of ~1.1×10^6 s^{-1} for 15 seconds in a rotating disc shear device.*

Sample	Pre-shear extracellular protein (mg mL^{-1})	Post-shear extracellular protein (mg mL^{-1})	Total protein available for release (mg mL^{-1})	% release
1	0.66	0.67	0.95	3.4
2	0.66	0.70	0.95	14.0
3	0.66	0.64	0.95	-7.0

Table 5.2.3 *Protein release resulting from shearing of a spheroplast suspension produced by overnight extraction at 60℃. Spheroplasts were sheared at a rate of ~1.1×10^6 s^{-1} for 15 seconds in a rotating disc shear device.*

The results show minimal cell breakage as a result of shearing. The mean protein release for 30°C spheroplasts was 2.5%, which is comparable to the mean G-6-PDH release (2.4%). Values for total protein and G-6PDH release should be similar as G-6PDH is an entirely cytoplasmic enzyme and approximately 97% of the total protein in the cell is located in the cytoplasm. The mean protein release for the 60°C spheroplasts was 3.5%, again indicating minimal cell breakage. The greater variation

observed in the release figures for 60°C spheroplasts can be attributed to the reduction in the total protein available for release; the difference between '0%' and '100%' release was sufficiently small that errors associated with the protein assay would have had a significant effect on the calculated '% release' value.

It appears from the results that the spheroplast integrity is unaffected by shear rates up to 1.1×10^6 s^{-1} and, in addition, increasing the extraction temperature has no appreciable effect on shear sensitivity. Spheroplasts are thought to be relatively flaccid and able to deform when subjected to a shearing force which would explain their insensitivity to shear. The results are in agreement with those of E. Fischer (PhD Thesis, 1996) and N. Murrell (PhD Thesis, 1998), both of whom observed minimal breakage of *E. coli* spheroplasts when exposed to shear in laboratory equipment and during centrifugation.

Following analysis of spheroplast breakage, the effect of shearing on centrifugal clarification efficiency was examined. Spheroplast suspensions were produced by overnight periplasmic extraction at 30°C and 60°C. Half of each suspension (~250 mL) was sheared using the rotating disk shear device. Suspensions were again sheared for 15 seconds at 27 000 rpm, in the presence of air-liquid interfaces. A centrifuge spin test, described in section 2.4.2.2, was performed on both sheared and non-sheared suspensions. 10 mL samples of each suspension were spun in the Beckman J2-M1 centrifuge using the JS 13.1 spin-out rotor at 6720 rpm for various time intervals between 3.5 and 47 minutes. (The centrifuge was operated at 6720 rpm to maintain consistency with later experiments). The clarification efficiency obtained at each run time was calculated based on optical density at 600nm (section 2.4.2.3). The equivalent Q/Σ corresponding to each run time has been calculated in Appendix 8, and the relationship between clarification efficiency and equivalent Q/Σ is shown in Figures 5.2.2 and 5.2.3.

The graphs indicate that exposure to shear resulted in a reduction in clarification efficiency during the centrifugation of spheroplasts produced at both extraction temperatures. The percentage reduction in clarification increased with increasing equivalent Q/Σ (i.e. as spin time decreased). For 30°C spheroplasts, the reduction in

clarification resulting from exposure to shear ranged from 0.2% at low Q/Σ to 7.0% at high Q/Σ. For 60°C spheroplasts, the reduction in clarification was slightly lower, ranging from 0.3% at low Q/Σ to 4.3% at high Q/Σ.

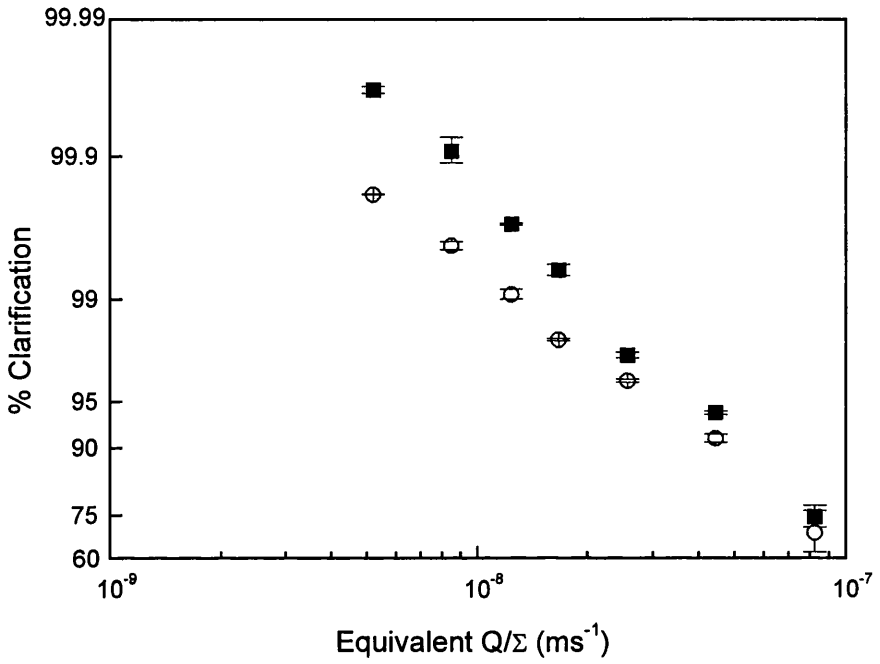

Figure 5.2.2 *Relationship between clarification efficiency and equivalent Q/Σ for sheared (O) and non-sheared (■) spheroplasts produced by overnight periplasmic extraction at 30℃. Spheroplasts were recovered in the laboratory J2-M1 centrifuge operated at 6720 rpm (RCF = 3720g) using the JS 13.1 rotor. Spheroplasts were sheared at a rate of ~1.1×10^{6} s^{-1} for 15 seconds in a rotating disc shear device. Error bars represent the standard deviation for triplicate spin tests using the same feed material. Results show a reduction in clarification efficiency for sheared spheroplasts compared to non-sheared spheroplasts. The reduction in clarification ranges from 0.2% at low Q/Σ to 7.0% at high Q/Σ.*

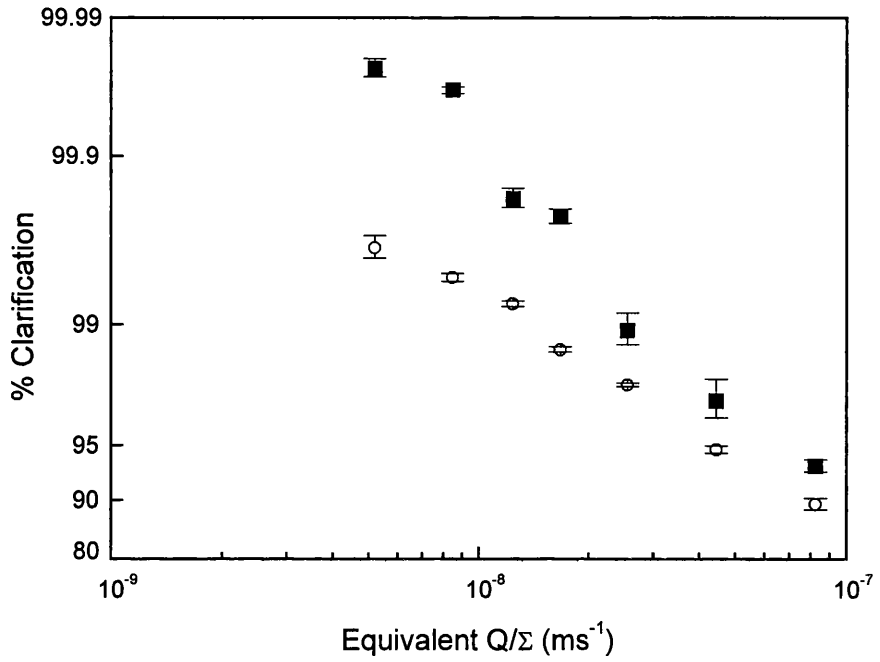

Figure 5.2.3 *Relationship between clarification efficiency and equivalent Q/Σ for sheared (O) and non-sheared (■) spheroplasts produced by overnight periplasmic extraction at 60℃. Spheroplasts were recovered in the laboratory J2-M1 centrifuge operated at 6720 rpm (RCF = 3720g) using the JS 13.1 rotor. Spheroplasts were sheared at a rate of ~1.1×10^6 s^{-1} for 15 seconds in a rotating disc shear device. Error bars represent the standard deviation for triplicate spin tests using the same feed material. Results show a reduction in clarification efficiency for sheared spheroplasts compared to non-sheared spheroplasts. The reduction in clarification ranges from 0.3% at low Q/Σ to 4.3% at high Q/Σ.*

The reduction in clarification is likely to result from a change in the particle size distribution of sheared spheroplast suspensions, with an increase in the proportion of smaller particulates which require longer centrifugation time for sedimentation. Reduction in the average particle size also provides an explanation for the greater reduction in clarification efficiency observed at higher Q/Σ. Hewitt *et al.*, (1998), studied the effect of fluid mechanical stress on *E. coli* strain W3110 during continuous cultivation in an agitated bioreactor. Their results showed that exposure of continuous cultures to high aeration and agitation rates (3 vvm and 1200 rpm respectively) had no effect on cell physiology, cell size or cell integrity. However, exposure to agitation rates of 1200 rpm for 7 hours did result in the stripping away of the outer polysaccharide layer of the cell. (Experiments were performed in a 5L

cylindrical glass bioreactor (162 mm diameter × 300 mm total height) using a working volume of 4L and employing two 82 mm six-bladed paddle type impellers). Hence, the exposure of spheroplasts to much higher rates of agitation within the shear device may have resulted in damage to the outer membrane, releasing submicron sized particles that are more difficult to clarify by centrifugation. Alternatively, shearing may change the particle size distribution simply by breaking up cell clumps or aggregates.

5.2.3 Clarification of spheroplast suspensions using a tubular bowl and a disk stack centrifuge

Clarification of spheroplast suspensions was performed using a tubular bowl centrifuge (the CARR P6 Powerfuge, CARR Separations Inc, Franklin, MA) and a disk stack centrifuge (the Westfalia CSA-1, Westfalia Separator, Milton Keynes, UK). Technical specifications of the centrifuges are given in Appendix 6 (CARR) and Appendix 7 (CSA-1). Centrifuge performance was assessed by carrying out process mass balances at the operating flow rate required for 95% clarification. Spheroplast suspensions for the centrifugation trials were produced by periplasmic extraction as described in section 2.4.1.3.

5.2.3.1 Centrifuge recovery

Initially, recovery curves were produced to determine the flow rates required for 95% recovery. The centrifuges were operated at a range of flow rates and the clarification efficiency achieved at each flow rate was calculated. The flow rates used are given in section 2.4.2.4-a and the corresponding Q/Σ values have been calculated in Appendix 9. The relationship between clarification efficiency and Q/Σ for the CSA-1 and CARR centrifuges are illustrated in Figures 5.2.4 and 5.2.5 respectively.

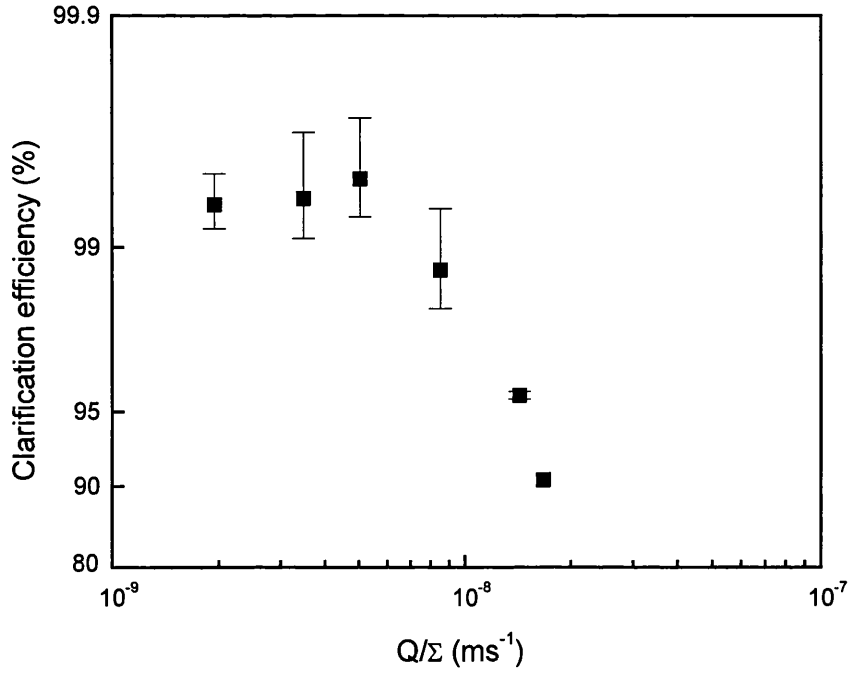

Figure 5.2.4 *Relationship between clarification efficiency and Q/Σ for the removal of spheroplasts using the CSA-1 disk stack centrifuge. Error bars represent the standard deviation of triplicate sample measurements taken at regular intervals prior to breakthrough at each flow rate.*

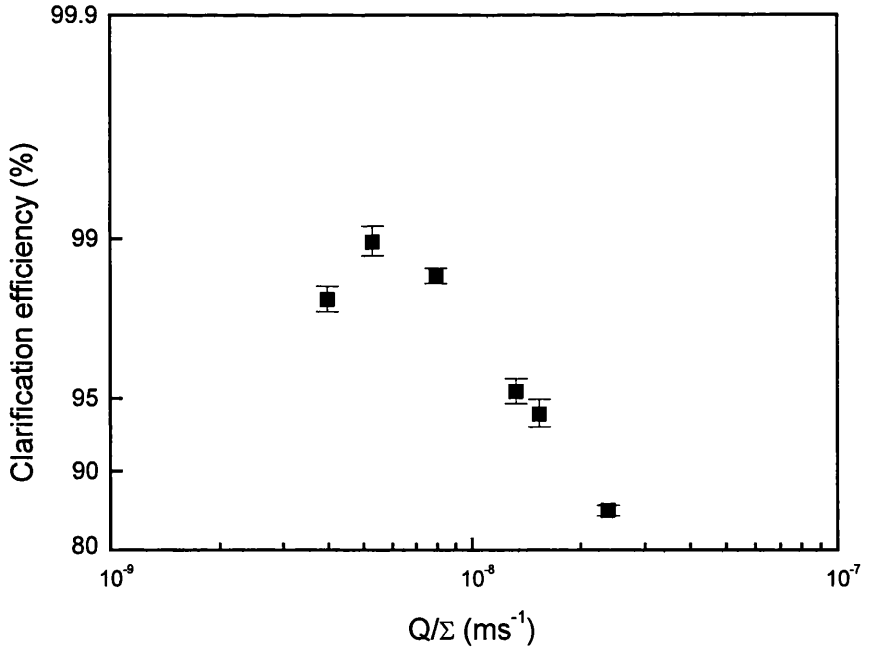

Figure 5.2.5 *Relationship between clarification efficiency and Q/Σ for the removal of spheroplasts using the tubular bowl CARR P6 Powerfuge. Error bars represent the standard deviation of triplicate sample measurements taken at regular intervals prior to breakthrough at each flow rate.*

For the CSA-1, clarification increased with decreasing flow rate, as expected. Decreasing the flow rate leads to improved recovery because the residence time of particles in the centrifuge bowl is increased. Good recovery (>99%) was achieved at low volumetric throughputs, however no advantage in terms of solids recovery was gained by operating below 30 Lhr^{-1} (Q/Σ, 5.2×10^{-9} ms^{-1}). From the graph, the flow rate required for 95% clarification was determined to be 81 Lhr^{-1} (corresponding Q/Σ = 1.39×10^{-8} ms^{-1}).

Similarly for the CARR, decreasing the flow rate resulted in improved clarification, with a maximum recovery of 99% achieved at 20 Lhr^{-1} (Q/Σ, 5.3×10^{-9} ms^{-1}). No advantage was gained from operating the centrifuge below 20 Lhr^{-1}. The flow rate required for 95% clarification was found to be 53 Lhr^{-1} (corresponding Q/Σ = 1.41×10^{-8} ms^{-1}).

5.2.3.2 Centrifuge mass balances

Centrifuge mass balances were carried out as described in section 2.4.2.4-b. All mass balance runs were performed using the same spheroplast feed stream. The flow rates used and clarification efficiencies achieved (based on optical density and solids fractions) are given in Table 5.2.4.

The CSA-1 was initially operated with full discharge. Triplicate mass balance runs were performed; the mean values obtained for Fab', protein and liquid recovery in the supernatant and solids streams are given in Table 5.2.5.

The small size of the CSA-1 meant it could not be operated with a proper partial discharge as the minimum time the bowl could be opened for (~ 2 seconds) was longer than the time required for partial discharge (~0.7 seconds). Therefore, to gain an indication of the properties of the solids stream following partial discharge, the centrifuge was opened following the processing of one bowl volume of material and the solids were sampled directly from within the bowl. The results of a single 'partial discharge mimic' run are given in Table 5.2.6.

	CSA-1		CARR
	Full discharge	Partial discharge	
Flow rate (Lhr^{-1})	81	81	53
% Clarification:			
OD basis	96	96	94
Solids fraction basis	91	91	88

Table 5.2.4 *Flow rates employed for centrifuge mass balance runs and clarification efficiencies achieved based on optical density at 600nm and solids volume fraction.*

Process stream	% Yield		
	Fab'	Protein	Liquid
Supernatant	73	72	77
Solids	24	35	23
Total (supernatant + solids)	97	107	100

Table 5.2.5 *Fab', protein and liquid recovery in the supernatant and solids streams following the processing of one 'centrifuge bowl' volume of spheroplast suspension using the CSA-1 disk stack centrifuge. Following the processing of one bowl volume, solids were ejected by full discharge. The centrifuge was operated at a bowl speed of 9840 rpm and a feed flow rate of 81 Lhr^{-1}.*

	% Yield		
	Fab'	Protein	Liquid
Supernatant	87	86	92
Solids	6	5	4
Total (supernatant + solids)	93	91	96

Table 5.2.6 *Fab', protein and liquid recovery in the supernatant and solids streams following the processing of one 'centrifuge bowl' volume of spheroplast suspension using the CSA-1 disk stack centrifuge. Following the processing of one bowl volume, the centrifuge was opened and solids sampled from within the bowl to gain an indication of solids stream properties following partial discharge. The centrifuge was operated at a bowl speed of 9840 rpm and a feed flow rate of 81 Lhr^{-1}.*

Process stream	% Yield		
	Fab'	Protein	Liquid
Supernatant	94	90	96
Solids	-	-	-
Total (supernatant + solids)	-	-	-

Table 5.2.7 *Fab', protein and liquid recovery in the supernatant and solids streams following the processing of one 'centrifuge bowl' volume of spheroplast suspension using the CARR P6 Powerfuge. The centrifuge was operated at a bowl speed of 15 320 rpm and a feed flow rate of 53 Lhr^{-1}.*

Due to the limited availability of feed material, the mass balance runs performed using the CARR Powerfuge were carried out in duplicate. Mean values of Fab',

protein and liquid recovery in the supernatant stream are given in Table 5.2.7. Because the solids ejected from the CARR were considerably drier than those discharged from the CSA-1, it was not possible to measure the extracellular protein and Fab' concentrations or the solids fraction of the solids stream.

Analysis of the clarification efficiencies in Table 5.2.4 shows that the flow rates required to give 95% clarification were successfully predicted from the recovery verses Q/Σ curves, however clarification measured by OD was slightly higher than the recovery determined from solids fractions.

The data in Tables 5.2.5-5.2.7 indicates that during disk stack and tubular bowl centrifugation, the recovery of Fab' and protein follows liquid recovery. The CARR recovered more of the liquid, producing drier solids, hence recoveries of Fab' and protein were higher (>90%). Operation of the CSA-1 with full discharge resulted in loss of 23% of liquid, hence approximately 24% of Fab' was also lost in the solids stream. Results from sampling solids directly from the bowl in the CSA-1 suggest operation of this machine with a partial discharge will result in reduced loss of liquid and hence improved Fab' recovery; yields of Fab' in the supernatant stream were 87%, compared to 73% during operation with full discharge. However, due to the presence of both solids and liquid in the bowl it was very difficult to obtain a 'representative' solids sample, therefore the precise figures in Table 5.2.6 should be treated with caution. The lower liquid losses in the solids stream produced by tubular bowl centrifugation, and by partial discharge compared to full discharge during disk stack centrifugation were confirmed by dry cell weight analysis of the solids streams. Dry cell weight data is given in Table 5.2.8.

Centrifuge	Discharge mechanism	Solids DCW (gDCW (g solids)$^{-1}$)
CSA-1 Disk stack	Full discharge	0.073
CSA-1 Disk stack	Partial discharge	0.227
CARR Tubular bowl	-	0.270

Table 5.2.8 *Dry cell weights (DCW) of solids streams produced by disk stack centrifugation employing full and partial discharge mechanisms and by tubular bowl centrifugation.*

The results of the centrifugation mass balances, which showed that Fab' recovery follows the recovery of liquid, are contradictory to observations of N. Weir (personal communication) and G. Zapata (Erdmann, 1998), both of whom found that antibody fragments preferentially associated with the solids stream during large scale centrifugation following periplasmic extraction or cell lysis. The centrifugal operation referred to by N. Weir was performed at a much larger scale than the experiments described here. The centrifuge used was an Alpha Laval MBUX 510 (Alpha Laval Separation Ltd., Camberley, UK), operated at a bowl speed of 7500 rpm and a feed flow rate of 1200-1600 Lhr^{-1}. Little data is available regarding the experiments on which the observations of G. Zapata are based, however the effect was only observed in 'large-scale' centrifuges and was referred to as one of the 'hidden problems' of scale up. Hence it is likely that the effect of preferential partitioning of product with the solids phase is only associated with centrifugation at very large scale, and may additionally be dependent upon the specific equipment used or the properties of individual feed streams.

The centrifuge of choice for the clarification of spheroplast suspensions based on the results of the centrifugation trials is the tubular bowl centrifuge, as the solids produced are drier and consequently liquid recovery and Fab' yields are greater. However, the operating flow rate required to achieve 95% clarification using the CARR tubular bowl was lower for the than for the Westfalia CSA-1, hence longer processing times would be required. Processing time may be significant in the purification of a labile product and therefore is an additional factor which must be taken into consideration when specifying equipment for a particular unit operation in a purification process.

5.2.4 Scale-down of spheroplast removal

Approaches to centrifuge scale-down have been discussed in the introduction to this chapter (section 5.1.4). They include the modification of full-scale equipment to reduce the volume of feed material required to study clarification (Maybury *et al.*, 1998), and the operation of laboratory equipment to simulate the performance of an industrial machine (Maybury *et al.*, 2000). Both techniques have been shown to

accurately predict the recovery performance of an industrial disk stack separator for the clarification of shear insensitive material. In the following section, the techniques are assessed in their ability to predict the recovery performance of the CSA-1 disk stack centrifuge during processing of shear sensitive spheroplast suspensions.

Recovery curves for the clarification of spheroplast suspensions were obtained using the CSA-1 operated in full-scale and scale-down configurations and for the Beckman J2-M1 laboratory centrifuge operated as an ultra scale-down model of the CSA-1. The same feed suspension (produced by periplasmic extraction as described in section 2.4.1.3) was used for all centrifugation runs.

Scale-down of the CSA-1 was achieved using a series of interlocking inserts which reduced the number of active disks (and therefore the separation area), the bowl volume and the solids holding space as described in section 2.4.2.6. Recovery curves were obtained for the CSA-1 operated in full-scale and scale-down configuration by measuring the clarification efficiency at different flow rates. The flow rates used are given in section 2.4.2.6, and the corresponding Q/Σ values have been calculated in Appendix 10. To allow clarification performance of the disk stack centrifuge to be compared to the laboratory centrifuge, it was necessary to use a correction factor to account for deviations from the ideal-flow assumed in Sigma theory. Maybury *et al.*, (2000) found that recovery performance of the CSA-1 was accurately predicted by the laboratory centrifuge during the processing of shear-insensitive particles using correction factors of 0.4 and 1.0 for the disk stack and laboratory machines respectively. Therefore a correction factor of 0.4 was assumed in the calculation of Q/Σ for the CSA-1.

The Beckman J-2 M-1 laboratory centrifuge was operated as an ultra scale-down mimic of the CSA-1 using the approach of Maybury *et al.*, (2000). The centrifuge was operated at 6720 rpm to give the same mean RCF as experienced in the CSA-1, as recommended by Ambler (1952) (calculation of the bowl speed which produced the required RCF is given in Appendix 8). In theory, however, the centrifugal force should not affect recovery performance as long as the Q/Σ is maintained. Recovery curves were obtained by measuring the clarification efficiency at a range of spin

times (i.e. by performing the centrifuge spin test described in section 2.4.2.2). The spin times used and calculations of the corresponding equivalent Q/Σ are given in Appendix 8. A correction factor of 1.0 was assumed for the batch centrifuge.

Although the laboratory centrifuge can be operated to mimic the RCF and Q/Σ produced by the industrial machine, the high shear in the feed zone of the industrial centrifuge is not reproduced in the laboratory device. Previous work (section 5.2.2) showed that although cell integrity is maintained during exposure to high shear, shearing can affect clarification efficiency. Therefore, recovery curves were prepared for the laboratory centrifuge using both non-sheared spheroplasts and samples of the spheroplast suspension which had been exposed to shear rates of 1.1×10^{6} s^{-1} for 15 seconds using the rotating disc shear device.

Recovery curves for the CSA-1 operated in full-scale and scale-down configurations, and for the laboratory centrifuge clarification of both non-sheared and sheared spheroplast suspensions are compared in Figure 5.2.6. The results show that recovery performance of the full-scale disk stack centrifuge was over predicted by both the scale-down disk stack and the ultra scale-down laboratory centrifuge.

Over-prediction of clarification by the scale-down disk stack was thought to be due to reduced shear in the feed zone of the centrifuge. Although the separation area and bowl volume were reduced by the scale-down inserts, no alterations were made to the centrifuge feed zone, which is where the process stream experiences the highest shear. The scale-down disk stack was operated at lower flow rates than the full-scale machine to maintain Q/Σ, however reducing the flow rate also decreases shear rates in the feed zone. The results in section 5.2.2 showed that shearing can reduce clarification; thus the improved clarification in the scale-down disk-stack can be attributed to the reduced shear in the centrifuge feed zone.

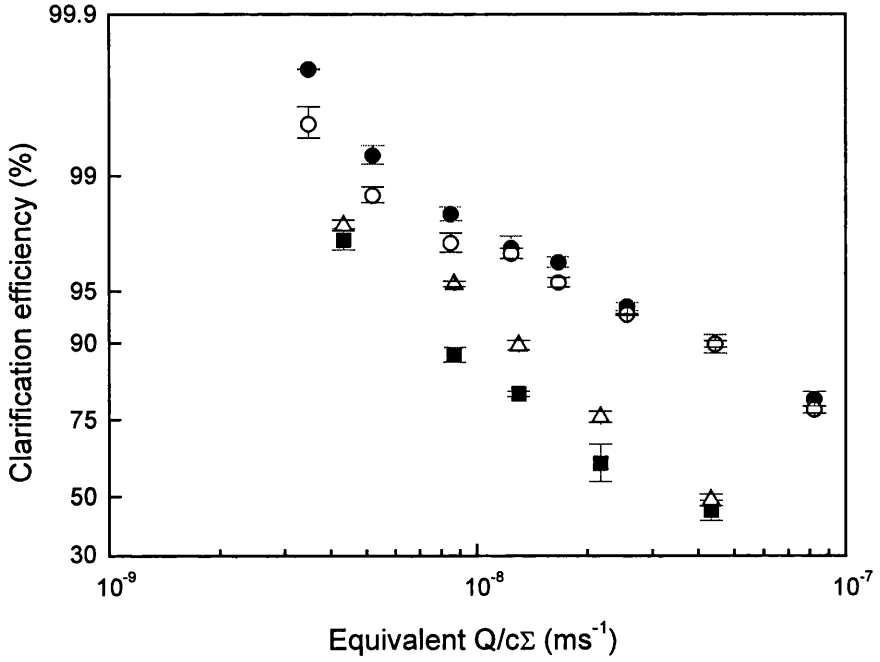

Figure 5.2.6 *Comparison of clarification of a spheroplast suspension achieved using the CSA-1 disk stack centrifuge in full-scale (■) and scale-down (Δ) operation, and the laboratory J2-M1 centrifuge operated using sheared (O) and non-sheared (●) spheroplasts. The same spheroplast feed stream was used for all operations. The CSA-1 was operated at a bowl speed of 9810 rpm. The J2-M1 centrifuge was operated using the JS 13.1 rotor at a bowl speed of 6720 rpm to produce the same relative centrifugal force as in the disk stack machine (RCF = 3720g). Spheroplasts were sheared at a rate of ~1.1×10^6 s^{-1} for 15 seconds in a rotating disc shear device. Efficiency factors (c) of 0.4 and 1.0 were used for the disk stack and laboratory centrifuge respectively.*

Recovery performance of the CSA-1 was poorly predicted by the ultra scale-down laboratory equipment. The over-prediction of recovery by the laboratory centrifuge during clarification of non-sheared spheroplast suspensions was expected as material is exposed to only very low shear in the batch centrifuge. Maybury *et al.*, (2000) also found that recovery of shear-sensitive material in the laboratory centrifuge over-predicted recovery performance of the disk stack separator. A slight reduction in clarification of sheared compared to non-sheared spheroplasts was observed, however the reduction was less than observed in previous experiments (Figures 5.2.2 and 5.2.3), indicating variations in the sensitivity of different spheroplast suspensions to shear. The results show that although shear rates in the rotating disk shear device are thought to be greater than those produced in the feed zone of the CSA-1, the

shear conditions within the CSA-1 are not effectively mimicked by the laboratory device.

The observed variation in the sensitivity of spheroplast suspensions to shear may be due to intrinsic differences in the properties of individual feed streams. Variation may also in part result from inherent errors associated with the experimental technique used to determine clarification efficiency during the spin test. Following clarification in the laboratory centrifuge, the 'supernatant' and 'slurry' streams are separated by pouring the supernatant into a clean tube. The optical density of the supernatant is then recorded to allow calculation of clarification efficiency. At low equivalent Q/Σ (i.e. following long spins), the pouring technique is quite reproducible because most of the slurry is well compacted and supernatant and slurry streams are well defined. However, at higher equivalent Q/Σ (i.e. following short spins), the distinction between supernatant and slurry is much less well-defined, and the pouring of a single extra 'drop' of supernatant can considerably affect the optical density and hence clarification value obtained. Following all spin tests performed however, visible differences were apparent in the clarity of the supernatant following the centrifugation of sheared and non-sheared spheroplast suspensions, confirming that the reduction in clarification following shearing *is* a real phenomenon.

The assessment of scale-down techniques for the modelling of recovery performance in the disk stack centrifuge has revealed that the recovery of shear sensitive material in the CSA-1 is poorly mimicked by both the scale-down CSA-1 and the ultra scale-down laboratory equipment. A more detailed study of the effects of shear within the industrial centrifuge and the rotating disc shear device, including an analysis of the effects of shearing and centrifugation on particle size distribution, is required to fully define the effects of shear on centrifugal clarification. In addition, improved methods for reproducing the shear in laboratory equipment and in the feed zone of the scale-down disk stack need to be developed before such techniques can be used confidently to predict the recovery of shear sensitive material in an industrial machine.

5.3 Summary

A common problem associated with the centrifugation of biological material is the cell disruption or product damage resulting from exposure to very high shear rates in the centrifuge feed zone. The effect of shear on purified 4D5 Fab' and spheroplast suspensions produced by periplasmic extraction has been assessed using a rotating disc shear device. Exposure to shear rates of up to 1.1×10^{6} s^{-1} for 15 seconds, which is comparable to the shear in an industrial centrifuge, did not damage purified 4D5 Fab' or affect spheroplast integrity. However, shearing was found to reduce the clarification achieved during centrifugation in a laboratory batch centrifuge, possibly by breaking up cell clumps or shearing off material from the cell surface, thereby altering the particle size distribution of the suspension.

The centrifugal clarification of spheroplast suspensions has been studied using a disk stack and a tubular bowl centrifuge. For both centrifuges, Fab' recovery appeared to follow the recovery of liquid. The tubular bowl centrifuge produced drier solids and recovered more liquid than the disk stack, hence higher yields of Fab' were achieved. The discharging mechanism of the disk stack centrifuge requires that the solids remain sufficiently wet to flow out of the bowl. As a result, the solids ejected from the disk stack contain considerably more liquid than the tubular bowl solids, and, consequently, Fab' yields in the supernatant stream are lower. Liquid losses during disk stack centrifugation can be reduced by operation with a partial rather than a full discharge.

Techniques developed to allow the study of centrifugal clarification at reduced scale have been assessed in their ability to predict the recovery performance of an industrial disk stack centrifuge. A scale-down version of the disk stack machine and ultra scale-down laboratory equipment over-predicted the clarification of spheroplast suspensions achieved using the full-scale disk stack centrifuge. The poor modelling of full-scale clarification was thought to result from the inability to accurately reproduce shear effects in scale-down equipment. A better understanding of the effect

of shear on biological process streams and improved characterisation of shear fields in both the disk stack centrifuge and the rotating disc shear device are required to allow improvements in the techniques available for modelling centrifugal clarification at reduced scale.

6. A COMPARISON OF CHROMATOGRAPHIC METHODS FOR THE PURIFICATION OF 4D5 Fab'

6.1 Introduction

Two process alternatives are available for the purification of 4D5 Fab' from *E. coli* periplasmic extracts. Fab' may be recovered from periplasmic extracts by packed bed chromatography following process stream clarification. Alternatively, Fab' may be purified directly from whole (unclarified) periplasmic extracts by expanded bed chromatography.

In this chapter, a preliminary study is made into the purification of 4D5 Fab' from clarified and unclarified periplasmic extracts by packed bed and expanded bed protein A affinity chromatography respectively. The two methods of chromatographic purification are compared on the basis of process yield, matrix capacity and the level of process stream purification achieved. The following sections (6.1.1-6.1.3) provide an introduction to expanded bed adsorption and its applications. Section 6.2.1 describes the experimental approach and the basis for process comparisons. The packed and expanded bed runs are summarised in sections 6.2.2 and 6.2.3 respectively. Finally, the two methods of purification are compared in section 6.2.4.

6.1.1 Conventional processing strategies

When designing a purification process, it is important to minimise both the number of unit operations and the processing time to ensure maximal yields and minimal product degradation. The recovery of proteins from cell suspensions or homogenates by packed bed chromatography requires prior clarification of the process stream. The traditional techniques employed for the removal of particulate matter are centrifugation and/ or microfiltration (Lee, 1989). Industrial centrifugation processes are less than 100% efficient and therefore it is usually necessary to combine them with a filtration step to obtain a particle free solution that can be applied to a packed

bed chromatography column. Microfiltration will yield a cell free solution, however liquid flux through the membrane is often dramatically reduced due to membrane fouling during the filtration process, leading to extended processing times and operational problems. Additional disadvantages of both unit operations include no volume reduction and little or no increase in product concentration. Product losses incurred at each stage of process stream clarification and the long processing times which may allow proteolytic degradation of the product both contribute to reduced process yields.

Expanded bed adsorption is a novel technique which allows purification of a protein directly from cell suspensions or homogenates without the requirement for prior process stream clarification. This usually allows higher product recovery in a shorter time period as fewer unit operations are required and the product will be separated from proteolytic enzymes earlier in the process sequence. The development and applications of expanded bed adsorption technology have been reviewed by Chase (1994) and Hjorth (1997); only a brief overview of expanded bed operation is given below.

6.1.2 Expanded bed adsorption

During expanded bed adsorption, liquid is pumped upwards through a particulate adsorbent which is not constrained by the presence of an upper adapter. The adsorbent expands and spaces open up between the particles, allowing cells and cell debris within the feed to pass through without blocking the bed. Adsorption of the product therefore occurs directly in the presence of cellular material.

Purpose-designed adsorbents and columns are required to achieve stable bed expansion and the low back mixing necessary for expanded bed operation. The adsorbents possess an increased density (usually achieved through the inclusion of a quartz or steel core) and a wider size distribution relative to conventional chromatography matrices. The combined effect is to give a 'stratified' bed in expanded mode, with the larger and denser particles in the lower sections of the bed and the smaller, lighter particles in the upper regions. This gives a more 'stable'

expanded bed in which individual adsorbent particles undergo no bulk movement. The increased mass of the adsorbent particles also allows operation of the expanded bed at higher flow rates to give improved productivities.

The columns used for expanded bed processes have two features that distinguish them from packed bed chromatography columns; a 'floating' upper adapter and a specially designed liquid distributor on the column inlet. The upper adapter is moveable so that its height can be adjusted during operation. The column inlet contains a perforated plate which generates a pressure drop and distributes liquid evenly across the whole diameter of the expanded bed, so that plug flow-through the column is achieved.

Expanded bed processes are generally operated in a similar manner to packed bed processes. The major difference relates to the direction of liquid flow; expansion, sample application and washing of the expanded bed being performed using an upward flow. After washing solids from the voids between the particles, the flow is stopped and the bed allowed to settle. Elution is usually performed using a downward flow at decreased velocity to minimise the volume of the eluted fraction.

6.1.3 Applications of expanded bed adsorption

Expanded bed adsorption has been used in a variety of processes for the recovery of proteins from process streams containing cells and/ or cell debris. Examples include the recovery of the intracellular enzyme glucose-6-phsophate dehydrogenase from unclarified yeast cell homogenates by anion-exchange chromatography (Chang and Chase, 1996), purification of extracellular inulinase from yeast cell suspensions using both anion and cation-exchange chromatography (Pessoa, 1996) and the recovery of the recombinant protein annexin V from *E. coli* homogenates using an ion-exchange adsorbent (Barnfield Frej *et al.*, 1994).

The use of expanded bed adsorption for the recovery of a periplasmic protein from cell-containing *E. coli* periplasmic extracts was described by Johansson *et al.*, 1996. The isolation of modified *Pseudomonas* exotoxin A from an *E. coli* spheroplast suspension by anion exchange expanded bed adsorption was compared to a conventional purification method involving centrifugation, microfiltration, and packed bed chromatography. The expanded bed process was found to be three times faster than the conventional route, gave slightly higher yields and produced a more concentrated product.

Expanded bed systems have also been used for the recovery of monoclonal antibodies from mammalian cell systems using immobilised protein A. Thommes *et al.*, (1996) utilised recombinant protein A coupled to a purpose-designed expanded bed matrix (Streamline rProtein A) for the recovery of mouse IgG from an unclarified hybridoma cell culture. A clarified, concentrated eluate of high purity was obtained. However, low product concentrations in the feed caused long sample application times (10-11 hours). The same protein A matrix was used for pilot scale purification of IgG from myeloma cell culture (Jagersten *et al.*, 1996). The purified antibody was found to be of comparable purity to that obtained following feedstock clarification and packed bed protein A chromatography.

Mammalian cell cultures are much more sensitive to shear forces than *E. coli* and yeast cells. Therefore they must be handled more carefully to avoid cell breakage and contamination of the process stream with DNA or intracellular proteases. Cell damage during passage through the expanded bed was assessed by Lutkemeyer *et al.*, 1999. No cell damage was detected during bench or pilot scale purification of IgG using an rProtein A matrix and operating flow rates of 300-450 cm hr^{-1}. Feuser *et al.*, (1999) also observed no measurable cell damage during the purification of IgG from hybridoma cell culture using a cation exchange resin (Streamline SP) or an affinity adsorbent (Streamline rProtein A). The hybridoma cells were however found to interact significantly with the cation exchange adsorbent, but not with the rProtein A matrix.

6.2 Results and Discussion

6.2.1 Experimental approach

Packed bed and expanded bed protein A affinity purification were compared on the basis of matrix capacity, Fab' recovery and purification factor achieved. To allow for process comparisons, a packed bed and an expanded bed rProtein A column were loaded to capacity and the Fab' concentration in the column flow-through was monitored. The matrix total binding capacity and dynamic binding capacities at different levels of Fab' breakthrough were then calculated using the following equations:

$$\text{Total Fab' bound to column} = \text{Total Fab' loaded to column} - \text{Total Fab' lost in breakthrough} \quad \textbf{(6.1)}$$

$$\text{Matrix capacity (mg mL}^{-1}\text{)} = \frac{\text{Total Fab' bound to column (mg)}}{\text{Volume of matrix in column (mL)}} \quad \textbf{(6.2)}$$

Equations 6.1 and 6.2 are based on the assumption that all Fab' retained on the column (i.e. not lost in the breakthrough) is bound to the column and would not be removed by washing.

Data from the chromatography runs was also used to estimate Fab' yields at different levels of breakthrough using the equation:

$$\text{\% Fab' recovery} = 100 \times \frac{\text{Total Fab' bound to column (mg)}}{\text{Total Fab' loaded onto column (mg)}} \quad \textbf{(6.3)}$$

Equation 6.3 again assumes that all retained Fab' is bound to the column and, additionally, that elution of the Fab' is 100% efficient.

Analysis of specific Fab' in the column feeds and purity of Fab' eluted allowed calculation of the process purification factor (PF) where:

$$PF = \frac{\text{Specific Fab' in column eluate}}{\text{Specific Fab' in column feed}} \quad \textbf{(6.4)}$$

$$\text{Specific Fab'} = \frac{\text{Fab' concentration (mg mL}^{-1}\text{)}}{\text{Protein concentration (mg mL}^{-1}\text{)}} \quad \textbf{(6.5)}$$

The column eluate in Equation 6.4 is defined as all the material eluted from the column. In some cases (particularly during processes such as ion exchange chromatography where the levels of purification achieved may be relatively low), the purification factor may be increased by only collecting the proportion of the eluate containing the highest concentration of product (eluate cutting). However, increased purity is only achieved at the expense of a reduction in product yield. Hence, for affinity chromatography where the level of purification is generally very high, there may be no significant advantage in terms of purification gained by eluate cutting.

The packed and expanded bed purification runs had to be performed at different scales of operation because a large scale packed bed protein A column was not available. A 1 mL HiTrap rProtein A column (Amersham Pharmacia Biotech, Uppsala, Sweden) was used for packed bed purification. For expanded bed purification, a Streamline 25 column was employed, using 25 mL Streamline rProtein A media (column and matrix both supplied by Amersham Pharmacia Biotech).

The two chromatography adsorbents utilised the same capture ligand but different base matrices. The ligand, recombinant protein A, has a cystein residue fused to the C-terminal, to allow oriented coupling to the base matrix and thus enhanced IgG binding capacities. The base matrix for packed bed chromatography was cross linked 4% agarose. For expanded bed adsorption, the base matrix was a cross-linked 4% agarose derivative that has been modified through the insertion of an inert, metal alloy core material to provide the required high density for stable bed expansion. The ligand density and total binding capacities for the packed and expanded bed matrices

are quoted by manufacturers as ~ 6 mg rProtein A/ mL medium and ~ 50 mg human IgG/ mL medium respectively.

6.2.2 Packed bed affinity chromatography

Packed bed affinity chromatography was performed according to the protocol detailed in section 2.4.3.1. 4D5 Fab' was purified from clarified periplasmic extracts produced by overnight extraction at 60°C (section 2.4.1.1). Prior to purification, the process stream was concentrated by ultrafiltration (section 2.4.4.2) to reduce the load time required for column saturation. 300 mL of clarified periplasmic extract was loaded onto the 1 mL HiTrap rProtein A column at a flow rate of 40 cm hr^{-1} (1 mL min^{-1}).

Chromatograms for the packed bed purification of 4D5 Fab' are illustrated in Figure 6.2.1. The breakthrough profile shows that column saturation was achieved early in the load cycle (earlier than predicted based on feed concentration and quoted matrix binding capacity, however this only became apparent following completion of the process when Fab' assays had been performed).

6.2.3 Expanded bed affinity chromatography

Expanded bed affinity chromatography was performed as outlined in section 2.4.3.2. The settled bed height of the Streamline adsorbent was 5 cm - the minimum allowable bed height for stable bed expansion. (Recommended sedimented bed heights are in the range 10-15 cm, however a smaller volume of matrix was used to increase the potential for achieving column saturation).

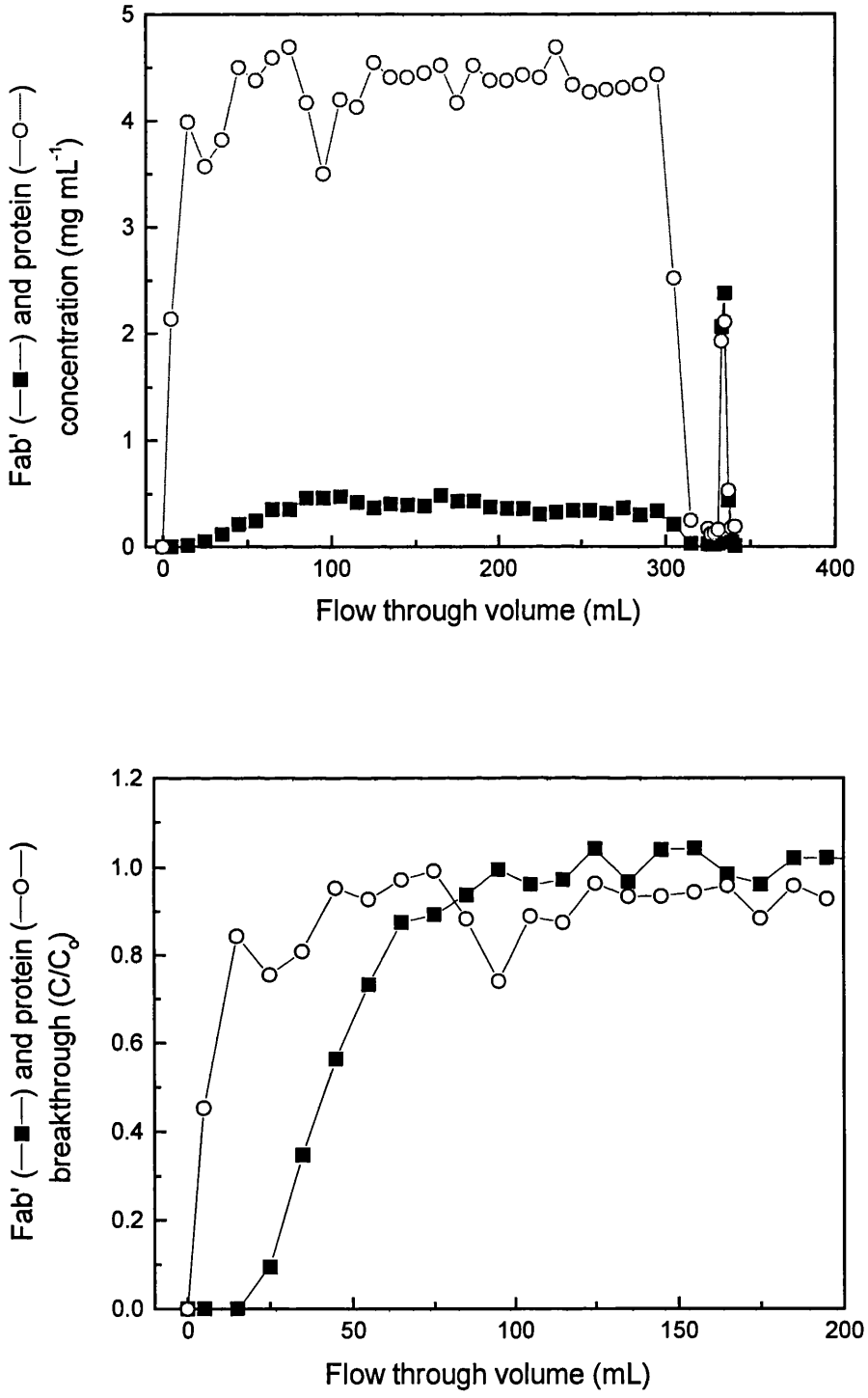

Figure 6.2.1 *Chromatograms for the purification of 4D5 Fab' from clarified periplasmic extracts by packed bed affinity chromatography. Fab' was purified on a 1 mL HiTrap rProtein A column at a flow rate of 40 cm hr^{-1}. The full chromatogram (upper plot) shows Fab' and protein concentrations in the column flow-through. The breakthrough portion of the chromatogram (lower plot) shows the concentration of Fab' or protein in the column flow-through relative to the feed concentration (C/C_o).*

4D5 Fab' was purified from whole (unclarified) periplasmic extracts produced by overnight extraction at 60°C (section 2.4.1.1). Initial expanded bed runs had to be terminated during column loading due to blocking of the lower adapter (column inlet) with cells or cell-associated material. To try and alleviate this problem, feed material was treated with benzonase, as described in section 2.4.3.2-a, prior to loading onto the column to break down extracellular nucleic acids. Following benzonase treatment, no problems with column blocking were encountered during the loading of unclarified periplasmic extract. (This approach has been widely reported by researchers, for example Johansson *et al.*, (1996), however the high cost of benzonase may render such treatment non-viable at scale. In addition, regulatory authorities may not find the use of nuclease treatment during processing acceptable for products destined for therapeutic use).

3L of unclarified periplasmic extract was loaded onto the Streamline column operated in expanded bed mode at a flow rate of 185 cm hr^{-1} (15 mL min^{-1}). Elution was performed in packed bed mode at a flow rate of 90 cm hr^{-1} (7.5 mL min^{-1}).

Chromatograms for the expanded bed purification of 4D5 Fab' are given in Figure 6.2.2. Breakthrough data shows that column saturation was not achieved during loading of the expanded bed. The volume of material required to saturate the bed had been estimated using data from the packed bed chromatography run. However, Fab' losses in the breakthrough during loading of the expanded bed were considerably greater (shown by the breakthrough curve), hence increased volumes of material were required for column saturation. Again this only became apparent once Fab' assays had been performed following completion of the process. However, the required process parameters for comparison with packed bed chromatography could still be estimated from the data obtained.

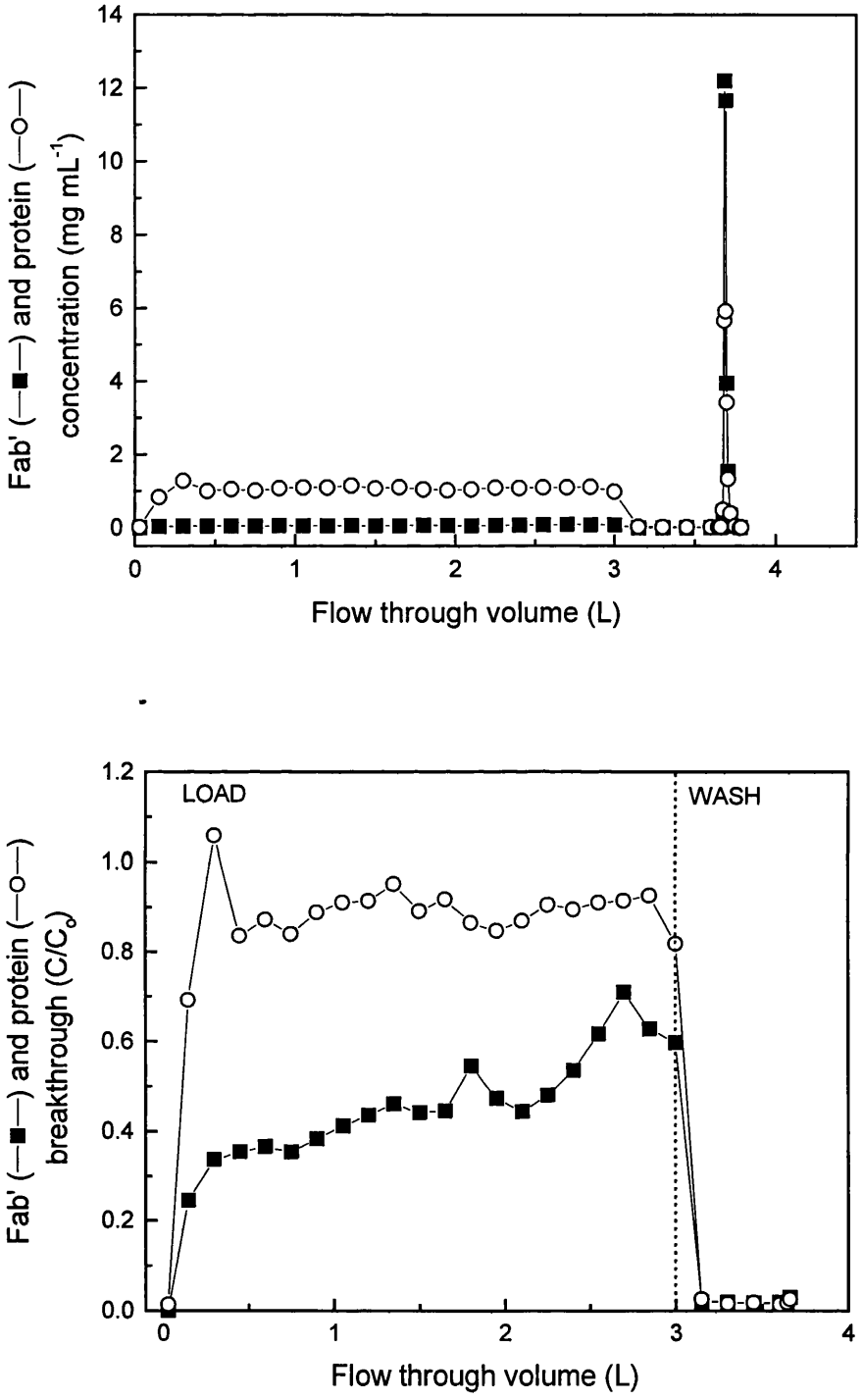

Figure 6.2.2 *Chromatograms for the purification of 4D5 Fab' from unclarified periplasmic extracts by expanded bed affinity chromatography. Fab' was purified using 25 mL Streamline rProtein A media in a 25mm diameter Streamline column. Load and wash cycles were performed in expanded bed mode at a flow rate of 185 cm hr^{-1}. Elution was performed in packed bed mode at 90 cm hr^{-1}. The full chromatogram (upper plot) shows Fab' and protein concentrations in the column flow-through. The breakthrough portion of the chromatogram (lower plot) shows the concentration of Fab' or protein in the column flow-through relative to the feed concentration (C/C$_o$).*

6.2.4 Comparison of packed and expanded bed affinity purification

The experimental data was used to estimate total binding capacities of the packed and expanded bed rProtein A media. The binding capacities for 4D5 Fab' are compared to the total capacities for human IgG quoted by manufacturers in Table 6.2.1. Lower capacities for Fab' are expected as the capacities are based on the mass of antibody bound per mL of media. The mass of Fab' is approximately one third that of whole IgG. Therefore, assuming IgG and Fab' bind to protein A in the same ratio, approximately one third the *mass* of Fab' compared to IgG will bind to the same volume of media. Furthermore, protein A binds to different sites on Fab' and IgG, and the affinity for the Fab' site is lower (Starovasnik *et al.*, 1999), which will reduce the binding capacity further. Measured binding capacities of packed and expanded bed media for Fab' were 12.5 and 13.5 mg mL^{-1} respectively, which is approximately one quarter that quoted for IgG (50 mg mL^{-1}).

Chromatography Method	Chromatography media	Total Binding Capacity (mg mL^{-1})	
		Quoted value (for IgG)	Experimental value (for Fab')
Packed bed chromatography	rProtein A Sepharose® Fast Flow	50	12.5
Expanded bed chromatography	Streamline rProtein A	50	13.5

Table 6.2.1 *Comparison of experimental and quoted values for the total binding capacity of packed bed and expanded bed chromatography media. Quoted values are those given by manufacturers for the binding of human IgG. Experimental values are for 4D5 Fab'.*

The breakthrough data for the two chromatography runs was used to estimate the Fab' yields and dynamic binding capacities of the chromatography media at different levels of Fab' breakthrough. The yields and capacities obtained are shown in Figures 6.2.3. and 6.2.4 respectively. For both packed and expanded bed chromatography, yields decreased and matrix dynamic capacity increased with increasing Fab' breakthrough, as expected. However, yields and capacities were appreciably greater for packed bed chromatography.

The observed differences can be attributed to the contrasting patterns of Fab' breakthrough. The packed and expanded bed breakthrough curves, adjusted for differences in column volumes and the Fab' concentration in feed streams, are compared in Figure 6.2.5. To adjust for differences in the feed concentration of Fab' it was assumed that the affinity of protein A for Fab' was independent of Fab' concentration for the range of Fab' concentrations 0.1-0.4 mg mL^{-1}.

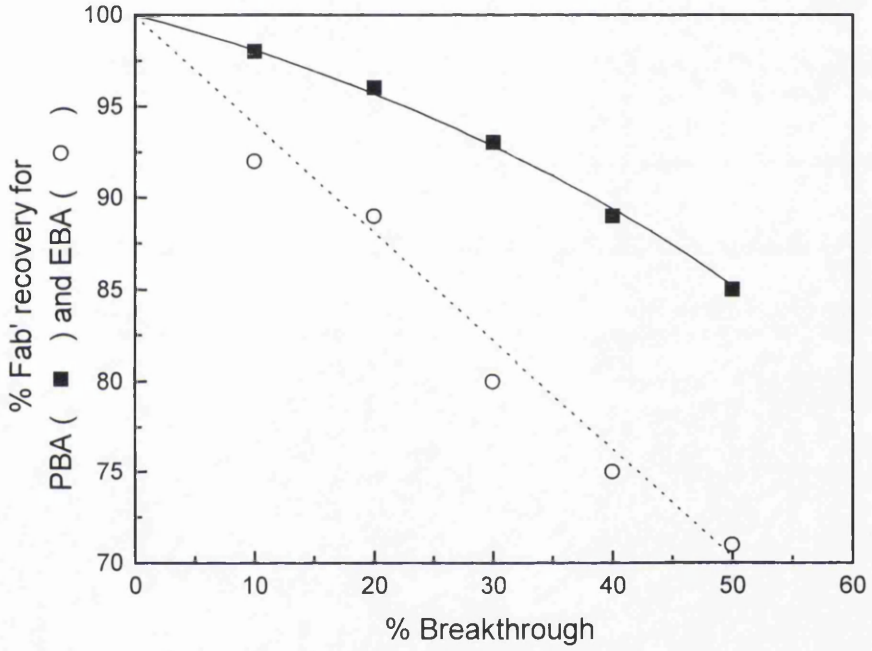

Figure 6.2.3 *Comparison of Fab' recovery at different levels of Fab' breakthrough for packed bed chromatography (PBA; trend shown by solid line) and expanded bed chromatography (EBA; trend shown by dotted line). PBA was performed using a 1 mL HiTrap rProtein A column at a flow rate of 40 cm hr^{-1}. EBA was performed using 25 mL Streamline rProtein A media in a 25 mm diameter Streamline column. Operating flow rates for EBA were 185 cm hr^{-1} (load and wash cycles, performed in expanded bed mode) and 90 cm hr^{-1} (elution cycle, performed in packed bed mode).*

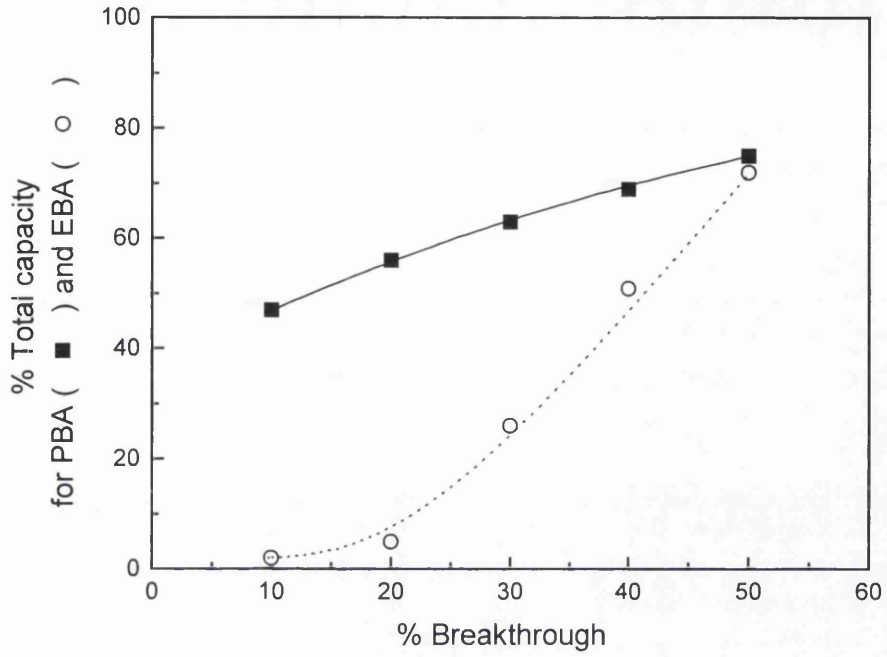

Figure 6.2.4 *Comparison of media capacity at different levels of Fab' breakthrough for packed bed chromatography (PBA; trend shown by straight line) and expanded bed chromatography (EBA; trend shown by dotted line). Media capacity is expressed as a percentage of the total binding capacity, which was estimated from the chromatography data as 12.5 mg mL^{-1} (packed bed media) and 13.5 mg mL^{-1} (expanded bed media). PBA was performed using a 1 mL HiTrap rProtein A column at a flow rate of 40 cm hr^{-1}. EBA was performed using 25 mL Streamline rProtein A media in a 25 mm diameter Streamline column. Operating flow rates for EBA were 185 cm hr^{-1} (load and wash cycles, performed in expanded bed mode) and 90 cm hr^{-1} (elution cycle, performed in packed bed mode).*

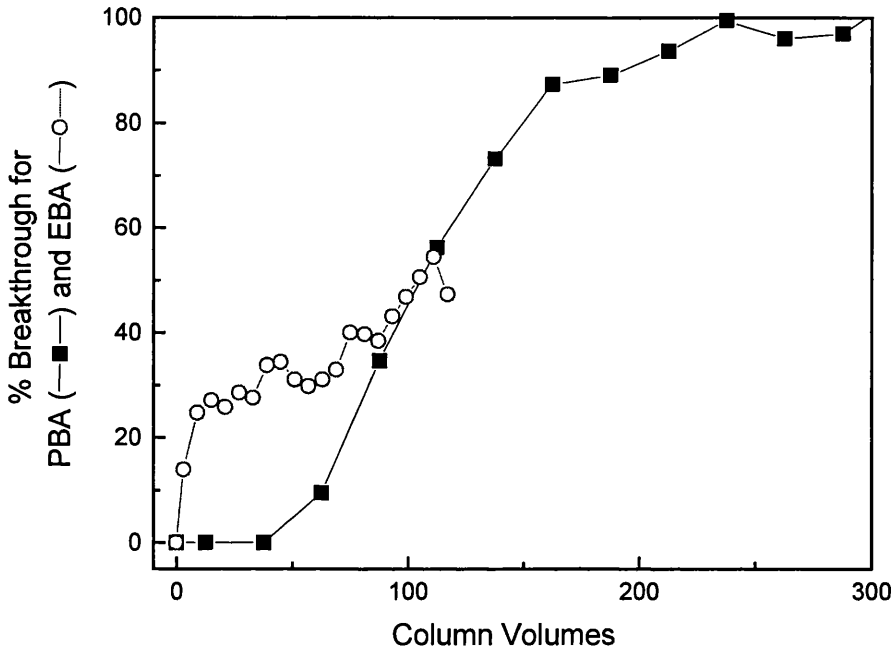

Figure 6.2.5 *Comparison of Fab' breakthrough curves for packed bed (PBA) and expanded bed (EBA) chromatography. Breakthrough curves have been adjusted to account for differences in the concentration of Fab' in the column feeds and for differences in column volumes. Data for EBA was only obtained up to 50% breakthrough.*

The pattern of breakthrough for packed bed chromatography was similar to the expected or 'traditional' chromatography breakthrough curve, however the breakthrough pattern for expanded bed adsorption was more unusual. Fab' concentration in the flow-through from the expanded bed immediately increased to ~30% of the feed concentration from the onset of column loading; the level of breakthrough then continued to rise but at a much slower rate compared to both the initial increase and the rate of increase in breakthrough for packed bed chromatography. The higher levels of Fab' loss in the expanded bed flow-through accounts for the lower Fab' yields compared to packed bed purification. In addition, the very low matrix capacities at low levels of breakthrough can also be attributed to the immediate breakthrough to ~30%.

Breakthrough from the expanded bed chromatography column was only monitored during one purification run, however similar patterns of breakthrough have also been observed during the expanded bed purification of alcohol dehydrogenase from yeast homogenates (personal communication, N. Willoughby). Losses of Fab' during column loading in the experiments described above may have been exaggerated as a result of using a minimal volume of chromatography media. Increasing the volume of media will increase the column residence time, allowing more time for Fab' binding and thereby reducing Fab' losses in the column flow-through. Use of a small bed volume may also have resulted in streaming, with some product bypassing the bed completely. Such an effect would have further exaggerated Fab' losses in the breakthrough.

When specifying operating conditions for a chromatographic purification process, there generally has to be a trade off between maximising the utilisation of expensive chromatography media (achieved by operation at high breakthrough) and minimising the loss of a high value pharmaceutical product (achieved by operation at low breakthrough). The trade off between product yield and matrix utilisation can be determined from a plot combining product recovery and matrix capacity data. Figure 6.2.6 shows such a plot for the expanded bed purification of 4D5 Fab'. The operating conditions which maximise matrix utilisation whilst minimising product losses are determined from the intersection of the two sets of data, in this case 50%

breakthrough. Operation at lower than 50% breakthrough will increase yields by reducing Fab' losses, however the chromatography media will not be used to optimum capacity. Operation at higher than 50% breakthrough will improve media utilisation but at the expense of product yield. Economic data relating matrix costs and product value is also required to provide a more detailed cost analysis of the process and allow identification of the optimal operating conditions.

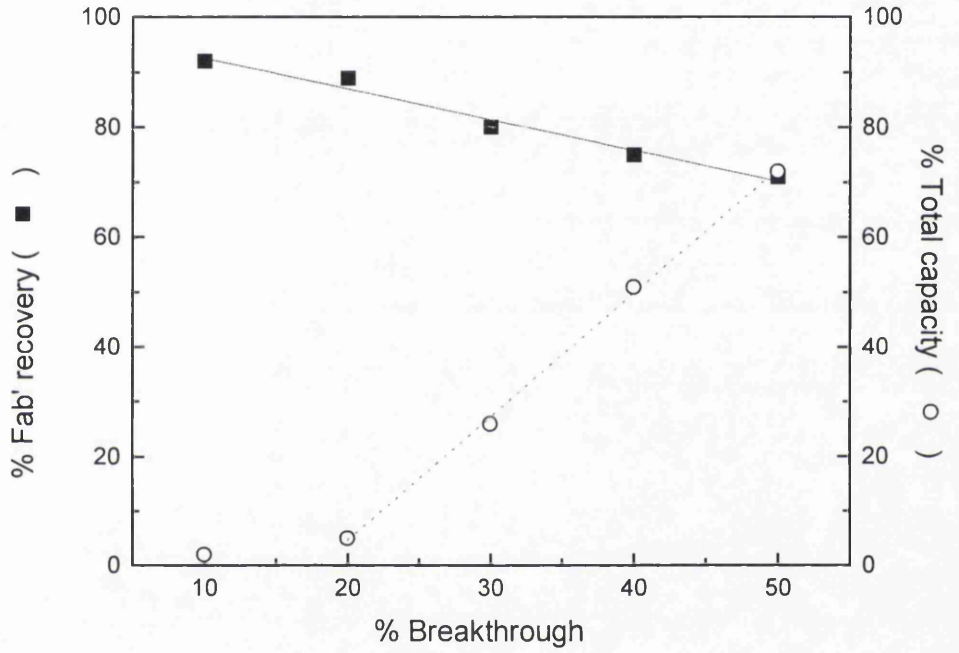

Figure 6.2.6 *Effect of the level of breakthrough on Fab' yield and matrix dynamic binding capacity for the expanded bed purification of 4D5 Fab' from E. coli unclarified periplasmic extracts. Such information, combined with cost data for product revenue and matrix price, could form the basis of an economic analysis for the expanded bed purification process.*

Finally, the degree of process stream purification attained using packed and expanded bed chromatography was compared. Similar levels of purification were achieved, shown by the similar purification factors (Table 6.2.2). Comparable levels of Fab' purity was also illustrated by SDS-PAGE analysis of the column eluates (Figure 6.2.7).

Process Stream	PBA		EBA	
	Specific Fab' (mg mL^{-1})	Purification factor (-)	Specific Fab' (mg mL^{-1})	Purification factor (-)
Column feed	0.078	-	0.101	-
Column eluate	1.1	14	1.26	12

Table 6.2.2 *Comparison of process stream purification achieved using packed bed (PBA) and expanded bed (EBA) affinity purification of 4D5 Fab'.*

On the basis of results from this study, packed bed affinity chromatography appears to be the more efficient purification method because of the higher Fab' yields and matrix capacities at low levels of breakthrough. However, the study does not consider additional processing factors such as operating time and process costs. A major advantage of expanded bed adsorption is the fact that it can be performed on unclarified feedstocks. Packed bed adsorption requires clarification of the process stream prior to application to the column, which can add considerable time and cost to the process, and will result in reduced process yields. A disadvantage of expanded bed adsorption however is the high cost of the chromatography media and the requirement for large volumes of buffers during column equilibration and washing, which will further increase the operational costs. A more detailed comparison of packed and expanded bed purification processes, which includes reference to process yields and operating time, is given in Chapter 8.

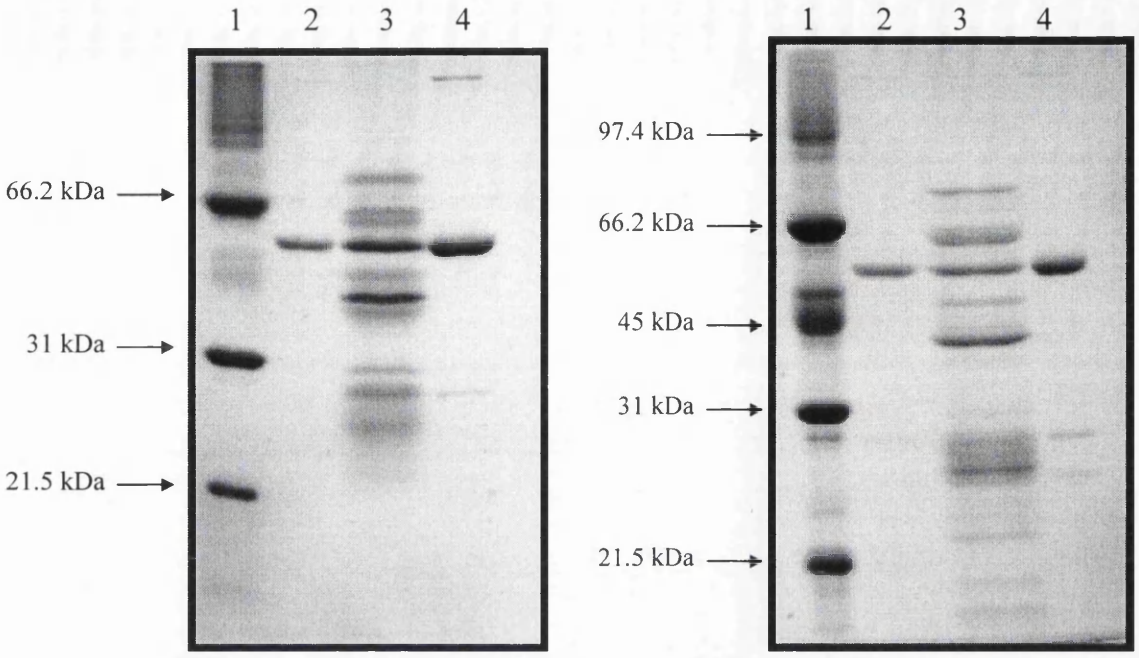

(a) Packed bed chromatography (b) Expanded bed chromatography

Figure 6.2.7 *SDS-PAGE analysis of Fab' purity following packed bed (a) and expanded bed (b) protein A affinity purification of 4D5 Fab'.*

(a) Packed bed affinity purification of 4D5 Fab'

Lane 1 Low molecular weight markers
Lane 2 Purified 4D5 Fab' standard
Lane 3 Column load (clarified E. coli periplasmic extract)
Lane 4 Column eluate (purified 4D5 Fab')

(b) Expanded bed affinity purification of 4D5 Fab'

Lane 1 Low molecular weight markers
Lane 2 Purified 4D5 Fab' standard
Lane 3 Column load (unclarified E. coli periplasmic extract)
Lane 4 Column eluate (purified 4D5 Fab')

6.2.5 Summary

Packed bed and expanded bed affinity purification of 4D5 Fab' have been compared on the basis of Fab' yield, matrix capacity and the degree of process stream purification achieved.

Fab' yields and dynamic binding capacities were greater for packed bed chromatography compared to expanded bed chromatography. Differences were attributed to the contrasting patterns of Fab' breakthrough, with considerably greater losses of Fab' in the flow-through from the expanded bed column. Estimates of the total binding capacity of the two matrices were similar; capacities of 12.5 mg mL^{-1} and 13.5 mg mL^{-1} were obtained for packed and expanded bed media respectively. The degree of purification was also similar for the two processes; a purification factor of 14 was recorded for packed bed purification and 12 for the expanded bed process.

This study provides only an initial insight into the differences between the chromatographic processes. A detailed assessment of processing time and costs would also be required to give a more comprehensive view of the advantages and disadvantages of the process alternatives.

7. BIOPROCESS MONITORING

7.1 Introduction

The monitoring of antibody fragments during production and purification processes has traditionally been performed by enzyme linked immunosorbant assay (ELISA). The ELISA is a multistage method which can take 3 hours or more to complete, therefore samples for ELISA analysis are generally stored until completion of the process and assayed together in one batch. This means the data generated can only provide an historical description of the completed process; the ELISA cannot be used to generate data in real time to allow decisions regarding the fate of the process to be made during process operation.

The optical biosensor has recently found application in monitoring of fermentation and chromatographic process (reviewed in Chapter 1). Advantages of the biosensor include the reduced sample processing time, with quantitative data available within minutes of sample addition to the device. Hence the biosensor has the potential to generate data regarding the state of the process in real time, providing the means for more effective process control.

During this study an optical biosensor employing a resonant mirror (Cush *et al.*, 1993) was used for the monitoring of 4D5 Fab' during fermentation and chromatographic purification. Two optical biosensor assays were developed as an alternative to ELISA. The first assay used protein A as the biosensor ligand, the second a mouse anti-human monoclonal antibody labelled HP6045.

Staphylococcal protein A has two distinct binding sites on human immunoglobulins. It will bind the Fc region of most IgG molecules and, in addition, has been shown to bind to an 'alternative' site within the Fab region of certain immunoglobulins independent of their heavy chain isotype (Ibrahim *et al.*, 1993). The Fab site that binds protein A has been localised to the V region of the Ig H chain and the ability to bind protein A is restricted to immunoglobulins that utilise heavy chain genes encoded by the VH (III) subfamily (Sasso *et al.*, 1991). Protein A has been shown to

bind 4D5 Fab' with an association constant, k_a, of 5.5 (±0.5) × 10^5 M^{-1} (Starovasnik *et al.*, 1999).

HP6045 is the capture antibody used in the ELISA and binds the CH1 domain of all subclasses of human immunoglobulin. Thus the HP6045 assay is generic for all human Fab whereas use of the protein A assay would be restricted to Fabs of the VH (III) subclass.

This chapter describes and compares the assays employed for quantification of 4D5 Fab'. The ELISA is characterised in section 7.2.1. Section 7.2.2 describes the protein A and HP6045 biosensor assays developed during this work. The biosensor assays are compared to ELISA in the ability to quantify antibody titres during the induction stage of *E. coli* fermentation in section 7.2.3.1. Finally, the protein A biosensor assay is assessed as a technique for the monitoring of chromatography breakthrough and elution during packed and expanded bed affinity purification in section 7.2.3.2.

7.2 Results and discussion

7.2.1 ELISA

The primary technique used for antibody quantification in this study was ELISA. A schematic representation of the ELISA used for the detection of 4D5 Fab' is illustrated in Figure 7.2.1, and the detailed protocol is given in section 2.3.1. The ELISA is a sandwich assay which detects correctly folded and assembled Fab' and furthermore is generic for all human Fabs containing the kappa light chain. However it does not provide a measure of Fab' activity.

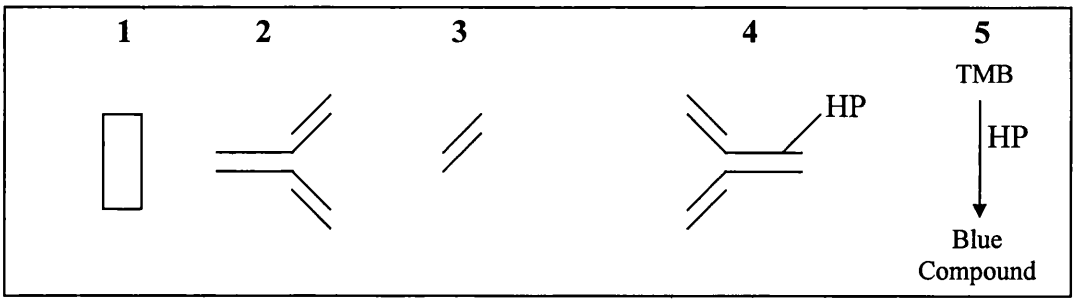

1. **Solid Phase** - 96 well microtitre plates

2. **Capture Antibody** - HP6045 (mouse anti-human monoclonal antibody - recognises CH1 domain of all subclasses of human immunoglobulin)

3. **Standard or Sample** - 4D5 Fab' antibody fragment

4. **Antibody-enzyme conjugate** - GD12 peroxidase (commercially available mouse anti-human monoclonal antibody directed against human kappa light chain, conjugated to horseradish peroxidase)

5. **Enzyme substrate** - TMB (converted by horseradish peroxidase to a blue coloured compound detected at 630nm)

Figure 7.2.1 *Schematic representation of ELISA used for the quantification of 4D5 Fab'.*

7.2.1.1 Assay calibration

All antibody concentrations determined by ELISA were measured by comparison with standard 4D5 Fab' solutions of known concentration. Standard curves were prepared by performing a 1 in 2 dilution series of a 1 $\mu g\ mL^{-1}$ standard solution of 4D5 Fab' on every plate each time the ELISA was performed. A typical ELISA standard curve is illustrated in Figure 7.2.2. Concentrations of unknown samples were read from within the linear range of the curve, typically 0.125-0.015 $\mu g(Fab')\ mL^{-1}$.

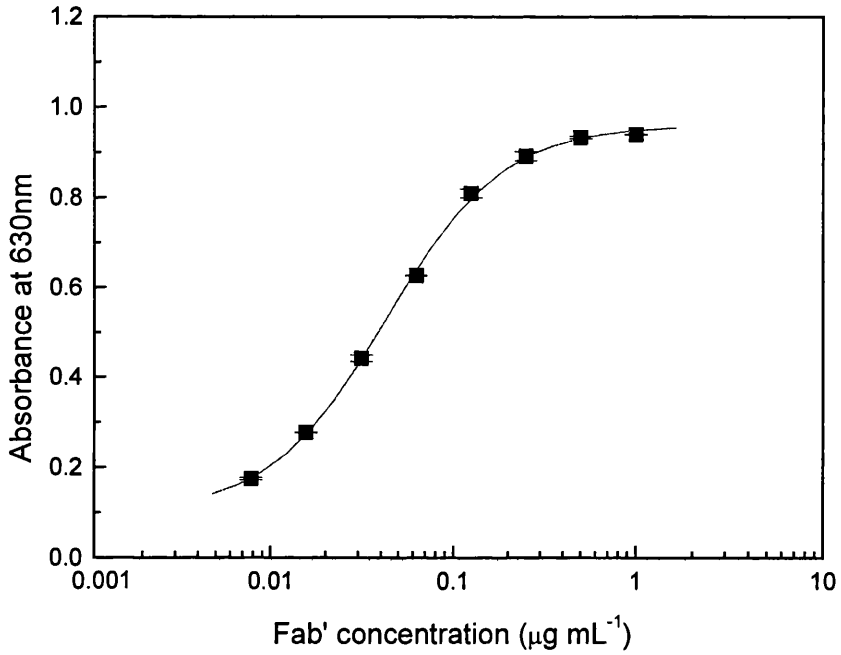

Figure 7.2.2 *Typical standard curve for the calibration of ELISA assays. Fab' concentrations in unknown samples are read from the linear region of the standard curve (0.125 - 0.015 μg mL^{-1}). Error bars represent the standard deviation of duplicate measurements.*

Initially 4D5 Fab' standards were obtained from Celltech Chiroscience (Slough, UK). Later, protocols were developed for the production of standards 'in house'. A summary of the methods involved in standard production is shown in Figure 7.2.3 and the specific protocols are outlined in section 2.3.3.

The initial 'in house' standard was purified from periplasmic extracts produced by overnight incubation at 30°C. However, later work characterising the periplasmic extraction process (Chapter 4) revealed that such preparations contained a large proportion of incomplete or partially degraded Fab' (Figure 4.2.5). Concentration of the standard was determined from its absorbance at 280nm, which provided a measure of total protein rather than complete, correctly assembled Fab' detectable by ELISA. The consequence of using such a standard for ELISA calibration would have been to overestimate the concentration of Fab' in unknown samples.

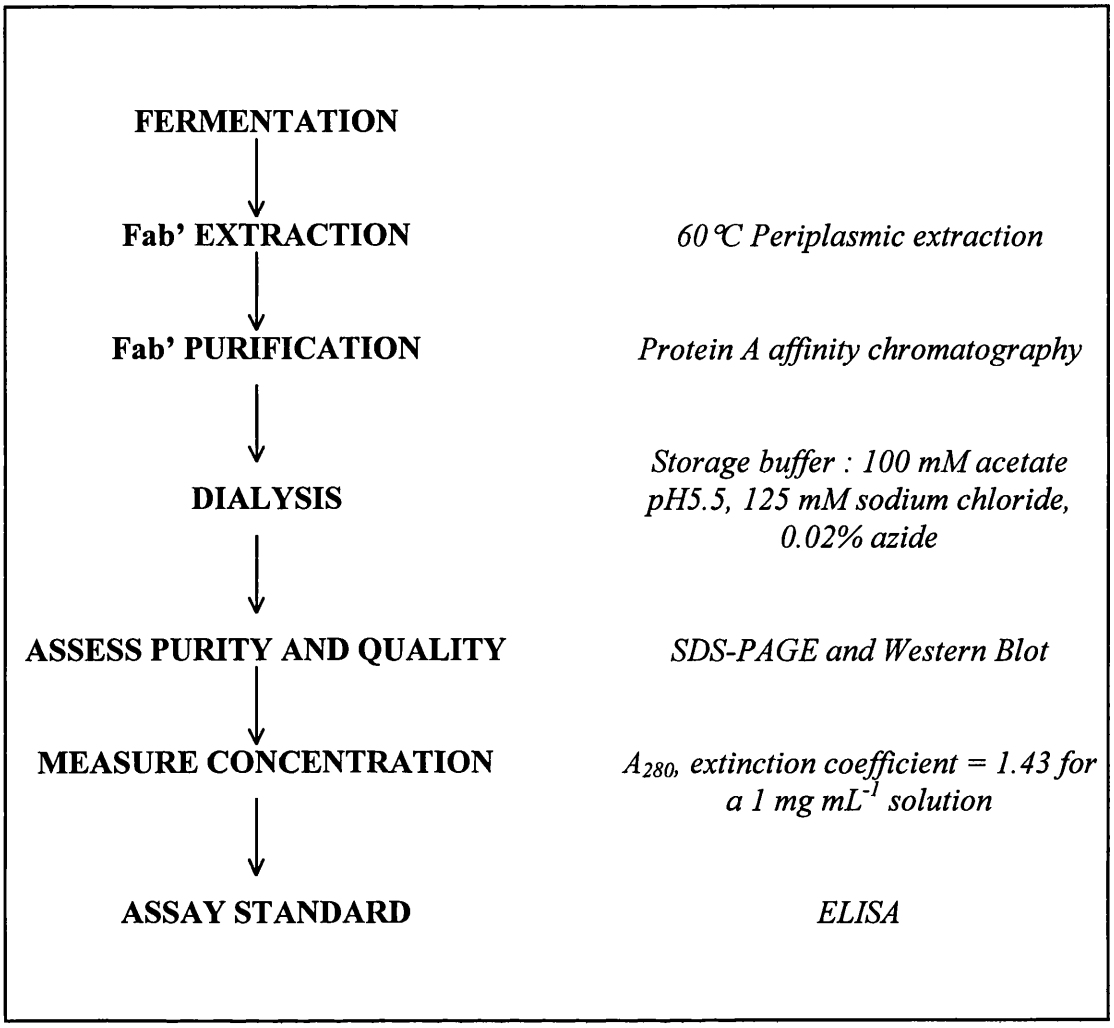

Figure 7.2.3 *Summary of the stages involved in the production of 4D5 Fab' standards.*

Subsequent standards were purified from periplasmic extracts obtained by overnight incubation at 60°C. Such preparations were appreciably 'cleaner' than those produced from 30°C extracts (Figure 4.2.5), containing predominantly correctly assembled, disulphide bonded Fab' and thus allowing a more accurate determination of the Fab' concentration in unknown samples.

The use of different antibody standards is thought to have contributed towards the variation in Fab' titres observed for the fermentations described in Chapter 3. Initial HCD fermentations (runs 1 and 2) produced very high Fab' titres (>600 mg L^{-1}), however titres recorded in later fermentations were notably lower (<230 mg L^{-1}). The reduction in titres was thought to be a direct consequence of switching from the old

standard (purified from 30°C extracts) to a new standard (produced from 60°C extracts) rather than being a real phenomenon. This highlights the importance of correct standard preparation and careful assessment of standard quality to ensure accurate determination of Fab' concentration and allow valid comparisons of Fab' titres in unknown samples.

7.2.1.2 Assay error

The error associated with the ELISA was estimated by performing 10 standard curves on the same microtitre plate and measuring the mean absorbance, the maximum deviation of any value from the mean and the 95% confidence interval (CI) for each concentration. The equations for calculation of 95% CI are given in Appendix 11. The maximum deviation of any value from the mean was ± 11%, and the maximum error of the mean at the 95% CI level was determined to be ± 5%. Because the method used to estimate error only takes into account a selection of the inaccuracies associated with the assay, the value of ± 11% was thought to give a more accurate indication of error, hence this is the value used to represent ELISA error in previous chapters of this thesis.

Sources of error include the large sample dilutions required prior to sample analysis (all samples must be diluted to within the linear range of the standard curve) and the propagation of errors caused by performing a dilution series of both standards and samples on each ELISA plate. The use of different standards, poor pipette calibration and the deterioration of assay reagents during storage can also contribute to the inaccuracies of the assay.

7.2.1.3 Non-specific binding

Before using the ELISA in the analysis of process samples a series of control experiments were carried out to determine background absorbance levels resulting from non-specific interactions between assay reagents. Standard curves were prepared using the combinations of reagents shown in Table 7.2.1. Where an antibody is shown as not being included, buffer alone was added to the wells and

plates were incubated according to the standard protocol. All control curves gave maximum absorbances of <0.060 confirming that no appreciable signal is produced as a result of non-specific interactions between assay reagents.

Experiment	Combination of reagents used				Non-specific interactions tested	Maximum absorbance
	HP6045	4D5 Standard	GD12 peroxidase	Substrate solution		
1	✓	✓	✓	✓	-	0.937
2	✓	✗	✓	✓	HP6045 - GD12	0.053
3	✓	✓	✗	✓	4D5 - substrate	0.051
4	✓	✗	✗	✓	HP6045 - substrate	0.049
5	✗	✓	✓	✓	Well - 4D5	0.055
6	✗	✗	✓	✓	Well - GD12	0.056
7	✗	✗	✗	✓	Well - substrate	0.059
8	✗	✗	✗	✗	Buffers	0.057

Table 7.2.1 *Summary of ELISA control experiments.*

Prior to the analysis of complex process samples it was also necessary to determine the effects of non-specific binding on the ELISA assay. Contaminants within process samples, particularly lipids and DNA, can interact through non-specific hydrophobic or ionic interactions with the surface of the solid phase (the wells of the microtitre plate) or with antibodies used in the assay. Such interactions may result in 'false positive' responses and should be minimised during assay development by selection of the correct reagents and buffer systems (Kuen *et al.*, 1993; Jones *et al.*, 1992). The sample conjugate buffer used for the dilution of samples, standards and the revealing antibody GD12 peroxidase contained NaCl, Tween and casein to minimise non-specific binding. Salt and Tween reduce ionic and hydrophobic interactions respectively whereas casein acts as a 'block', binding to sites on the wells of the ELISA plate not occupied by the coating antibody.

The effects of non-specific binding were determined by comparing standard curves prepared in sample conjugate buffer with those prepared by spiking purified antibody into control fermentation supernatant (supplied by D. Bracewell, Department of Biochemical Engineering, UCL). The control supernatant was obtained from an *E. coli* fermentation (strain BMH 71-18) expressing the D1.3 Fv antibody fragment (J. Harrison, PhD Thesis, 1996). D1.3 Fv is derived from the murine monoclonal antibody D1.3 IgG raised against hen egg lysozme and therefore should not interact

with antibodies employed for the ELISA assay, both of which are directed against constant regions of human antibodies. Purified 4D5 Fab' was spiked into the fermentation supernatant to a concentration of 1 μg mL^{-1}. This sample was assayed alongside 4D5 Fab' standard diluted to 1 μg mL^{-1} in sample conjugate buffer. Conjugate buffer and fermentation supernatant without antibody added were included as negative controls on the same ELISA plate.

The ELISA response curves obtained are shown in Figure 7.2.4. Both curves are within error of each other, indicating no appreciable interference from components of the fermentation broth. In addition, no detectable signal was obtained from either negative control providing further evidence that the ELISA is not subject to interference by non-specific binding.

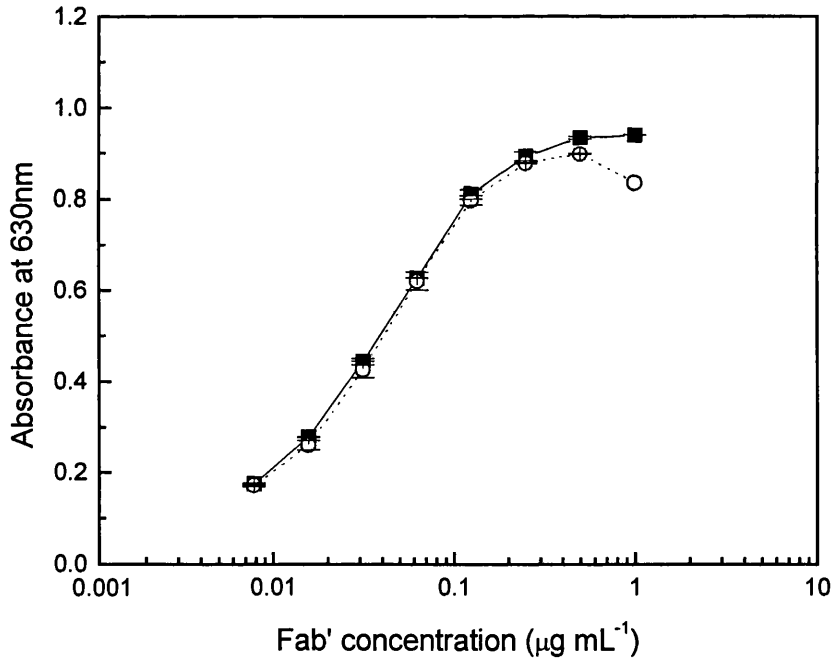

Figure 7.2.4 *ELISA calibration curves produced using Fab' standard diluted in sample conjugate buffer (-■-) or E. coli fermentation supernatant (···O···). Both curves are within error of each other indicating that contaminants within the fermentation supernatant do not interfere with the ELISA signal. Error bars represent the standard deviation of duplicate measurements.*

7.2.2 Optical biosensor assays

Carboxymethyl dextran cuvettes prepared with either protein A or HP6045 immobilised to the sensing surface were employed for antibody fragment quantification. Both capture ligands were immobilised using the standard protocol described in section 2.3.2.2. The amount of ligand immobilised was determined from the change in refractive index of the sensing surface (measured as the difference between pre- and post- immobilisation baselines). Typically, this was in the order of 1000-2000 arc seconds, corresponding to 1-2 ng (bound protein) mm^{-2} (Richalet-Secordel *et al.*, 1997).

7.2.2.1 Assay calibration

The interaction of 4D5 Fab' with each ligand was studied as described in section 2.3.2.3. The addition of known concentrations of purified 4D5 Fab' to the biosensor cuvette containing the appropriate capture ligand resulted in a series of characteristic binding curves differing in initial binding rate. A set of such binding curves for the protein A assay is illustrated in Figure 7.2.5. Linear regression applied to the initial ten seconds of each binding curve (as described by Holwill *et al.,* 1996) was used to determine the initial rate of binding and this in turn was plotted against concentration to produce a calibration curve for each assay.

Calibration plots for the protein A and HP6045 assays are illustrated in Figure 7.2.6. (In all calibration plots the 4D5 Fab' concentration shown is the concentration prior to dilution in the biosensor cuvette). A linear correlation clearly exists between instrument response and sample concentration for both assays, however the range of this correlation is notably greater for the protein A assay (working range 0-400 μg mL^{-1}) compared to the HP6045 assay (working range 0-200 μg mL^{-1}). The linear range is likely to be limited by the number of sites available for antibody binding at the sensor surface which, in turn, will be influenced by the amount of capture ligand immobilised and the orientation of immobilisation (Berney *et al.*, 1997). The larger size of HP6045 (~150 kDa) compared to protein A (45 kDa) means that fewer

HP6045 molecules will be immobilised, giving fewer sites for Fab' binding, which may explain the reduced assay range.

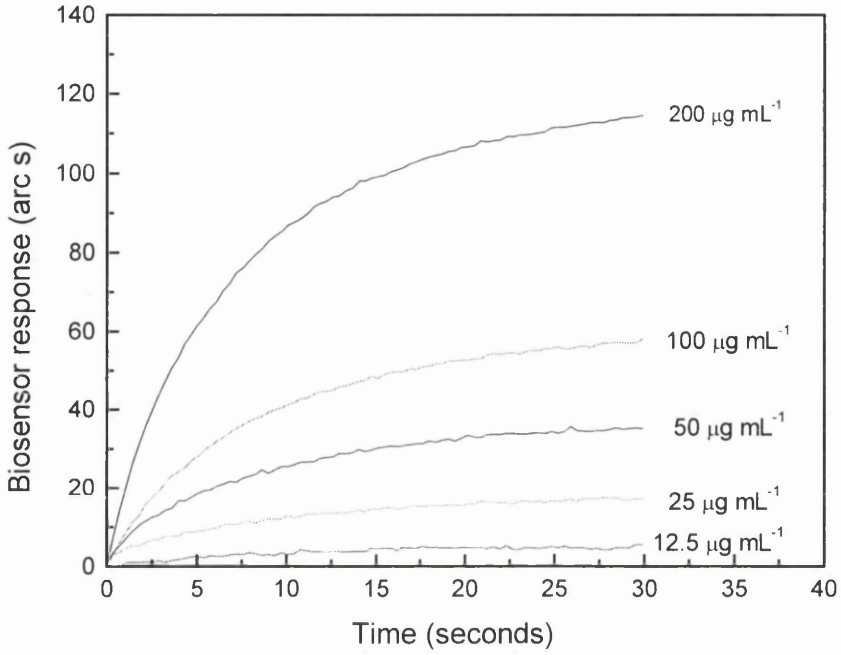

Figure 7.2.5 *Interaction curves for binding of 4D5 Fab' standard solutions of known concentration to immobilised protein A. Binding curves were produced using the IAsys optical biosensor. Linear regression was applied to the initial ten seconds of each interaction curve to determine the initial rate of binding, as described by Holwill et al., (1996).*

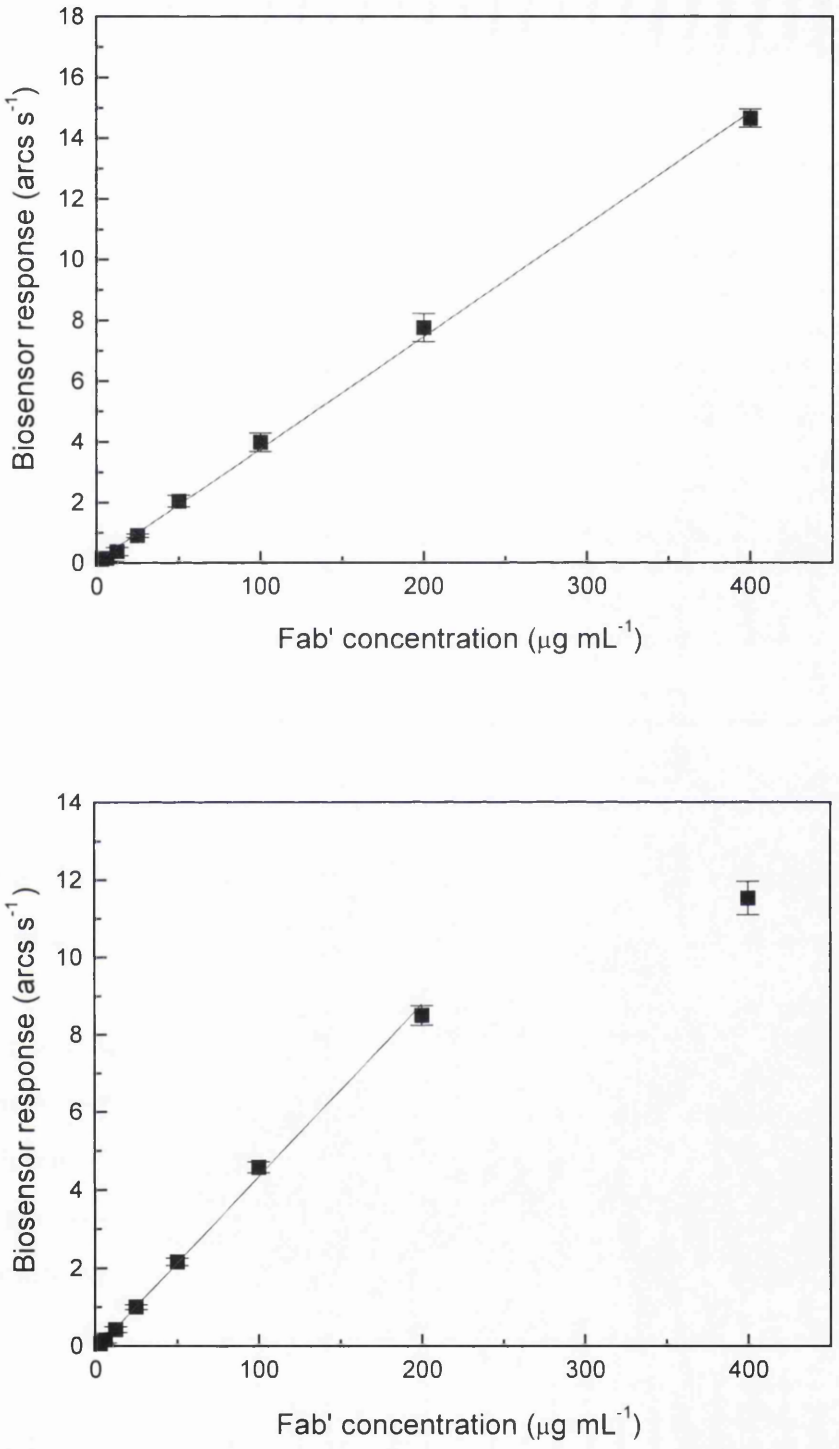

Figure 7.2.6 *Calibration curves for the interaction of purified 4D5 Fab' in buffer with protein A (upper plot) and HP6045 (lower plot). The linear relationship between initial rate of biosensor response and Fab' concentration is shown. Error bars represent the standard deviation of triplicate sample measurements.*

Variations in the amount of ligand immobilised resulted in differences in the magnitude of the biosensor response to specific concentrations of 4D5 Fab' and therefore variations in the slope of the standard curve. As a result, every cuvette required calibration. The gradient of the standard curve was also affected by the length of time for which the capture ligand had been stored prior to immobilisation. Therefore, only freshly reconstituted protein A or the latest HP6045 preparation was used for immobilisation purposes.

The effect of using different standards for assay calibration was assessed by calibrating a protein A and an HP6045 coated biosensor cuvette with two Fab' standards produced 'in house'. Both standards were purified from 60°C periplasmic extracts as described in section 2.3.3, and were initially shown to produce identical ELISA calibration curves. The biosensor calibration curves obtained are illustrated in Figure 7.2.7. It is apparent that both standards gave identical plots for the HP6045 cuvette, however the interaction between protein A and Fab' standard 1 was considerably stronger than between protein A and Fab' standard 2.

The standards were purified from different feedstocks, using slightly different chromatographic techniques. Standard 1 was purified on a 7 mL Streamline rProtein A column whereas standard 2 was purified using 1.66 mL POROS® 50A protein A affinity chromatography media. Details of media, columns and associated operating conditions are given in section 2.4.3.1. The use of different media and flow rates may have resulted in the purification of non-identical populations of Fab' molecules differing in their affinity for protein A. This identifies one of the potential problems associated with using a standard purified by affinity protein A chromatography to calibrate an assay based on the interaction between protein A and Fab'.

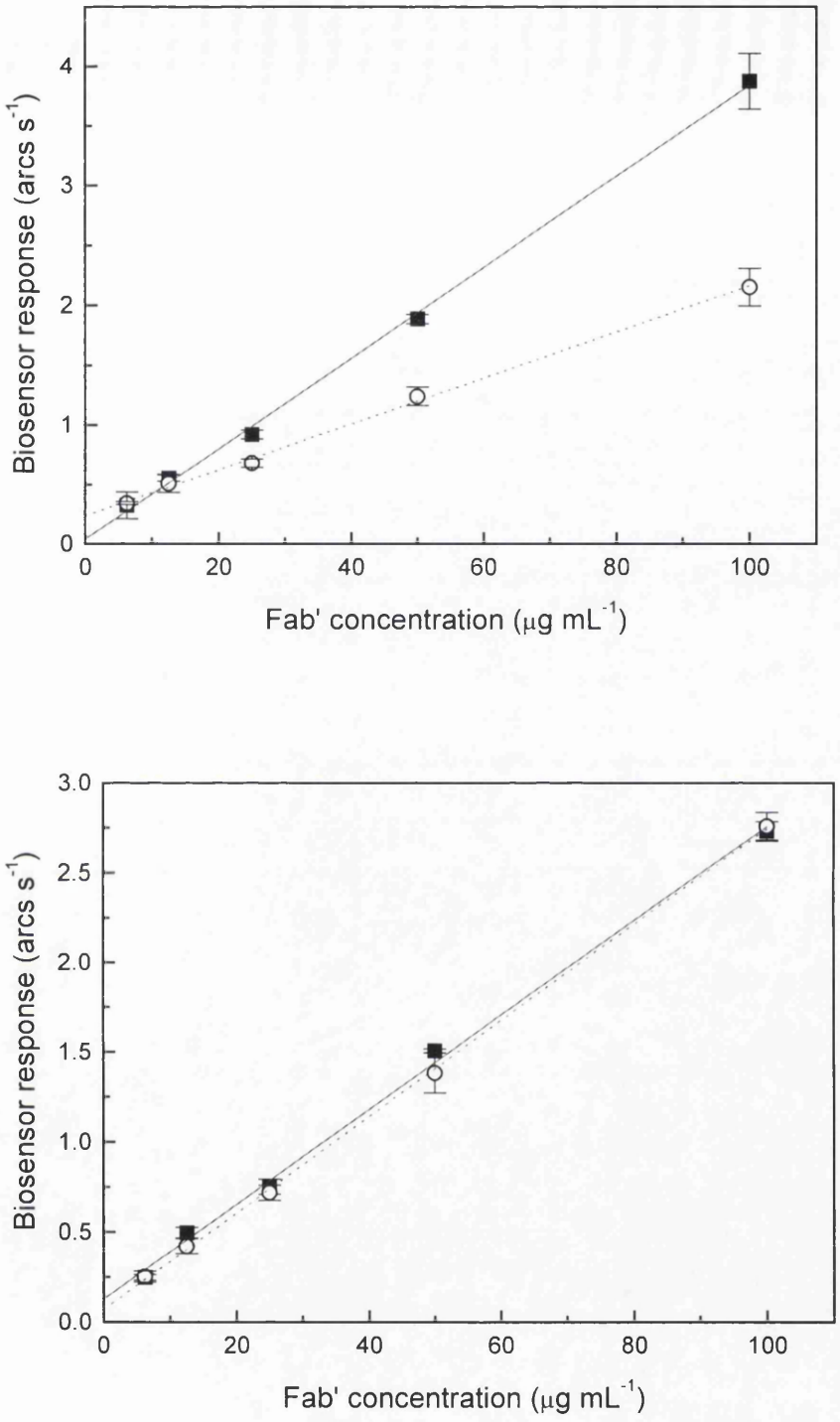

Figure 7.2.7 *Calibration of protein A (upper plot) and HP6045 (lower plot) biosensor cuvettes with two 4D5 Fab' standards produced in house. Standard 1, (-■-), standard 2 (···O···).*

7.2.2.2 Assay error and binding surface stability

To assess the stability of the binding surface and the error associated with each biosensor assay, ten replicate standard curves were prepared using six standard solutions covering the concentration range 200-6.25 μg mL^{-1}. Samples were applied in random order of concentration to minimise systematic error. The surface was regenerated between assays using 50 mM HCl.

Comparison of initial binding rate of the 10 interaction curves at each concentration for the protein A assay showed no decrease in biosensor response over the number of regeneration steps employed. The error associated with the assay increased at lower concentrations of 4D5 Fab'; the maximum error (95% CI) was ± 8% at Fab' concentrations ≥ 25 μg mL^{-1}, compared to ± 23% at concentrations ≤ 12.5 μg mL^{-1}.

Analysis of interaction curves for the HP6045 assay revealed a notable decrease in biosensor response following multiple addition and regeneration cycles. This is illustrated in Figure 7.2.8 which shows the initial rate measured for each standard concentration over the first five replicate applications to the biosensor. Degradation of the sensing surface was minimised by regenerating the surface between assays with 10 mM HCl instead of 50 mM HCl. Following ten replicate additions of the six standard solutions using 10 mM HCl for surface regeneration, the error at each concentration was calculated. As for the protein A assay, the error increased at lower Fab' concentrations; the maximum error of the mean (95% CI) was estimated at ± 9% at Fab' concentrations ≥ 25 μg mL^{-1} and ± 22% at Fab' concentrations ≤ 12.5 μg mL^{-1}.

Sources of error during biosensor analysis include fluctuation of the instrument response with time, alteration of the immobilised ligand due to repeated regeneration and variations in the precise volume of samples applied to the sensing surface. The latter is likely to be the most significant source of error. Pipettes were used for the manual addition of 20 μL samples to the biosensor cuvette. Errors associated with the pipetting of such small volumes can be high and will be more significant at low ligate concentrations. Such errors could be reduced by the use of an automated sample handling device.

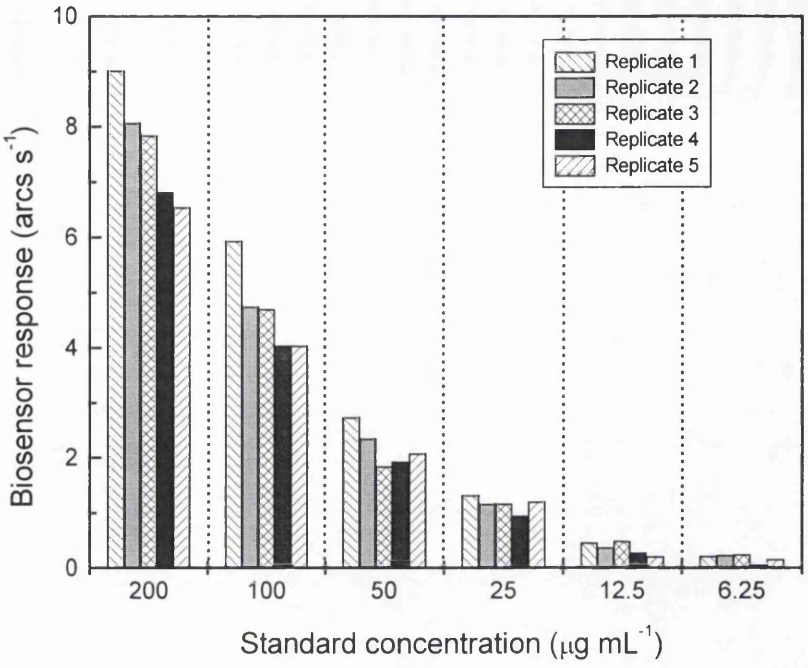

Figure 7.2.8 *Reproducibility plot for the interaction of 4D5 Fab' standard solutions with immobilised HP6045. Samples were applied in random order of concentration to avoid systematic error. The sensing surface was regenerated between assays using 50 mM HCl.*

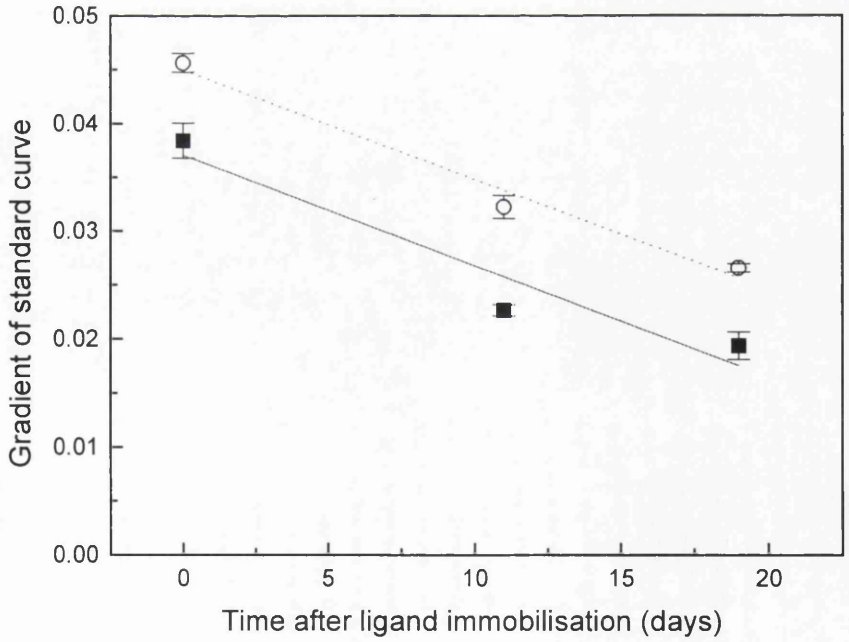

Figure 7.2.9 *Effect of storage time on the gradient of 4D5 Fab' calibration curves for carboxymethyl dextran cuvettes with protein A (-■-) or HP6045 (···O···) immobilised to the sensing surface. Error bars represent the standard deviation of triplicate measurements.*

Stability of the sensing surface over time was assessed by comparing standard curves for a protein A and an HP6045 cuvette prepared on the day of ligand immobilisation and following storage for 11 days and 19 days. Cuvettes were stored in PBS at 4°C. Figure 7.2.9 shows how the gradient of the standard curve decreased over time for both chips, indicating a degeneration of the sensing surface. Degeneration results from a combination of loss of ligand from the sensing surface due to repeated wash and regeneration steps, protein denaturation caused by harsh regeneration conditions and the natural denaturation over time. As a consequence of the observed degeneration, it was necessary to re-calibrated cuvettes every 2-3 days to ensure accurate concentration data.

7.2.2.3 Non-specific binding

Interference from non-specific binding during the analysis of complex bioprocess samples can be a major problem if quantitative data is required (A. Gill, PhD Thesis, 1996). To assess the effects of non-specific binding on the protein A and HP6045 biosensor assays, the interaction of fermentation supernatant obtained from another *E. coli* fermentation expressing the antibody fragment D1.3 Fv (supplied by D. Bracewell, UCL, see section 7.2.1.3) with immobilised protein A and HP6045 was assessed. Purified D1.3 Fv was initially shown not to interact with either protein A or HP6045.

For both biosensor assays an initial baseline was obtained by addition of PBS/T/S buffer to the biosensor cuvette. Buffer was replaced with fermentation supernatant for an interaction period of 5 minutes, after which the contents of the cuvette were replaced with PBS/T/S buffer and the effect on baseline examined. This procedure was repeated using fermentation broth supernatant spiked with purified Fab' at a concentration of 200 $\mu g\ mL^{-1}$. The results are illustrated in Figure 7.2.10. The initial increase in biosensor response following the addition of pure fermentation supernatant to the cuvette was caused by the change in refractive index. The return to baseline following buffer wash of the pure fermentation broth shows there to be no interaction between broth components and the cuvette sensing surface, compared to broth containing Fab'.

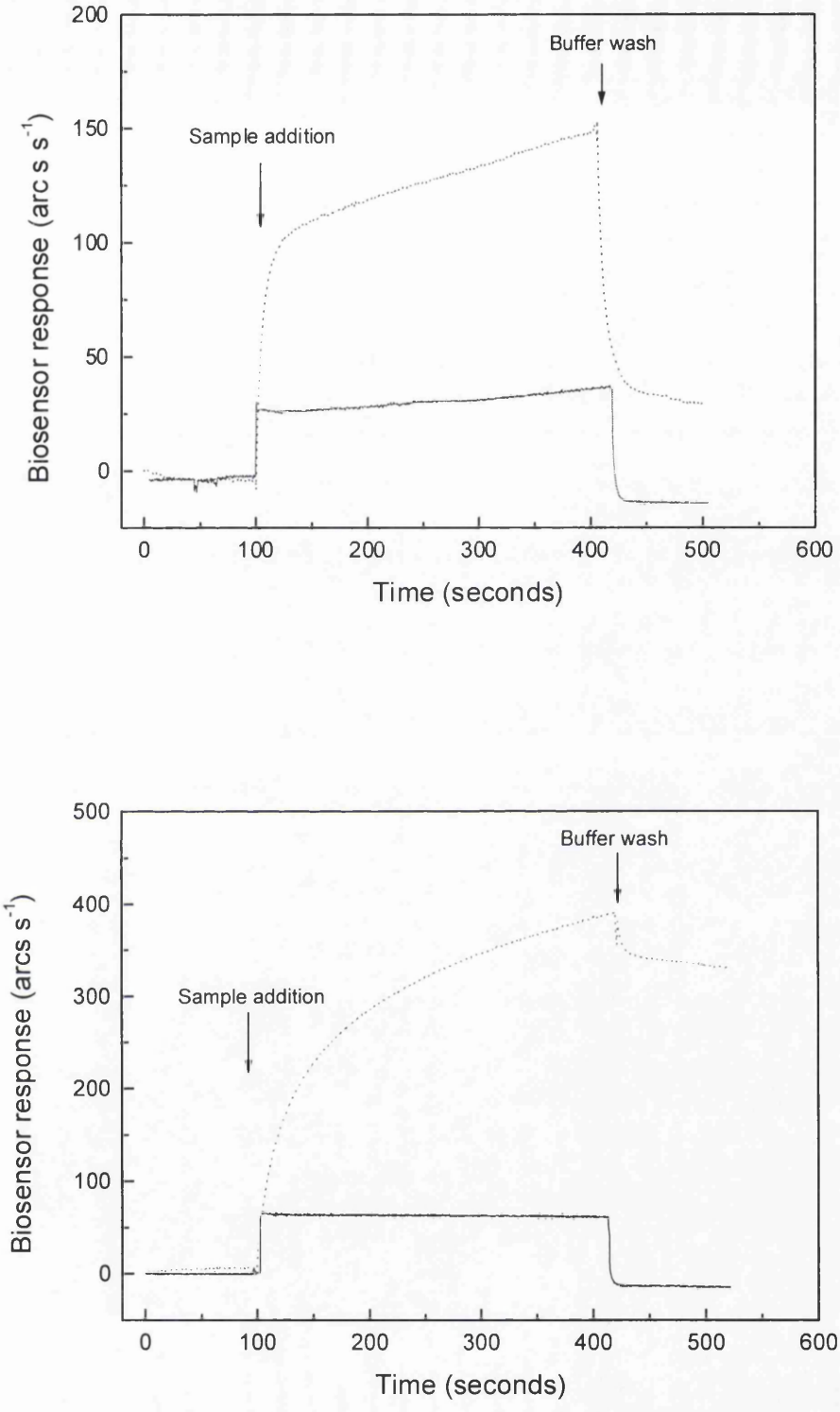

Figure 7.2.10 *Biosensor profiles showing the interaction of E. coli fermentation supernatant containing no Fab' (solid line) and spiked with purified 4D5 Fab' (dotted line) with immobilised protein A (upper plot) and HP6045 (lower plot).*

The work described in section 7.2.3.1 compares the use of ELISA and biosensor assays in the monitoring of periplasmic 4D5 Fab' during the induction phase of a fermentation. For this work it was felt necessary to gain a more accurate indication of the effect of background interference from components of the periplasmic extracts on signals obtained from both biosensor assays (it was envisaged that different background components may have differing effects on the biosensor signal).

A 'control' periplasmic extract was produced by taking cells harvested from fermentation HCD 4 and incubating overnight in periplasmic extraction buffer (section 2.4.1.1) at 60°C, 250 rpm. Endogenous 4D5 Fab' was then removed from the extract by packed bed protein A affinity chromatography using the protocol described in section 2.4.3.1. Fab' levels in the control extract following chromatography were determined by ELISA to be ~ 1 $\mu g\ mL^{-1}$ which is below the detection limit of both biosensor assays. Serial 1 in 2 dilutions of purified Fab' standard were performed in PBS and in the control periplasmic extract over the concentration range 200-6.25 $\mu g\ mL^{-1}$. The standard solutions were applied to immobilised protein A and HP6045 to produce calibration plots, illustrated in Figure 7.2.11.

The results indicate that interference from components of the periplasmic extract has an effect on the signal obtained from both assays. Interference caused an increase in recorded biosensor response for the HP6045 assay shown by the upwards shift in calibration curve for Fab' diluted in control periplasmic extract. The opposite effect is observed for the protein A assay; interference from periplasmic extract components actually cause a decrease in observed biosensor response, shown by the downward shift in calibration curve for Fab' diluted in control periplasmic extract. Such effects need to be taken into consideration when using these assays to obtain quantitative data from bioprocess samples.

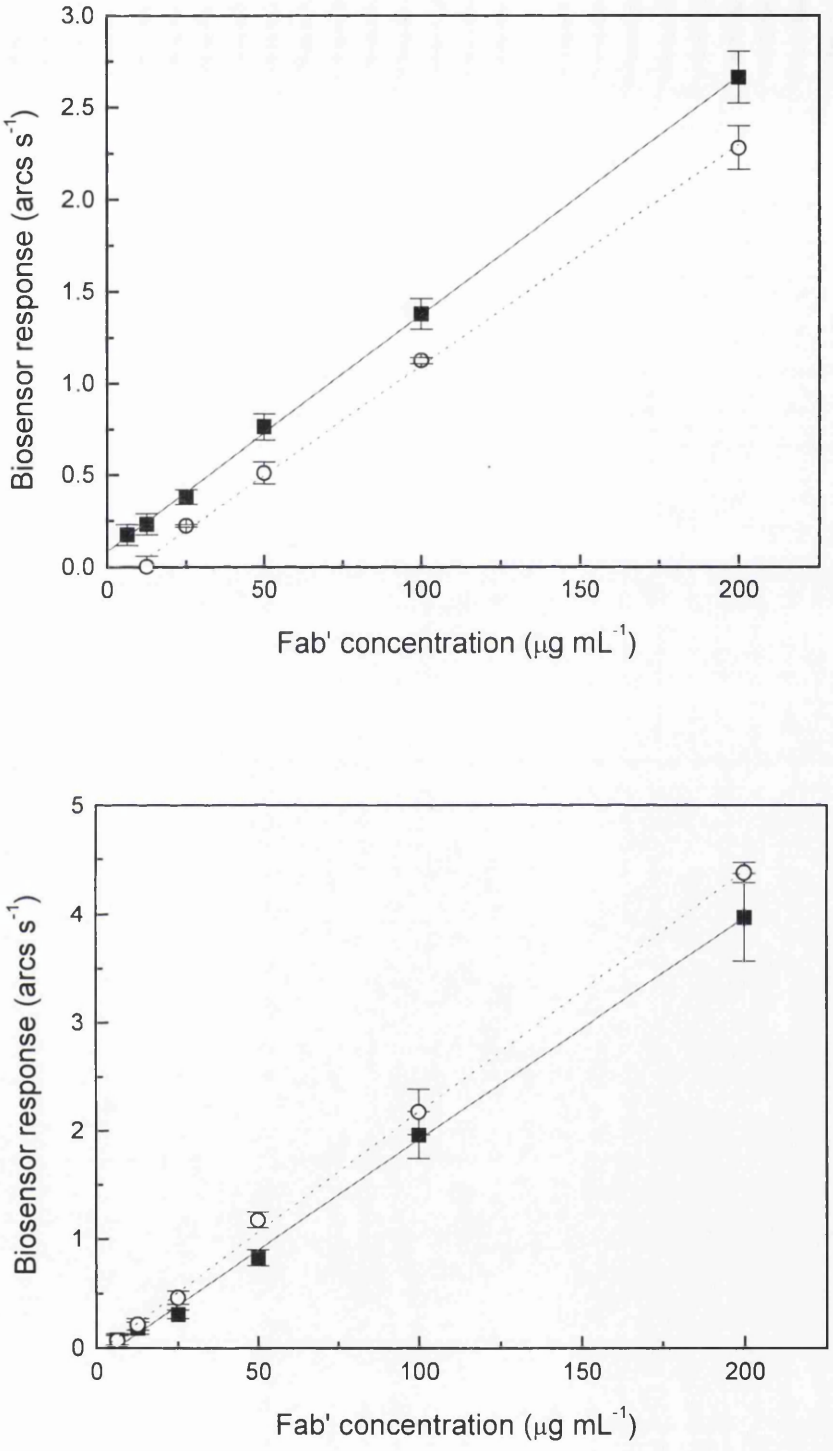

Figure 7.2.11 *Calibration curves for the interaction of purified 4D5 Fab' diluted in PBS (solid line) or control E. coli periplasmic extract (dotted line) with immobilised protein A (upper plot) and HP6045 (lower plot). Error bars represent the standard deviation of triplicate sample analyses.*

7.2.3 Bioprocess monitoring

In the following sections the biosensor assays are assessed as an alternative to ELISA for the quantitative detection of antibody fragments during fermentation and chromatographic purification processes.

7.2.3.1 Fermentation monitoring

The ELISA and biosensor assays were initially compared in their ability to produce quantitative data during the induction period of an *E. coli* fermentation. Fab' concentrations were measured in extracellular and periplasmic fermentation samples taken throughout the induction phase of the 450 L fermentation described in section 3.2.3. Periplasmic fractions were initially obtained by overnight extraction at 30°C. All assays were calibrated with the same standard. Calibration curves for the biosensor assays were produced using standards diluted in PBS. Extracellular and periplasmic Fab' accumulation profiles obtained using the three assay techniques are illustrated in Figures 7.2.12 and 7.2.13 respectively.

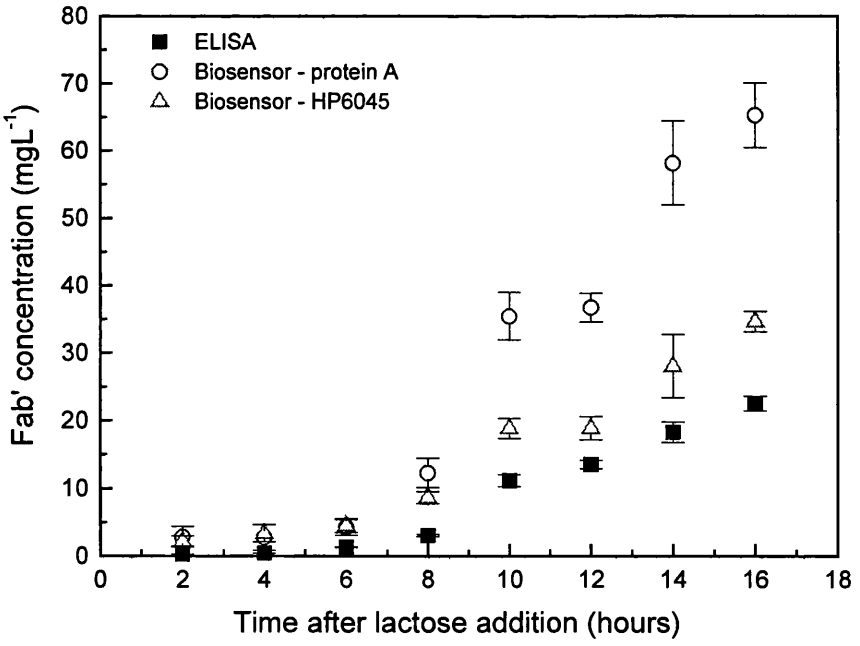

Figure 7.2.12 *Comparison of extracellular Fab' titres recorded by ELISA and biosensor assays in the induction phase of E. coli batch fermentation. Error bars represent the standard deviation of triplicate sample measurements.*

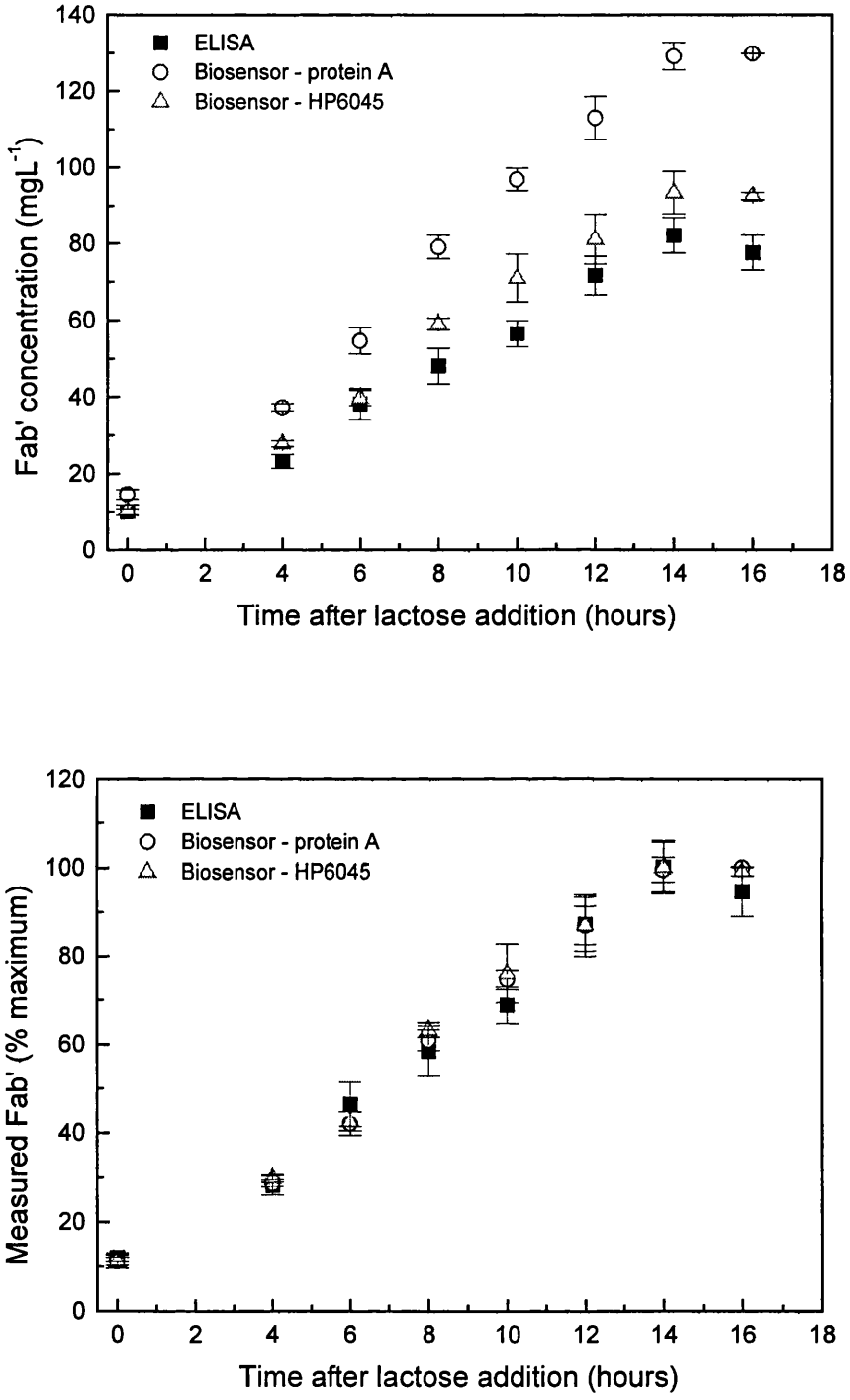

Figure 7.2.13 *Comparison of ELISA and biosensor assays in the monitoring of periplasmic Fab' during the induction phase of E. coli batch fermentation. The upper plot shows the Fab' titres recorded using each analytical method. Good correlation between Fab' accumulation profiles is illustrated when this data is expressed as a percentage of the maximum value (lower plot). Periplasmic fractions were obtained by overnight incubation in extraction buffer at 30℃. Error bars represent the standard deviation of triplicate sample measurements.*

A comparison of the profiles reveals similar trends in Fab' accumulation, however both biosensor assays measured appreciably higher titres than ELISA. The protein A assay recorded titres which were on average 60% higher than ELISA for the periplasmic samples and 200% higher for the extracellular samples. Concentrations recorded by the HP6045 biosensor assay were closer to ELISA; periplasmic titres were on average 15% higher and extracellular samples 55% higher than ELISA.

The high correlation in trends obtained using the three assays is illustrated in Figure 7.2.13 (lower plot), which expresses the periplasmic concentration data as a percentage of the maximum recorded titre.

The differences in concentration data were thought to be primarily due to inherent differences in the Fab' species detected by the three assays. The sandwich nature of the ELISA means it only records fully assembled Fab' molecules. The capture ligands used in the biosensor assays both bind separate regions of the Fab' heavy chain, hence these assays can potentially detect free heavy chain and any incomplete or partially degraded Fab' molecules containing the appropriate binding region of the Fab' heavy chain in addition to complete Fab' molecules. Fermentation samples are likely to contain a proportion of free heavy chain and incomplete Fab' which will be recorded by the biosensor assays but not ELISA, thus providing an explanation for the higher titres recorded by biosensor analysis.

To test this theory, Fab' titres recorded in periplasmic fractions obtained by overnight incubation in extraction buffer at 30°C were compared to Fab' titres recorded in equivalent periplasmic fractions obtained by overnight incubation at 60°C. Previous work has shown that operating the extraction at high temperature results in degradation of free heavy and light chain and incomplete or partially degraded Fab' fragments, whereas the complete, correctly folded Fab' molecule is stable and remains intact (Chapter 4). Fab' titres recorded by ELISA and biosensor assays in 30°C and 60°C periplasmic extracts are compared in Figures 7.2.14 and 7.2.15.

Fab' concentrations measured by ELISA are either within error or slightly lower in the 60°C periplasmic extracts compared to the 30°C extracts. Differences are likely to be due to degradation of free heavy and light chain which associate in solution and are therefore recorded in 30°C periplasmic extracts but are degraded by the high temperature during the 60°C extraction process.

Both biosensor assays record considerably lower Fab' titres in the 60°C extracts than the 30°C extracts, supporting the theory that these assays are detecting incomplete Fab' molecules which are degraded by the high temperature extraction. Further evidence of this is provided by an SDS-PAGE gel showing Fab' preparations obtained by protein A affinity purification from 30°C and 60°C periplasmic extracts (Figure 4.2.5). The gel shows periplasmic samples before and after purification by protein A affinity chromatography (using the protocols described in section 2.4.3.1). The protein bands in the elution fractions (lanes 4 and 6) represent the material within the periplasmic extracts which binds to protein A. It is evident from the increased number of bands in the elution fraction obtained from the 30°C extract (lane 4) that protein A binds a large amount of material in addition to the complete Fab' in the 30°C extract but not in the 60°C extract. The high temperature extraction produces a much 'cleaner' preparation in which the material that binds protein A is almost exclusively complete Fab' (lane 6).

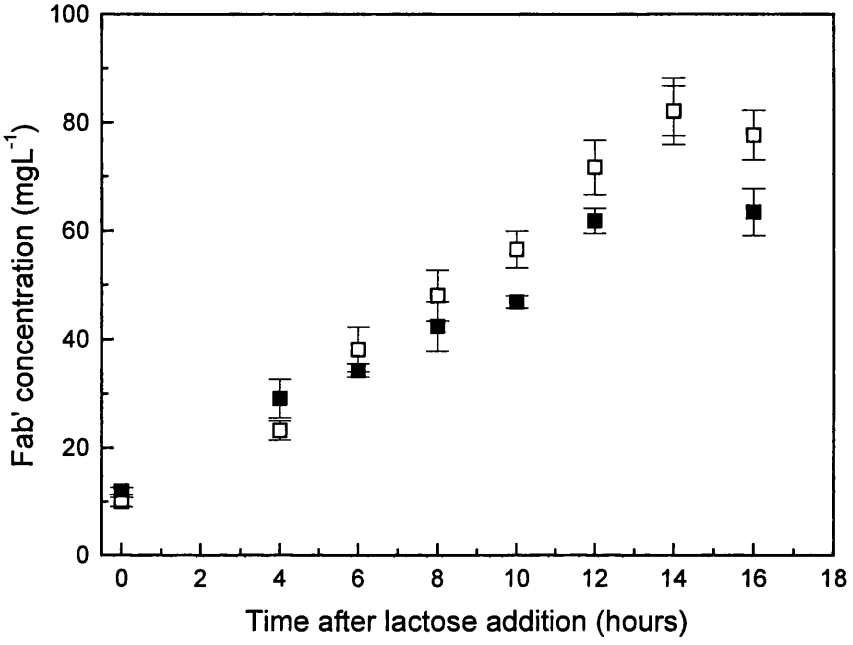

Figure 7.2.14 *Effect of extraction temperature on periplasmic Fab' titres recorded by ELISA. Periplasmic fractions were obtained by overnight incubation in extraction buffer at 30℃ (□) or 60℃ (■). Error bars represent the standard deviation of triplicate sample measurements.*

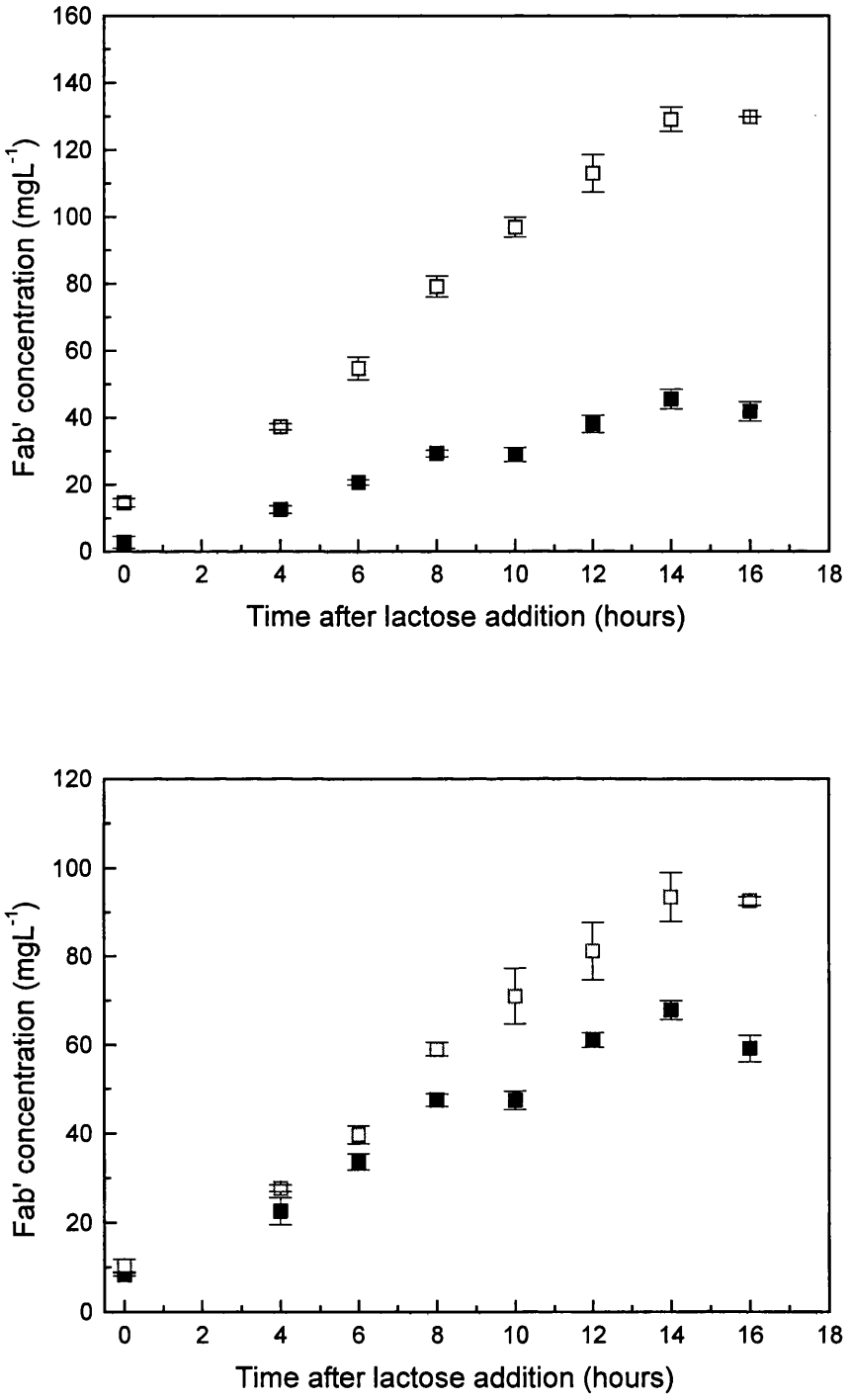

Figure 7.2.15 *Effect of extraction temperature on periplasmic Fab' titres recorded by protein A (upper plot) and HP6045 (lower plot) biosensor assays. Periplasmic fractions were obtained by overnight incubation in extraction buffer at 30℃ (□) or 60℃ (■). Error bars represent the standard deviation of triplicate sample measurements.*

The Fab' titres recorded by ELISA and biosensor assays in 60°C periplasmic extracts are compared in Figure 7.2.16. The graph shows improved correlation between the concentrations; titres measured by ELISA and the HP6045 biosensor assay are mainly within error, however titres recorded by the protein A biosensor assay average approximately 40% lower than those recorded by ELISA.

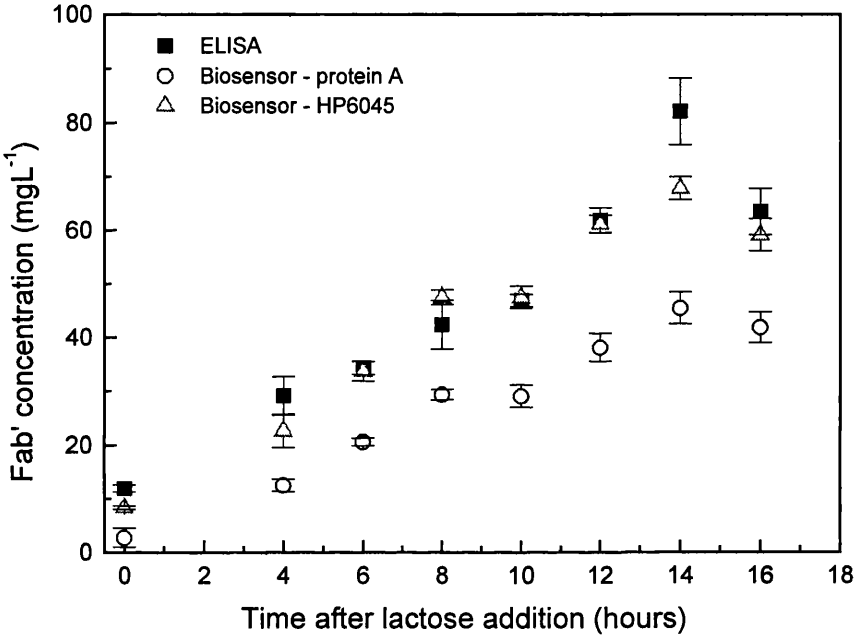

Figure 7.2.16 *Comparison of periplasmic Fab' titres recorded by ELISA and biosensor assays in the induction phase of E. coli batch fermentation. Periplasmic fractions were obtained by overnight incubation in extraction buffer at 60°C. Error bars represent the standard deviation of triplicate sample measurements.*

A final comparison was made in which Fab' concentrations were adjusted to take into account interference from components of the periplasmic extracts. The ELISA was shown not to be affected by non-specific binding (Figure 7.2.4), however background interference during the analysis of periplasmic extracts was shown to increase the biosensor response for the HP6045 assay and decrease the response for the protein A assay (Figure 7.2.11). To account for this, Fab' titres in the 60°C periplasmic extracts were read from calibration curves prepared using Fab' standard

diluted to known concentrations in control periplasmic extract rather than PBS (Figure 7.2.11). A comparison of the titres measured in 60°C periplasmic extracts taking background interference into account is shown in Figure 7.2.17. Improved correlation is observed between Fab' concentrations recorded by ELISA and the biosensor protein A assay, with the biosensor measuring ~25% lower titres than ELISA. Titres recorded by the HP6045 biosensor assay average ~15% lower than those measured by ELISA, showing slightly poorer correlation compared to when assay interference was not taken into account.

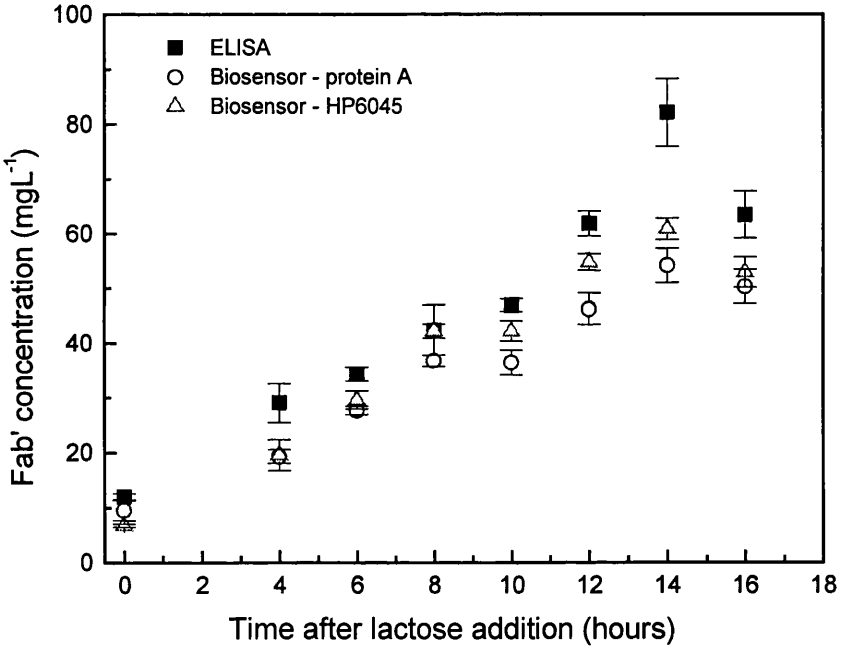

Figure 7.2.17 *Comparison of periplasmic Fab' titres recorded by ELISA and biosensor assays in the induction phase of E. coli batch fermentation. Fab' titres recorded by the biosensor assays have been adjusted to take into account background interference from components of the periplasmic extracts. Periplasmic fractions were obtained by overnight incubation in extraction buffer at 60°C. Error bars represent the standard deviation of triplicate sample measurements.*

Discrepancies remaining in the titres recorded by ELISA and the protein A biosensor assay may be related to the standard used for assay calibration. It has already been observed that the protein A assay interacts differently with different Fab' standards.

The use of protein A to purify the standards may result in the selection of a population of Fab' molecules with higher than average affinity for protein A. The consequence of using such a standard for calibration of the protein A biosensor assay would be to provide an underestimation of the Fab' concentration in unknown samples. This may provide the explanation for the protein A biosensor assay recording lower Fab' titres than both ELISA and the HP6045 biosensor assay. Furthermore, it again indicates one of the problems associated with using a protein A purified standard for calibration of an assay based on binding to protein A.

7.2.3.2 Monitoring of chromatography breakthrough and elution

Protein A affinity purification of 4D5 Fab' has been discussed in Chapter 6. During the packed and expanded bed affinity purification runs described in sections 6.2.2 and 6.2.3 respectively, 4D5 Fab' breakthrough and elution was monitored using ELISA and the protein A biosensor assay.

The 4D5 Fab' breakthrough profiles obtained for the packed bed chromatography run are shown in Figure 7.2.18. A 1 mL Pharmacia HiTrap rProtein A column was loaded with 300 mL of clarified *E. coli* periplasmic extract at a flow rate of 1 mL min^{-1} (40 cm hr^{-1}). Eluent from the column was passed through a spectrophotometer at 280nm to detect total protein. Fractions were assayed for 4D5 Fab' using ELISA and protein A biosensor assays. Concentration of 4D5 Fab' in the feed was also assayed using both techniques to allow calculation of the percentage breakthrough.

The breakthrough profiles illustrated in Figure 7.2.18 show extremely good correlation between ELISA and biosensor assays, indicating the potential of the biosensor to provide an accurate measure of breakthrough during column loading. Such information allows improved process control during process operation, providing the ability to maximise column utilisation whilst minimising product loss.

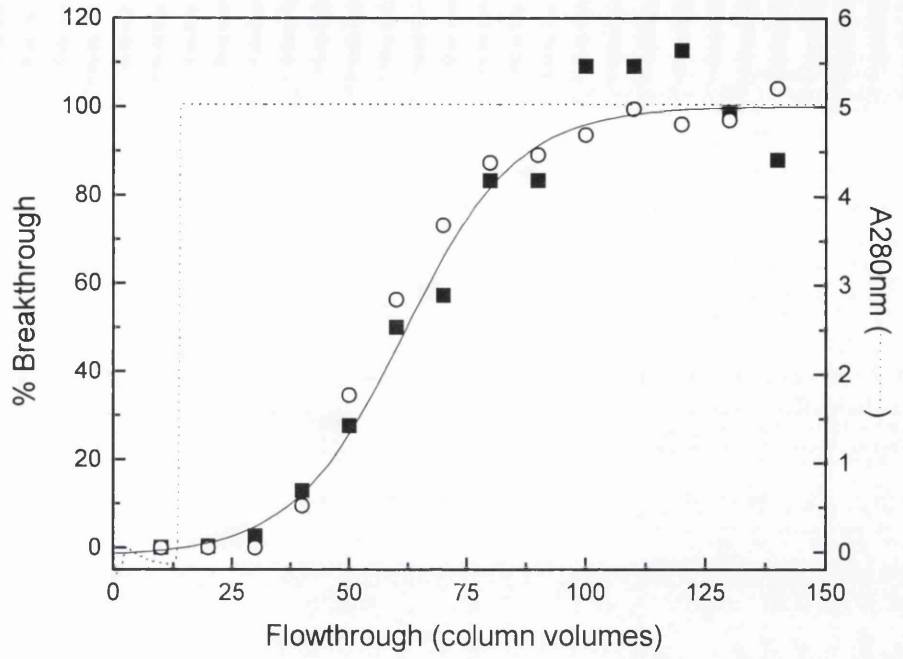

Figure 7.2.18 *Breakthrough of a 1 mL packed bed affinity protein A chromatography column monitored using ELISA (■) and biosensor protein A (O) assays. The column was loaded with clarified E. coli periplasmic extract at a flow rate of 1 mL* min^{-1} *(40 cm* hr^{-1}*).*

Breakthrough profiles were also obtained during expanded bed affinity purification (illustrated in Figure 7.2.19). A Streamline 25 column containing 25 mL Streamline rProtein A media was loaded with 3 L of whole (unclarified) *E. coli* periplasmic extract at a flow rate of 15 mL min^{-1} (185 cm hr^{-1}). Eluent from the column was again passed through a spectrophotometer at 280nm to detect total protein. Due to the large number of fractions collected, assays were only performed on the first fraction of every ten. For ELISA analysis, spheroplasts were removed prior to assay by centrifugation. Assays performed using the protein A biosensor assay were carried out on samples both before and after spheroplast removal to allow the effect of the presence of spheroplasts on the biosensor signal to be assessed.

Again good correlation is observed between biosensor and ELISA data in Figure 7.2.19, although the biosensor recorded on average slightly lower levels of breakthrough. The presence of spheroplasts in the samples did not adversely effect biosensor signals, moreover the sensor response to samples containing spheroplasts showed improved correlation to ELISA data compared to clarified samples. This provides further evidence of the suitability of the protein A biosensor assay for monitoring breakthrough during expanded bed purification, and shows the biosensor can be used confidently to measure Fab' titres directly in the column eluate without the need for spheroplast removal prior to analysis.

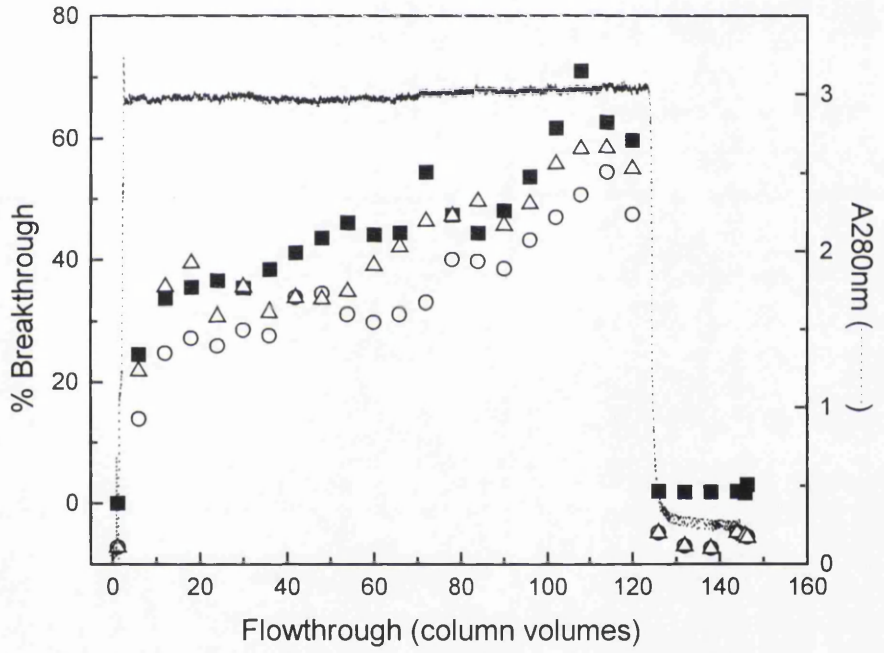

Figure 7.2.19 *Breakthrough of a Streamline 25 expanded bed column containing 25 mL Streamline rProtein A media, monitored using ELISA (■) and protein A biosensor assay (O, unspun samples; Δ, samples spun prior to assay to remove spheroplasts). The column was loaded with E. coli periplasmic extract at a flow rate of 15 mL* min^{-1} *(185 cm* hr^{-1}*).*

Elution of 4D5 Fab' from both the packed bed and the expanded bed protein A columns was also monitored using ELISA and biosensor analysis. Comparable results were obtained for both chromatographic processes, therefore only data from the expanded bed elution will be discussed.

Elution of 4D5 Fab' from the expanded bed was performed in sedimented bed mode at a flow rate of 7.5 mL min^{-1} (90 cm hr^{-1}). Fractions were diluted to the appropriate concentration (~1 μg mL^{-1}) prior to assay by ELISA, however samples were not diluted for biosensor analysis. This was because the biosensor assay was being assessed in its ability to produce on-line data for process control, and any required dilution of the process stream may be difficult to assess and to perform during on-line analysis.

The elution profiles obtained are illustrated in Figure 7.2.20. The profiles show the measured 4D5 Fab' concentration in each fraction, the eluate stream absorbance at 280nm (which is an indication of total protein content) and the % Fab' recovery calculated from the Fab' concentration data. Analysis of the profiles shows that the assay data correlates well with the A280nm trace and furthermore that both biosensor and ELISA identify the same fractions as containing product. Concentrations determined by ELISA however are considerably greater than those measured using the protein A biosensor assay. In addition Fab' recovery determined from ELISA data is >100% whereas recovery based on biosensor data is only ~14%. This suggests that the biosensor assay is underestimating Fab' titres in the elution fractions. A probable explanation is that the concentration of Fab' in some of the fractions were so high that they were out of the linear calibration range. More accurate data may have been obtained by diluting the fractions prior to biosensor analysis, however this was not done for the reasons described previously. Although the concentration data provided by the biosensor assay was inaccurate, the data still provides a reliable indication of the fractions containing the product and hence could be used confidently to select the required product containing fractions for further purification. Identification of product-containing fractions by directly assaying for the product is both more accurate and more reliable than relying simply on correlations with A280 data.

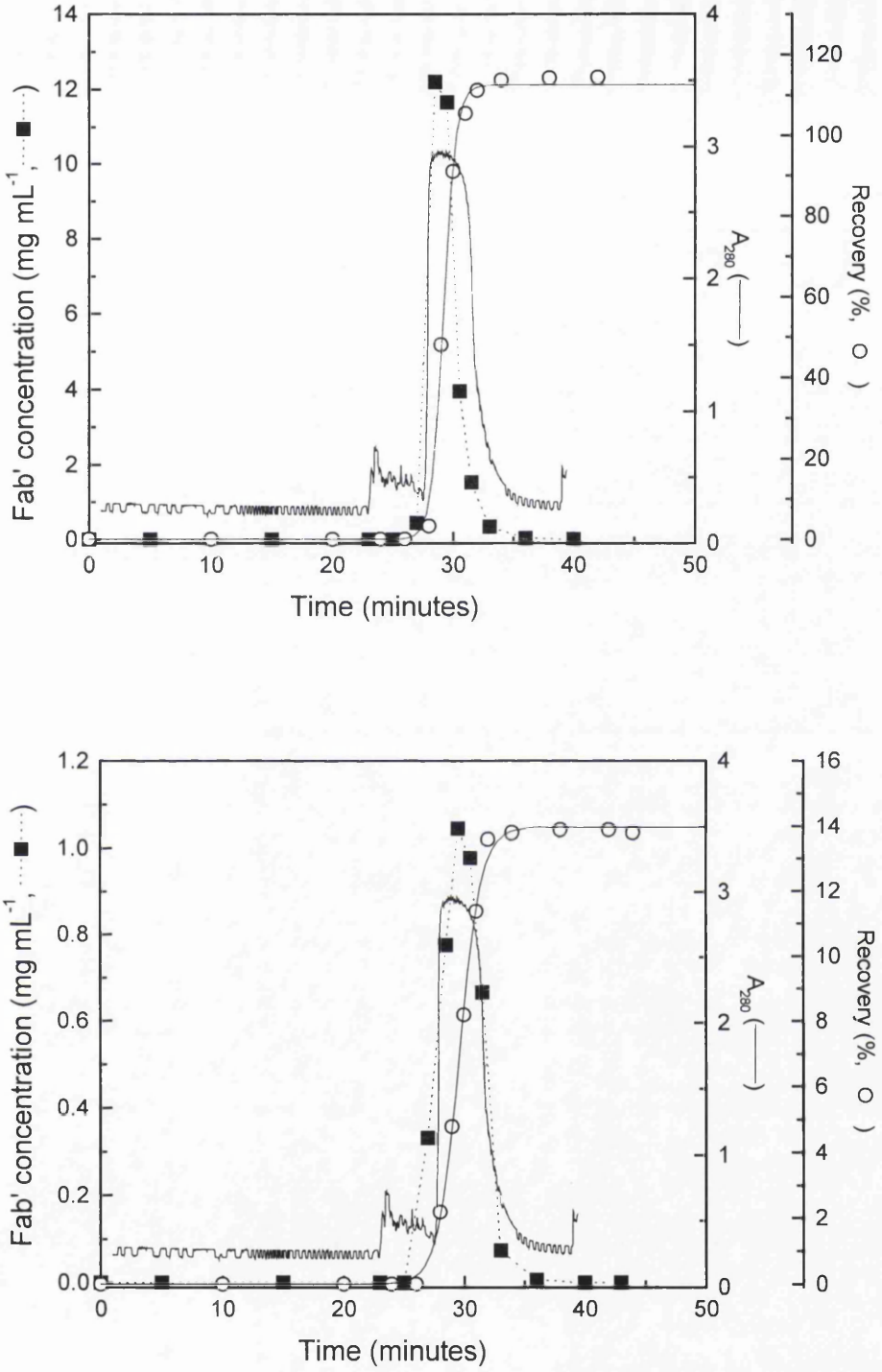

Figure 7.2.20 *Elution of 4D5 Fab' from a Streamline 25 expanded bed column containing 25 mL Streamline rProtein A media, monitored using ELISA (upper plot) and protein A biosensor assay (lower plot). Fab' was eluted at a flow rate of 7.5 mL min^{-1} (90 cm hr^{-1}).*

7.3 Summary

Two biosensor assays have been developed and compared to ELISA as analytical techniques for the monitoring of 4D5 Fab' during fermentation and chromatographic purification. One biosensor assay utilised protein A as the capture ligand, the other HP6045 (the capture antibody used in ELISA). Specific advantages of the biosensor include reduced sample preparation time and reduced assay time, with an assay turnaround time of several minutes compared to several hours for ELISA.

Both biosensor and ELISA assays required calibration with 4D5 Fab' standards of known concentration. ELISA standard curves had to be prepared on every plate each time the ELISA was performed. Due to differences in the quantity of ligand immobilised and deterioration of the sensing surface over time, each biosensor cuvette required calibration after ligand immobilisation and following storage for more than 2-3 days.

Methods were developed for the preparation of 4D5 Fab' standards 'in house'. The method employed was found to have a considerable effect on quality of the standard which in turn affected assay calibration, with improved quality standards purified from periplasmic extracts obtained by overnight incubation at 60°C rather than 30°C.

The protein A biosensor assay was shown to react differently to different Fab' standards, which was thought to be a result of differences in methods of standard purification by protein A affinity chromatography. The effect identifies one of the problems associated with using a protein A based purification technique to purify standards for use in an assay based on interaction with protein A.

The error associated with the ELISA assay was calculated to be ± 5% at a 95% confidence interval. This was lower than the errors of the biosensor assays, which were up to ± 9% for Fab' concentrations ≥ 25 $\mu g\ mL^{-1}$ and ± 23% at Fab' concentrations ≤ 12.5 $\mu g\ mL^{-1}$.

The ELISA was found to be unaffected by non-specific binding, however contaminants within process samples were shown to effect both biosensor assays. The biosensor response was increased in the presence of process contaminants in the case of the HP6045 assay, whereas a decrease in response was observed in the presence of process contaminants for the protein A assay.

The two biosensor assays were compared to ELISA in the ability to provide quantitative data of product accumulation during the induction phase of an *E. coli* fermentation. Good correlation was observed between the product accumulation profiles obtained with the three assay techniques. In addition, correct sample preparation and consideration of non-specific binding effects allowed quantitative data to be obtained from both biosensor assays which was comparable to ELISA data.

The protein A biosensor assay was also assessed as a technique for the on-line analysis of chromatography breakthrough and elution. The assay was successfully used to monitor breakthrough from a packed bed and an expanded bed affinity chromatography column, even in the presence of spheroplasts. The assay also successfully identified product-containing fractions during elution from the expanded bed column, however dilution of the fractions would be required to allow accurate concentration determination.

The results clearly demonstrate the potential of the optical biosensor as a technique for real time process monitoring to allow improved process control. However, due to a higher associated error, interference from non-specific binding and problems associated with biosensor calibration, the ELISA is still the method of choice for accurate quantification of 4D5 Fab' in process samples.

8. PROCESS MASS BALANCES

8.1 Introduction

This chapter draws together the results from the analysis of individual unit operations by comparing process alternatives for the recovery and purification of 4D5 Fab' from *E. coli* fermentation broth. The process options which have been studied are illustrated in Figure 8.1.1. Process comparisons are made on the basis of Fab' yield, level of purification achieved and total process operating time.

When designing a process for the production and purification of antibody fragments, the initial decision which must be made relates to fermentation design; whether the product should be fully retained within the periplasm or whether a degree of leakage into the extracellular broth should be encouraged. Advantages of periplasmic expression include easier purification from the relatively clean periplasmic extracts compared to purification from the complex mix of metabolic by-products in the extracellular medium. Extracellular expression has the further disadvantage that exposure to the extracellular environment for long time periods may have a detrimental effect on product quality, with protease activity or deamidation reactions resulting in antibody degradation. Chapter 3 illustrated how a fermentation process could be modified to improve retention of product within the periplasmic space. However, successful periplasmic retention can be more difficult to achieve at large scale. Therefore it is important to consider fully options for the purification of both periplasmic and extracellular material.

Four purification processes, illustrated in Figure 8.1.1, have been studied. Three focus on the recovery of exclusively periplasmic product whereas the fourth allows recovery of both periplasmic and extracellular antibody fragments. For the recovery of purely periplasmic product, a cell harvest step is needed at the end of the fermentation. Efficient cell harvest requires not only that as many cells as possible are recovered, but also that cell breakage during recovery is minimised. Breakage will result in both product losses and the release of intracellular contaminants such as proteases, lipids and DNA which may degrade product or cause processing problems

in later purification stages. For this process study, the use of a tubular bowl centrifuge for cell harvest has been assumed, as improved dewatering is achieved compared to disk stack centrifugation. However, the use of a tubular bowl centrifuge for large scale processing maybe limited by the size of commercially available machines. (The largest available tubular bowl is the CARR P24 Powerfuge (CARR Separations Inc., Franklin, MA) which has a bowl size of 66L, achieves a relative centrifugal force of up to 15 000g and can be operated at flow rates of up to 4000 L hr^{-1}).

Product is released from harvested cells by the process of periplasmic extraction. Selective release of periplasmic material is desired to produce a concentrated liquid stream of antibody whilst minimising contamination of the process stream with intracellular products. Performing the extraction process at high temperature offers the additional advantage of process stream purification by degrading both contaminating *E. coli* proteins and incomplete or incorrectly folded antibody fragments.

Following periplasmic release, Fab' can be purified directly from unclarified periplasmic extracts by expanded bed affinity chromatography. Alternatively, Fab' may be recovered by packed bed affinity chromatography following the clarification of periplasmic extracts by centrifugation and depth filtration. Process stream clarification can be achieved using a disk stack or a tubular bowl centrifuge. Again the aim is to maximise both clarification and dewatering whilst minimising cell breakage.

A more novel processing alternative which allows the recovery of both extracellular and periplasmic product involves performing the extraction process on whole fermentation broth. Fab' can then be harvested directly from whole broth extracts by expanded bed affinity purification.

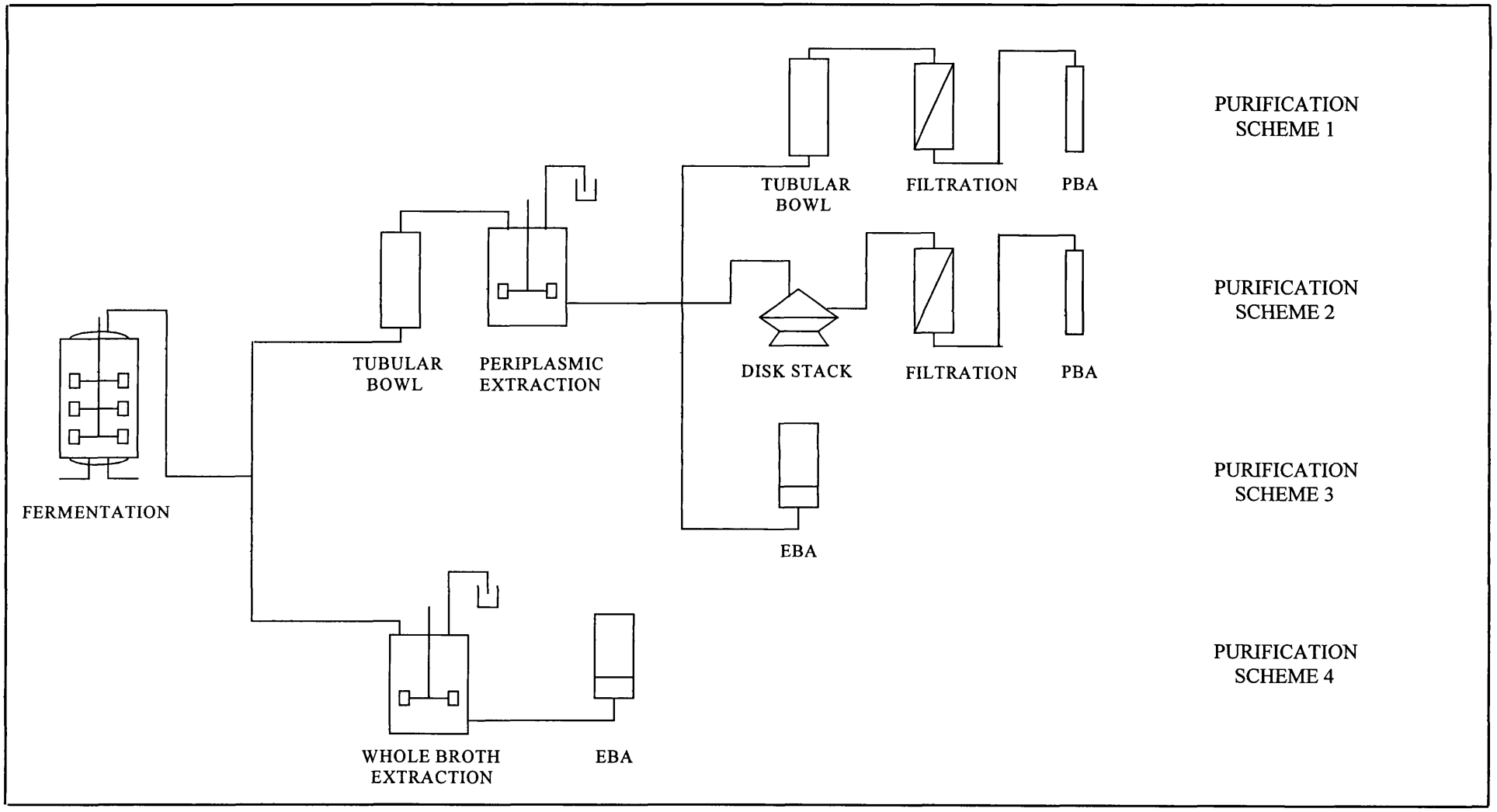

Figure 8.1.1 *Process options for the recovery of 4D5 Fab' from E. coli fermentation broth. EBA, expanded bed adsorption; PBA, packed bed adsorption.*

In the following sections three examples of specific process alternatives are initially examined in the context of alternative purification schemes. Section 8.2.1 compares periplasmic and whole broth extraction. In section 8.2.2 the use of a disk stack centrifuge and a CARR tubular bowl centrifuge are compared for the clarification of spheroplast suspensions. Section 8.2.3 assesses packed bed and expanded bed purification routes for the recovery of Fab' from periplasmic extracts. Finally, in section 8.2.4, the whole recovery processes illustrated in Figure 8.1.1 are compared on the basis of yield, purification and processing time.

8.2 Results and discussion

8.2.1 Periplasmic verses whole broth extraction

Important process considerations for comparison of the alternative extraction procedures include:

- Fab' yield
- Process stream purification - degradation of contaminating *E. coli* proteins
  - degradation of incorrectly assembled or partially degraded Fab'
- Fab' quality following extraction (physiochemical characteristics, affinity, efficacy)
- Process time

Periplasmic and whole broth extraction were compared as individual unit operations in Chapter 4. Fab' yields were higher for periplasmic extraction (85% Fab' yield) than for whole broth extraction (41% yield). However, the two procedures showed similar degrees of process stream purification, and produced Fab' preparations of similar quality as judged by Western blotting of periplasmic extracts and SDS-PAGE analysis of Fab' purified from the extracts by affinity chromatography.

To compare periplasmic and whole broth extraction as alternative processing routes, the cell harvest step prior to periplasmic extraction must also be taken into consideration. This will allow a more comprehensive indication of relative process yields and operating times. A comparison of the two extraction routes based on the processing of 100L fermentation broth is illustrated in Figure 8.2.1. The use of a Sharples AS26 tubular bowl centrifuge (Alfa-Laval Engineering Ltd.) was assumed for the cell harvest process. The flow rate required for 95% cell recovery was determined experimentally during the harvest of fermentation 150L3. The AS26 centrifuge has a bowl volume of 6.0L, hence two centrifuge bowls are required for the harvest of 100L fermentation broth containing 10% (v/v) solids. The estimated operating time for cell harvest therefore includes 15 minutes to allow for the centrifuge to be run down and the bowl to be changed. Other assumptions made are listed in Table 8.2.1. Fab' yields and purification factors for the extraction processes were determined experimentally in Chapter 4.

Yields for the periplasmic extraction route are reduced from 85% to 65% by taking into account the centrifugation step, firstly because all the extracellular product is discarded and secondly because the efficiency of centrifugal cell harvest is less than 100%. In addition, the processing time is increased for the periplasmic route and operating costs will be greater because of the requirement for an additional unit operation. Differences in process time and operating costs will become more significant as the operational scale is increased. Thus, although a direct comparison of yields for the individual extraction processes suggested periplasmic extraction is by far the more efficient option, comparison in the wider context of a purification scheme has shown that following optimisation, the whole broth extraction process may present a more viable process alternative which offers the additional advantages of lower operating costs and reduced process time.

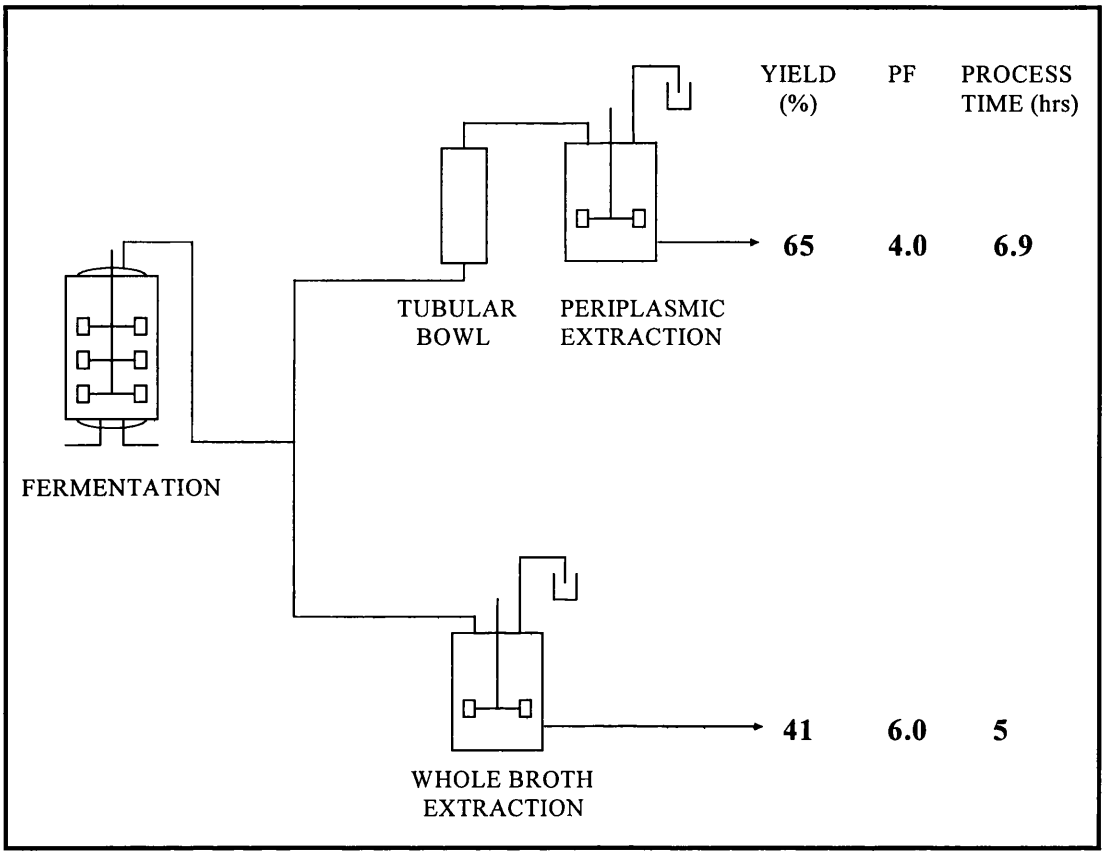

Figure 8.2.1 *Comparison of periplasmic and whole broth extraction based on the processing of 100L fermentation broth. Comparisons are based on process yield, purification factor (PF) and the total process operating time. Assumptions made are given in Table 8.2.1.*

OPERATION	PROCESS VARIABLE	ASSUMED VALUE
Fermentation	Scale	100 L
	Solids fraction	10% (v/v)
	Fab' titres	200 mg L^{-1}
	Fab' distribution:	
	Periplasmic	80% (160 mg L^{-1})
	Extracellular	20% (40 mg L^{-1})
Cell harvest (AS26 tubular bowl centrifuge)	Flow rate	60 L hr^{-1}
	*Process time	1.92 hours
	Cell recovery	95%
Periplasmic extraction	Extraction time	5 hours
	Fab' yield	85%
	Purification factor	4.0
Whole broth extraction	Extraction time	5 hours
	Fab' yield	41%
	Purification factor	6.0

Table 8.2.1 *Assumptions for the comparison of periplasmic and whole broth extraction processes. *Includes 15 minutes to allow for running down of the centrifuge and changing of the centrifuge bowl.*

8.2.2 Tubular bowl verses disk stack centrifugation

Important process considerations for the centrifugal clarification of spheroplast suspensions include:

- Product yield
- Dewatering
- Shear damage (to both Fab' product and spheroplasts)
- Processing time

A tubular bowl centrifuge (the CARR P6 Powerfuge) and a disk stack centrifuge (the Westfalia CSA-1 centrifuge) were compared for the clarification of periplasmic extracts in Chapter 5. Results indicated that Fab' yields were higher using the tubular bowl because of the improved liquid recovery (dewatering). No damage to the Fab' or to cells was observed during either centrifugation process.

Yields and operating times for the clarification of 100L periplasmic extract by disk stack and tubular bowl centrifugation are compared in Figure 8.2.2. Process parameters used in the comparison are listed in Table 8.2.2. Process times are based on operation at the flow rate required for 95% clarification. The operating flow rates and process yields were both determined for small-scale centrifuges (the CSA-1 has a bowl volume of 0.6L; the CARR P6 Powerfuge has a bowl volume of 1.0L). Larger scale machines would have to be used for the processing of 100L periplasmic extract, however it has been assumed that the same process parameters would still apply. No additional time has been allowed for discharging the tubular bowl centrifuge as it has also been assumed that the machine utilised would have a bowl volume sufficient to allow processing of the entire extract in one batch.

Results indicate that although yields are higher for the tubular bowl, processing times are longer because the flow rate required to achieve 95% clarification is lower. Again the difference in process time will become more significant at increased scale. Processing time may be an important factor in the purification of labile products.

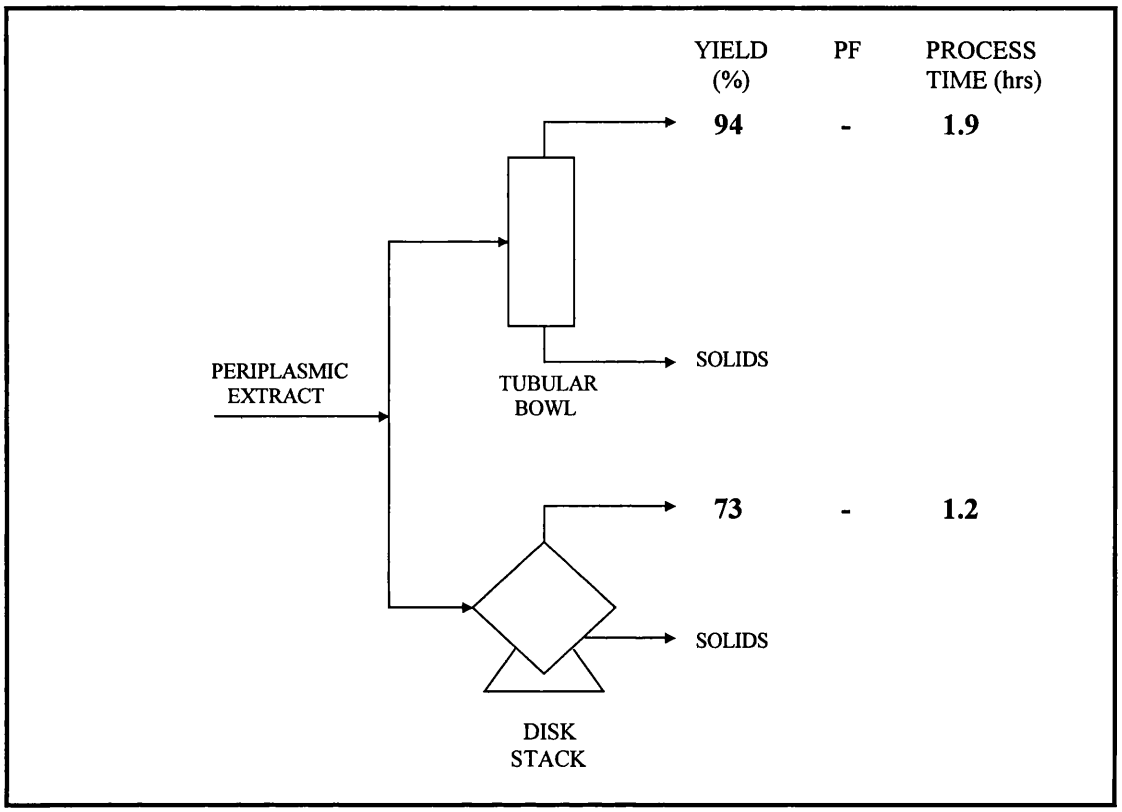

Figure 8.2.2 *Comparison of tubular bowl and disk stack centrifugation for the clarification of 100L periplasmic extract. Comparison is based on process yield, purification factor (PF) and the total process operating time. Assumptions made are given in Table 8.2.2.*

CENTRIFUGE	PROCESS VARIABLE	ASSUMED VALUE
Tubular bowl centrifuge (CARR Powerfuge)	Process stream volume	100L
	Process stream solids content	10% (v/v)
	Centrifuge flow rate	53 Lhr^{-1}
	Process time	1.89 hours
	Clarification	95%
Disk stack centrifuge	Process stream volume	100L
	Process stream solids content	10% (v/v)
	Centrifuge flow rate	81 Lhr^{-1}
	Process time	1.23 hours
	Clarification	95%

Table 8.2.2 *Assumptions for the comparison of tubular bowl and disk stack centrifugation for the removal of spheroplasts from periplasmic extracts.*

8.2.3 Packed bed verses expanded bed chromatography

Processing factors to be taken into consideration in the comparison of packed and expanded bed purification include:

- Product yield
- Purification factor
- Process time
- Matrix capacity and cost
- Overall processing costs

Packed and expanded bed purification were compared on the basis of process yield, matrix capacity and purification in Chapter 6. Packed bed chromatography was found to give higher yields and show improved matrix binding capacities, whereas levels of purification were similar for the two chromatographic operations.

Although the results indicated packed bed adsorption to be the more efficient method of purification, a disadvantage associated with this route is the initial requirement for process stream clarification. A comparison of packed and expanded bed processes, taking into account feedstock clarification by tubular bowl centrifugation and filtration is shown in Figure 8.2.3. Assumptions for the comparison are given in Table 8.2.3. Detailed calculations for the determination of column volumes and process times for the chromatographic purifications are given in Appendix 12.

The results show higher yields of Fab' for the process involving packed bed adsorption, with similar levels of purification achieved in both recovery schemes. A disadvantage of the packed bed purification route however is the considerably greater process operating time.

Additional factors which have not been taken into consideration include operational costs and process reliability. Expanded bed adsorption suffers the disadvantage of requiring specifically designed media which is expensive, and large volumes of

buffers which further add to the overall operational costs. During experimentation, operational problems associated with use of the expanded bed were also identified. The processing of high cell density feed streams frequently resulted in blocking of the lower adapter (column inlet). This was alleviated by nuclease treatment of the feed prior to column loading during purification from periplasmic extracts, however problems with column blocking were still encountered following nuclease treatment during the processing of whole broth extracts. Frequently encountered operational problems such as this will also influence decisions when specifying a purification scheme.

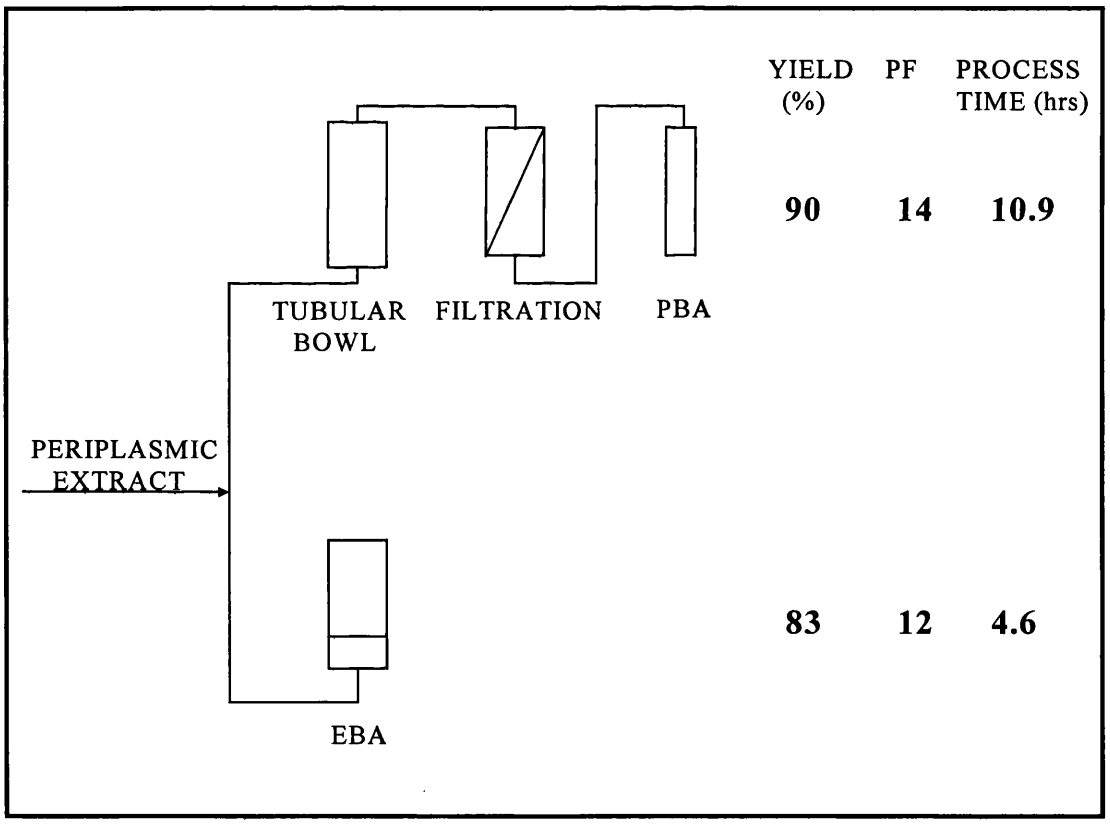

Figure 8.2.3 *Comparison of packed bed (PBA) and expanded bed (EBA) purification of 4D5 Fab' from 100L periplasmic extract. Comparison is based on process yield, purification factor (PF) and the total process operating time. Assumptions made are given in Table 8.2.3.*

OPERATON	PROCESS VARIABLE	ASSUMED VALUE
Centrifugation (Tubular bowl)	Process stream volume	100L
	Process stream solids content	10% (v/v)
	Centrifuge flow rate	53 Lhr^{-1}
	Process time	1.89 hours
	Clarification	95%
	Liquid recovery	96%
	Fab' recovery	94%
Filtration	Process time	2 hours
	Fab' recovery	98%
	Liquid recovery	100%
Packed bed chromatography	Column volume	2.0 L
	Column dimensions	50 mm × 100 cm
	Chromatography media	Protein A Sepharose 4 fast flow
	Flow rate	1000 cm hr^{-1}
	Process time	6.96 hours
	Fab' yield (10% breakthrough)	98%
	Purification factor	14
Expanded bed chromatography	Column	Streamline 200
	Column dimensions	20 cm × 15 cm
	Bed volume	4.7 L
	Chromatography media	Streamline rProtein A
	Flow rate	185 cm hr^{-1} (load and wash) 90 cm hr^{-1} (elution)
	Process time	4.59 hours
	Fab' yield (27% breakthrough)	83%
	Purification factor	12

Table 8.2.3 *Assumptions for the comparison of packed and expanded bed chromatography in the purification of 4D5 Fab' from 100L E. coli periplasmic extract. Detailed calculations for the determination of column volumes and process times for the chromatographic purifications are given in Appendix 12.*

8.2.4 Overall process mass balances

This chapter concludes with a comparison of complete purification schemes based on overall yield, purification factor and process time. The results, shown in Figure 8.2.4, give the yields for individual unit operations as well as the overall process yields. Detailed calculations of the column sizes, process volumes and process times for the chromatographic purification steps are given in Appendix 12. In addition, the process

yield, purification factor and operation time for each unit operation in each of the four purification schemes are given in Appendix 13.

The most efficient process based on yield alone is the 'traditional' purification route involving Fab' recovery from clarified periplasmic extracts by packed bed chromatography (58% yield), followed by the more novel method of Fab' purification from unclarified periplasmic extracts by expanded bed adsorption (54% yield). The least efficient process is the one focusing on recovery of Fab' directly from whole broth extracts by expanded bed adsorption (35% yield).

In contrast, the most efficient process based on both purification factor and operational time is the whole broth extraction route. The traditional purification scheme involving periplasmic extraction and packed bed chromatography, which gave the highest overall yield, proved to be the least efficient with respect to operating time. In addition, the process providing the second highest yield of Fab' (expanded bed affinity purification of Fab' from periplasmic extracts) proved the least effective with regard to process stream purification.

Thus each recovery process has associated advantages and disadvantages, and the most appropriate purification route will be determined by the specific requirements of the individual process. For example, in the recovery of a labile product, minimising process time may be of paramount importance, whereas for a product destined for therapeutic application, the process giving highest degree of purification may be preferred.

The comparisons made provide only an initial insight into the relative merits of the process alternatives. A number of other significant factors including process cost, scale-up potential and the quality of Fab' produced (in terms of physiochemical characteristics and *in vivo* efficacy) also need to be taken into consideration to allow selection of the most efficient and economical purification scheme.

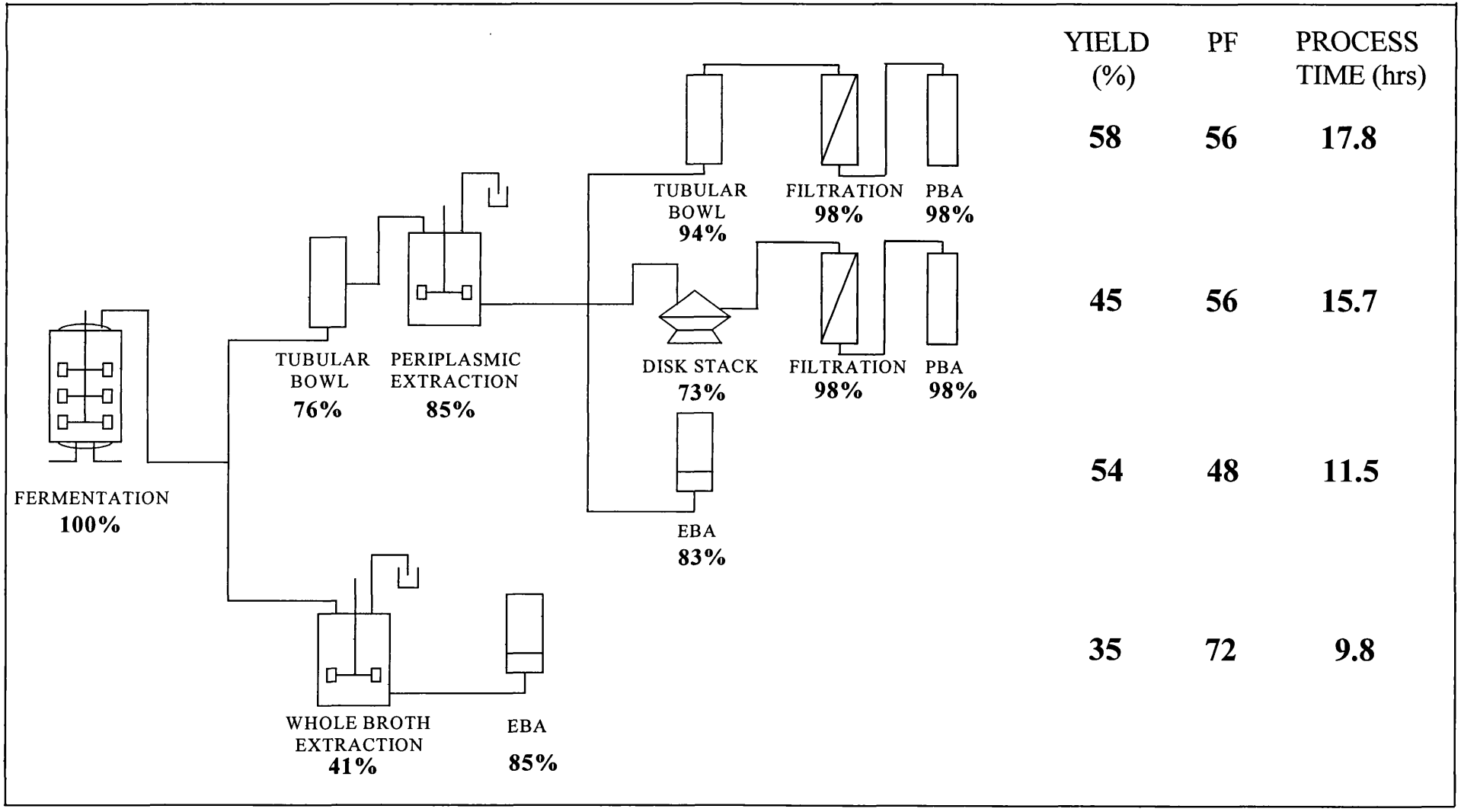

Figure 8.2.4 *Comparison of process options for the purification of 4D5 Fab' from E. coli fermentation broth. Processes are compared on the basis of process yield, purification factor (PF) and processing time. All assumptions on which the analysis is based are given in Tables 8.2.1-8.2.3. The figure beneath each unit operation represents the Fab' yield.*

8.3 Summary

This study has highlighted some of the operational factors which must be taken into consideration during the design and specification of a production and purification process based on an *E. coli* expression system. By comparing four alternative purification schemes, the study has illustrated that there is no single 'ideal' process, rather each purification route has associated advantages and disadvantages that need to be taken into consideration. Therefore, prior to process specification, the criteria for the final product must be defined to determine the objectives of the purification scheme. Only when the process objectives have been defined can the most appropriate purification route be elucidated.

9. CONCLUSIONS

During this project, novel process options for the production of antibody fragments using an *Escherichia coli* expression system have been developed and characterised, and techniques designed to facilitate process design, integration and control have been assessed by application to the experimental system under investigation.

Initially, a fermentation process designed for the periplasmic expression of a Fab' antibody fragment was characterised. Using the original fermentation protocol, antibody titres of up to 200 mg L^{-1} were achieved, however over the course of the induction period over 50% of the Fab' leaked into the extracellular broth. The fermentation was modified to increase the control of product location by reducing leakage into the medium. Following process modifications, antibody titres were increased to ~680 mg L^{-1} and, more significantly, 80-90% of product was consistently retained within the periplasmic space. Tight control of product location was maintained following scale up of the fermentation to 450L. However a number of problems associated with operating such a process at large scale were identified, including oxygen limitation, poor temperature control, foaming and difficulties keeping large quantities of lactose in solution.

A novel method for the specific release of periplasmic proteins was characterised. 85% recovery of periplasmic Fab' was achieved by suspending cells in a Tris-EDTA extraction buffer at 60°C. Operation of the extraction process at high temperature offered the additional advantages of process stream purification by the degradation of both contaminating *E. coli* proteins and incomplete or incorrectly folded Fab' fragments.

Fab' release and protein degradation during periplasmic extraction were modelled at scales from 65 mL to 100 L using simple first order kinetics. Fab' release appeared to occur instantaneously during cell resuspension at all scales. The extent of protein degradation varied with different feed material and the rate of protein degradation was lower at large scale. Process variation with different feed material is difficult to

predict and highlights one of the potential difficulties associated with the design and use of models for predicting the performance of biological processes.

The periplasmic extraction process was performed on whole fermentation broth with the aim of allowing the recovery of both extracellular and periplasmic antibody fragments. However yields were considerably lower than for periplasmic extraction, with only 41% Fab' recovered. Reduced yields were thought to be due to a combination of increased Fab' degradation (possibly due to the reduced thermal stability of extracellular Fab') and a less efficient extraction procedure.

Removal of spheroplasts generated by periplasmic extraction was compared using a tubular bowl and a disk stack centrifuge. Operating both machines at the flow rate required for 95% clarification, 94% Fab' was recovered using the tubular bowl, compared to 73% using the disk stack centrifuge. The higher recovery achieved with the tubular bowl was shown to be directly due to the greater level of dewatering achievable.

A scale-down version of the disk stack centrifuge and ultra-scale-down laboratory equipment were assessed for their ability to predict the recovery performance of the full-scale disk stack separator. Both scale-down and ultra-scale-down equipment were found to over-predict the recovery performance of the disk stack centrifuge during the clarification of spheroplast suspensions. The poor results were thought to reflect the inability to mimic accurately the shear fields in the industrial machine.

Expanded bed and packed bed adsorption were compared for the purification of 4D5 Fab' from unclarified and clarified periplasmic extracts respectively. Packed bed adsorption resulted in higher Fab' yields and showed greater dynamic binding capacities compared to expanded bed purification. The differences were attributed to the contrasting patterns of Fab' breakthrough, with considerably greater losses of Fab' in the flow through from the expanded bed column. The results however were based on single process runs performed at different scales of operation. For a more accurate comparison the two processes should ideally be optimised individually for the specific system under analysis and then directly compared at equivalent scales using the same feed material.

Optical biosensor assays were developed and compared to the more traditional ELISA for the monitoring of Fab' accumulation during fermentation. The two techniques yielded similar accumulation profiles, however Fab' titres recorded by the assays differed considerably. Discrepancies were found to be due to subtle differences in the species detected by each assay and to interference from contaminants within process samples. Correct sample preparation minimised these discrepancies and resulted in comparable measured titres from each technique. The biosensor was also used to monitor breakthrough and elution during chromatographic purification. The sensor was shown to provide an accurate indication of breakthrough during column loading and also correctly identified product containing fractions during column elution.

The thesis concluded with a series of mass balance studies which compared the relative efficiencies of the different processing routes conducted at pilot scale. The mass balance studies highlighted the fact that there is unlikely to be a single 'ideal' purification scheme. The most suitable process will depend upon the specific requirements of the individual system under consideration. In the case of antibody fragment production processes where the ultimate product is a therapeutic for the treatment of chronic illness, the emphasis will be on maximising yields and minimising costs. Without a full economic analysis it is not possible to determine which of the four processes studied would prove the most economical. Based on yields alone, it is evident that the traditional process involving periplasmic extraction, clarification and packed bed adsorption is the preferred option. However, if loss of product during spheroplast removal continues to result in reduced yields at large scale, the process route involving expanded bed purification of the product directly from unclarified periplasmic extracts (which removes the requirement for a centrifugal clarification step) is likely to become a more attractive alternative, particularly following further optimisation of the expanded bed process.

Even when concentrating exclusively on antibody fragment production processes, the most suitable purification scheme will depend on the individual process under analysis. For example, the proportion of product which leaks into the supernatant during antibody fragment fermentations is, to an extent, dependent upon the nature of

the fragment being expressed. For a product which is naturally 'leaky' optimisation of the 'whole broth extraction' route may provide the most economical process, particularly as this process contains the smallest number of unit operations. Similarly, the success of expanded bed adsorption (including the potential for column blocking) is dependent upon the antibody fragment being expressed as this can affect the properties of the cells at fermentation harvest and therefore also the properties of the periplasmic or whole broth extract. Hence, a process involving expanded bed adsorption may be the most economical route for one antibody product, however it may be unfeasible to use the same process for a different product which produces an extract with a greater tendency to aggregate and block the column inlet.

To conclude, it remains clear that the most suitable purification strategy for antibody fragment production processes is system-specific, and will only become apparent following analysis of the specific process under consideration. The techniques of scale-down, modelling and rapid monitoring have all been developed to facilitate process analysis and specification of the most appropriate purification strategy.

10. FUTURE WORK

Each section of the thesis has highlighted areas of interest which require further investigation. Chapter 3 illustrated how a fermentation could be designed to minimise leakage of periplasmic product into the extracellular broth. However, the specific factors responsible for controlling leakage were not identified. Further work is required to elucidate the relative effects of different factors on periplasmic retention, such as the addition of calcium and magnesium prior to induction, phosphate limitation and induction temperature. Further analysis of the effects of scale on periplasmic retention would also be useful for the design of large-scale production processes.

The key requirements of a fermentation process for the production of biopharmaceuticals are consistency and reproducibility at different scales of operation. The process should also be well controlled and straightforward to operate at small-scale so that potential large-scale operational problems are avoided. The fermentation studied not only showed considerable variation in growth patterns and product titres at small-scale, but also required a complex set of carbon source and nutrient additions at specific stages of culture growth which would be difficult to reproduce effectively on scale-up. Reproducibility of the fermentation could be improved by further development of the inoculum train to provide a more consistent inoculum culture. The fermentation protocol should also be simplified to improve control and consistency of operation. Potential simplifications include exponential feeding of glycerol to remove the requirement for batch glycerol additions and to allow control of both growth rate and the point of induction. Additionally the development of lactose feeding strategies may simplify process operation during the induction phase, and feeding of phosphate could enable precise control of phosphate concentration at the point of induction (which may affect product partitioning between the periplasm and the extracellular broth). In cases where the emphasis is on high product yields, it may also be possible to increase titres by further increasing the biomass at induction, or by adding nutrient supplements such as amino acids during the induction phase.

Performing the Tris-EDTA extraction process on whole fermentation broth is a potential method for increasing yields by allowing the recovery of both extracellular and periplasmic product. However further assessment of the thermal stability and quality of the extracellular Fab', and optimisation of the extraction process in the presence of whole fermentation broth is required before the true potential of this technique can be realised. If successful, this method of extraction will be particularly attractive in processes where the Fab' is naturally 'leaky' and a considerable quantity of the product is located in the fermentation broth at the end of the induction period.

Current methods for the scale-down of centrifuges do not provide an accurate prediction of the recovery performance of industrial machines during the processing of shear sensitive biological materials. The reason is thought to lie in the inability to reproduce accurately shear fields in the scale-down equipment. More accurate methods for estimating the levels of shear in the centrifuge feed zone based on computational flow dynamics are currently being developed. Improved techniques for the reproduction of shear in scale-down and ultra-scale-down equipment are also required. This may necessitate modifications to the centrifuge feed zone in the scale-down version of the disk stack machine. Additional studies into the effect of shear on spheroplast suspensions, including the effect on particle size distribution would provide a more accurate indication of the differences resulting from processing in full-scale and scale-down equipment.

The development of a scale-down model of the disk stack centrifuge which accurately mimics the observed partitioning of Fab' with the solids phase during large-scale operation would greatly facilitate process development to minimise Fab' losses during this recovery operation. It is thought that the partitioning could be minimised by altering the ionic strength of the process stream, thereby reducing charge interactions between the Fab' and the solids. A scale-down model of the centrifuge would allow a range of feed streams of varying ionic strength to be tested in a short time period, so that the optimal operating conditions could be rapidly determined at minimal expense.

Expanded bed adsorption provides a method for the purification of antibody fragments directly from unclarified feedstocks. However blocking of the bed inlet is a common problem during processing of high cell density or high viscosity feed streams. During this study column blocking was alleviated by benzonase treatment of the feed prior to the processing of periplasmic extracts. However, blocking still occurred following benzonase treatment during processing of whole broth extracts. Also, addition of nuclease to process streams may not be permitted by regulatory authorities in the purification of products destined for therapeutic use. Therefore alternative methods need to be developed to minimise the potential for blocking. Redesign of the bed distributor may be required. Alternatively, mild homogenisation of the process stream may break up cell clumps within the feed stream and thus alleviate the problem for certain feedstocks. Given that certain feedstocks are more likely to cause column blockage than others, it would also be useful to develop a scale-down model of the expanded bed to allow assessment of process performance and identification of potential operational problems at small-scale, early during the development of a purification scheme.

Limitations of expanded bed adsorption include the high cost of affinity adsorbents and limitations on the scale of operation. The high cost of affinity matrices means ion exchange chromatography is the only practical option for large scale processing. Current limitations on the scale of operation of the expanded bed may restrict the utility of this technique until larger columns and higher capacity matrices can be designed.

The results of the biosensor studies clearly indicate the potential of this device for the real-time monitoring and control of a bioprocess sequence. The biosensor assays could be improved by further reducing non-specific binding and developing methods to increase the uniformity and stability of the binding surface by oriented coupling of ligands, which may also increase assay range. Additional assays could also be developed for the detection of different product variants such as free heavy and light chain during fermentation and purification processes.

A mass balance approach was used for the comparison of process options for the purification of Fab' fragments from *E. coli* fermentation broth. The study illustrated a method for the comparison of process alternatives and highlighted the operational factors that should be taken into consideration when designing a purification scheme. However, the actual results were of limited use as a number of the values used were based on single process runs or on operations which had not been optimised for the process under investigation. Ideally, for a more thorough analysis of process alternatives, each unit operation should be optimised individually and then the four purification schemes should be assessed at equivalent scales of operation using the same feed material. In addition, a full economic analysis and a more detailed assessment of the quality of the product following each purification sequence is required to give a more accurate indication of the most suitable and efficient purification route.

APPENDIX 1: Expression vector for the antibody fragment 4D5 Fab'

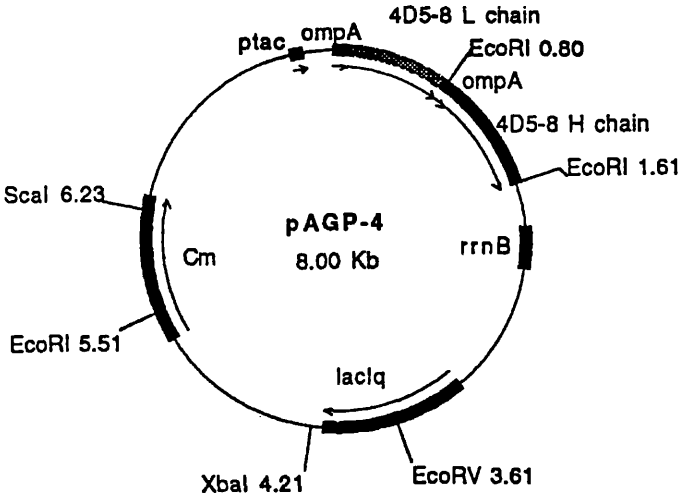

Figure A1.1 *Plasmid pAGP-4, used for expression of the antibody fragment 4D5 Fab' in Escherichia coli. Restriction sites marked are the estimated position.*

APPENDIX 2: Properties of feed material used for downstream processing trials

Table A2.1 indicates the source of material for each major downstream processing experiment and gives the properties of the fermentation broth at the time of cell harvest. All cell paste was frozen at -70°C following cell harvest, until required for DSP trials.

Fermentation	DCW ($g\ L^{-1}$)	Fab' concentration ($mg\ L^{-1}$)		DSP Trials
		Periplasmic	Extracellular	
HCD4 (10L)	37	202	15	Laboratory scale PE
HCD5 (10L)	38	132	49	WBE
150L2	37	117	43	Scale-down centrifugation trials
450L	48	78	23	2L and 100L PE CARR/ CSA-1 comparisons PBA and EBA

Table A2.1 *Properties of feed material used in downstream processing trials. Dry cell weights (DCW) and Fab' concentrations given are those measured immediately prior to cell harvest at the end of the fermentation. DSP, downstream processing; PE, periplasmic extraction; WBE, whole broth extraction; PBA, packed bed adsorption; EBA, expanded bed adsorption.*

APPENDIX 3: Derivation of equations for modelling of antibody release and protein degradation during periplasmic extraction

Antibody release and protein degradation during periplasmic extraction were modelled using first order kinetics. Derivations of the relevant equations are given below.

A3.1 Derivation of equations used for modelling antibody release

If it is assumed that the release of antibody from cells is a first order process, then it can be described by the equation:

$$\frac{dA}{dt} \propto (A_m - A) \qquad \textbf{(A3.1)}$$

or

$$\frac{dA}{dt} = k_1(A_m - A) \qquad \textbf{(A3.2)}$$

where A = antibody released ($\mu g\ mL^{-1}$)

A_m = maximum antibody available for release ($\mu g\ mL^{-1}$)

k_1 = rate constant for antibody release (s^{-1})

t = time (s)

Integration of equation A3.2, assuming the boundary conditions

1. $A = 0$ when $t = 0$
2. $A \rightarrow A_m$ as $t \rightarrow \infty$

gives the relationship:

$$\ln\left(\frac{A_m}{A_m - A}\right) = k_1 t \qquad \textbf{(A3.3)}$$

or rearranged,

$$A = A_m(1 - e^{-k_1 t}) \qquad \textbf{(A3.4)}$$

Integration of equation A3.2, assuming the boundary conditions

1. $A = A_0$ when $t = 0$
2. $A \rightarrow A_m$ as $t \rightarrow \infty$

gives the relationship:

$$\ln\left(\frac{A_m - A_o}{A_m - A}\right) = k_1 t \qquad \textbf{(A3.5)}$$

or, rearranged,

$$A = A_m\left(1 - e^{-k_1 t}\right) + A_o e^{-k_1 t} \qquad \textbf{(A3.6)}$$

A3.2 Derivation of equations used for modelling protein degradation

If it is assumed that the temperature-related denaturation of protein is a first order process, then it can be described by the equation:

$$-\frac{dP}{dt} \propto \left(P - P_f\right) \qquad \textbf{(A3.7)}$$

or,
$$-\frac{dP}{dt} = k_2\left(P - P_f\right) \qquad \textbf{(A3.8)}$$

where P = functional (non-denatured) protein (mg mL^{-1})

P_f = functional protein remaining at the end of the denaturation process (i.e. protein which is stable at the temperature employed, mg mL^{-1})

k_2 = rate constant for protein degradation (s^{-1})

t = time (s)

Integration of equation A3.8, assuming the boundary conditions:

1. $P = P_m$ at $t = 0$ (where P_m is the total protein available for denaturation)
2. $P \rightarrow P_f$ as $t \rightarrow \infty$

gives the relationship:

$$-\ln\left(\frac{P - P_f}{P_m - P_f}\right) = k_2 t \qquad \textbf{(A3.9)}$$

or, rearranging,

$$P = P_m e^{-k_2 t} + P_f(1 - e^{-k_2 t}) \qquad \textbf{(A3.10)}$$

APPENDIX 4: Periplasmic extraction scale up

Periplasmic extraction was scaled up by maintaining constant power per unit volume at the different scales of operation.

Power per unit volume given by following correlation:

$$\frac{P}{V} = \frac{P_o \rho N^3 D_I^5}{V} \qquad \textbf{(A4.1)}$$

where P = Power (W)

P_0 = impeller power number (-)

ρ = density (kg m^{-3})

N = impeller speed (rps)

D_I = impeller diameter (m)

V = liquid volume (m^3)

Constant power per unit volume was maintained by appropriate setting of the impeller rotational speed. Impeller speeds required to achieve a constant power per unit volume of 45 W m^{-3} are given in Table A4.1.

Extraction vessel	0.1L Stirred tank	3L Bioreactor	150L Bioreactor
Extraction volume	0.065L	2L	100L
P_o	5	10	15
ρ (kg m^{-3})	1014	1014	1014
N (rpm)	**250**	**151**	**128**
N (rps)	4.17	2.52	2.13
D_I (m)	0.024	0.056	0.125
V (m^3)	6.5×10^{-5}	2×10^{-3}	0.1
P/V (W m^{-3})	**45**	**45**	**45**

Table A4.1 *Impeller rotational speeds required to maintain constant power per unit volume at the different scales of operation for periplasmic extraction.*

APPENDIX 5: Equations for Σ values of the laboratory batch centrifuge, the tubular bowl and the disk stack centrifuge

Sigma theory was developed by Ambler in 1952 as a method of comparing the performance of different scales or designs of centrifuge. The sigma value, Σ, indicates the required area of a gravity settling tank with the same clarifying capacity as the centrifuge under the same conditions. Equations for the Σ factor of the laboratory batch centrifuge, the tubular bowl and the disc stack centrifuge are given below.

A5.1 The laboratory batch centrifuge

In the laboratory batch centrifuge, cylindrical containers are rotated with the axis of the cylinder at right angles to the axis of rotation. The Σ value for the laboratory batch centrifuge is given by the equation:

$$\Sigma = \frac{\omega^2 V}{2g \ln\left(\frac{2r_2}{r_1 + r_2}\right)} \qquad \textbf{(A5.1)}$$

where V = liquid volume (m^3)

r_1 = distance from the centre of rotation to the liquid surface (m)

r_2 = distance from the centre of rotation to the surface of the sedimented cake (m)

ω = angular velocity (rad s^{-1})

A5.2 The tubular bowl centrifuge

The Σ value for the tubular bowl centrifuge is given by the equation:

$$\Sigma = \frac{\omega^2 \pi L}{g} \frac{r_2^2 - r_1^2}{\log_e\left(\frac{2r_2^2}{r_2^2 + r_1^2}\right)} \qquad \textbf{(A5.2)}$$

where L = length of bowl (m)

r_1 = distance from centre of rotation to the liquid surface (m)

r_2 = distance from centre of rotation to the surface of the bowl (m)

A5.3 The disk stack centrifuge

The Σ value for the disk stack centrifuge is given by the equation:

$$\Sigma = 2\pi . n\omega^2 \frac{(r_o^3 - r_i^3)}{3g \tan\theta} F_L \qquad \textbf{(A5.3)}$$

where n = number of disks in the disk stack (-)

θ = lower angle of conical disk (rad)

r_o = outer disk radius (m)

r_i = inner disk radius (m)

F_L is a correction factor to account for rib spacers on the disks which hold the disks apart. The rib spacers occupy area within the disk stack and hence reduce the equivalent settling area of the machine.

$$F_L = 1 - \frac{3 z_L b_c}{4\pi . r_2} \frac{1 - (r_o/r_i)^2}{1 - (r_o/r_i)^3} \qquad \textbf{(A5.4)}$$

where F_L = Σ correction factor to account for disk ribs (-)

z_L = number of ribs per disk (-)

b_c = rib width (m)

APPENDIX 6: Technical data for the CARR Powerfuge

A6.1 Data for calculation of Σ

Length of bowl (L)	0.1273 m
Distance from centre of rotation to the liquid surface (r_1)	0.0508 m
Distance from centre of rotation to the surface of the bowl (r_2)	0.0762 m
Centrifuge rotational speed (ω)	1602 rad s^{-1} (15 300 rpm)

A6.2 CARR Powerfuge specifications

Bowl volume	1.0 L
Solids holding volume	0.9 L
Σ value at 15300 rpm	1037 m^2
Correction factor	0.9-1.0

The correction factor for the CARR is close to unity because the tubular bowl has simpler flow patterns than most centrifuges and therefore operates more closely to the Sigma theory prediction (and the implied assumptions).

APPENDIX 7: Technical data for the Westfalia CSA-1 disk stack centrifuge

A7.1 Data for calculation of Σ

Number of disks in the disk stack (n)	45
Lower angle of conical disk (θ)	0.66 rad
Outer disk radius (r_o)	0.053 m
Inner disk radius (r_i)	0.021 m
Centrifuge rotational speed (ω)	1027 $rads^{-1}$ (9810 rpm)
Number of ribs per disk (z_L)	6
Rib width (b_c)	0.005 m

A7.2 CSA-1 specifications

Bowl volume	0.6 L
Solids holding volume	0.3 L
Minimum discharge interval	2 min
Σ value at 9810 rpm	1602 m^2

A7.3 CSA-1 scale-down configuration

Number of active disks in the disk stack	12
Bowl volume	0.13
Solids holding volume	0.089
Σ value at 9810 rpm	427 m^2

APPENDIX 8: Determination of operating conditions of the laboratory centrifuge required to predict the recovery performance of an industrial disk stack centrifuge

The Beckman J2-M1 laboratory centrifuge, operated with the JS 13.1 swing out rotor, was used to predict recovery performance of the Westfalia CSA-1 disk stack separator. The laboratory centrifuge was operated at the same RCF as the CSA-1 and the relationship between clarification efficiency and equivalent Q/Σ compared to that obtained for the industrial machine.

Section A8.1 shows calculation of the rotational speed of the laboratory centrifuge required to produce the same RCF as the CSA-1 operating at 9810 rpm. Section A8.2 details the method and equations used to calculate the equivalent Q/Σ of the laboratory machine, and shows the centrifuge spin times and corresponding Q/Σ used for assessment of recovery performance.

A8.1 Calculation of operating speed of the laboratory centrifuge required to give the same RCF as the CSA-1

A8.1.1 Calculation of RCF of CSA-1 operating at 9810 rpm

$$RCF = \frac{r_{ln}\omega^2}{g} \qquad \textbf{(A8.1);} \qquad r_{ln} = \frac{r_o - r_i}{\ln\left(r_o / r_i\right)} \qquad \textbf{(A8.2)}$$

For the CSA-1 $r_i = 0.021$ m

$r_o = 0.053$ m

$\omega = 1027$ rads^{-1}

$\Rightarrow$ RCF = 3716

A8.1.2 Calculation of laboratory centrifuge rotational speed

$$RCF_{LAB} = RCF_{CSA\text{-}1} = 3716$$

$$RCF_{LAB} = \frac{r_{ln(LAB)}\omega^2}{g} \quad \textbf{(A8.3);} \qquad r_{ln(LAB)} = \frac{r_2 - r_1}{\ln\left(r_2/r_1\right)} \quad \textbf{(A8.4)}$$

For the laboratory centrifuge $r_1 = 0.044$ m

$r_2 = 0.114$ m

$$\Rightarrow r_{ln(LAB)} = 0.0735 \text{ m}$$

$$\omega = \sqrt{\frac{g(RCF_{LAB})}{r_{ln(LAB)}}} \quad \textbf{(A8.5)}$$

$\Rightarrow \omega = 704$ rads^{-1} (= 6723 rpm)

A8.2 Calculation of equivalent Q/Σ for the laboratory centrifuge

The equation defining recovery performance for a laboratory batch centrifuge (derived in full by Ambler, 1959) is:

$$\frac{Q}{\Sigma} = \frac{2g\ln\left(\frac{2r_2}{r_1 + r_2}\right)}{\omega^2 t} \quad \textbf{(A8.6)}$$

where r_1 = distance from the centre of rotation to the liquid surface (m)

r_2 = distance from the centre of rotation to the surface of the sedimented cake (m)

ω = the angular velocity around the centre of rotation (rad s^{-1})

t = the total time for centrifuging (s)

For a batch centrifuge, Q is defined as:

$$Q = \frac{V}{t} \qquad \textbf{(A8.7)}$$

where V = the volume of material in the centrifuge tube (L)

t = the run time of the centrifuge at constant speed (s)

Equation A8.6 applies for constant speed of operation only. It has been adapted by Maybury *et al.*, (2000) to account for the acceleration and deceleration periods of the centrifuge bowl.

The modified equation is:

$$\frac{Q}{\Sigma} = \frac{6g\ln\left(\frac{2r_2}{r_1 + r_2}\right)}{\omega^2(3 - 2x - 2y)t_c} \qquad \textbf{(A8.8)}$$

where y = the fraction of overall centrifugation time for acceleration (-)

x = the fraction of overall centrifugation time for deceleration (-)

t_c = total centrifugation time (s)

Equation A8.8 is based on the assumption that the acceleration and deceleration periods are represented by linear relationships. Analysis of the centrifuge acceleration profile (Maybury *et al.*, 2000) shows that the initial acceleration phase (0-500 rpm) and the end of the deceleration phase (500-0 rpm) are non-linear. However, the contribution of these regions to the overall Q/Σ was found to be small (<1%); therefore they have been ignored. Hence, for the calculation of Q/Σ values, the total centrifugation time, t_c, was taken as the time between the bowl speed reaching 500 rpm during the acceleration phase and reducing to 500 rpm during deceleration.

The centrifuge run times and corresponding Q/Σ values used in the centrifuge spin tests to determine the relationship between clarification efficiency and equivalent Q/Σ are shown in Table A8.1 The 'centrifuge run time' given in Table A8.1 is the

actual run time set on the centrifuge control panel. This corresponds to the time from the beginning of acceleration to the beginning of deceleration. The time taken for the centrifuge to accelerate to 500 rpm was measured at approximately 15 seconds, therefore the relationship between the centrifuge run time (in minutes) and t_c is given by the equation:

Centrifuge run time = (t_c - time for centrifuge deceleration + 15)/60 **(A8.9)**

Table A8.1 shows that as the centrifuge run time varies, the duration of operation at the maximum speed of 6720 rpm varies, however the duration of the acceleration and deceleration stages remains constant.

Centrifuge run time (mins)	Equivalent Q/Σ (ms^{-1})	Total centrifugation time (t_c) (s)	Time for centrifuge acceleration (s)	Total time at 6720 rpm (s)	Time for centrifuge deceleration (s)
3.5	8.24×10^{-8}	290	76	120	94
6	4.45×10^{-8}	439	76	269	94
10	2.56×10^{-8}	679	76	509	94
15	1.67×10^{-8}	981	76	811	94
20	1.24×10^{-8}	1282	76	1112	94
29	8.49×10^{-9}	1819	76	1649	94
47	5.20×10^{-9}	2899	76	2729	94

Table A8.1 *Centrifuge run times and corresponding Q/Σ values used for the construction of recovery curves for the laboratory centrifuge. The centrifuge run time is the actual run time set on the centrifuge control panel and corresponds to the time from the beginning of centrifuge acceleration to the beginning of deceleration. The total centrifugation time (t_c) is the time used for calculation of Q/Σ values and corresponds to the time between the bowl speed reaching 500 rpm during the acceleration phase and reducing to 500 rpm during deceleration.*

APPENDIX 9: Operational flow rates and corresponding Q/Σ values for the CSA-1 disk stack centrifuge and CARR Powerfuge

Tables A9.1 and A9.2 show the feed flow rates and corresponding Q/Σ values used during experimentation to determine the relationship between clarification efficiency and Q/Σ for the Westfalia CSA-1 disk stack centrifuge and the CARR P6 Powerfuge. Equations used for calculations of the relevant Σ factors are given in Appendix 5.

Feed flow rate (Lhr^{-1})	Bowl speed (rpm)	Σ (m^2)	Q/Σ (ms^{-1})
11.2	9810	1602	1.9×10^{-9}
20.2	9840	1612	3.5×10^{-9}
29.2	9840	1612	5.0×10^{-9}
49.4	9840	1612	8.5×10^{-9}
83.2	9840	1612	1.4×10^{-9}
98.9	9870	1642	1.7×10^{-8}

Table A9.1 *Feed flow rates and corresponding Q/Σ values used to determine the relationship between clarification efficiency and Q/Σ for the Westfalia CSA-1 disk stack centrifuge. (Σ values were calculated using equation A5.3).*

Feed flow rate (Lhr^{-1})	Bowl speed (rpm)	Σ (m^2)	Q/Σ (ms^{-1})
15	15 320	1040	4.0×10^{-9}
20	15 320	1040	5.3×10^{-9}
30	15 320	1040	8.0×10^{-9}
50	15 320	1040	1.3×10^{-8}
58	15 320	1040	1.5×10^{-8}
90	15 320	1040	2.4×10^{-8}

Table A9.2 *Feed flow rates and corresponding Q/Σ values used to determine the relationship between clarification efficiency and Q/Σ for the CARR P6 Powerfuge (tubular bowl centrifuge). (Σ values were calculated using equation A5.2).*

APPENDIX 10: Operational flow rates and corresponding Q/Σ values for CSA-1 in full stack and scale-down configurations

Tables A10.1 shows the feed flow rates and corresponding Q/Σ values used during preparation of recovery curves for the CSA-1 centrifuge operated in full-scale and scale-down configurations. Σ factors for the CSA-1 are given in Appendix 7.

CSA-1 (Full-scale)			CSA-1 (Scale-down)		
Flow rate (Lhr^{-1})	Q/Σ (ms^{-1})	Q/cΣ (ms^{-1})	Flow rate (Lhr^{-1})	Q/Σ (ms^{-1})	Q/cΣ (ms^{-1})
100	1.73×10^{-8}	4.33×10^{-8}	27	1.73×10^{-8}	4.33×10^{-8}
50	8.67×10^{-9}	2.17×10^{-8}	13	8.67×10^{-8}	2.17×10^{-8}
30	5.20×10^{-9}	1.30×10^{-8}	8	5.20×10^{-9}	1.30×10^{-8}
20	3.47×10^{-9}	8.68×10^{-9}	5.3	3.47×10^{-9}	8.68×10^{-9}
10	1.73×10^{-9}	4.33×10^{-9}	2.7	1.73×10^{-9}	4.33×10^{-9}

Table A10.1 *Flow rates and corresponding Q/Σ values used in the preparation of recovery curves for the CSA-1 disk stack centrifuge operated in full-scale and scale-down configurations. To account for non-ideal flow a correction factor, c, of 0.4 was used in the calculation of Q/Σ.*

APPENDIX 11: Equations for the calculation of assay error

The error associated with ELISA and biosensor assays was measured by repeating a calibration curve for each assay 10 times and calculating the error of the mean for each concentration using the equations given below:

1. Standard error of the mean , $SE = \frac{\sigma}{\sqrt{n}}$ **(A11.1)**

2. 95% confidence interval, 95% CI = tSE **(A11.2)**

3. Error of the mean at 95% $CI = \frac{CI}{x}100$ **(A11.3)**

where x = mean value for each concentration

σ = standard deviation for each concentration

n = number of times each assay was repeated (=10)

t = t value obtained from t-tables for (n-1) degrees of freedom at the 95% confidence interval

APPENDIX 12: Mass balance analysis: calculation of operating parameters for packed and expanded bed purification processes

Chapter 8 compares four process for the purification of antibody fragments from *E. coli* fermentation broth. Each purification scheme concludes with a protein A packed or expanded bed affinity purification step. The following sections show the calculations for the determination of column size, process yield, process stream volume and operating time for these chromatographic purification processes.

A12.1 Purification Scheme 1

The individual unit operations, associated yields and overall process yields for purification scheme 1 are give in Table A12.1.

	UNIT OPERATION	YIELD (%)	OVERALL YIELD (%)
1	Fermentation	100	100
2	Tubular Bowl Centrifugation	76	76
3	Periplasmic Extraction	85	64.6
4	Tubular Bowl Centrifugation	94	60.7
5	Filtration	98	59.5
6	Packed Bed Adsorption (PBA)	?	?

Table A12.1 *Individual unit operation yields and total process yields for purification scheme 1.*

A12.1.1 Calculation of column size required for packed bed adsorption

Fermentation assumptions	Scale 100L
	Solids fraction 10% (v/v)
	Fab' yield 200 mg L^{-1}
	Total Fab' 20 g
Process yield following filtration	59.5%
∴Total Fab' to be processed by PBA	20 × 0.595 = 11.9 g

Assuming the process is operated at 10% Fab' breakthrough, this will give 98% Fab' yield and a dynamic binding capacity of 47% of the total matrix binding capacity (determined from Figures 6.2.3 and 6.2.4, Chapter 6).

Total matrix binding capacity	12.5 mg mL^{-1}
(determined experimentally for rProtein A	
Sepharose® Fast Flow, Table 6.2.1, Chapter 6)	
Dynamic binding capacity (at 10% breakthrough)	12.5×0.47 = 5.9 mg mL^{-1}
Volume of matrix required to purify 11.9g Fab'	11.9/ 5.9 = 2L

Therefore it was assumed an XK 50 mm × 100 cm column (Amersham Pharmacia Biotech, Uppsala, Sweden) containing 2L protein A Sepharose 4 Fast Flow chromatographic media (Amersham Pharmacia Biotech) would be used for the purification.

A12.1.2 Calculation of operating time for the packed bed adsorption process in purification scheme 1

Assumptions following periplasmic extraction:

Volume of process stream	100L
Solids fraction of process stream	10% (v/v)
Liquid volume of process stream	100 × 0.9 = 90L
Liquid recovery by tubular bowl centrifugation	96%
(determined experimentally, Table 5.2.7, Chapter 5)	
Liquid recovery during filtration (assumed)	100%
Volume of liquid to be process by PBA	90 × 0.96 × 1.0 = 86.4L

Assuming the chromatographic process is operated at a flow rate of 1000 cm hr^{-1} (= 19.6 L hr^{-1}), the total process time is determined as shown in Table A12.2.

CHROMATOGRAPHIC STAGE	VOLUME (CV)	VOLUME (L)	TIME (hr)
Column equilibration	10	20	1.02
Load	-	86.4	4.41
Wash	5	10	0.51
Elution	10	20	1.02
TOTAL TIME	-	-	6.96

Table A12.2 *Calculation of operating time for the packed bed purification of Fab' in purification scheme 1.*

A12.2 Purification Scheme 2

The individual unit operations, associated yields and overall process yields for purification scheme 2 are give in Table A12.3.

	UNIT OPERATION	YIELD (%)	OVERALL YIELD (%)
1	Fermentation	100	100
2	Tubular Bowl Centrifugation	76	76
3	Periplasmic Extraction	85	64.6
4	Disk Stack Centrifugation	73	47.2
5	Filtration	98	46.3
6	Packed Bed Adsorption (PBA)	?	?

Table A12.3 *Individual unit operation yields and total process yields for purification scheme 2.*

A12.2.1 Calculation of column size required for packed bed adsorption

Fermentation assumptions	Scale	100 L
	Solids fraction	10% (v/v)
	Fab' yield	200 mg L^{-1}
	Total Fab'	20 g
Process yield following filtration	46.3%	
∴ Total Fab' to be processed by PBA	$20 \times 0.463 = 9.3$ g	

Assuming the process is operated at 10% Fab' breakthrough, this will give 98% Fab' yield and a dynamic binding capacity of 47% of the total matrix binding capacity (determined from Figures 6.2.3 and 6.2.4, Chapter 6).

Total matrix binding capacity	12.5 mg mL^{-1}
(determined experimentally for rProtein A	
Sepharose® Fast Flow, Table 6.2.1, Chapter 6)	
Dynamic binding capacity (at 10% breakthrough)	12.5×0.47 = 5.9 mg mL^{-1}
Volume of matrix required to purify 9.3g Fab'	9.3/ 5.9 = 1.6 L

Therefore, it was assumed an XK 50 mm × 100 cm column containing 1.6 L protein A Sepharose 4 Fast Flow chromatographic media would be used for the purification.

A12.2.2 Calculation of operating time for the packed bed adsorption process in purification scheme 2

Assumptions following periplasmic extraction:

Volume of process stream	100L
Solids fraction of process stream	10% (v/v)
Liquid volume of process stream	100 × 0.9 = 90L
Liquid recovery by disk stack centrifugation	77%
(determined experimentally, Table 5.2.5, Chapter 5)	
Liquid recovery during filtration (assumed)	100%
Volume of liquid to be process by PBA	90 × 0.77 × 1.0 = 69.3L

Assuming the chromatographic process is operated at a flow rate of 1000 cm hr^{-1} (= 19.6 L hr^{-1}), the total process time is determined as shown in Table A12.4.

CHROMATOGRAPHIC STAGE	VOLUME (CV)	VOLUME (L)	TIME (hr)
Column equilibration	10	16	0.82
Load	-	69.3	3.54
Wash	5	8	0.41
Elution	10	16	0.82
TOTAL TIME	-	-	5.59

Table A12.4 *Calculation of operating time for the packed bed purification of Fab' in purification scheme 2.*

A12.3 Purification Scheme 3

The individual unit operations, associated yields and overall process yields for purification scheme 3 are give in Table A12.5.

	UNIT OPERATION	YIELD (%)	OVERALL YIELD (%)
1	Fermentation	100	100
2	Tubular Bowl Centrifugation	76	76
3	Periplasmic Extraction (PE)	85	64.6
4	Expanded bed adsorption (EBA)	?	?

Table A12.5 *Individual unit operation yields and total process yields for purification scheme 3.*

A12.3.1 Calculation of column size required for expanded bed adsorption

Fermentation assumptions	Scale 100L
	Solids fraction 10% (v/v)
	Fab' yield 200 mg L^{-1}
	Total Fab' 20 g
Process yield following PE	64.6%
∴ Total Fab' to be processed by EBA	20 × 0.646 = 12.9 g

Because expanded bed columns are only available in a limited range of sizes, it was assumed a Streamline 200 column (20 cm × 15 cm) would be used, containing 4.7 L Streamline rProtein A media (both manufactured by Amersham Pharmacia Biotech, Uppsala, Sweden).

The total binding capacity of the Streamline rProtein A matrix was determined experimentally to be 13.5 mg(Fab') mL^{-1}(matrix) (Table 6.2.1, Chapter 6). Therefore, the total binding capacity of 4.7 L matrix is 63.5 g(Fab').

Total Fab' to be processed	12.9 g
Total binding capacity of matrix	63.5 g(Fab')
∴ binding capacity of matrix utilised (following complete loading of the Fab')	100 × 12.9/ 63.5 = 20%

Operating at a binding capacity of 20% of the total matrix capacity gives the following process parameters (from Figure 6.2.6, Chapter 6):

Level of Fab' breakthrough	27%
Fab' yield	83%

A12.3.2 Calculation of operating time for the expanded bed adsorption process in purification scheme 3

Volume to be processed	100L

Assuming the equilibration, load and wash steps are performed at a flow rate of 185 cm hr^{-1} (= 58.1 L hr^{-1}) and elution is carried out at a flow rate of 90 cm hr^{-1} (= 28.3 L hr^{-1}), the total process time is determined as shown in Table A12.6.

CHROMATOGRAPHIC STAGE	VOLUME (CV)	VOLUME (L)	TIME (hr)
Column equilibration	10	47	0.81
Load	-	100	1.72
Wash	5	23.5	0.40
Elution	10	47	1.66
TOTAL TIME	-	-	4.59

Table A12.6 *Calculation of operating time for the packed bed purification of Fab' in purification scheme 3.*

A12.4 Purification Scheme 4

The individual unit operations, associated yields and overall process yields for purification scheme 4 are give in Table A12.7.

	UNIT OPERATION	YIELD (%)	OVERALL YIELD (%)
1	Fermentation	100	100
2	Whole Broth Extraction (WBE)	41	41
3	Expanded bed adsorption (EBA)	?	?

Table A12.7 *Individual unit operation yields and total process yields for purification scheme 4.*

A12.4.1 Calculation of column size required for expanded bed adsorption

Fermentation assumptions	Scale	100L
	Solids fraction	10% (v/v)
	Fab' yield	200 mg L^{-1}
	Total Fab'	20 g
Process yield following WBE	41%	
∴ Total Fab' to be processed by PBA	$20 \times 0.41 = 8.2$ g	

For the reasons described previously (section A12.3.1), it was assumed a Streamline 200 column (20 cm × 15 cm) would be used, containing 4.7 L Streamline rProtein A media.

The total binding capacity of the Streamline rProtein A matrix was determined experimentally to be 13.5 mg(Fab') mL^{-1}(matrix) (Table 6.2.1, Chapter 6). Therefore, the total binding capacity of 4.7 L matrix is 63.5 g(Fab').

Total Fab' to be processed	8.2 g
Total binding capacity of matrix	63.5g Fab'
$\therefore$ binding capacity of matrix utilised (following complete loading of the Fab')	$100 \times 8.2/ 63.5 = 13\%$

Operating at a binding capacity of 13% of the total matrix capacity gives the following process parameters (Figure 6.2.6, Chapter 6):

Level of Fab' breakthrough	24%
Fab' yield	85%

A12.4.2 Calculation of operating time for the expanded bed adsorption process in purification scheme 4

Volume to be processed	110L

Assuming the equilibration, load and wash steps are performed at a flow rate of 185 cm hr^{-1} (= 58.1 L hr^{-1}) and elution is carried out at a flow rate of 90 cm hr^{-1} (= 28.3 L hr^{-1}), the total process time is determined as shown in Table A12.8.

CHROMATOGRAPHIC STAGE	VOLUME (CV)	VOLUME (L)	TIME (hr)
Column equilibration	10	47	0.81
Load	-	110	1.89
Wash	5	23.5	0.40
Elution	10	47	1.66
TOTAL TIME	-	-	4.76

Table A12.8 *Calculation of operating time for the packed bed purification of Fab' in purification scheme 4.*

APPENDIX 13: Mass balance analysis summary

Chapter 8 compares four purification schemes for the recovery of antibody fragments from *E. coli* fermentation broth. Tables A13.1-A13.4 show the yield, purification factor and operating time calculated for each unit operation in each of the four purification schemes.

UNIT OPERATION	YIELD (%)	PURIFICATION FACTOR (-)	OPERATING TIME (hours)
Fermentation	100	-	-
Tubular Bowl Centrifugation	76	-	1.92
Periplasmic Extraction	85	4.0	5
Tubular Bowl Centrifugation	94	-	1.89
Filtration	98	-	2
Packed Bed Adsorption	98	14	6.96
PROCESS TOTAL	**58%**	**56**	**17.8 hours**

Table A13.1 *Yield, purification factor and operating time calculated for each unit operation in purification scheme 1.*

UNIT OPERATION	YIELD (%)	PURIFICATION FACTOR (-)	OPERATING TIME (hours)
Fermentation	100	-	-
Tubular Bowl Centrifugation	76	-	1.92
Periplasmic Extraction	85	4.0	5
Disk Stack Centrifugation	73	-	1.23
Filtration	98	-	2
Packed Bed Adsorption	98	14	5.59
PROCESS TOTAL	**45%**	**56**	**15.7 hours**

Table A13.2 *Yield, purification factor and operating time calculated for each unit operation in purification scheme 2.*

UNIT OPERATION	YIELD (%)	PURIFICATION FACTOR (-)	OPERATING TIME (hours)
Fermentation	100	-	-
Tubular Bowl Centrifugation	76	-	1.92
Periplasmic Extraction	85	4.0	5
Expanded bed adsorption	83	12	4.59
PROCESS TOTAL	**54%**	**48**	**11.5 hrs**

Table A13.3 *Yield, purification factor and operating time calculated for each unit operation in purification scheme 3.*

UNIT OPERATION	YIELD (%)	PURIFICATION FACTOR (-)	OPERATING TIME (hours)
Fermentation	100	-	-
Whole Broth Extraction	41	6.0	5
Expanded bed adsorption	85	12	4.76
PROCESS TOTAL	**35%**	**72**	**9.8 hrs**

Table A13.4 *Yield, purification factor and operating time calculated for each unit operation in purification scheme 4.*

NOMENCLATURE

A	absorbance	-
A	antibody released	mg mL^{-1}
A_m	maximum antibody available for release	mg mL^{-1}
A_o	initial antibody release	mg mL^{-1}
b_c	rib width	m
c	concentration	mg mL^{-1}
c	Σ correction factor to account for non-ideality	-
C_{AD}	Fab' concentration in solids stream	mg mL^{-1}
C_{AF}	Fab' concentration in feed stream	mg mL^{-1}
C_{AS}	Fab' concentration in supernatant stream	mg mL^{-1}
C_{PD}	protein concentration in solids stream	mg mL^{-1}
C_{PF}	protein concentration in feed stream	mg mL^{-1}
C_{PS}	protein concentration in supernatant stream	mg mL^{-1}
d_s	diameter of particle	m
D	dilution factor	-
D_I	impeller diameter	m
E	extinction coefficient	mL μmol^{-1} cm^{-1}
F_L	Σ correction factor to account for disk ribs	-
g	acceleration due to gravity	m s^{-2}
G	centrifugal force term	-
k_1	rate constant for Fab' release	s^{-1}
k_2	rate constant for protein degradation	s^{-1}
k_a	molar association constant	M^{-1}
K	dimensional constant (equation 4.1)	$P^{-2.9}$
l	path length	cm
L	length of bowl	m
N	number of passes through homogeniser	-
N	impeller speed	rps
n	number of active disks in the disk stack	-
OD	optical density	-
P	pressure	Pa

P	power	W
P	functional protein	$mg\ mL^{-1}$
P_f	remaining functional protein at end of process	$mg\ mL^{-1}$
P_m	total functional protein	$mg\ mL^{-1}$
P_o	impeller power number	-
P_S	Extracellular protein/ enzyme concentration in sheared sample	$mg\ mL^{-1}$
P_0	Background protein/ enzyme concentration	$mg\ mL^{-1}$
P_{100}	Total enzyme/ protein available for release	$mg\ mL^{-1}$
Q	volumetric flow rate	$m^3\ s^{-1}$
R	protein released	$mg\ g^{-1}$
R_m	maximum protein available for release	$mg\ g^{-1}$
r	radial position of particle	m
r_1	inner radius	m
r_2	outer radius	m
r_e	effective radius of the centrifuge	m
r_i	inner disk radius	m
r_o	outer disk radius	m
RCF	relative centrifugal force	-
s_e	effective settling distance	m
t	time	s
v_{FDIS}	volume solids fraction of solids stream	-
v_{FF}	volume solids fraction of feed stream	-
v_{FSUP}	volume solids fraction of supernatant stream	-
V_{DIS}	volume of solids stream	L
V_{FEED}	volume of feed stream	L
V_{SUP}	volume of supernatant stream	L
V_g	settling velocity under gravity	$m\ s^{-1}$
V_Z	settling velocity in a centrifugal field	$m\ s^{-1}$
V	volume	m^3
y	the fraction of overall centrifugation time for acceleration	-
x	the fraction of overall centrifugation time for deceleration	-
Z_l	number of ribs per centrifuge disk	-

Greek symbols

ε	extinction coefficient	mL mg^{-1} cm^{-1}
θ	lower angle of conical disk	rad
μ	suspension dynamic viscosity	Ns m^{-2}
ν	volume of sample in cuvette	mL
ρ	density	kg m^{-3}
ρ_S	density of the particles	kg m^{-3}
ρ_L	density of the suspending fluid	kg m^{-3}
Σ	equivalent centrifuge separating area	m^2
ω	the angular velocity around the centre of rotation	rad s^{-1}

REFERENCES

Ahlstrom, B., Edebo, L. 1994. Selective release of the periplasmic enzyme β-lactamase from *Escherichia coli* with tetradecyl betainate. FEMS Microbiology Letters **119**:7-12

Altshuler, G.L., Dzwiewulski, D.M., Sowek, J.A., Belfort, G. 1986. Continuous hybridoma growth and monoclonal antibody production in hollow-fibre reactor-separators. Biotechnology and Bioengineering **28**: 646-658

Amann, E., Brosius, J., Ptashne, M. 1983. Vectors bearing a hybrid *trp-lac* promoter useful for regulating expression of cloned genes in *Escherichia coli*. Gene **25**: 167-178

Ambler, C. M. 1952. The evaluation of centrifugal performance. Chemical Engineering Progress **48**: 150-158

Ambler, C. M. 1959 The theory of scaling up laboratory data for the sedimentation type centrifuge. Journal of Biochemical and Microbiological Technology and Engineering **1**: 185-205

Ames, G.F-L., Prody, C., Kustu, S. 1984. Simple, rapid and quantitative release of periplasmic proteins by chloroform. Journal of Bacteriology **160**: 1181-1183

Ariga, O., Watari, T., Andoh, Y., Fujishita, Y., Sano, Y. 1989. Release of thermophilic α-amylase from transformed *Escherichia coli* by addition of glycine. Journal of Fermentation and Bioengineering **68**: 243-246

Arnold, F.H. 1991. Metal-affinity separations: a new dimension in protein processing. Bio/Technology **9**: 151-156

Bagshawe, K.D., Sharma, S., Burke, P.J., Melton, R.G., Knox, R.J. 1999. Developments with targeted enzymes in cancer therapy. Current Opinion in Immunology **11**: 579-583

Baker, K., Ison, A., Freedman, R., Jones, W., James, D. 1997. Real-time monitoring of recombinant protein concentration in animal cell cultures using an optical biosensor. The Genetic Engineer and Biotechnologist **17**: 69-74

Barnfield Frej, A-K., Hjorth, R., Hammarstrom, A. 1994. Pilot scale recovery of recombinant annexin V from unclarified *Escherichia coli* homogenate using expanded bed adsorption. Biotechnology and Bioengineering **44**: 922-929

Bentley, W.E., Madurawe, R.D., Gill, R.T., Shiloach, M., Chase, T.E., Pulliam-Holoman, T.R., Valdes, J.J. 1998. Generation of a histidine-tagged antibotulinum toxin antibody fragment in *E. coli*: effect of post-induction temperature on yield and IMAC binding-affinity. Journal of Industrial Microbiology and Biotechnology **21**: 275-282

Berney, H., Roseingrave, P., Alderman, J., Lane, W., Collins, J.K. 1997. Biosensor surface characterisation: confirming multilayer immobilisation, determining coverage of the biospecies and establishing detection limits. Sensors and Actuators B **44**: 341-349

Berry, M.J., Davies, J. 1992. Use of antibody fragments in immunoaffinity chromatography: Comparison of Fv fragments and paralog peptides. Journal of Chromatography **597**: 239-245

Berry, M.J., Wattam, T.A.K., Willets, J., Linder, N., De Graaf, T., Hunt, T., Gani, M., Davis, P.J., Porter, P. 1994. Assay and purification of Fv fragments in fermenter cultures: design and evaluation of generic binding reagents. Journal of Immunological Methods **167**: 173-182

Better, M., Chang, C.P., Robinson, R.R., Horwitz, A.H. 1988. *Escherichia coli* secretion of an active chimeric antibody fragment. Science **240**: 1041-1043

Better, M., Horwitz, A.H. 1989. Expression of engineered antibodies and antibody fragments in microorganisms. Methods in Enzymology **178**: 476-496

Better, M., Horwitz, A.H. 1993. *In vivo* expression of correctly folded antibody fragments from microorganisms. ACS Symposium Series **526**: 203-217

Bibila, T.A., Robinson, D.K. 1995. In pursuit of the optimal fed-batch process for monoclonal antibody procuction. Biotechnology Progress **11**: 11-13

Bird, R.E., Walker, B.W. 1991. Single chain antibody variable regions. Trends in Biotechnology **9**: 132-137

Birdsell, D.C., Cota-Robles, E.H. 1967. Production and ultrastructure of lysozyme and ethylenediaminetetraacetate-lysozyme spheroplasts of *Escherichia coli.* Journal of Bacteriology **93**: 427-437

Boss, M.A., Kenten, J.H., Wood, C.R., Emtage, J.S. 1984. Assembly of functional antibodies from immunoglobulin heavy and light chains synthesised in *E. coli.* Nucleic Acids Research **12**: 3791-3806

Bracewell, D.G., Gill, A., Hoare, M., Lowe, P.A. An in-line flow injection optical biosensor for real-time bioprocess monitoring. In preparation.

Bracewell, D. G., Gill, A., Hoare, M., Maule, C. H. 1998. An optical biosensor for real-time chromatography monitoring: Breakthrough determination. Biosensors and Bioelectronics **13**: 847-853

Bradford, M. 1976. A rapid and sensitive method for quantification of microgram quantities of protein using the principle of protein-dye binding. Analytical Biochemistry **72**: 248-254

Bregegere, F., Schwartz, J., Bedouelle, H. 1994. Bifunctional hybrids between the variable domains of an immunoglobulin and the maltose binding protein of

Escherichia coli: production, purification and antigen binding. Protein Engineering **7**: 271-280

Brown, D.E., Kavanagh, P.R. 1987. Cross-flow separation of cells. Process Biochemistry **22**: 96-101

Brunner, K.H., Hemfort, H. 1988. Centrifugal Separation in Biotechnological Processes. In Advances in Biotechnological Processes **8**; Mizrahi, A., Alan, R., Ed.; Liss Inc., New York: 1-50

Buchner, J., Rudolph, R., 1991. Renaturation, purification and characterisation of recombinant Fab fragments produced in *Escherichia coli*. Biotechnology **9**: 157-162

Burks, E.A., Iverson, B.L. 1995. Rapid, high yield recovery of a recombinant digoxin binding single chain Fv from *Escherichia coli*. Biotechnology Progress **11**: 112-114

Byfield, M.P., Abuknesha, R.A. 1994. Biochemical aspects of biosensors. Biosensors and Bioelectronics **9**: 373-400

Cabilly, S. 1989. Growth at Sub-optimal temperatures allows the production of functional, antigen-binding Fab fragments in *Escherichia coli*. Gene **85**: 553-557

Cabilly, S., Riggs, A.D., Pande, H., Shively, J.E., Holmes, W.E., Rey, M., Perry, J., Wetzel, R., Heyneker, H.L. 1984. Generation of antibody activity from immunoglobulin polypeptide chains produced in *E. coli*. Proceedings of the National Academy of Science USA **81**: 3273-3277

Carter, P., Kelley, R.F., Rodrigues, M.L., Snedcor, B., Covarrubias, M., Velligan, M.D., Wong, W.L.T., Rowland, A.M., Kotts, C.E., Carver, M.E., Yang, M., Bourell, J.H., Shepare, H.M., Henner, D. 1992a. High level *Escherichia coli* expression and production of a bivalent humanised antibody fragment. Bio/Technology **10**: 163-167

Carter, P., Merchant, A.M. 1997. Engineering antibodies for imaging and therapy. Current Opinion in Biotechnology **8**: 449-454

Carter, P., Presta, L., Gorman, C.M., Ridgway, J.B.B., Henner, D., Wong, W.L.T., Rowland, A.M., Kotts, C., Carver, M.E., Shepard, H.M. 1992b. Humanization of an anti-p185^{HER2} antibody for human cancer therapy. Proceedings of the National Academy of Science USA **89**: 4285-4289

Caulcott, C.A. 1984. Competition between plasmid-positive and plasmid-negative cells. Biochemical Society Transactions **12**: 1140-1142

Caulcott, C.A., Dunn, A., Robertson, H.A., Cooper, N.S., Brown, M.E., Rhodes, P.M. 1987. Investigation of the effect of growth environment on the stability of low-copy-number plasmids in *Escherichia coli*. Journal of General Microbiology **133**: 1881-1889.

Chang, Y.K., Chase, H.A. 1996. Ion-exchange purification of G6PDH from unclarified yeast-cell homogenates using expanded bed adsorption. Biotechnology and Bioengineering **49**: 204-216

Chase, H.A. 1994. Purification of proteins by adsorption chromatography in expanded beds. Trends in Biotechnology **12**: 296-303

Chester, K.A., Hawkes, R.E. 1995. Clinical issues in antibody design. Trends in Biotechnology **13**: 294-300

Chester, K.A., Robson, L., Keep, P.A., Pedley, R.B., Boden, J.A., Hawkins, R.E., Begent, R.H.J. 1994. Production and tumour-binding characterisation of a chimeric anti-CEA Fab expressed in *Escherichia coli*. International Journal of Cancer **57**: 67-72

Cush, R., Cronin, J. M., Stewart, W. J., Maule, C. H., Molloy, J., Goddard, N. J. 1993. The Resonant Mirror: a novel optical biosensor for direct sensing of

biomolecular interactions Part I: principle of operation and associated instrumentation. Biosensors and Bioelectronics **8**: 347-364.

Datar, J., Rosen, C-G. 1987. Centrifugal separation in the recovery of intracellular protein from *Escherichia coli*. The Chemical Engineering Journal **34**: B49-B56

Donovan, R.S., Robinson, C.W., Glick, B.R. 1996. Review: Optimising inducer and culture conditions for expression of foreign proteins under control of the *lac* promoter. Journal of Industrial Microbiology **16**: 145-154

Dorai, H., McCartney, J.E., Hudziak, R.M., Tai, M-S., Laminet, A.A., Houston, L.L., Huston, J.S., Oppermann, H. 1994. Mammalian cell expression of single-chain Fv (scFv) antibody proteins and their C-terminal fusions with interleukin-2 and other effector domains. Bio/Technology **12**: 890-897

Erdmann, J. 1998. Mab Purification Strategies. Genetic Engineering News, April 15, p26

Fahrner, R.L., Blank, G.S. 1999(a). Real-time control of antibody loading during protein A affinity chromatography using on-line assay. Journal of Chromatography A **849**: 191-196

Fahrner, R.L., Blank, G.S. 1999(b). Real-time monitoring of recombinant antibody breakthrough during protein A affinity chromatography. Biotechnology and Applied Biochemistry **29**: 109-112

Fahrner, R.L., Lester, P.M., Blank, G.S., Reifsnyder. 1998. Real-time control of purified product collection during chromatography of recombinant human insulin-like growth factor-I using an on-line assay. Journal of Chromatography A **827**: 37-43

Feuser, J., Halfar, M., Lutkemeyer, D., Ameskamp, N., Kula, M-R., Thommes, J. 1999. Interaction of mammalian cell culture broth with adsorbents in expanded bed adsorption of monoclonal antibodies. Process Biochemistry **34**: 159-165

Fischer, E.J. 1996. Impacts of separation processes on protein recovery from cells and cell spheroplasts. PhD Thesis, University of London.

Fischer, R., Drossard, J., Emans, N., Commandeur, U., Hellwig, S. 1999. Towards molecular farming in the future: *Pichia pastoris*-based production of single-chain antibody fragments. Biotechnology and Applied Biochemistry **30**: 117-120

Foor, F., Morin, N., Bostian, K.A. 1993. Production of L-dihydroxyphenylalanine in *Escherichia-coli* with the tyrosine phenol-lyase gene cloned from *Erwinia-herbicola.* Applied and Environmental Microbiology **59**: 3070-3075

Forsberg, G., Forsgren, M., Jaki, M., Norin, M., Sterky, C., Enhorning, A., Larsson, K., Ericsson, M., Bjork, P. 1997. Identification of framework residues in a secreted recombinant antibody fragment that control production level and localisation in *Escherichia coli.* Journal of Biological Chemistry **272**: 12430-12436

Francisco, J.A., Campbell, R., Iverson, B.L., Georgiou, G. 1993. Production and fluorescence-activated cell sorting of *Escherichia coli* expressing a functional antibody fragment on the external surface. Proceedings of the National Academy of Sciences USA **90**: 10444-10448

French, C., Keshavarz-Moore, E., Ward, J. 1996. Large scale production and recovery of a recombinant protein from the periplasm of *Escherichia coli.* Enzyme and Microbial Technology **19**: 332-338

Freyre, F.M., Vazquez, J.E., Ayala, M., CanaanHaden, L., Bell, H., Rodriguez, I., Gonzalez, A., Cintado, A., Gavilondo, J.V. 2000. Very high expression of an anti-carcinoembryonic single chain Fv antibody fragment in the yeast *Pichia pastoris.* Journal of Biotechnology **76**: 157-163

Fuchs, P., Breitling, F., Dubel, S., Seehaus, T., Little, M. 1991. Targeting recombinant antibodies to the surface of *Escherichia coli*: Fusion to a peptidoglycan associated lipoprotein. Bio/Technology **9**: 1369-1372

Gandecha, A.R., Owen, M.R.L., Cockburn, B., Whitlam, G.C. 1992. Production and secretion of a bifunctional Staphylococcal protein A::antiphytochrome single-chain Fv fusion protein in *Escherichia coli*. Gene **122**:361-365

Gavit, P., Walker, M., Wheeler, T., Bui, P., Lei, S-P., Weickmann, J. 1992. Purification of a mouse-human chimeric Fab secreted from *E. coli*. Biopharm January/February: 28-34

Gill, A. 1996. The evaluation of an optical biosensor for at-line monitoring and control of a bioprocess. PhD Thesis, University of London.

Gill, A., Bracewell, D. G., Hoare, M., Lowe, P.A. 1998. Bioprocess monitoring: An optical biosensor for real-time bioproduct analysis. Journal of Biotechnology **65**: 69-80

Gill, A., Harrison, J., Holwill, I., Lowe, P. A., Hoare, M. 1996. Determination of bioactive protein product produced during fermentation using an optical biosensor. Protein and Peptide Letters **3**: 199-206

Glockshuber, R., Malia, M., Pfitzinger, I., Pluckthun, A. 1990. A comparison of strategies to stabilise immunoglobulin Fv fragments. Biochemistry **29**: 1362-1367

Hames, B.D., Rickwood, D. 1990. Gel electrophoresis of proteins: a practical approach (2^{nd} edition). Oxford: IRL Press at Oxford University Press.

Han, K., Lim, H.C., Hong, J. 1992. Acetic acid formation in *Escherichia coli* fermentation. Biotechnology and Bioengineering **39**: 663-671

Harris, B. 1999. Exploiting antibody-based technologies to manage environmental pollution. Trends in Biotechnology: **17**: 290-296

Harrison, J. 1996. Production of recombinant antibody fragments in microorganisms. PhD Thesis, University College London.

Harrison, J. S., Kesharvarz-Moore, E., Dunnill, P., Berry, M. J., Fellinger, A., Frenken, L. 1997. Factors affecting the fermentative production of a lysozyme-binding antibody fragment in *Escherichia coli*. Biotechnology and Bioengineering **53**: 611-622

Hetherington, P.J., Follows, M., Dunnill, P., Lilly, M.D. 1971. Release of protein from bakers yeast (*Saccharomyces cerevisiae*) by disruption in an industrial homogeniser. Transaction of the Institution of Chemical Engineers **49**: 142-148

Hewitt, C.J., Boon, L.A., McFarlane, C.M., Nienow, A.W. 1998. The use of flow cytometry to study the impact of fluid mechanical stress on *Escherichia coli* W3110 during continuous cultivation in an agitated bioreactor. Biotechnology and Bioengineering **59**: 612-620

Hjorth, R. 1997. Expanded bed adsorption in industrial bioprocessing: recent developments. Trends in Biotechnology **15**: 230-235

Hoare, M., Narendranathan, T.J., Flint, J.R., Heywood-Waddington, D., Bell, D.J., Dunnill, P. 1982. Disruption of protein precipitates during shear in couette flow and in pumps. Industrial and Engineering Chemistry Fundamentals **21**: 402-406

Holliger, P., Hoogenboom, H. 1998. Antibodies come back from the brink. Nature Biotechnology **16**: 1015-1016

Holliger, P., Wing, M., Pound, J.D., Bohlen, H., Winter, G. 1997. Retargeting serum immunoglobulin with bispecific diabodies. Nature Biotechnology **15**: 632-636

Holms, W.H. 1986. The central metabolic pathways of *Escherichia coli*: Relationship between flux and control at a branch point, efficiency of conversion to biomass, and excretion of acetate. Current Topics in Cell Regulation **28**: 69-105

Holwill, I., Gill, A., Harrison, J., Hoare, M., Lowe, P.A. 1996. Rapid analysis of biosensor data using initial rate determination and its application to bioprocess monitoring. Process Control and Quality **8**: 133-145.

Horn, U., Strittmatter, W., Krebber, A., Knupfer, U., Kujau, M., Wenderoth, R., Muller, K., Matzku, S., Pluckthun, A., Riesenberg, D. 1996. High volumetric yields of functional dimeric miniantibodies in *Escherichia coli*, using an optimised expression vector and high-cell-density fermentation under non-limited growth conditions. Applied Microbiology and Biotechnology **46**: 524-532

Hudson, P.J. 1998. Recombinant antibody fragments. Current Opinion in Biotechnology **9**: 395-402

Hudson, P.J. 1999. Recombinant antibody constructs in cancer therapy. Current Opinion in Immunology **11**: 548-557

Hudziak, R.M., Lewis, G.D., Winget, M., Fendly, B.M., Shepard, H.M., Ullrich, A. 1989. p185-HER2 monoclonal-antibody has antiproliferative effects *in vitro* and sensitises human-breast tumour-cells to tumour necrosis factor. Molecular Cell Biology **9**:1165-1172

Ibrahim, S., Kaartinen, M., Seppala, I., Matosoferreira, A., Makela, O. 1993. The alternative binding site for protein A in the Fab fragment of immunoglobulins. Scandinavian Journal of Immunology **37**: 257-264

Inbar, D., Hochman, J., Givol, D. 1972. Localisation of antibody-combining sites within the variable portions of heavy and light chains. Proceedings of the National Academy of Sciences USA **69**: 2659-2662

Jacobsen, F.S., Hanson, J.T., Wong, P-Y., Mulkerrin, M., Deveney, J., Reilly, D., Wong, S.C. 1997. Role of high-performance liquid chromatographic protein analysis in developing fermentation processes for recombinant human growth hormone, relaxin, antibody fragments and lymphotoxin. Journal of Chromatography A **763**: 31-48

Jagersten, C., Johansson, S., Pardon, R., Bonnerjea, J. 1996. Abstracts, Recovery of Biological Products, American Chemical Society: 46

Johansson, H.J., Jagersten, C., Shiloach, J. 1996. Large scale recovery and purification of periplasmic recombinant protein from *E. coli* using expanded bed adsorption chromatography followed by new ion exchange media. Journal of Biotechnology **48**: 9-14

Johnson, B.H., Hecht, M.H. 1994. Recombinant proteins can be isolated from *E. coli* cells by repeated cycles of freezing and thawing. Bio/Technology **12**: 1357-1360

Jones, S.L., Cox, J.C., Shepherd, J.M., Rothel, J.S., Wood, P.R., Radford, A.J. 1992. Removal of false-positive reactions from plasma in an enzyme immunoassay for bovine interferon-γ. Journal of Immunological Methods **155**: 233-240

Kapralek, F., Jecmen, P., Sedlacek, J., Fabry, M., Zadrazil, S. 1991. Fermentation conditions for high-level expression of the *tac*-promoter-controlled calf prochymosin cDNA in *Escherichia coli* HB 101. Biotechnology and Bioengineering **37**: 71-79

Karlsson, R., Michaelsson, A., Mattsson, L. 1991. Kinetic analysis of antibody-antigen interactions with a new biosensor based analytical system. Journal of Immunological Methods **145**: 229-240

Katsui, N., Tsuchido, T., Hiramatsu, R., Fujikawa, S., Takano, M., Shibasaki, I. 1982. Heat-induced blebbing and vesiculation of the outer membrane of *Escherichia coli*. Journal of Bacteriology **151**: 1523-1531

Kelley, R.F., O'Connell, M.P., Carter, P., Presta, L., Eigenbrot, C., Covarrubias, M., Snedecor, B., Bourell, J.H., Vetterlein, D. 1992. Antigen binding thermodynamics and antiproliferative effects of chimeric and humanized anti-p185^{HER2} antibody Fab fragments. Biochemistry **31**: 5434-5441

Kempken, R., Preissmann, A., Berthold, W. 1995. Assessment of a disc stack centrifuge for use in mammalian cell separation. Biotechnology and Bioengineering **46**: 132-138

Keshavarz Moore, E., Hoare, M., Dunnill, P. 1990. Disruption of baker's yeast in a high-pressure homogeniser: New evidence on mechanism. Enzyme and Microbial technology **12**: 764-770

King, D.J., Byron, O.D., Mountain, A., Weir, N., Harvey, A., Lawson, A.D.G., Proudfoot, K.A., Baldock, D., Harding, S.E., Yarranton, G.T., Owens, R.J. 1993. Expression, purification and characterisation of B72.3 Fv fragments. Biochemical Journal **290**: 723-729

Kipriyanov, S.M., Moldenhauer, G., Little, M. 1997. High level production of soluble single chain antibodies in small-scale *Escherichia coli* cultures. Journal of Immunological Methods **200**: 69-77

Knappik, A., Pluckthun, A. 1995. Engineered turns of a recombinant antibody improve its *in-vivo* folding. Protein Engineering **8**: 81-89

Kohler, G., Milstein, C. 1975. Continuous cultures of fused cells secreting antibody of predefined specificity. Nature **256**: 495-497

Kortt, A.A., Lah, M., Oddie, G.W., Gruen, C.L., Burns, J.E., Pearce, L.A., Atwell, J.L., McCoy, A.J., Howlett, G.J., Metzger, D.W., Webster, R.G., Hudson, P.J. 1997. Single-chain Fv fragments of anti-neuraminidase antibody NC10 containing five- and ten-residue linkers form dimers and with zero-residue linker a trimer. Protein Engineering **10**: 423-433

Korz, D.J., Rinas, U., Hellmuth, K., Sanders, E.A., Deckwer, W-D. 1995. Simple fed-batch technique for high cell density cultivation of *Escherichia coli*. Journal of Biotechnology **39**: 59-65

Kreitman, R.J. 1999. Immunotoxins in cancer therapy. Current Opinion in Immunology **11**: 570-578

Kuen, L.S., Ming, C.H., Fan, Y.S. 1993. Background noise in ELISA procedures. Influence of the pH of the coating buffer and correlations with serum IgM concentration. Journal of Immunological methods **163**: 277-278

Laemmli, U.K. 1970. Cleavage of structural proteins during assembly of the head of bacteriophage T4. Nature 227: 680-685

Leatherbarrow, R.J., Rademacher, T.W., Dwek, R.A., Woof, J.M., Clark, A., Burton, D.R., Richardson, N., Feinstein, A. 1985. Effector functions of a monoclonal aglycosylated mouse IgG2a: binding and activation of complement component C1 and interaction with human monocyte F_C receptor. Molecular Immunology **22**: 407-415

Lee, J-H., Choi, Y-H., Kang, S-K., Park, H-H., Kwon, I-B. 1989. Production of human leukocyte interferon in *Escherichia coli* by control of growth rate in fed-batch fermentation. Biotechnology Letters **11**: 695-698

Lee., S-M. 1989. The primary stages of protein recovery. Journal of Biotechnology **11**:103-118

Lee, S-M., Gustafson, M.E., Pickle, D.J., Flickinger, M.C., Muschik, G.M., Morgan, A.C. 1986. Large-scale purification of a murine antimelanoma monoclonal antibody. Journal of Biotechnology **4**:189-204

Lee, S.Y. 1996. High cell-density culture of *Escherichia coli*. Trends in Biotechnology **14**: 98-105

Levy, M.S., Collins, I.J., Yim, S.S., Ward, J.M., Titchener-Hooker, N., Shamlou, P.A., Dunnill, P. 1999. Effect of shear on plasmid DNA in solution. Bioprocess Engineering **20**: 7-13

Lutkemeyer, D., Ameskamp, N., Tebbe, H., Wittler, J., Lehmann, J. 1999. Estimation of cell damage in bench- and pilot-scale affinity expanded-bed chromatography for the purification of monoclonal antibodies. Biotechnology and Bioengineering **65**: 114-119

Ma, J.K.C. 1995. Antibody expression in plants. ACS Symposium Series **604**: 56-59

Martineau, P., Jones, P., Winter, G. 1998. Expression of an antibody fragment at high levels in the bacterial cytoplasm. Journal of Molecular Biology **280**: 117-127

Maybury, J.P., Hoare, M, Dunnill, P. 2000. The use of laboratory centrifugation studies to predict performance of industrial machines: studies of shear insensitive and shear sensitive materials. Biotechnology and Bioengineering **67**: 265-273

Maybury, J.P., Mannweiler, K., Titchener-Hooker, NJ., Hoare, M., Dunnill, P. 1998. The performance of a scaled down industrial disk stack centrifuge with a reduced feed material requirement. Bioprocess Engineering **18**: 191-199.

McCarroll, L., King, L.A. 1997. Stable insect cell cultures for recombinant protein production. Current Opinion in Biotechnology **8**: 590-594

Mhatre, R., Nashabeh, W., Schmalzing, D., Yao, X., Fuchs, M., Whitney, D., Regnier, F. 1995. Purification of antibody Fab fragments by cation-exchange chromatography and pH gradient elution. Journal of Chromatography A **707**: 225-231

Murkes, J., Carlsson, C-G. 1978. Mathematical modelling and optimisation of centrifugal separation. Filtration and Separation Jan/ Feb: 18-22

Murrell, N.J. 1998. An engineering study of the recovery of shear sensitive biological materials by high speed disk stack centrifugation. PhD Thesis, University of London.

Naglak, T.J., Wang, H.Y. 1990. Recovery of a foreign protein from the periplasm of *Escherichia coli* by chemical permeabilisation. Enzyme and microbial Technology **12**: 603-611

Neri, D., de Lalla, C., Petrul, H., Neri, P., Winter, G. 1995. Calmodulin as a versatile tag for antibody fragments. Bio/Technology **13**: 373-377

Neu, H.C., Heppel, L.A. 1964. The release of ribonuclease into the medium when *Escherichia coli* cells are converted to spheroplasts. Journal of Biological Chemistry **239**: 3893-3900

Neubauer, P., Hofmann, K. 1994. Efficient use of lactose for the *lac* promoter-controlled overexpression of the main antigenic protein of the foot and mouth disease virus in *Escherichia coli* under fed-batch fermentation conditions. FEMS Microbiology Reviews **14**:99-102

Neuberger, M.S., Williams, G.T., Fox, R.O. 1984. Recombinant antibodies possessing novel effector functions. Nature **312**: 604-608

Nose, M., Wigzell, H. 1983. Biological significance of carbohydrate chains on monoclonal antibodies. Proceedings of the National Academy of Sciences USA **80**: 6632-6636

Nossal, N.G., Heppel, L.A. 1966. The release of enzymes by osmotic shock from *Escherichia coli* in exponential phase. Journal of Biological Chemistry **241**: 3055-3062

Ostlund, C. 1996. Large-scale purification of monoclonal antibodies. Trends in Biotechnology: 288-293

Pack, P., Kujau, M., Schroeckh, V., Knupfer, U., Wenderoth, R., Reisenberg, D., Pluckthun, A. 1993. Improved bivalent miniantibodies, with identical avidity as whole antibodies, produced by high cell density fermentation of *Escherichia coli*. Bio/Technology **11**: 1271-1277

Paliwal, S.K., Nadler, T.K., Wang, D.I.C., Regnier, F.E. 1993. Analytical Chemistry **65**: 3363-3367

Park, J.W., Hong, K., Carter, P., Asgari, H., Guo, L.Y., Keller, G.A., Wirth, C., Shalaby, R., Kotts, C., Wood, W.I., Papahadjopoulos, D., Benz, C.C. 1995. Development of anti-p185^{HER2} immunoliposomes for cancer therapy. Proceedings of the National Academy of Sciences USA **92**: 1327-1331

Pessoa, A., Hartmann, R., Vitolo, M., Hustedt, H. 1996. Recovery of extracellular inulinase by expanded bed adsorption. Journal of Biotechnology **51**: 89-95

Petermann, M.L., Pappenheimer, A.M. 1941. The ultracentrifugal analysis of diptheria proteins. Journal of Physical Chemistry **45**: 1

Pfeifer, T.A. 1998. Expression of heterologous proteins in stable insect cell culture. Current Opinion in Biotechnology **9**: 518-521

Pierce, J.J., Turner, C., Keshavarz-Moore, E., Dunnill, P. 1997. Factors determining more efficient large-scale recovery of a periplasmic enzyme from *E. coli* using lysozyme. Journal of Biotechnology **58**: 1-11

Pluckthun, A. 1991. Antibody engineering: advances from the use of *Escherichia coli* expression systems. Bio/Technology **9**: 545-551

Pluckthun, A., Skerra, A. 1989. Expression of functional antibody Fv and Fab fragments in *Escherichia coli*. Methods in Enzymology **178**: 497-515

Pohlner, J., Kramer, J., Meyer, T.F. 1993. A plasmid system for high-level expression and *in vitro* processing of recombinant proteins. Gene **130**: 121-126

Porter, R.R. 1959. The hydrolysis of rabbit γ-globulin and antibodies with crystalline papain. Biochemical Journal **73**: 119-126

Raag, R., Whitlow, M. 1995. Single-chain Fvs. FASEB Journal **9**: 73-80

Randen, I., Potter, K.N., Li, Y.C., Thompson, K.M., Pascual, V., Forre, O., Natvig, J.B., Capra, J.D. 1993. Complementary -determining region-2 is implicated in the binding of Staphylococcal protein-A to human-immunoglobulin V(H) III variable regions. European Journal of Immunology **23**: 2682-2686

Reichmann, L., Foote, J., Winter, G. 1988. Expression of an antibody Fv fragment in myeloma cells. Journal of Molecular Biology **203**: 825-828

Reiter, Y., Brinkmann, U., Lee, B., Pastan, I. 1996. Engineering antibody Fv fragments for cancer therapy: Disulfide-stabilized Fv fragments. Nature Biotechnology **14**: 1239-1245

Reznikoff, W.S., Abelson, J.N. 1980. The *lac* promoter. In: The Operon (Miller, J.H., Reznikoff, W.S. eds), 221-224, Cold Spring Harbor Laboratory, Cold Spring Harbor, NY.

Richalet-Secordel, P.M., Rauffer-Bruyere, N., Christensen, L.L.H., Ofenloch-Haehnle, B., Seidel, C., Van Regenmortel, M.H.V. 1997. Concentration measurement of unpurified proteins using biosensor technology under conditions of partial mass transport limitation. Analytical Biochemistry **249**: 165-173

Rodrigues, M.L., Snedecor, B., Chen, C., Wong, W.L.T., Garg, S., Blank, G.S., Maneval, D., Carter, P. 1993. Engineering Fab' fragments for efficient $F(ab)_2$ formation in *Escherichia coli* and for improved *in vivo* stability. Journal of Immunology **151**: 6954-6961

Ryan, W., Parulekar, S.J. 1991. Recombinant Protein Excretion in *Escherichia coli* JM109(pUC8): Effects of plasmid content, ethylenediaminetetraacetate, and phenethyl alcohol on cell membrane permeability. Biotechnology and Bioengineering **37**: 430-444

Sambrook, J., Fritsch, E. F., Maniatis, T. Molecular Cloning: A Laboratory Approach, second edition. 1989. Cold Spring Harbour Laboratory Press. Cold Spring Harbour, NY.

Sasso, E.H., Silverman, G.J., Mannik, M. 1991. Human IgA and IgG $F(ab')_2$ that bind to Staphylococcal protein-A belong to the VHIII-subgroup. Journal of Immunology **147**: 1877-1883

Sauer, T., Robinson, C.W., Glick, B.R. 1989. Disruption of native and recombinant *Escherichia coli* in a high-pressure homogeniser. Biotechnology and Bioengineering **33**: 1330-1342

Schugerl, K., Hitzmann, B., Jurgens, H., Kullick, T., Ulber, R., Weigal, B. 1996. Challenges in integrating biosensors and FIA for on-line monitoring and control. Trends in Biotechnology **14**: 21-31

Schutte, H., Kroner, K.H., Hustedt, H., Kula, M-R. 1983. Experiences with a 20 litre industrial scale bead mill for the disruption of microorganisms. Enzyme and Microbial Technology **5**: 143-148

Segal, D.M., Weiner, G.J., Weiner, L.M. 1999. Bispecific antibodies in cancer therapy. Current Opinion in Immunology **11**: 558-562

Shalaby, M.R., Shepard, H.M., Presta, L., Rodrigues, M., Beverley, P.C.L., Feldmann, M., Carter, P. 1992. Development of humanized bispecific antibodies reactive with cytotoxic lymphocytes and tumour cells overexpressing the HER2 protooncogene. Journal of Experimental Medicine **175**:217-225

Shibui, T., Munakata, K., Matsumoto, R., Ohta, K., Matsushima, R., Morimoto, Y., Nagahari, K. 1993. High-level production and secretion of a mouse chimeric Fab fragmenta with specificity to human carcino embryonic antigen in *Escherichia coli*. Applied Microbiology and Biotechnology **38**: 770-775

Shibui, T., Nagahari, K. 1992. Sectetion of a functional Fab fragment in *Escherichia coli* and the influence of culture conditions. Applied Microbiology and Biotechnology **37**: 352-357

Shusta, E.V., Raines, R.T., Pluckthun, A., Wittrup, K.D. 1998. Increasing the secretory capacity of *Saccharomyces cerevisiae* for production of single-chain antibody fragments. Nature Biotechnology **16**: 773-777

Simmons, L.C., Yansura, D.G. 1996. Translational level is a critical factor for the secretion of heterologous proteins in *Escherichia coli*. Nature Biotechnology **14**: 629-634

Skerra, A., Pfitzinger, I., Pluckthun, A. 1991. The functional expression of antibody Fv fragments in *Escherichia coli*: improved vectors and a generally applicable purification technique. Bio/Technology **9**: 273-278

Skerra, A., Pluckthun, A. 1988. Assembly of a functional immunogloblulin Fv fragment in *Escherichia coli*. Science **240**: 1038-1041

Skerra, A., Pluckthun, A. 1991. Secretion and *in vivo* folding of the F_{ab} fragment of the antibody McPC603 in *Escherichia coli*: influence of disulphides and *cis*-prolines. Protein Engineering **4**: 971-979

Slamon, D.J., Godolphin, W., Jones, L.A., Holt, J.A., Wong, S.G., Keith, D.E., Levin, W.J., Stuart, S.G., Udove, J., Ulrich, A., Press, M. 1989. Studies of the HER-2/*neu* proto-oncogene in human breast and ovarian cancer. Science **244**: 707-712

Smith, M.D. 1996. Antibody production in plants. Biotechnology Advances **14**: 267-281

Sommerville Jr., J.E., Goshorn, S.C., Fell, H.P., Darveau, R.P. 1994. Bacterial aspects associated with the expression of a single-chain antibody fragment in *Escherichia coli.* Applied Microbiology and Biotechnology **42**: 595-603

Starovasnik, M.A., O'Connell, M.P., Fairbrother, W.J., Kelley, F.R. 1999. Antibody variable region binding by Staphylococcal protein A: Thermodynamic analysis and location of the Fv binding site on E-domain. Protein Science **8**: 1423-1431

Stocklein, W., Schmid, R.D. 1990. Flow-injection immunoanalysis for the on-line monitoring of monoclonal antibodies. Analytica Chimica Acta **234**: 83-88

Straight, J.V., Ramkrishna, D., Parulekar, S.J., Jansen, N.B. 1989. Bacterial growth on lactose: an experimental investigation. Biotechnology and Bioengineering **34**: 705-716

Swamy, K.H.S., Goldberg, A.L. 1982. Subcellular distribution of various proteases in *Escherichia coli*. Journal of Bacteriology **149**: 1027-1033

Takagi, H., Morinaga, Y., Tsuchiya, M., Ikemura, H., Inouye, M. 1988. Control of folding of proteins secreted by a high expression secretion vector, pIN-III-*omp*A: 16-fold increase in production of active subtilisin in *Escherichia coli*. Biotechnology **6**: 948-950

Tempest, D.W., Wouters, J.T.M. 1981. Microbial behaviour in chemostat culture. Enzyme and Microbial Tecnnology **3**: 283-290

Thommes, J., Bader, A., Halfar, M., Karau, A,m Kula, M-R. 1996. Isolation of monoclonal antibodies from cell containing hybridoma broth using a protein A coated adsorbent in expanded beds. Journal of Chromatography A **752**: 111-122

Trail, P.A., Bianchi, A.B. 1999. Monoclonal antibody drug conjugstes in the treatment of cancer. Current Opinion in Immunology **11**: 584-588

Tsuchido, T., Katsui, N., Takeuchi, A., Takano, M., Shibaski, I. 1985. Destruction of the outer membrane permeability barrier of *Escherichia coli* by heat treatment. Applied Environmental Microbiology **50**: 298-303

Tsumoto, K., Nakaoki, Y., Ueda, Y., Ogasahara, K., Yutani, K., Watanabe, K., Kumagai, I. 1994. Effect of the order of antibody variable regions on the expression of single-chain HyHEL10 Fv fragment in *E. coli* and the thermodynamic analysis of its antigen binding properties. Biochemical and Biophysical Research Communications **201**: 546-551

Tyler, J.E. 1990. Microencapsulation of mammalian cells. In Large-Scale Mammalian Cell Culture Technology; Lubiniecki, A.S., Ed.; Marcel-Dekker, Inc., New York: 343-361

Vaara, M. 1992. Agents that increase the permeability of the outer membrane. Microbiological Reviews **56**: 395-411

Weir, A.N.C., Bailey, N.A. 1997. Process for obtaining antibodies utilising heat treatment. United States Patent 5,665,866.

Wheelwright, S.M. 1987. Designing downstream processes for large scale protein purification. Bio/Technology **5**: 789-793

Wong, S.L., Wu, X.C., Yang, L.P., Ng, S.C., Hudson, N. 1995. Production and purification of antibody using *Bacillus subtilis* as an expression host. ACS Symposium Series **604**: 100-107

Wu, S.C., Ye, R.Q., Wu, X.C., Ng, S.C., Wong, S.L. 1998. Enhanced secretory production of a single-chain antibody fragment from *Bacillus subtilis* by coproduction of molecular chaperones. Journal of Bacteriology **180**: 2830-2835

Yoon, S.K., Kang, W.K., Park, T.H. 1993. Fed-batch operation of recombinant *Escherichia coli* containing *trp* promoter with controlled specific growth rate. Biotechnology and Bioengineering **43**: 995-999

Zapata, G., Ridgway, J.B.B., Mordenti, J., Osaka, G., Wong, W.L.T., Bennett, G.L., Carter, P. 1995. Engineering linear $F(ab')_2$ fragments for efficient production in

Escherichia coli and enhanced antiproliferative activity. Protein Engineering **8**: 1057-1062

Zhu, Z., Zapata, G., Shalaby, R., Snedecor, B., Chen, H., Carter, P. 1996. High level secretion of a humanized bispecific diabody from *Escherichia coli.* Biotechnology **14**: 192-196

Zimmermann, J.J.F., Oddie, K., Langer, R., Cooney, C.L. 1991. The release of heparinase from the periplasmic space of *Flavobacterium heparinum* by three step osmotic shock. Applied Biochemistry and Biotechnology **30**: 137-148